Hydrogeology and Simulated Effects of Ground-Water Withdrawals from the Floridan Aquifer System in Lake County and in the Ocala National Forest and Vicinity, North-Central Florida

U.S. GEOLOGICAL SURVEY
Water-Resources Investigations Report 02-4207

Prepared in cooperation with:
Lake County Water Authority
St. Johns River Water Management District
Southwest Florida Water Management District

Hydrogeology and Simulated Effects of Ground-Water Withdrawals from the Floridan Aquifer System in Lake County and in the Ocala National Forest and Vicinity, North-Central Florida

By Leel Knowles, Jr., Andrew M. O'Reilly, *and* James C. Adamski

U.S. GEOLOGICAL SURVEY

Water-Resources Investigations Report 02–4207

Prepared in cooperation with the

Lake County Water Authority
St. Johns River Water Management District
Southwest Florida Water Management District

USGS
science for a changing world

Tallahassee, Florida
2002

U.S. DEPARTMENT OF THE INTERIOR
GALE A. NORTON, Secretary

U.S. GEOLOGICAL SURVEY
Charles G. Groat, Director

For additional information
write to:

District Chief
U.S. Geological Survey, WRD
Suite 3015
227 North Bronough Street
Tallahassee, FL 32301

Copies of this report can be purchased from:

U.S. Geological Survey
Branch of Information Services
Box 25286
Denver, CO 80225-0286
888-ASK-USGS

Additional information about water resources in Florida is available on the World Wide Web at **http://fl.water.usgs.gov**

CONTENTS

FIGURES

TABLES

CONVERSION FACTORS AND VERTICAL DATUM

Multiply	By	To obtain
	Length	
inch (in.)	2.54	centimeter
foot (ft)	0.3048	meter
mile (mi)	1.609	kilometer
	Area	
square foot (ft^2)	0.0929	square meter
square mile (mi^2)	2.590	square kilometer
square mile (mi^2)	259	hectare
	Flow	
cubic foot per second (ft^3/s)	0.02832	cubic meter per second
inch per year (in/yr)	25.4	millimeter per year
	Hydraulic Conductivity	
foot per day (ft/d)	0.3048	meter per day
	Leakance	
foot per day per foot [(ft/d)/ft]	1.000	meter per day per meter
	Transmissivity*	
foot squared per day (ft^2/d)	0.0929	meter squared per day

*The standard unit for transmissivity is cubic foot per day per square foot times foot of aquifer thickness [(ft^3/d)/ft^2]ft. In this report, the mathematically reduced form, foot squared per day (ft^2/d), is used for convenience.

Temperature in degrees Fahrenheit (°F) may be converted to degrees Celsius (°C) as follows: °C=(°F-32)/1.8.

Sea level: In this report, "sea level" refers to the National Geodetic Vertical Datum of 1929 (NGVD of 1929)--a geodetic datum derived from a general adjustment of the first-order level nets of both the United States and Canada, formerly called Sea Level Datum of 1929.

Altitude: In this report, altitude refers to distance above or below sea level.

Horizontal coordinate information is referenced to the North American Datum of 1927 (NAD27).

Acronyms and additional abbreviations:

ET	evapotranspiration
FAS	Floridan aquifer system
ICU	intermediate confining unit
LCWA	Lake County Water Authority
LFA	Lower Floridan aquifer
MCU	middle confining unit
MSCU	middle semiconfining unit
mg/L	milligrams per liter
Mgal/d	million gallons per day
NOAA	National Oceanic and Atmospheric Administration
Ocala NF	Ocala National Forest
RASA	Regional Aquifer Systems Analysis
SJRWMD	St. Johns River Water Management District
SFWMD	South Florida Water Management District
SWFWMD	Southwest Florida Water Management District
SAS	surficial aquifer system
TDEM	time domain electromagnetic measurements
USFS	U.S. Department of Agriculture, Forest Service
USGS	U.S. Geological Survey
UFA	Upper Floridan aquifer

List of Symbols

Roman

A	Area of sediments constituting the riverbed, [L^2]
AR	Artificial recharge from agricultural and golf-course irrigation and reclaimed water application, in inches
BD	Boundary leakage or net outflow crossing study-area boundary, in inches
BF	Total base flow, in inches
BF_{FAS}	Total base flow from the Floridan aquifer system, in inches
BF_{SAS}	Total base flow from the surficial aquifer system, in inches
C_{riv}	Conductance of sediments constituting the riverbed specified in the River package, [L^2/T]
D_e	Extinction depth, [L]
E_l	Lake evaporation, [L/T]
ET	Evapotranspiration, [L/T]
ET_a	Evapotranspiration extracted from artificial recharge before the water percolates to the water table, [L/T]
ET_n	Natural evapotranspiration, which is evapotranspiration in the absence of artificial recharge, [L/T]
$ET_{\mathrm{n,ex}}$	Excess natural evapotranspiration exceeding $ET_{n,min}$, [L/T]
$ET_{n,min}$	Minimum natural evapotranspiration, [L/T]
h	Simulated water-table altitude, [L]
H_{riv}	Stream or lake water-level altitude specified in the River Package, [L]
$K_{h,sa}$	Horizontal hydraulic conductivity of surficial aquifer system, [L/T]
$K_{h,lf}$	Horizontal hydraulic conductivity of Lower Floridan aquifer, [L/T]
$K_{h,uf}$	Multiplier for horizontal hydraulic conductivity of Upper Floridan aquifer, dimensionless
$K_{v,ic1}$	Vertical hydraulic conductivity of intermediate confining unit, less than or equal to 50 feet thick, [L/T]
$K_{v,ic2}$	Vertical hydraulic conductivity of intermediate confining unit, greater than 50 feet thick, [L/T]
$K_{v,ms}$	Multiplier for vertical hydraulic conductivity of middle semiconfining unit and middle confining unit, Upper Floridan aquifer, [L/T]
$K_{v,riv}$	Vertical hydraulic conductivity of sediments constituting the riverbed, [L/T]
L	Length unit
m	Thickness of sediments constituting the riverbed, [L]
N	Net recharge, [L/T]
N_a	Artificial net recharge, [L/T]
N_{cbl}	Net recharge at closed-basin lakes, [L/T]
N_n	Natural net recharge, [L/T]
$N_{n,max}$	Maximum natural net recharge, [L/T]

$N_{n,min}$	Minimum natural net recharge, [L/T]
no	Number of water-level and flow observations
np	Number of parameters estimated with inverse model
N_{SAS}	Net recharge to the surficial aquifer system, in inches
N_{UFA}	Net recharge to the Floridan aquifer system, in inches
O_{cbl}	Overland runoff to a closed-basin lake, [L/T]
O_s	Overland runoff to a surface-water body other than a closed-basin lake, [L/T]
O_{sa}	Overland runoff to a surface-water body as a result of artificial recharge, [L/T]
O_{sn}	Natural overland runoff, which is overland runoff in the absence of artificial recharge, to a surface-water body other than a closed-basin lake, [L/T]
$O_{sn,ex}$	Excess natural overland runoff exceeding $O_{sn,min}$, [L/T]
$O_{sn,min}$	Minimum natural overland runoff, [L/T]
P	Precipitation, [L/T]
Q_{riv}	Volumetric flow rate simulated by the River Package, [L^3/T]
R_a	Artificial recharge, [L/T]
$R_{ex,max}$	Maximum rate of combined excess evapotranspiration and excess overland runoff, [L/T]
RF	Rainfall, in inches
RO	Overland runoff, in inches
SE	Standard error of regression
SP	Springflow, in inches
S_y	Specific yield of the aquifer in which the water table is located or equal to 1 for a closed-basin lake, dimensionless
SSWR	Sum of squared, weighted residuals, dimensionless
T	Time unit
VAN_{lf}	Vertical anisotropy of Lower Floridan aquifer, dimensionless
VAN_{sa}	Vertical anisotropy of surficial aquifer system, dimensionless
VAN_{uf}	Vertical anisotropy of Upper Floridan aquifer, dimensionless
W	Pumpage from the Floridan aquifer system, in inches
w_k	Weight for the k^{th} water level, [L^{-2}], or flow, [$(L^3/T)^{-2}$]
y_k	k^{th} observed water level, [L], or flow, [L^3/T]
$\hat{y}_k$	k^{th} simulated water level, [L], or flow, [L^3/T]
z_{bot}	Altitude of the bottom of sediments constituting the riverbed specified in the River Package, [L]
z_{ls}	Mean land-surface altitude in model cell, [L]

Greek

ΔH	Change in water-table altitude or closed-basin lake level, [L/T]
ΔS	Total net change in storage, in inches
ΔS_{al}	Change in storage in the aquifer in which the water table is located and in closed-basin lakes, [L/T]
ΔS_{aq}	Change in storage in the aquifer in which the water table is located, [L/T]
ΔS_{cbl}	Change in closed-basin lake storage, [L/T]
ΔS_{FAS}	Net change in storage of the Floridan aquifer system, in inches
ΔS_{SAS}	Net change in storage of the surficial aquifer system, in inches

Hydrogeology and Simulated Effects of Ground-Water Withdrawals from the Floridan Aquifer System in Lake County and in the Ocala National Forest and Vicinity, North-Central Florida

By Leel Knowles, Jr., Andrew M. O'Reilly, *and* James C. Adamski

ABSTRACT

The hydrogeology of Lake County and the Ocala National Forest in north-central Florida was evaluated (1995-2000), and a ground-water flow model was developed and calibrated to simulate the effects of both present day and future ground-water withdrawals in these areas and the surrounding vicinity. A predictive model simulation was performed to determine the effects of projected 2020 ground-water withdrawals on the water levels and flows in the surficial and Floridan aquifer systems.

The principal water-bearing units in Lake County and the Ocala National Forest are the surficial and Floridan aquifer systems. The two aquifer systems generally are separated by the intermediate confining unit, which contains beds of lower permeability sediments that confine the water in the Florida aquifer system. The Floridan aquifer system has two major water-bearing zones (the Upper Floridan aquifer and the Lower Floridan aquifer), which generally are separated by one or two less-permeable confining units.

The Floridan aquifer system is the major source of ground water in the study area. In 1998, ground-water withdrawals totaled about 115 million gallons per day in Lake County and 5.7 million gallons per day in the Ocala National Forest. Of the total ground water pumped in Lake County in 1998, nearly 50 percent was used for agricultural purposes, more than 40 percent for municipal, domestic, and recreation supplies, and less than 10 percent for commercial and industrial purposes.

Fluctuations of lake stages, surficial and Floridan aquifer system water levels, and Upper Floridan aquifer springflows in the study area are highly related to cycles and distribution of rainfall. Long-term hydrographs for 9 lakes, 8 surficial aquifer system and Upper Floridan aquifer wells, and 23 Upper Floridan aquifer springs show the most significant increases in water levels and springflows following consecutive years with above-average rainfall, and significant decreases following consecutive years with below-average rainfall. Long-term (1940-2000) hydrographs of lake and ground-water levels and springflow show a slight downward trend; however, after the early 1960's, this downward trend generally is more pronounced, which corresponds with accumulating rainfall deficits and increased development.

The U.S. Geological Survey three-dimensional ground-water flow model MODFLOW-2000 was used to simulate ground-water flow in the surficial and Floridan aquifer systems in Lake County, the Ocala National Forest, and adjacent areas. A steady-state calibration to average 1998 conditions was facilitated by using the inverse modeling capabilities of MODFLOW-2000. Values of hydrologic properties from the

calibrated model were in reasonably close agreement with independently estimated values and results from previous modeling studies. The calibrated model generally produced simulated water levels and flows in reasonably close agreement with measured values and was used to simulate the hydrologic effects of projected 2020 conditions.

Ground-water withdrawals in the model area have been projected to increase from 470 million gallons per day in 1998 to 704 million gallons per day in 2020. Significant drawdowns were simulated in Lake County from average 1998 to projected 2020 conditions: the average and maximum drawdowns, respectively, were 0.5 and 5.7 feet in the surficial aquifer system, 1.1 and 7.6 feet in the Upper Floridan aquifer, and 1.4 and 4.3 feet in the Lower Floridan aquifer. The largest drawdowns in Lake County were simulated in the southeastern corner of the County and in the vicinities of Clermont and Mount Dora. Closed-basin lakes and wetlands are more likely to be affected by future pumping in these large drawdown areas, as opposed to other areas of Lake County. However, within the Ocala National Forest, drawdowns were relatively small: the average and maximum drawdowns, respectively, were 0.1 and 1.0 feet in the surficial aquifer system, 0.2 and 0.8 feet in the Upper Floridan aquifer, and 0.3 and 0.8 feet in the Lower Floridan aquifer.

Projected 2020 withdrawals from the Floridan aquifer system caused decreases from average 1998 conditions in the following simulated flows: combined rates of excess evapotranspiration and excess overland runoff (which represent evapotranspiration and overland runoff that occur in excess of their assumed minimum rates); groundwater discharge to streams, lakes, and wetlands; and springflow. The largest simulated flow decreases for first- or second-magnitude springs in Lake County were at Apopka (28 percent), Seminole (12 percent), and Bugg Springs (9 percent). The largest simulated flow decrease for first- or second-magnitude springs in the Ocala National Forest was at Juniper Springs (4 percent).

Particle-tracking analyses were used to delineate areas that contribute recharge to selected springs. Based on average 1998 conditions, the contributing area for Apopka Spring covers approximately 30 square miles and has an average contributing recharge flux of 15 inches per year, and the contributing area for Alexander Springs covers approximately 76 square miles and has an average contributing recharge flux of 18 inches per year. The contributing area for Alexander Springs changed little as a result of projected 2020 conditions because relatively little pumping exists in the vicinity of the spring's contributing area. However, the size of the contributing area for Apopka Spring decreased to 26 square miles and the average contributing recharge flux decreased to 13 inches per year as a result of projected 2020 conditions.

INTRODUCTION

The Floridan aquifer system (FAS), particularly the Upper Floridan aquifer (UFA), is the primary source of ground water in peninsular Florida. The FAS is being increasingly stressed as a result of increased pumping and below-average rainfall. Future water-use projections indicate as much as a 100 percent increase in the demand for ground water across central Florida from 1995 to 2020. Much of this increased demand for ground water results from the urban expansion of the Orlando and south-central Marion County areas of central Florida.

The study (model) area is about 4,800 square miles (mi^2) and includes Lake County, the Ocala National Forest (Ocala NF), and the surrounding adjacent counties in north-central Florida (fig. 1). Lake County (1,150 mi^2) and the Ocala NF (690 mi^2) are characterized by diverse landforms including numerous lakes, streams, wetlands, and springs. Urban development in Lake County is increasing rapidly, whereas little development has occurred or is expected to occur within the Ocala NF. Lake County contains numerous communities and small towns and is located 25 miles (mi) or more west and northwest of Orlando, which accounts for some of the population increase in recent years. The Ocala NF, although relatively undeveloped, contains several small communities and private lands (about 75 mi^2) including Astor, Salt Springs, and Lynne.

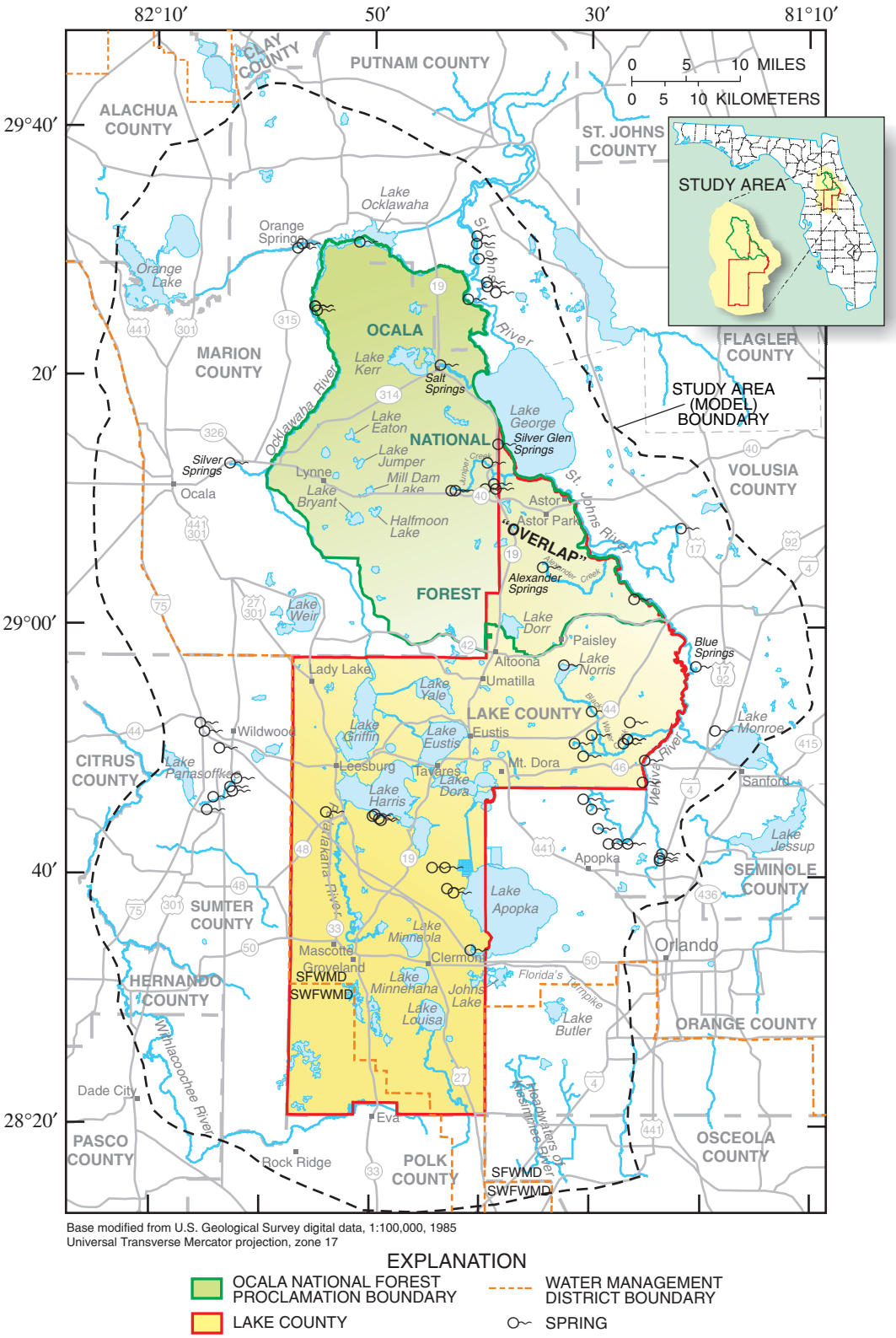

Base modified from U.S. Geological Survey digital data, 1:100,000, 1985
Universal Transverse Mercator projection, zone 17

EXPLANATION

- OCALA NATIONAL FOREST PROCLAMATION BOUNDARY
- LAKE COUNTY
- WATER MANAGEMENT DISTRICT BOUNDARY
- SPRING

Figure 1. Location of study (model) area.

These communities generally lie along the Ocala NF outer perimeter, hereafter called the Ocala NF Proclamation "Boundary." The area of the Ocala NF that encompasses the northeastern part of Lake County is hereafter called the "overlap." Also, urban expansion in the Ocala area and southwestern Marion County has extended toward the Ocala NF and currently has reached areas near the western and southwestern edges of the Ocklawaha River-Ocala NF boundary (fig. 1).

Background

Since 1960, the rates of ground-water pumping for municipal (public supply), domestic, and agricultural use have increased steadily in the central Florida peninsula. Demands for public supply are increasing mainly in response to continuing growth in population. Population in central Florida (which includes Lake, Marion, Volusia, Orange, Seminole, Oceola, and Brevard Counties) has increased by about 260 percent from about 683,270 in 1960 (University of Florida, 1976) to 2,469,200 in 1995 (University of Florida, 1996). Population for the same area is expected to increase by at least 57 percent from 1998 to 3,884,700 by 2020 (Smith and Nogle, 1999). Population in Lake and Marion Counties increased nearly 300 percent, from 109,000 in 1960 to more than 401,500 in 1995. An additional 100 percent increase in population is expected in Lake and Marion Counties from 1995 to 2020. Meanwhile, water levels of lakes, streams, the surficial aquifer system (SAS), and the FAS in the central Florida peninsula generally have decreased. Although much of the decline in water levels can be attributed to persistent below-average rainfall, increased pumping probably also is a factor in the general decline of water levels throughout the central Florida area. Annual ground-water withdrawals from the FAS in Lake and Marion Counties increased from about 61 million gallons per day (Mgal/d) in 1965 to about 166 Mgal/d in 1998 (Richard Marella, U.S. Geological Survey, written commun., 1999). Pumping rates for agricultural uses declined slightly during the 1980's, mainly as a result of reductions in irrigated citrus acreage and reduced citrus processing following several tree-killing freezes. During the 1990's, water use generally shifted away from citrus irrigation to public supply, recreation, turf irrigation, and domestic use. Ground water withdrawn from the UFA in Lake and Marion Counties is expected to increase by more than 50 percent from 166 Mgal/d in 1998 to more than 250 Mgal/d in 2020 (Brian McGurk, St. Johns River Water Management District; and Lou Motz, University of Florida, written commun., 1999).

Prior to the 1990's, ground-water pumping generally occurred from low-capacity wells widely distributed through Lake and Marion Counties; however, as public-supply and domestic use continues to increase, the tendency could be to concentrate more pumping into smaller areas. Consequently, effects from pumping will be more pronounced and localized, particularly in central parts of Lake and Marion Counties. In contrast, pumping in the Ocala NF has been and is expected to remain relatively small and stable. However, increased ground-water pumping from adjacent areas in Lake and Marion Counties could affect ground-water flow conditions within the Ocala NF in the future. The need for better conservation and management of ground-water resources in Lake County is increasing because of the rapid population growth in the county. An understanding of the water resources of the area, including the responses of lake stages, aquifer water levels, and springflows to ground-water pumping in Lake County and in the Ocala NF vicinity is needed so that water managers can develop strategies to meet the growing water-supply demands.

To address the water-resource needs, the Lake County Water Authority (LCWA), St. Johns River Water Management District (SJRWMD), Southwest Florida Water Management District (SWFWMD), and the U.S. Department of Agriculture, Forest Service (USFS), are participating in cooperative programs with the U.S. Geological Survey (USGS) to collect hydrologic data. Included in these programs are surface-water data-collection networks with the LCWA, SJRWMD, and USFS, as well as semiannual measurements of ground-water levels in the SAS and FAS with the SJRWMD and SWFWMD. In 1995, the USGS, with the aforementioned cooperators, began a 5-year study (1995-2000) to evaluate the ground-water resources of Lake County and the Ocala NF and to determine the potential effects of increased ground-water withdrawals on those resources. Most data for this study were collected from September 1997 through December 1998.

Purpose and Scope

This report presents a description of the hydrogeology of Lake County and the Ocala NF and quantifies the effects of future ground-water withdrawals

from the Floridan aquifer system. Ground-water level, surface-water stage and discharge, springflow, and water-use data are presented. Well log interpretations were used to determine the lithology and better understand the hydrogeology. Water-quality data collected during the study are presented by Adamski and Knowles (2001). A numerical model of the ground-water flow system was constructed and used to evaluate the effects of projected increases in ground-water withdrawals on water levels in the surficial and Floridan aquifer systems and on springflow from the Upper Floridan aquifer. Although the primary focus of this study was in Lake County and the Ocala NF, ground-water withdrawals in adjacent central Florida counties necessitated expansion of the model area to include a more regional system (fig. 1).

Previous Studies

Hydrologic data were collected systematically from 1966-70 for a summary report of water resources for east-central Florida, including Lake County, by Lichtler (1972). Knochenmus and Hughes (1976) provided a detailed description of the surface- and ground-water flow system in Lake County and presented the results of a 3-year investigation to assess the availability and quality of surface- and ground-water resources, and the effects of anthropogenic stresses on the hydrologic system in Lake County. Faulkner (1973) provided a detailed report of the stratigraphy, structural geology, and ground-water flow system of the proposed Cross-Florida Barge Canal right-of-way, with emphasis in the Ocala area. Tibbals (1975) conducted aquifer tests on the upper 100 feet (ft) of the FAS in the barge canal right-of-way to provide information about the potential exchange of water between the proposed canal and the aquifer. A quantitative appraisal of east-central Florida's water resources, inclusive of all but extreme western Lake County, also was done by Tibbals (1990) as part of the Regional Aquifer Systems Analysis (RASA). Lithologic and borehole data for the Green Swamp area of south Lake County are provided by Grubb and others (1978). Adamski and Knowles (2001) presented the results of a water-quality study for 217 water samples taken from the SAS and UFA in Lake County and the Ocala NF. O'Reilly and others (2002) described the hydrogeologic and water-quality characteristics of the Lower Floridan aquifer, in east-central Florida, including parts of Lake County. Hydrogeology and results of simulating the ground-water flow system surrounding and including parts of the study area are presented by Motz (1995), Murray and Halford (1996), O'Reilly (1998), Spechler and Halford (2001), Sepúlveda (2002), and McGurk and Presley (in press).

Acknowledgments

The authors wish to thank the U.S. Department of Agriculture, Forest Service, for access and assistance in the Ocala NF and the many residents and public officials who contributed information useful to the investigation; granted permission to drill new wells; and permitted access to wells, lakes, and springs to collect water-level and flow measurements and water samples. The authors also are grateful to Mr. Joe M. Branham for supplying flow measurements and hydrogeologic information for Bugg Spring; Mr. Joseph A. Bishop, Lake Forestry Station, Florida Department of Agriculture, for access and gage installation in the Seminole State Forest; and Mr. Walter D. Wood of Lake County Water Resources Management for well access and for providing historic hydrologic data from wells located on county lands.

DESCRIPTION OF STUDY AREA

The study area, which includes Lake County and the Ocala NF, is located 25 mi or more west and northwest of Orlando in north-central Florida (fig. 1). Lake County is predominantly rural with a few, mostly widely scattered, but steadily growing towns such as Leesburg, Tavares, Eustis, Clermont, and Lady Lake. While the Ocala NF remains mostly undeveloped, urban expansion in Marion County is approaching the southwestern and western edges of the Forest. The study area was defined by delineating estimated ground-water flow divides of the UFA around Lake County and the Ocala NF where possible (fig. 2). Specified-head boundaries were used to define the ground-water model study area in the southeastern section across northern Osceola and western Orange Counties, and in the southwestern section across western Sumter and southwestern Marion Counties. The model boundary is described in detail later in this report.

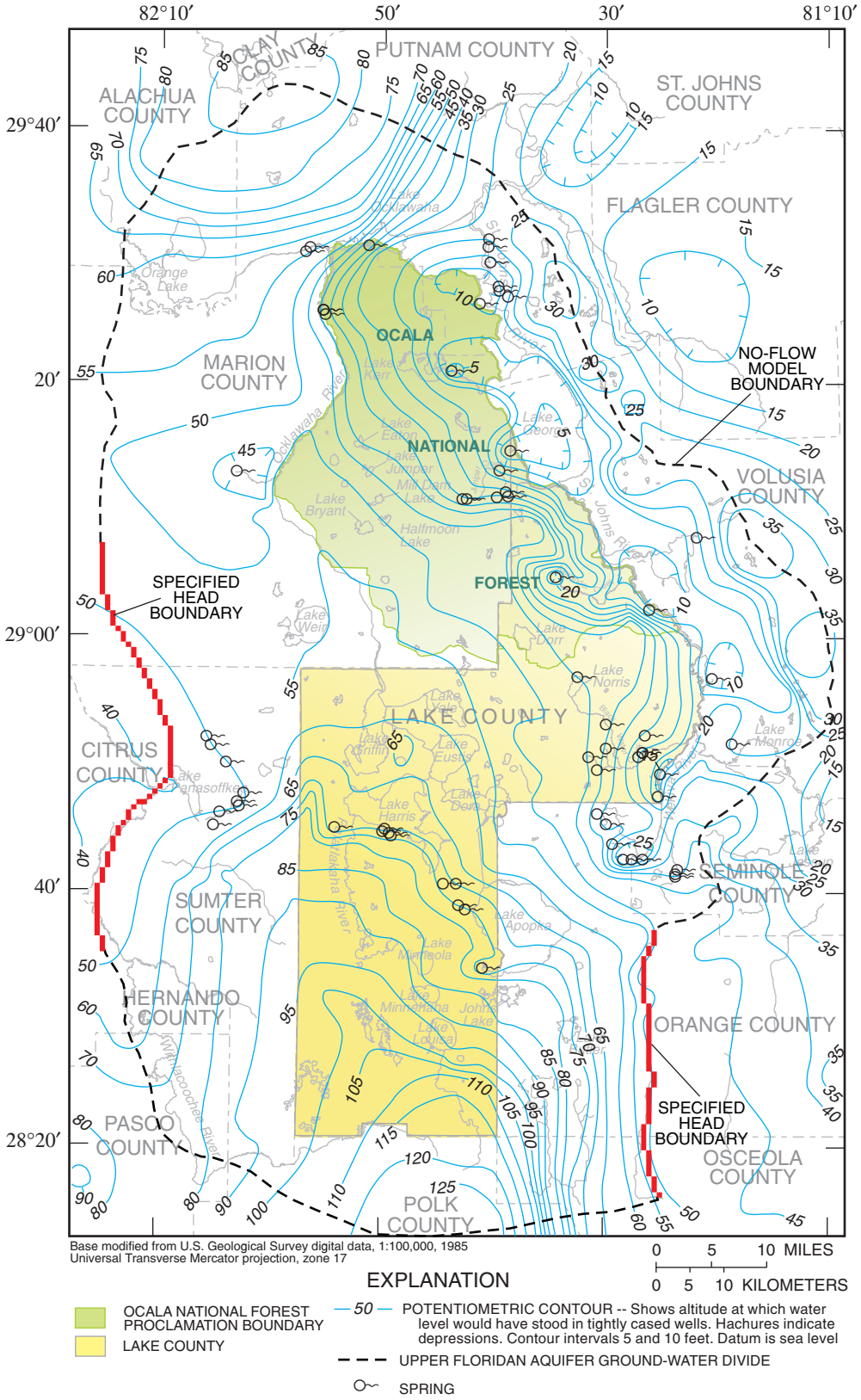

Figure 2. Model boundary delineated using the May 1998 potentiometric surface of the Upper Floridan aquifer (modified from Adamski, 1998).

Physiography

Lake County and the Ocala NF are in the Central Highlands topographic division described by Cooke (1945). Within this division, Puri and Vernon (1964) described 25 landforms, 8 of which occur in Lake County and 4 in the Ocala NF (fig. 3). In general, the landforms are of three basic types: ridges, valleys, and uplands. All of these landforms show strong lineation parallel with the present-day Atlantic Coast, which implies a coastal origin. Land-surface elevations in the study area range from near sea level to more than 300 ft above sea level.

Ridges characterize land areas with the highest altitudes. Two of these ridge systems—the Mount Dora Ridge and Lake Wales Ridge—extend into and across Lake County and the Ocala NF. These ridges are a series of gently rolling hills that trend northwest-southeast and include up to 200 ft or more of surficial sands. The Lake Wales Ridge is, in general, the higher of the two, with hilltop elevations ranging from 200 to more than 300 ft above sea level. The highest point in peninsular Florida is Sugarloaf Mountain (312 ft) located at the northern end of the Lake Wales Ridge west of Lake Apopka in Lake County (fig. 3). Ridges also are characterized by closed-basin lakes, water-table depths greater than 100 ft, and subsurface drainage, but surface-drainage features generally are absent. The Mount Dora Ridge contains some of the highest-altitude lakes in peninsular Florida.

The Central Valley, a second common landform, terminates the northern end of the Lake Wales Ridge and offsets the ridge from the Mount Dora Ridge to the east. The Central Valley is characterized by large lakes (the Ocklawaha chain), flat terrain, and relatively high surface runoff. In the Central Valley, water levels in SAS wells are at or only a few feet below land surface, and water flows above land surface from many UFA artesian wells.

The third common landform is the upland, of which there are three in the study area: Lake Upland, Marion Upland, and Sumter Upland. Uplands are characterized by moderate land-surface elevations and relief, numerous closed-basin lakes that become connected during high water, shallow lakes, and moderate water-table depths. Drainage from the uplands generally is poor, so that surface water can take as long as many weeks to drain following extended periods of heavy rainfall.

Drainage

Lake County and the Ocala NF are drained by both surface and subsurface drainage systems. Surface drainage mainly is by the Palatlakaha River, Ocklawaha River, and other tributaries to and including the St. Johns River (fig. 1). Small areas in the southwestern and southeastern parts of Lake County are drained by the Withlacoochee River and the headwaters of the Kissimmee River, respectively. Annual surface runoff for the Ocala NF likely is much smaller in comparison to Lake County because drainage generally is poor, and surface runoff to the St. Johns and Ocklawaha Rivers primarily is received by tributaries draining lands surrounding the Ocala NF.

Prior to about 1960, the natural surface-drainage system generally was not well developed and stream channels existed only as high-water connectors between lakes or wetlands. During the 1960's, many channels were deepened and improved to facilitate drainage as the area developed. Flow through the Ocklawaha chain-of-lakes is regulated by control structures.

The St. Johns River, Wekiva River, and Black Water Creek drain the northeastern part of Lake County (fig. 1). Black Water Creek flows southeast to its confluence with the Wekiva River, which then flows northeast to the St. Johns River. Black Water Creek and the St. Johns River have nearly parallel alignments, but flow in opposite directions. Very little, if any, surface drainage occurs in the high ridge areas as evidenced by the absence of surface-water features. Rather, nearly all of the precipitation infiltrates to the SAS or directly to the UFA, or is lost by evapotranspiration (ET).

The Ocklawaha River, Alexander Creek, and Juniper Creek drain the western and eastern parts of the Ocala NF. Most of the flow in these streams is supplied by springs and diffuse ground-water discharge from the UFA, which is controlled by stream stage. High stream stages whether caused by rainfall, tidal influences, or control structures suppress the ground-water contribution to streams. This condition can be observed along Lake Ocklawaha, which is regulated to maintain a water level approximately 15-20 ft above the natural stream stage. Discharge from submerged springs in Lake Ocklawaha increased by a magnitude of 10 or more when the regulated stage was lowered by approximately 9 ft during the winter of 1998-99, based on measurements made by the USGS.

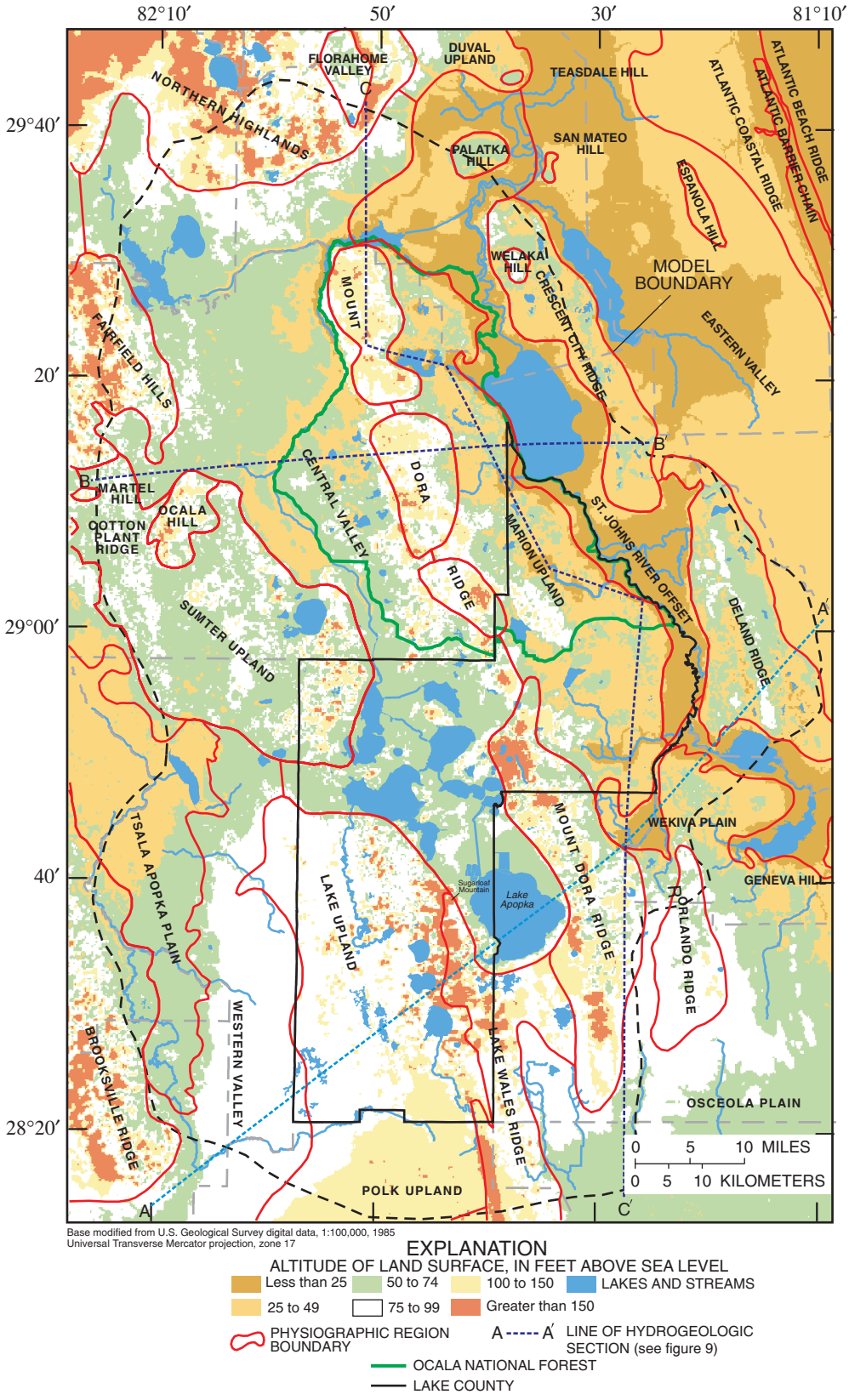

Figure 3. Topography, physiographic regions (modified from White, 1970), and locations of hydrogeologic sections.

A substantial amount of ground water discharges from the UFA as springs and seeps (65 of which are identified in this report). Most springs are located along or near the Ocklawaha, St. Johns, and Wekiva Rivers, but a few small springs are located in central Lake County on the south shore of Lake Harris and extending to the west shore of Lake Apopka. Silver Springs, the largest spring in the study area and located just west of the Ocala NF, near the city of Ocala, has an annual mean flow of 788 cubic feet per second (ft^3/s) for 1932-2000. Other springs, with average discharges greater than 100 ft^3/s, include Blue, Silver Glen, and Alexander Springs (fig.1).

From the early 1900's to the 1960's, drainage wells were drilled into the UFA, particularly in the city of Ocala and in western Orange County. Some drainage wells were drilled in partially plugged sinkholes or excavated retention ponds to augment the natural internal drainage as storm runoff increased with urban expansion. Others were drilled near lakes to control lake stages and prevent flooding of roads or residential areas. Many drainage wells have been plugged and are no longer in use. State regulations now prohibit the drilling of any additional drainage wells.

Climate

Climate in the study area is subtropical and typically characterized by warm and humid, rainy summers and temperate, dry winters. Summer daily maximum air temperatures typically exceed 90 degrees Fahrenheit (^oF), and occasionally exceed 100 ^oF. Winter daily minimum air temperatures generally are mild with occasional freezes, mainly from December to March each year. The mean annual air temperatures at Ocala and Clermont are 70.8 ^oF and 72.0 ^oF, respectively, for 1971-2000 (National Oceanic and Atmospheric Administration, 1935-99 and 2000). Mean monthly air temperatures range from 58.1 ^oF and 59.8 ^oF at Ocala and Clermont, respectively, in January to 81.7 ^oF at Ocala in July and 81.7 ^oF at Clermont in July and August. Mean annual precipitation at Ocala and Clermont is about 50 inches (in.) for 1971-00 with 50-55 percent typically falling during the summer.

Substantial rainfall events generally are associated with diurnal summer thunderstorms, summer or autumn tropical systems, and wet autumn, winter, or spring frontal systems (Winsberg, 1990). Typically, the frequency of high-intensity thunderstorms increases each year during late May and early June, peaking in July and August before becoming less frequent after early October. April and November typically are the driest months. Patterns of temperature and rainfall, however, vary within the study area and are influenced by large lakes that are slower in response to change in temperature than the surrounding land areas. Tropical systems can affect the study area during the summer and generate copious amounts of rainfall, which provides significant ground-water recharge. Occasionally, tropical systems affecting the area extend well into autumn. Rains associated with tropical and wet frontal systems generally are more widespread than those associated with summer thunderstorms. Recharge to the ground-water system can be substantial during wet winter months especially because evapotranspiration (ET) and pumping rates are at their annual minimum (Knowles, 1996, and R. Marella, U.S. Geological Survey, 1999, oral commun.).

Land and Water Use

Land use in Lake County in 1998 consisted of agriculture (30 percent), predominantly citrus and plant nurseries; National/State Forests and preserves (18 percent); rangeland (7 percent); urban (7 percent); open water and wetlands (36 percent); and some localized sand, rock, and peat mining (2 percent). From 1977 to 1994, agricultural land use declined from about 43 to 30 percent with freeze-killed citrus groves being replaced mostly by urban development.

USFS land covers about 89 percent of the area within the Proclamation Boundary of the Ocala NF and includes several recreation sites, transportation corridors, and lands designated for other special uses (Richard B. Shellfer, U.S. Department of Agriculture, Forest Service, 1999, oral commun.). The communities of Astor, Paisley, Lynne, and Salt Springs are located along or within the Boundary. Of the Ocala NF, 63 percent is designated as land suitable for timber management or harvest, 11 percent is private residential, 6.5 percent is wilderness, about 1 percent is for U.S. Navy bombing practice, and less than 1 percent is recreational sites. The remaining 18 percent is used as transportation corridors and access roads (2,300 mi). Although mining currently is not practiced in the Ocala NF, a few small claypits are used for road maintenance within the forest area.

Ground water withdrawn from the FAS in Lake County is used for numerous purposes (fig. 4). In 1998, Lake County pumped about 115 Mgal/d (110 Mgal/d from the UFA and 5 Mgal/d from the LFA)—less than 48 percent for agricultural use; about

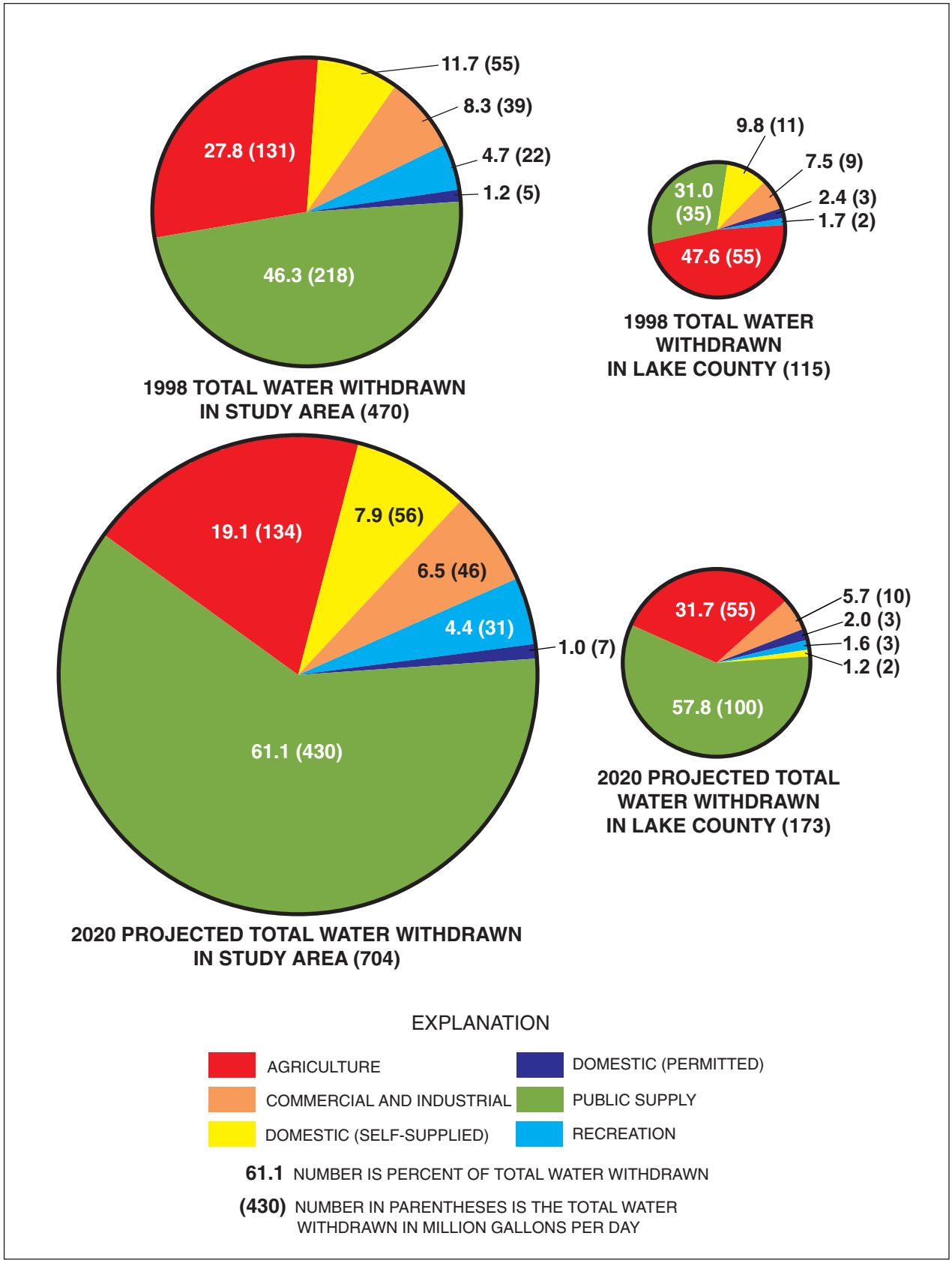

Figure 4. Distribution of water withdrawals from the Floridan aquifer system.

45 percent for municipal, domestic, and recreation use; and more than 7 percent for commercial or industrial use. Domestic water use is subdivided into subcategories: self-suppled and permitted. Self-supplied water use generally consists of water withdrawn from private (homeowner) wells with casings 4 inches or less in diameter. Permitted water use consists of larger private and community wells with casings 6 inches or larger in diameter. Total water pumped in Lake County is projected to be 173 Mgal/d (162 Mgal/d from the UFA and 11 Mgal/d from the LFA) by 2020—less than 63 percent municipal, domestic, and recreation; about 32 percent agriculture; and less than 6 percent commercial or industrial (Brian McGurk, St. Johns River Water Management District, 1999, written commun.). Currently, about 15 percent of all water pumped from the UFA in Lake County is returned to the ground-water system as artificial recharge by land application, mostly in the southeastern and central areas of the County; and by septic systems distributed throughout the county (Richard Marella, U.S. Geological Survey, 1999, oral commun.).

Nearly all water withdrawn in the Ocala NF is from the UFA and is used for domestic and recreation purposes at scattered communities, recreation sites, and private residences. In 1998, water use totaled 5.7 Mgal/d, with about 60 percent being returned as artificial recharge to the ground-water system by septic systems (Richard Marella, U.S. Geological Survey, 1999, oral commun.), mainly in communities and at recreation sites in the Ocala NF. Additional analysis of 1998 water-use data since the publication of Adamski and Knowles (2001) resulted in an updated value (from about 2 Mgal/d to about 5.7 Mgal/d) for water use in the Ocala NF. The magnitude and type of water use in the Ocala NF is not expected to change significantly by 2020.

Data-Collection Network

Data-collection sites were inventoried based on a review of existing data in the study area. Additional sites were added to define better the characteristics of the hydrologic system and the relation between water levels in the SAS and the potentiometric surface of the UFA. Data include rainfall; stream stage and discharge; lake stage; and ground-water levels (figs. 5, 6, and 7; app. A, B, and C). Additional hydrologic, lithologic, and water-use data were acquired from the USGS, SJRWMD, LCWA, USFS, SWFWMD, SFWMD, Lake County Water Resources Management, Florida Geological Survey, and National Oceanic and Atmospheric Administration (NOAA) computer and paper files.

The lake and ground-water monitoring network (figs. 6 and 7; apps. B and C) includes existing sites measured by the USGS, SJRWMD, or SWFWMD; 10 new lake staff gages (6 in the Ocala NF and 4 in Lake County); 27 new wells tapping the SAS (12 each in Lake County and the Ocala NF, and 3 in the overlap area); and 1 new well tapping the UFA in the Ocala NF. Several of the new SAS wells were constructed adjacent to UFA wells to determine the local head difference between the aquifers. Synoptic water-level data were collected bi-monthly during the 16-month period, September 1997 to December 1998, to provide "instantaneous" measurements. Continuous water-level recorders were installed at two of the paired-well sites.

More than 1,300 lithologic, geophysical, and geological logs were analyzed to determine the stratigraphy and lithology of the SAS, the intermediate confining unit (ICU), and the FAS in the study area. Four additional UFA wells were logged and core samples were collected from 35 SAS wells and boreholes drilled during the study. Altitudes and thicknesses of lithologic units and control points interpreted from these logs were interpolated using a minimum curvature method to construct generalized lithologic maps of the study area.

HYDROGEOLOGY

The principal water-bearing units in the study area, the SAS and FAS (fig. 8), are separated by the ICU, which contains beds of lower permeability that confine the FAS. The FAS has two major water-bearing zones, the UFA and the Lower Floridan aquifer (LFA), which generally are separated by the less permeable middle semiconfining unit (MSCU) or the middle confining unit (MCU). Underlying the FAS is the sub-Floridan confining unit, which contains low-permeability limestone, dolomite, and anhydrite. The bottom of the freshwater flow system is defined either by the sub-Floridan confining unit or the depth at which the chloride concentration of the water is greater than 5,000 milligrams per liter (mg/L) in the FAS, whichever is shallower. Generalized hydrogeologic sections based on well logs are shown in figure 9.

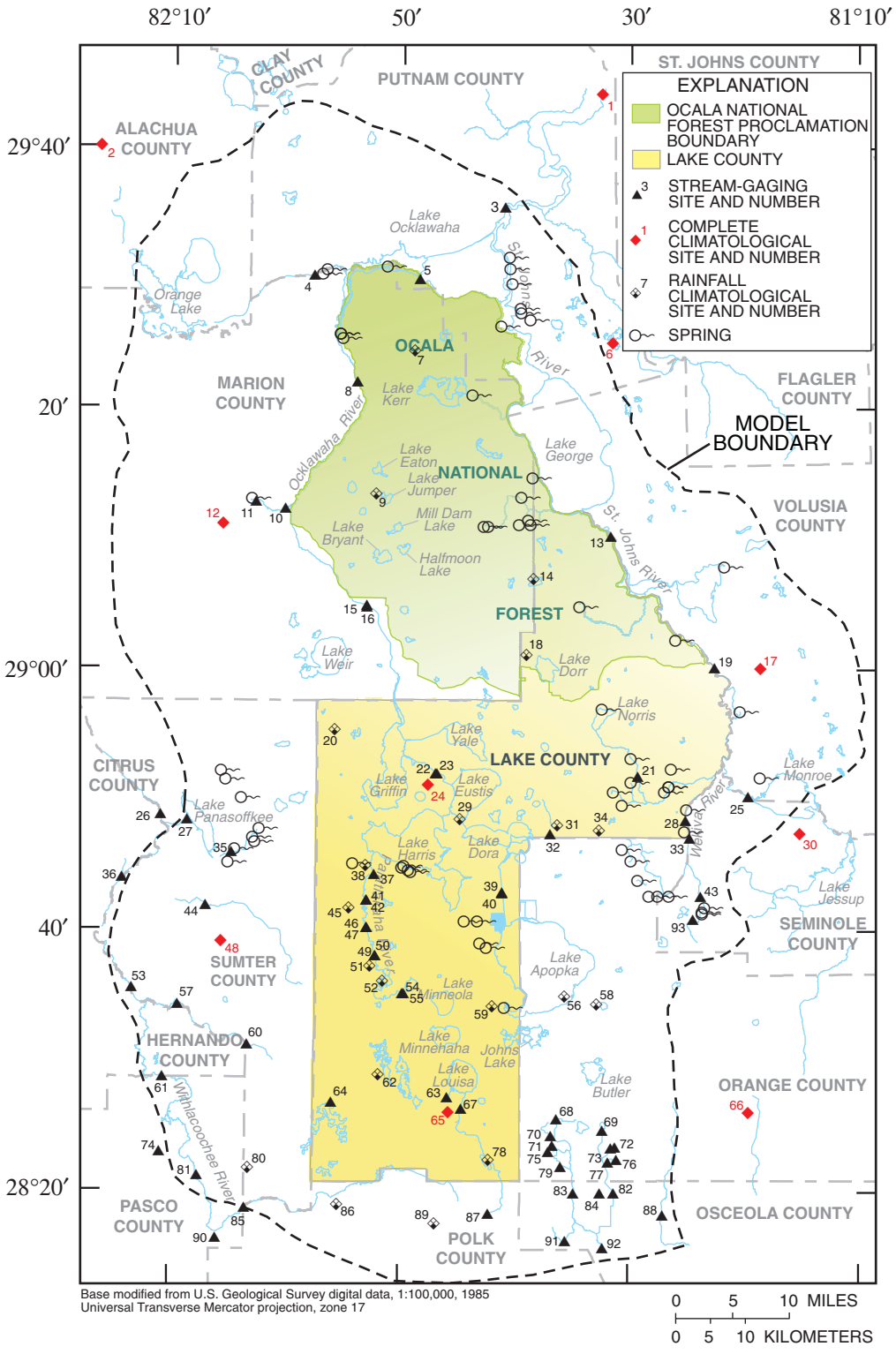

Figure 5. Locations of stream-gaging and climatological data-collection sites (numbers refer to appendix A).

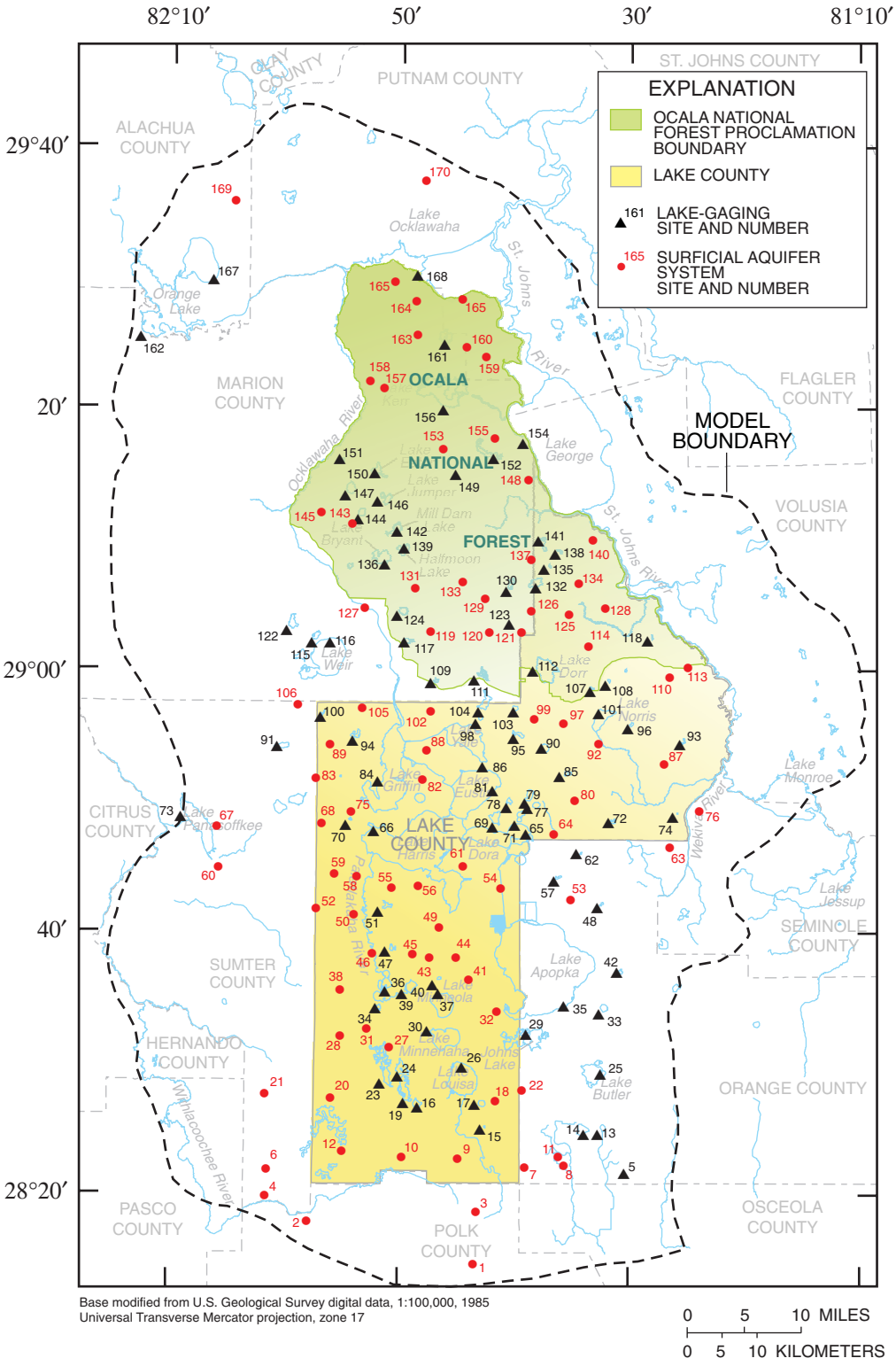

Figure 6. Locations of lake-gaging and surficial aquifer system well data-collection sites (numbers refer to appendix B).

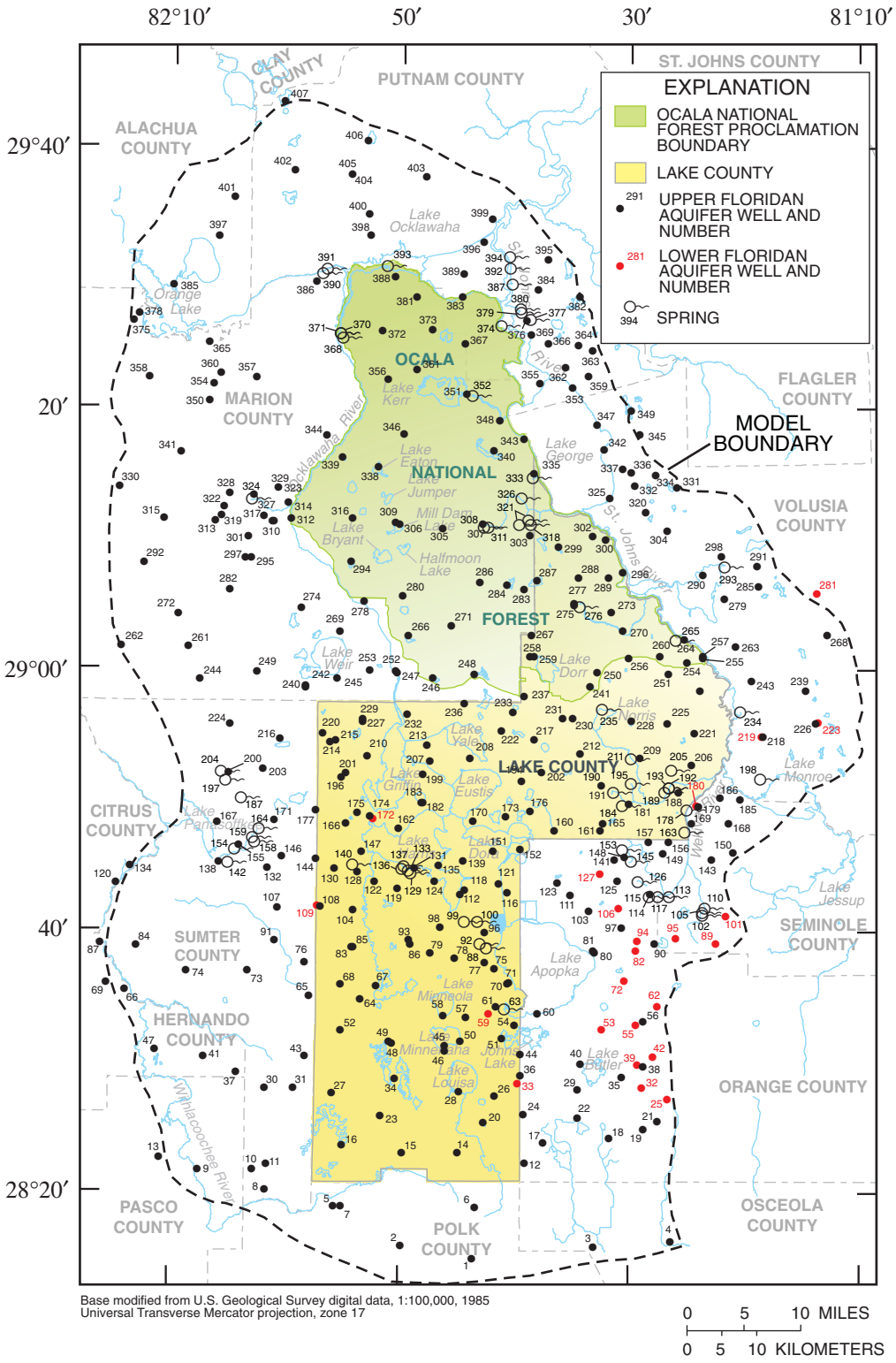

Figure 7. Locations of springs and Floridan aquifer system well sites (numbers refer to appendix C).

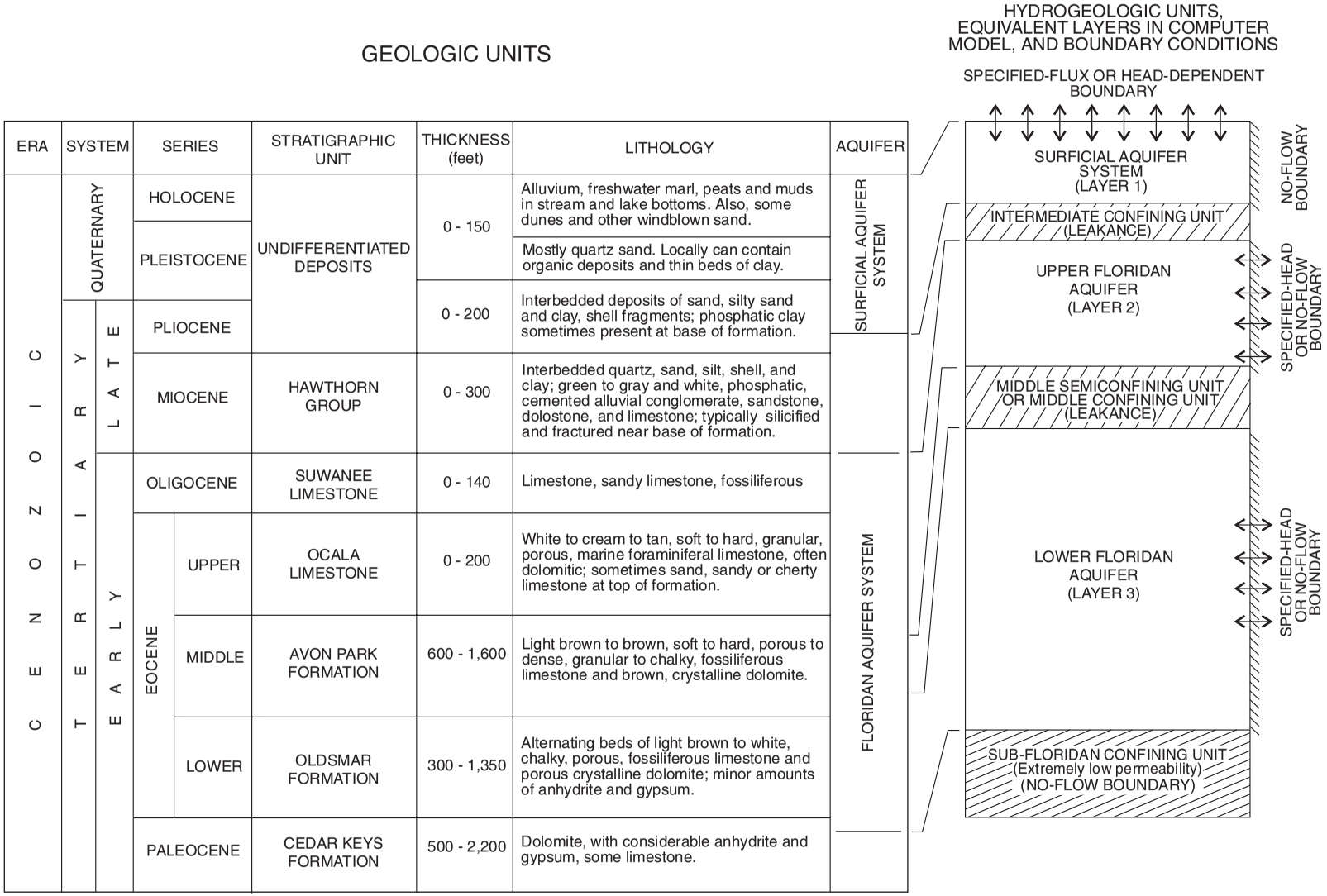

Figure 8. Geologic units, hydrogeologic units, and equivalent layers and boundary conditions used in the ground-water flow model.

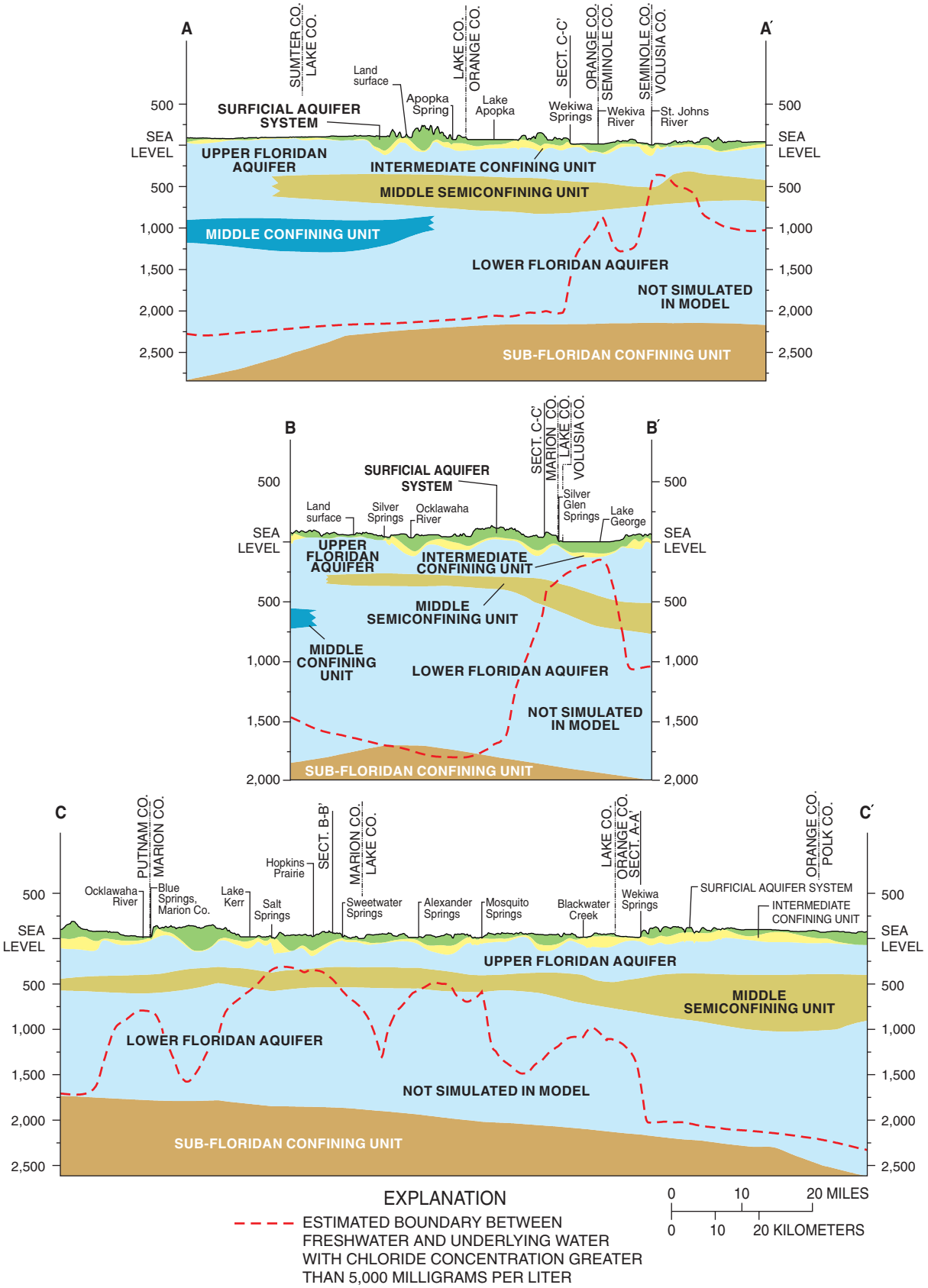

Figure 9. Hydrogeologic sections A-A', B-B', and C-C' (locations of sections shown in fig. 3).

Stratigraphy

The Florida Plateau is a large, tectonically stable carbonate platform that has accumulated thick deposits of Paleocene and Eocene limestones, dolomites, some evaporites, and a comparatively thin post-Eocene sequence of sand and clay (Faulkner, 1973). These sedimentary deposits overlie the post-Paleozoic Coastal Plain Floor and are about 4,000 ft thick, of which 1,500 to 2,500 ft are pre-Tertiary in age and the remainder is Tertiary and younger (fig. 8). Oligocene-age and older sediments were deposited while most of the carbonate platform was submerged in a shallow sea environment. Evaporites were deposited in shallow, land-locked marine basins on emergent areas of the platform during lower sea-level stands.

The basal Tertiary unit is the Cedar Keys Formation of late Paleocene age. The Cedar Keys Formation generally has extremely low permeability and thus functions as the sub-Floridan confining unit at the base of the FAS. Conformably overlying the Cedar Keys are about 600-800 ft of the lower Eocene Oldsmar Formation, composed mostly of limestone with some interbedded dolomite and minor amounts of evaporites, anhydrite, and gypsum (fig. 8). The Avon Park Formation, a thick sequence of marine limestone and dolomite, conformably overlies the Oldsmar Formation and is characterized by alternating layers of soft to hard, fossilferous brown, crystalline dolomite and light-brown to tan limestone (fig. 8). The Avon Park Formation typically is highly fractured and vugular.

An erosional unconformity separates the Avon Park Formation from the overlying Ocala Limestone of late Eocene age. The Ocala Limestone has eroded entirely in some parts of Marion County and southwestern Lake County. In these areas, the Avon Park Formation is present at or relatively near land surface (less than 50-ft depth); however, in other parts of the study area, the top of the Ocala Limestone ranges from near land surface to more than 250 ft below land surface. The Ocala Limestone is composed of white to cream or tan limestone, which usually is fossilferous and soft to hard (fig. 8). Geologists' logs indicate that some Ocala Limestone contains chert, either as irregular masses, thin layers, or localized caps. Differential erosion of the limestone surface has caused the formation of pinnacles and a wide variation in the altitude of the surface of the limestone, resulting in a mature karst terrain featuring rolling hills and numerous sinkhole depressions. Overlying the Ocala Limestone in some parts of Florida is the Suwannee Limestone of Oligocene age. The Suwannee Limestone has undergone extensive erosion and is present only in the southwestern part of the study area (Miller, 1986).

The Hawthorn Group of Miocene age unconformably overlies the Ocala Limestone and, where present, ranges in thickness from less than 5 ft to 150 ft (fig. 8). The thickest units are associated with fill deposits in paleosinks that typically are not expressed at the surface. The Hawthorn Group consists mostly of marine sand interbedded with clay, sandy phosphatic clay, cemented alluvial conglomerate, and in some places, basal units of hard dense or fractured limestone or dolomite. In much of western Marion and southwestern Volusia Counties, much of the sediments of the Hawthorn Group have eroded and the remaining deposits commonly cap the hilltops. Elsewhere in the study area, the Hawthorn Group is more continuous.

Overlying the Hawthorn Group across much of the study area is a variety of mostly siliclastic sediments of Pliocene to Holocene age that range in thickness from 0 to 200 ft (fig. 8). Undifferentiated Pliocene to Holocene sediments that overlie the Hawthorn Group typically include phosphatic, nonmarine clayey sands, marine and lacustrine sand, shell marl, and sandy clay. Thin beds of Pleistocene clays on the Mount Dora Ridge (fig. 3) locally support lakes and small water-filled sinks.

Structure

The carbonate rocks of the Florida Plateau were deposited in shallow transgressive and regressive seas over the southeastward-plunging Peninsula Arch, which probably originated during the late Paleozoic or early Mesozoic Era when crustal stresses caused a gentle upward warping of the Coastal Plain Floor (Faulkner, 1973). The Peninsular Arch is the primary structural control for sediments deposited during Mesozioc and early Eocene time (Faulkner, 1973, p. 24). The axis of the subsurface arch trends northwest to southeast through the Ocala NF in eastern Marion County, northeastern Lake County, northwestern Orange County, and southwestern Volusia County. During middle-late Eocene time, the Ocala Uplift formed in western Marion and Sumter Counties, approximately parallel to the trend of the Peninsula Arch. As the Ocala Uplift developed, tensional stresses caused a series of extensive vertical and lateral

fracture systems in the rock strata at the top and along the sides of the Uplift. Many of these fractures that border the Ocala NF to the north and west have vertical displacements of up to 100 ft or more (Faulkner, 1973, p. 40).

Numerous cavern systems exist in the Ocala Limestone, most of which are oriented along fracture systems of the Ocala Uplift. Flow of acidic water through the fracture systems resulted in further dissolution of the rock surrounding the original fractures, increasing the size and innerconnection of the fractures. Millions of years ago, extensive cavern systems were formed when the Ocala Limestone was closer to the land surface. Presently, the same processes are still occurring.

The fracture system also influenced the locations of the Ocklawaha River, Silver Springs, and many springs in the St. Johns River Basin (fig. 1). Faulkner (1973) concluded that the Lower Ocklawaha River valley and the area to the east of it have been structurally lowered. As a result, low-permeability sediments of the Hawthorn Group are present east of the river, but have been eroded from the higher areas of the Mount Dora Ridge. The apparent relative downward displacement of the sediments east of the river resulted in these low-permeability beds of the Hawthorn Group blocking eastward flow of ground water in the underlying limestone (fig. 9, sections A-A' and B-B'). As a result, ground water is forced upward and has surfaced in this region at what is now Silver Springs (Faulkner, 1973). Highly interconnected secondary porosity has developed in the UFA (Ocala Limestone) in and around these springs, where transmissivity values locally can be on the order of 10^6 feet squared per day (ft^2/d) (Tibbals, 1990). Other first-magnitude springs located near the St. Johns River and smaller springs in Lake Ocklawaha probably developed by similar processes.

Surficial Aquifer System

The SAS is the uppermost, unconfined water-bearing unit in the study area and is composed principally of fine- to coarse-grained quartz sand, silt, and interbedded clay, peat, marl, and shell. These deposits generally are discontinuous, and the lithology and texture of the deposits can vary considerably locally both vertically and laterally. The upper 5-15 ft of the unit consist predominately of fine-grained, well-sorted sand of Holocene age overlying Pleistocene-age sediments, which range from 0 to 150 ft thick. For purposes of this study, the base of the SAS was defined by the first occurrence of persistent beds of Pliocene or Miocene age containing at least 50 percent silt, clay, limestone, or dolomite. In the study area, the altitude of the base of the SAS generally ranges from 200 ft below to greater than 100 ft above sea level (fig. 10). Thickness of the SAS is highly variable and ranges from 0 ft (SAS absent) in parts of the Lake Upland, Sumter Upland, and the DeLand Ridge to nearly 300 ft in parts of the Central Valley, Mount Dora and Lake Wales Ridges, and the Marion Upland (figs. 3 and 10). Along the St. Johns and Wekiva Rivers, the SAS generally is 10-20 ft thick. Elsewhere, the thickness of the SAS generally is about 50-60 ft thick.

The vertical hydraulic conductivity of samples from the SAS reported by Knochenmus and Hughes (1976) was found to be highly variable and ranged from 0.03 to 160 feet per day (ft/d). In some areas, discontinuous and relatively low-permeability beds of reddish-brown to gray hardpan are present within a few feet of the land surface. These layers of hardpan are composed of slightly to well-indurated, organic, iron-oxide cemented sand and clay.

The unconfined SAS serves as a filter bed and reservoir for storing precipitation that eventually recharges the underlying FAS. However, the SAS has little potential as a major source of ground water compared to the FAS, although wells completed in the Pleistocene-age sands are pumped for irrigation and mining in some areas along the Mount Dora Ridge.

The upper boundary of the SAS is defined by the water table. In swampy lowlands and flatlands, the water table generally is at or near land surface throughout most of the year. Generally, the water table follows the shape of land-surface topography in a subdued manner, but can be as much as 150 ft or more below land surface in some areas. In addition to the influence of topography, the slope of the water table varies depending on hydrologic conditions, such as rainfall and ET rates; subsurface drainage to lakes and streams; and vertical leakage of water to the UFA. During wet periods when infiltration exceeds ET, the slope of the water table towards lakes or streams steepens as the storage of water in the SAS increases. During dry periods, the slope flattens as water drains from storage and is lost to ET or to seepage to lakes or streams.

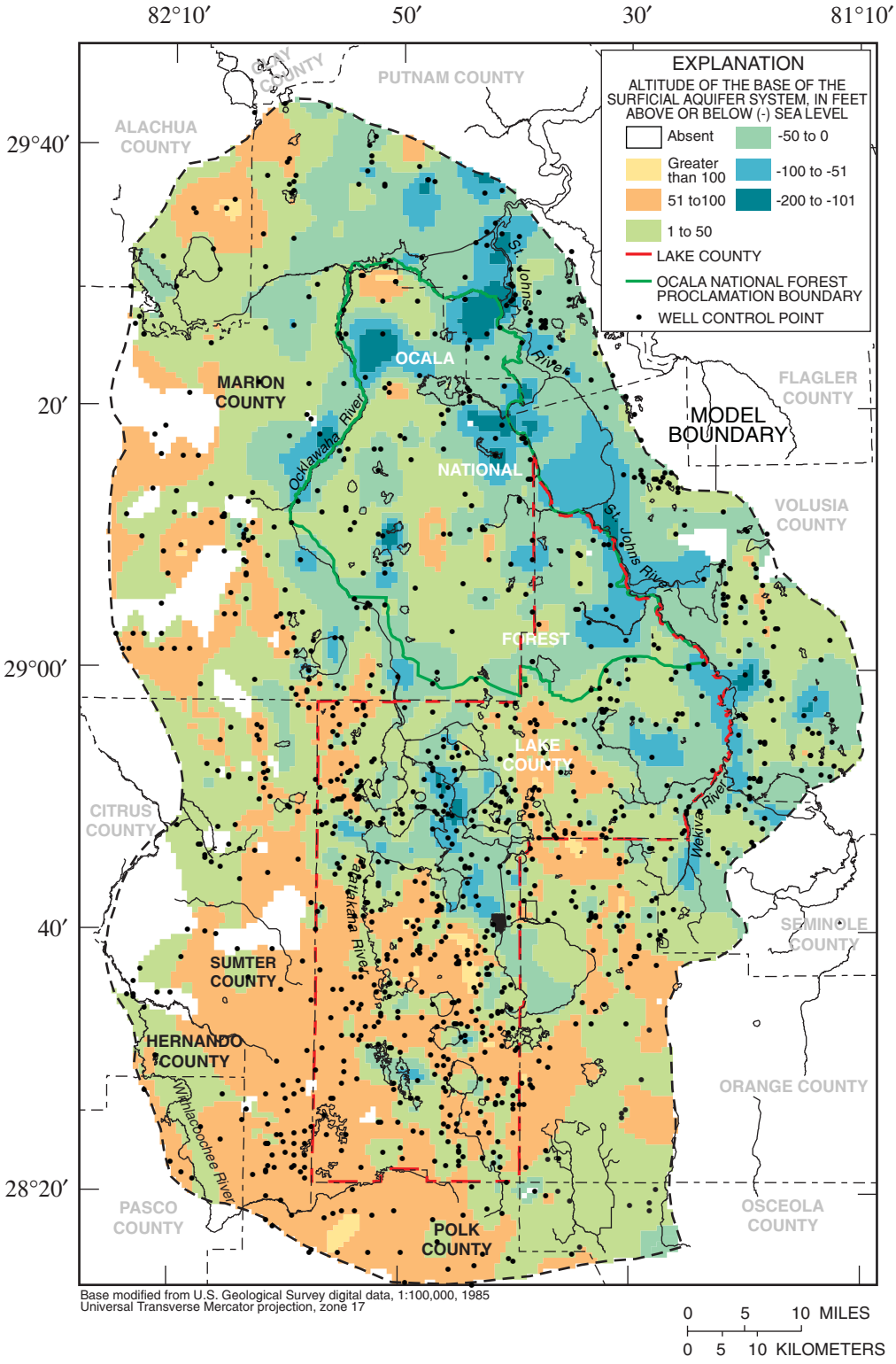

Figure 10. Generalized altitude of the base of the surficial aquifer system.

The water-bearing properties of the SAS vary considerably across the study area and depend largely upon aquifer thickness, lithology, grain-size distribution, sorting, packing, and cementation of the sediments within the aquifer. Horizontal hydraulic conductivity values of the SAS were determined from slug tests performed on 30 SAS wells in Lake County and the Ocala NF. The values ranged from 0.2 to 35 ft/d, having a geometric mean of 8 ft/d, with the highest values in areas of the Mount Dora Ridge, Lake Wales Ridge, and Marion Upland. These values are in agreement with results of 21 slug tests from Seminole County, where horizontal hydraulic conductivity of the SAS ranged from 0.5 to 40 ft/d with a geometric mean of 8 ft/d (Spechler and Halford, 2001). CH2MHill (1989) reported horizontal hydraulic conductivity of the SAS ranged from 25 to 160 ft/d based on slug tests conducted in the Lake Wales Ridge in extreme southwestern Orange County.

Intermediate Confining Unit

The ICU, which underlies the SAS, generally consists of the Hawthorn Group of late-to-middle Miocene age and, locally, low-permeability beds of Pliocene age. Throughout most of the study area, the ICU serves as a confining layer (except where breached by sinkholes) that restricts the vertical movement of water between the overlying SAS and the underlying UFA. The unit is composed principally of an interbedded mixture of marine sediments including locally highly phosphatic sand and pebbles, clay and limestone; montmorillonitic clay and shell; and basal lenses of sandy, dolomitic, phosphatic limestone. Lower zones of the ICU, which are composed of shell or high-permeability carbonate rocks, can yield a limited supply of potable water. Some basal units of the Hawthorn Group consist of high-permeability carbonate rocks that generally are not in direct hydraulic connection with the UFA in the study area, except locally where these rocks are highly fractured. The base of the ICU, interpreted from well logs, is defined where the downward occurrence of phosphatic sediments is absent.

The thickness of the ICU typically is considered to be the thickness of the Hawthorn Group. However in some areas, particularly in western Volusia and northern Marion Counties, the upper part of the ICU includes mostly Hawthorn-Group phosphatic sands, so that the actual confining part of the unit is thinner than the total thickness of the Hawthorn Group. In many areas, low-permeability Pliocene clays and silts overlie the Hawthorn Group. Therefore, the thickness of the ICU as defined in this report will refer to the sediments that collectively confine the FAS, which includes all or part of the Hawthorn Group and part or none of the overlying Pliocene-age sediments.

Well logs indicate that the ICU ranges in thickness from 0 (where the UFA is unconfined) to 150 ft thick in the study area (fig. 11). Locally, the unit can be thin or absent, especially across parts of Sumter and western Marion Counties, along the northern extension of the Mount Dora Ridge, and in parts of western Volusia County east of the St. Johns River. The ICU is thickest in the Central Valley, the Lake Upland, the southern extension of the Mount Dora Ridge, and the St. Johns River Offset (figs. 3 and 11). The vertical hydraulic conductivity of the ICU is highly variable across the study area, ranging from 0.01 to 0.53 ft/d (Knochenmus and Hughes, 1976). Tibbals (1990) reported leakance values ranging from $1x10^{-6}$ to $6x10^{-4}$ feet per day per foot ((ft/d)/ft). The diverse lithology and range of hydraulic conductivity values of the ICU reflects the variety of depositional environments that occurred during the Pliocene and Miocene Epochs.

Floridan Aquifer System

The FAS is a thick sequence of carbonate rocks (limestones, dolomitic limestones, and dolomite) of Eocene to Oligocene age that are generally high in permeability and hydraulically connected in varying degrees. The FAS in the study area ranges in thickness from 900 to 2,000 ft (Miller, 1986, plate 27), and is subdivided on the basis of the vertical occurrence of two zones of relatively high permeability, the UFA and the LFA, which generally are separated by the MSCU or MCU.

The top of the youngest pre-Miocene sediments is considered to be the top of the UFA. The Suwannee Limestone has been removed by past erosional processes in most of the study area (Miller, 1986). The Ocala Limestone also is absent in some areas, particularly in areas of southwestern Lake County and the adjacent counties, as a result of past erosional processes. The top of the UFA in these areas is defined by the dolomitic limestones of the Avon Park Formation. A generalized map of the altitude of the top of the UFA is shown in figure 12. The surface of the UFA is irregular and paleokarstic.

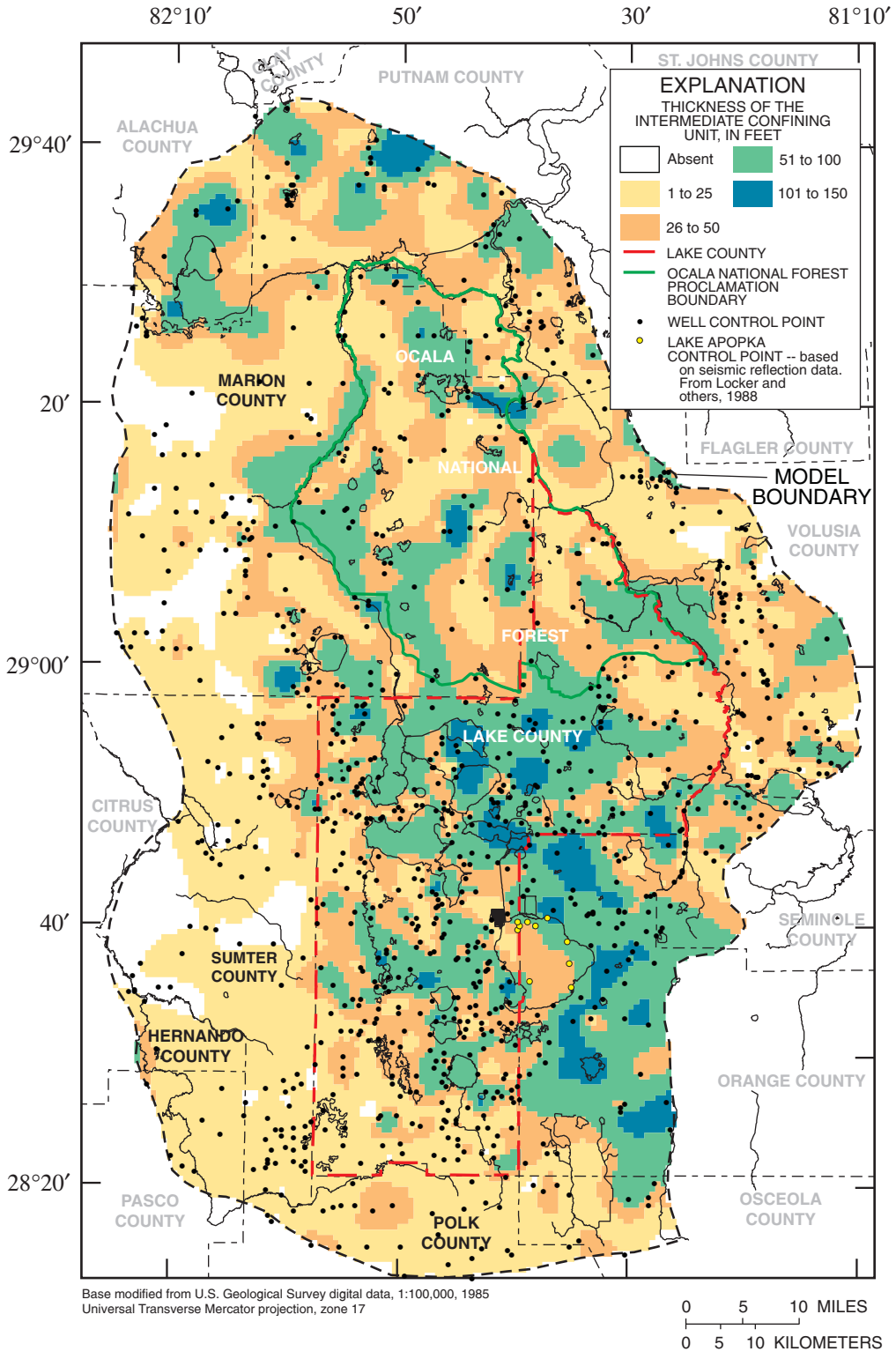

Figure 11. Generalized thickness of the intermediate confining unit.

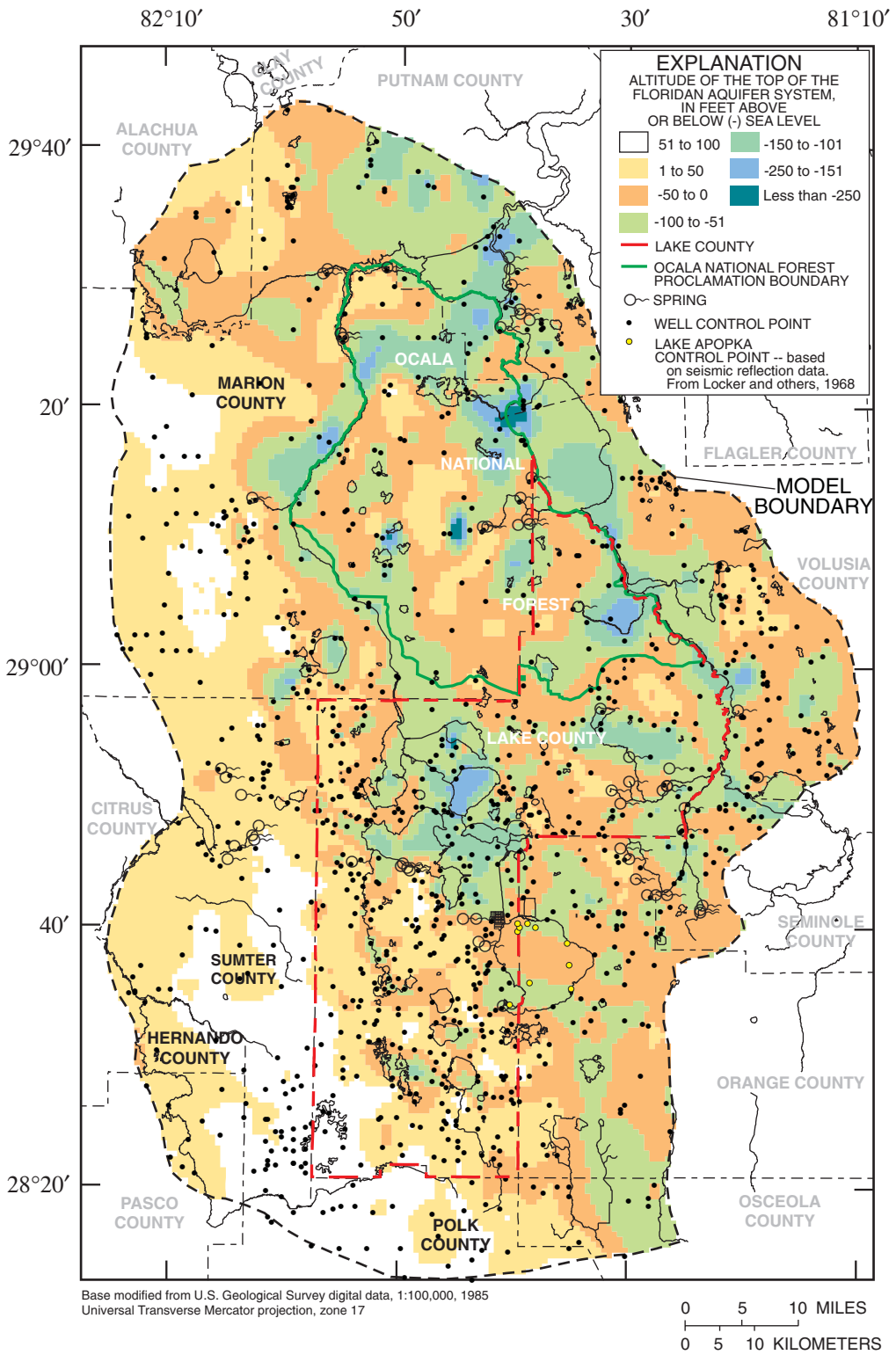

Figure 12. Generalized altitude of the top of the Floridan aquifer system.

The altitude of the UFA ranges from nearly 100 ft above sea level in northwestern Polk County, southern and eastern Sumter County, and in areas of western Marion County to more than 250 ft below sea level southeast of Salt Springs and in north-central Marion County. The top of the UFA is highest along the crest of the Ocala Uplift, which extends through the western part of the study area, and is lowest along large dissolution features and sinkholes in and near the St. Johns and Ocklawaha River basins surrounding the eastern and northern edges of the Ocala NF. As shown in figure 12, the deeply eroded surface of the pre-Miocene carbonate sediments trends northwest-southeast and extends from Osceola County, across western Orange County and central Lake County, then along the Ocklawaha River to the St. Johns River; and also extends along the entire St. Johns River in the study area. Sinkhole-type depressions on the surface of the UFA are common; however, many of these features are small and localized, and are not shown in figure 12. The thickness of the UFA averages about 300 ft through most of the study area, and ranges from 200 ft thick or less in the southwestern part of the Ocala NF and in extreme northwestern Lake County to more than 400 ft thick in the extreme northeastern part of the Ocala NF and southwestern Lake County. The base of the UFA is shown in figure 13.

Throughout most of the study area, the MSCU or MCU separates the UFA and LFA (fig. 8). Miller (1986, p. B56-59) describes the MSCU and MCU as two, separate, distinct units. The MSCU is composed of beds of relatively less permeable limestone and dolomitic limestone and extends across most of the study area (fig. 14). In the western one-third of the study area, the MCU is composed primarily of gypsiferous dolomite and dolomitic limestone, which forms a much less leaky confining unit than the MSCU and functions hydraulically as the base of the freshwater flow system in the FAS in west-central Florida (Tibbals, 1990, p. E14). Because the MSCU and MCU are two distinct units, a discontinuity exists in the base of the UFA along the western edge of the study area (fig. 13). For the purpose of this study, the MSCU and the MCU (or the combined layers where overlapped) are hereafter referred to as the MSCU/MCU.

The MSCU/MCU ranges in thickness from more than 1,000 ft in northern Polk County and extreme southern Lake County to less than 100 ft in west-central Marion and southeastern Alachua Counties where it becomes thin or absent. In Lake County, the thickness of the MSCU/MCU averages about 250 ft across northern parts of the county and about 750 ft across southwestern parts of the county. The MCU is not known to exist in the Ocala NF; the MSCU is fairly uniform in thickness, ranging from about 100 ft along the Ocklawaha River to more than 300 ft in extreme northeastern Lake County.

The LFA, which underlies the MSCU/MCU, includes about the bottom one-third of the Avon Park Formation and all of the Oldsmar Formation. The aquifer is highly productive and is composed of alternating beds of limestone and fractured dolomite. Permeability within this aquifer is related mostly to secondary porosity developed along bedding planes, joints, and fractures (Miller, 1986). The top of the LFA dips from northwest to southeast across the study area with altitudes ranging from 400 ft below sea level in central Marion County and the Ocala NF to more than 1,000 ft below sea level in areas to the south and west of, and including, southern Lake County (Miller, 1986, plate 31). The LFA averages about 1,400 ft in thickness across the study area, ranging from about 1,200 ft in the northern part of the Ocala NF to 1,500 ft or more in western Lake County and much of northern Sumter County. The altitude of the base of the LFA also dips from northwest to southeast and ranges from about 1,500-1,800 ft below sea level in central Marion County to about 2,500 ft below sea level in southwestern Lake County (fig. 15). The base of the LFA is underlain by the sub-Floridan confining unit.

Occurrence of Brackish (or Saline) Water

The northern and eastern parts of Lake County and the Ocala NF (although well inland) contain naturally occurring brackish or moderately saline ground water in the UFA at relatively shallow depths along the St. Johns River and its tributaries. Saline, connate ground water (particularly enriched in chloride and sulfate) moves upward from the LFA into lower parts of the UFA in discharge areas along the lower Wekiva River near the Lake-Seminole County line, in the St. Johns River along the Lake-Marion-Volusia-Putnam County line, across the northern part of the Ocala NF, and along the lower Ocklawaha River, particularly Lake Ocklawaha. Springs in these areas (fig. 7) discharge brackish water mixed with the fresher water circulating in the upper parts of the UFA (Adamski and Knowles, 2001). The approximate depth to water containing 5,000 mg/L chloride concentration in the FAS is shown in figure 16.

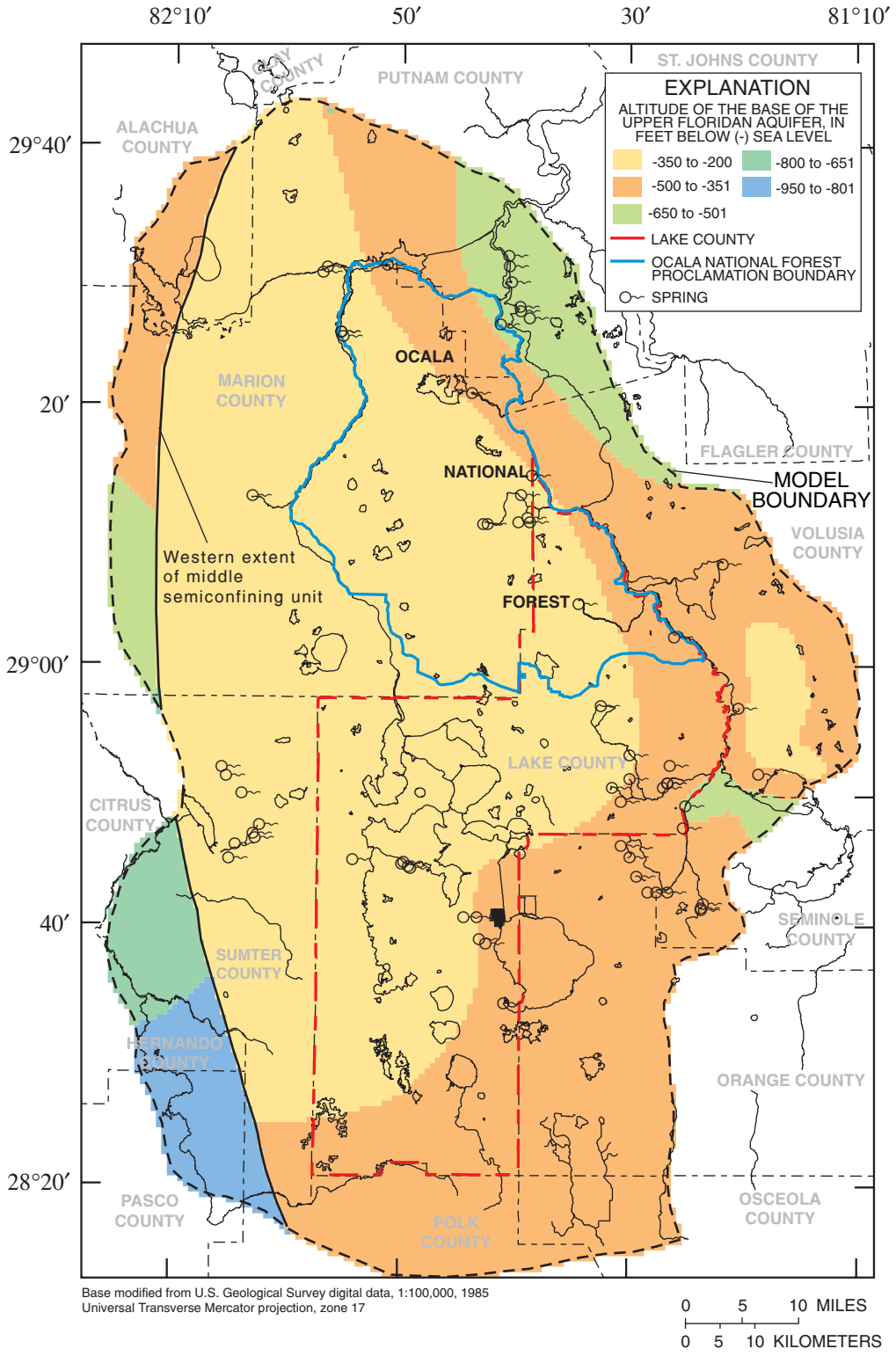

Figure 13. Generalized altitude of the base of the Upper Floridan aquifer (modified from McGurk and Presley, in press; and Miller, 1986).

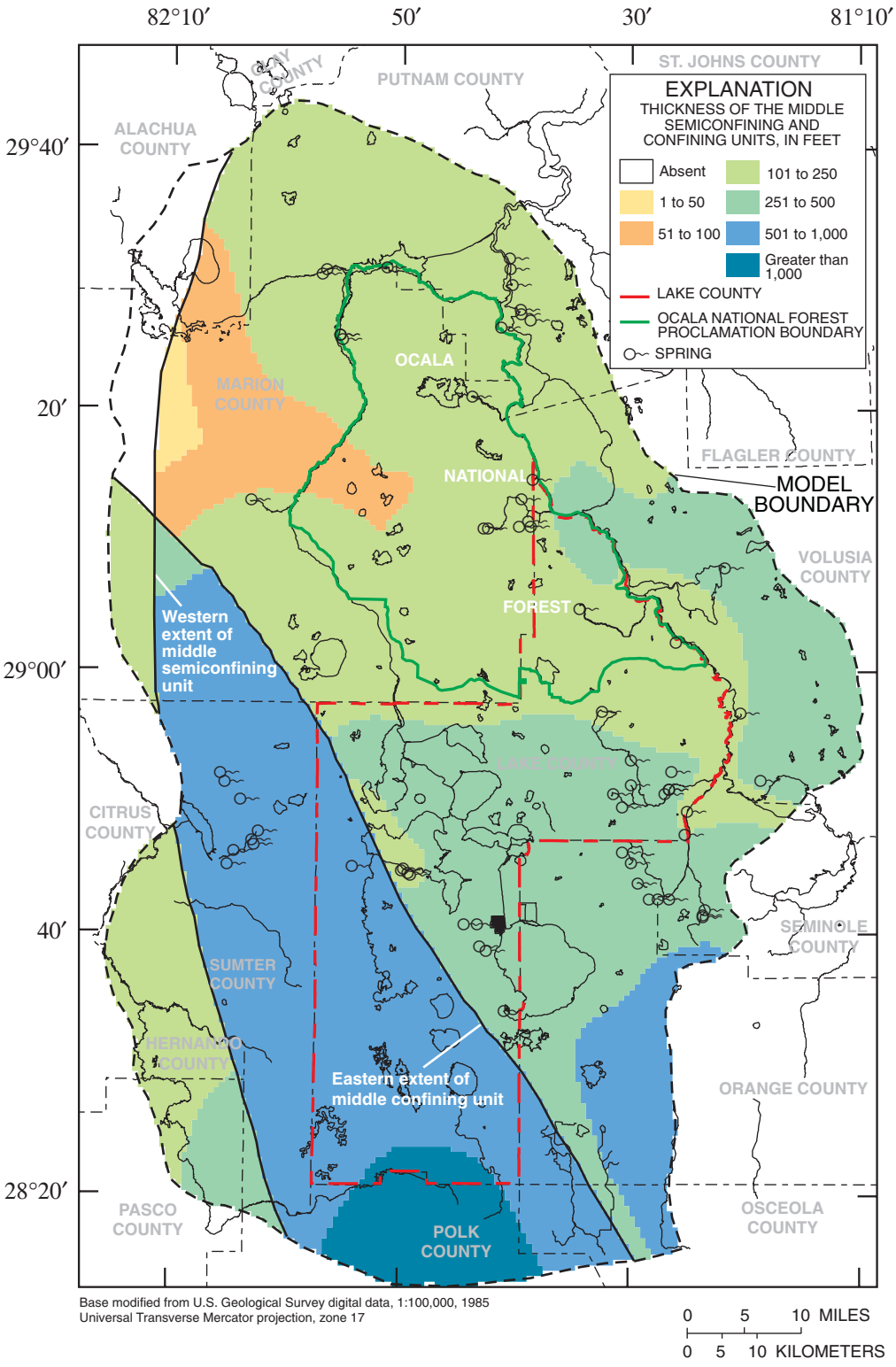

Figure 14. Generalized thickness of the middle semiconfining and confining units (modified from McGurk and Presley, in press; and Miller, 1986).

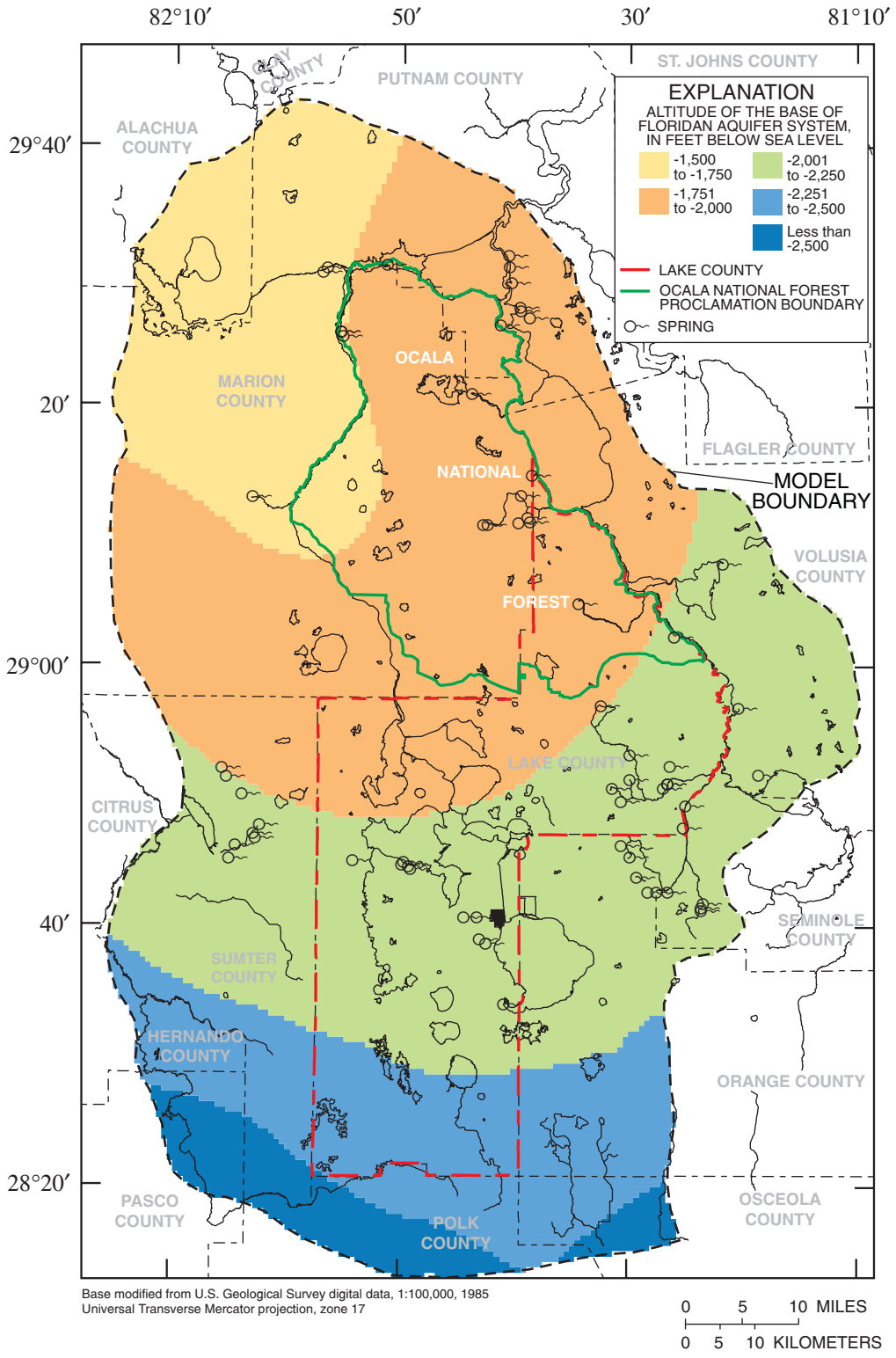

Figure 15. Generalized altitude of the base of the Floridan aquifer system (from Miller, 1986).

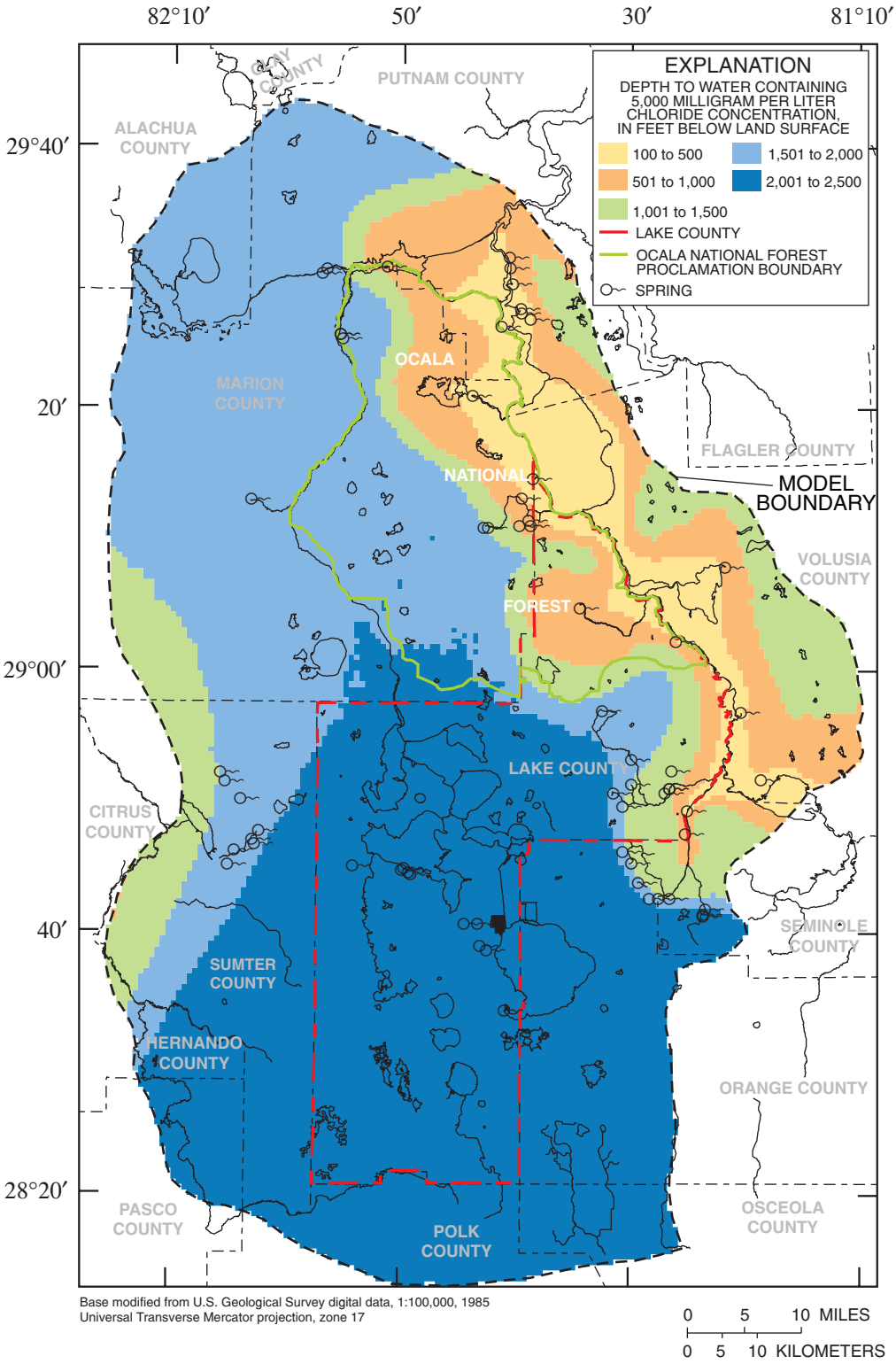

Figure 16. Generalized depth to water containing 5,000 milligram per liter chloride concentration in the Floridan aquifer system (modified from McGurk and others, 1998; and Sprinkle, 1989).

The map is based primarily on chloride-concentration data collected from monitor wells and test drilling in the study area; and to a lesser degree, time domain electromagnetic measurements (TDEM) that were collected in the mid- to late-1980's (McGurk and others, 1998; and Nicasio Sepúlveda, U.S. Geological Survey, 1999, written commun.). The depth to water containing at least 5,000 mg/L chloride concentration ranges from less than 200 ft along the St. Johns River to nearly 2,500 ft below land surface in southern Sumter and Lake Counties. The thickest section of freshwater in the FAS in the study area is located across much of southern and central Lake County, extending into the southwestern part of the Ocala NF.

Hydraulic Characteristics

The transmissivity of the UFA varies widely across the study area and is a function of both primary and secondary porosity. Secondary porosity features that enhance permeability result from dissolution of the limestone aquifer matrix along bedding planes, joints, and fractures, but because of the irregular distribution and innerconnection of such features, transmissivity of the aquifer can vary widely. The transmissivity of the UFA varies throughout the study area and ranges from 3,750 to 2,000,000 ft^2/d, generally increasing northward from Lake County to central Marion County. Pride and others (1966) estimated the transmissivity of the UFA in the Green Swamp area of southern Lake County to be 3,750 to 39,200 ft^2/d. Knochenmus and Hughes (1976) estimated that the transmissivity of the UFA averages about 40,000 ft^2/d in Lake County. The highest transmissivity values in the study area occur locally around many of the larger UFA springs. Faulkner (1973) reported an average transmissivity of greater than 2,000,000 ft^2/d in the vicinity of Silver Springs and Ocala in central Marion County.

The storage coefficient of most confined carbonate aquifers ranges from about $1x10^{-5}$ to $1x10^{-3}$ (Lohman, 1972). Storage coefficient values for the UFA are more uniform than values of transmissivity, and typically range from $5x10^{-4}$ to $1x10^{-3}$ (Tibbals, 1990).

Few data are available to quantify the hydraulic properties of the MSCU that separates the UFA and LFA. The leakance of the MSCU, as estimated by Tibbals (1990) and Murray and Halford (1996), was a uniform value of about $5x10^{-5}$ (ft/d)/d except in spring areas along the St. Johns River. There, the leakance of the MSCU likely is very high because of a deep fracture system that provides a good hydraulic connection between the UFA and LFA.

The transmissivity of the LFA varies throughout the study area and is less well known than that of the UFA. Tibbals (1981) estimated transmissivity values of about 30,000 ft^2/d in most of the Ocala NF and southern Lake County, about 60,000 ft^2/d in central and northern Lake County, and about 130,000 ft^2/d in western Orange County. Murray and Halford (1996) reported an aquifer test conducted near Apopka in northwestern Orange County (fig. 1) yielded a transmissivity value of 632,000 ft^2/d. Additional transmissivity values for the LFA from 10 aquifer tests in Orange County were reported by O'Reilly and others (2002).

Estimates of storage coefficient for the LFA are based on sparse information, however, the storage coefficient values for the LFA are likely similar to those for the UFA. Values of storage coefficient calculated from aquifer tests of the LFA in Orange County ranged from $4x10^{-3}$ to $2x10^{-4}$ (Tibbals, 1990).

Recharge

Recharge areas of the UFA cover much of the study area and include well-drained and poorly drained soils, swamps, closed-basin lakes, and sinkholes. The UFA is recharged by the downward movement of water through the SAS and, where present, the ICU. The rate of recharge varies with the vertical hydraulic conductivity and thickness of the SAS and ICU, and the magnitude of the downward head gradient. The annual recharge rate to the UFA averages about 7 inches per year (in/yr) in Lake County (Knochenmus and Hughes, 1976). Recharge rates range from as high as 20-30 in/yr or greater on the Lake Wales and Mount Dora Ridges to 0 in/yr in the St. Johns River Offset areas of Lake County and the Ocala NF (O'Reilly, 1998; Murray and Halford, 1996). Less than 1 in/yr of lateral ground-water inflow is estimated to enter the UFA in Lake County from Polk County (Knochenmus and Hughes, 1976). An indeterminate amount of additional lateral ground-water inflow enters the UFA in the Ocala NF from western Marion and northern Lake Counties. Additional recharge also occurs through drainage wells drilled into the UFA to dispose of excess surface water in Ocala and western Orange County. Recharge to the SAS, and consequently to the UFA, is augmented locally by artificial recharge—wastewater land application, rapid-infiltration basins, and septic systems.

Discharge

Discharge from the UFA to the SAS occurs where the potentiometric surface of the UFA is higher than the water table of the SAS. In some areas, the potentiometric surface of the UFA is above land surface. Wells that tap the UFA in these areas are known as flowing artesian wells. Discharge from the UFA in Lake County, the Ocala NF, and vicinity generally occurs through numerous springs, a few flowing wells, and as diffuse ground-water discharge along the St. Johns River, Wekiva River, Ocklawaha River, the south shore of Lake Harris, and the western shore of Lake Apopka.

Springflow from the UFA in the study area for 1998 was estimated at nearly 1,300 Mgal/d (6 in/yr), of which 236 Mgal/d (4.3 in/yr) was from Lake County and 227 Mgal/d (6.9 in/yr) was from the Ocala NF. Silver Springs, the largest spring in the study area, has an annual mean flow of 788 ft^3/s (1932-2000); Alexander Springs, the largest in Lake County, has an annual mean flow of 106 ft^3/s (1931-2000); and Silver Glen Springs, the largest in the Ocala NF, has an annual mean flow of 102 ft^3/s (1931-2000) (fig.7). Spring discharge (from as many as 20 springs reported in the Lake Ocklawaha area) and ground-water discharge from the UFA in and along the lower Ocklawaha River are substantially suppressed by elevated river stages regulated at the outlet of Lake Ocklawaha.

Potentiometric Surface of the Upper Floridan Aquifer

Potentiometric surface maps of the UFA in the northern and central Florida peninsula are published semiannually by the USGS in cooperation with various State and local agencies. The potentiometric surface of the UFA represents the altitude to which water levels will rise in tightly cased wells. Area-wide potentiometric-surface maps of the LFA commonly are not constructed because of the sparsity of wells tapping only the LFA. Many wells that tap the LFA also tap the UFA and are not hydraulically isolated from the UFA by well casing. O'Reilly and others (2002) present potentiometric-surface maps of the LFA in east-central Florida, including parts of Lake County, for September 1998 and May 1999. A potentiometric-surface map of the UFA in the study area was constructed using water-level measurements made by the USGS in approximately 292 wells in May 1998, including 30 new wells identified for the purposes of this study (fig. 2).

Water levels in the UFA respond to seasonal variations in rainfall on a regional scale and to pumping on a local scale. Generally, the potentiometric surface of the UFA in the study area is lowest during May or June near the end of the dry season and highest in September or October near the end of the wet season. During 1998, however, the potentiometric surface was highest during March and lowest during December. This was attributed to extremely wet conditions during the (El Niño) winter of 1997-98, followed by a 4-month-long drought, and then drier than average conditions during the summer wet season. Still, the potentiometric surface of the UFA across the study area generally was slightly higher in 1998 than most years during the 1990's. Increased pumping during the spring and early summer drought locally increased declines in water levels.

The potentiometric surface of the UFA in May 1998 ranges from greater than 125 ft above sea level in northern Polk County to less than 5 ft above sea level at Lake George (fig. 2). In the study area, water in the UFA flows from potentiometric-surface highs in northern Polk and southwestern Clay and Putnam Counties to potentiometric-surface lows located in discharge areas. Ground water in Lake County generally flows in a north to northeast direction. In the Ocala NF, ground water generally flows eastward. Water-level measurements from UFA wells in May 1998 generally were about the average of the water-level measurements made during 1998.

Widely spaced potentiometric-surface contours can indicate highly transmissive areas of the UFA, such as the southwestern part of the Ocala NF and areas of northeastern Lake County south of the overlap (fig. 2). In contrast, closely spaced contours can indicate low transmissivity areas, such as areas directly west of the St. Johns River in Lake County and along the Ocklawaha River (fig. 2). There are two possible explanations for this area of low transmissivity. One is a change in lithology, possibly related to depositional environments. Corings from UFA wells in northernmost Lake County indicate that the top of the Ocala Limestone is cherty in some places and sandy in other places. Many of the UFA wells in this area also have partially collapsed holes, indicating a weakened, fractured, or sandy substructure. Another possible explanation is the presence of subsurface structural features. If such features exist, they could result in the juxtaposition of permeable zones in the west against less permeable zones in the east, as described by Faulkner (1973). As ground water flows laterally toward the St. Johns River, less permeable layers could

act as barriers, forcing water to the surface at numerous springs and seeps, and as diffuse ground-water discharge where the ICU is breached, thin, or absent.

Long-Term Trends

In the early 1930's, a large data-collection network was developed by State and Federal agencies in cooperation with the USGS to record rainfall, lake stage, ground-water levels, and springflow. Data from this network were used to identify hydrologic trends of sites in the study area.

Rainfall and Lake Stage

Rainfall in the study area is characterized by variation of rainfall amounts from place to place, as well as from day to day and year to year. On an annual basis, however, there are cycles of wet seasons (June through September) and dry seasons (October through May). This variation in rainfall results in seasonal trends in surface- and ground-water levels and springflow. In the study area, the long-term average annual rainfall is about 51 in., with 55-60 percent falling during the 4-month wet season and 40-45 percent falling during the 8-month dry season (National Oceanic and Atmospheric Administration, 1935-99). This average is based on 65 years of record from four climatological sites in the study area. An additional 25 sites were used to analyze rainfall data for the study period, December 1997-98 (fig. 5).

Cumulative daily rainfall distribution based on the 29 climatological sites in the study area for December 1997-November 1998 is shown in figure 17. The total measured rainfall for the study period was 57.02 in., or slightly above the average annual rainfall of about 51 in. A wetter than usual winter during 1997-98 was followed by a prolonged 4-month period with little or no rain, thereby shortening the wet season rainfall by about a month. The greatest recharge to the SAS occurs when the rising slope of the cumulative rainfall curve is steepest—such as during the periods of December 1997 through March 1998 and July 1998 through September 1998.

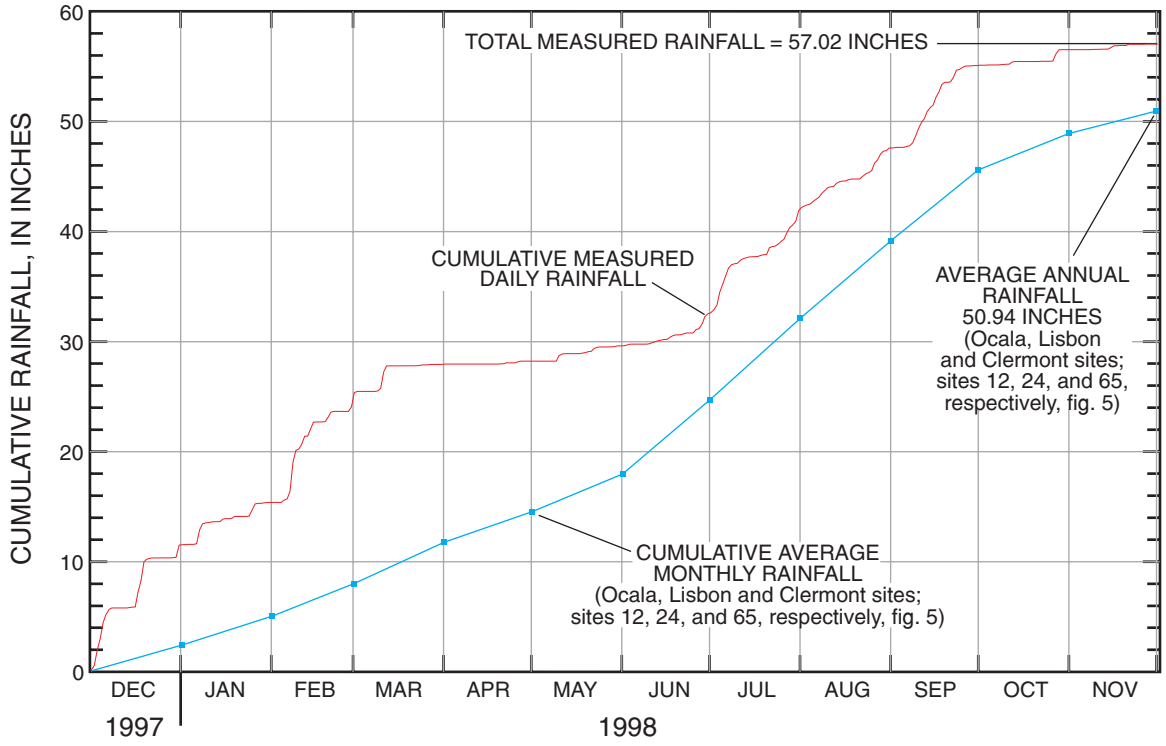

Figure 17. Cumulative daily rainfall distribution for climatological sites in the study area December 1997 - November 1998.

Long-term, multiyear cycles in rainfall are difficult to discern primarily because of the lack of available long-term rainfall record within the study area. The longest rainfall records available in the study area begin in 1935 and include Clermont, Lisbon, Ocala, and Bushnell (sites 65, 24, 12, and 48, respectively) (fig. 5 and app. A). Graphs of cumulative departure from average rainfall at these sites from 1935 to 2000 are shown in figure 18A. A rising slope indicates above-average rainfall (excess), whereas a declining slope shows below-average rainfall (deficit). For example, the long-term record at Lisbon shows that from 1935 to 1961 there was a total excess of about 84 in., an average excess of 3.1 in/yr. However, from 1961 to 1991 (a period dominated by drought conditions), the rainfall deficit totaled about 127 in., an average deficit of 4.2 in/yr. In contrast, the record at Clermont shows a slight deficit for 1939-69 and a slight surplus since 1970, indicating that rainfall trends are not necessarily the same at all sites in the study area.

Responses of lake stage are highly related to cycles and distribution of rainfall (fig. 18B). The most significant rises and falls in lake stage follow consecutive years with above-average and below-average rainfall, respectively. For example, the lowest (1995) and highest (1961) annual mean lake stages of Lake Weir coincide with the maximum cumulative rainfall deficit and excess, respectively, at both Ocala and Lisbon. For the period, 1935-2000, lake stages generally were highest during 1936-38, 1946, 1950, 1960, 1984, and 1996; and lowest during 1957, 1981, and 1994. The long-term (1940-2000) hydrograph of Lake Harris (fig. 18B) shows no discernible trends, whereas Lakes Griffin, Weir, and Bryant show a slight downward trend. After the early 1960's, declines in lake stages generally are more pronounced, which corresponds well with the accumulating rainfall deficits of the same time period.

The magnitude of lake water-level fluctuations is related to the leakance of the lake bottom, but also to the hydraulic gradients beneath and surrounding the lake. Lakes located where a large, downward hydraulic gradient exists between the SAS and the UFA typically fluctuate more than those lakes located where the downward gradient is very small or reversed. For example, Deerhaven Lake (high downward gradient) has fluctuated nearly 7 ft over 18 years, whereas, Lake Dorr (little or no downward gradient) has fluctuated by less than 1 ft over 34 years.

Lakes are designated as either closed-basin (seepage) or flow-through (drainage). Closed-basin lakes are internally drained and have no surface inlet or outlet, whereas, flow-through lakes have a surface inlet and outlet, and surface water flows through the lakes, which often are regulated by structures along streams interconnecting these lakes. Lake water either evaporates, infiltrates through the lake bottom, or is pumped for irrigation.

Lake water-level duration curves show the time that given values of lake water-surface elevations were exceeded for the period of record (fig. 19), and provide a frame of reference to determine the water levels in lakes relative to the long-term water levels (represented by the curves). For example, the water level in Lake Bryant, a closed-basin lake, can be expected to be below 53 ft above sea level, 65 percent of the time, based on available record (500 observations made 1936-2000). Conversely, lake water levels will exceed 53 ft above sea level, 35 percent of the time. Annual mean lake water level in 1998 for Lake Bryant was 51.26 ft above sea level (based on 4 measurements) which, based on 64 years of record, was exceeded about 83 percent of the time (fig. 19). Similarly for the remaining closed-basin lakes, annual mean lake water level for Lake Weir in 1998 was 55.32 ft above sea level (based on 52 measurements) and for Lake Dorr was 43.28 ft above sea level (based on 51 measurements) in 1998, which was exceeded about 80 percent of the time (1942-99) and 81 percent of the time (1965-2000), respectively.

For the flow-through lakes, annual mean lake water levels for Lakes Louisa, Harris, and Griffin were 94.79 ft (based on 52 measurements), 62.86 ft (based on 362 measurements), and 58.53 ft above sea level (based on 364 measurements) in 1998, respectively, which were exceeded 80 percent of the time (1957-2000), 70 percent of the time (1936-99), and 75 percent of the time (1944-99), respectively. The curves shown in figure 19 indicate that, in general, the water levels of the closed-basin lakes fluctuate slightly less than those of the flow-through lakes; however, the closed-basin lakes (selected based on the longevity of data record) also are located in areas where the downward gradient between the SAS and the UFA is nearly zero. Therefore, these closed-basin lakes may not represent the magnitude of the water-level fluctuations that occur in other closed-basin lakes located where a much larger downward gradient exists between the SAS and the UFA in the study area.

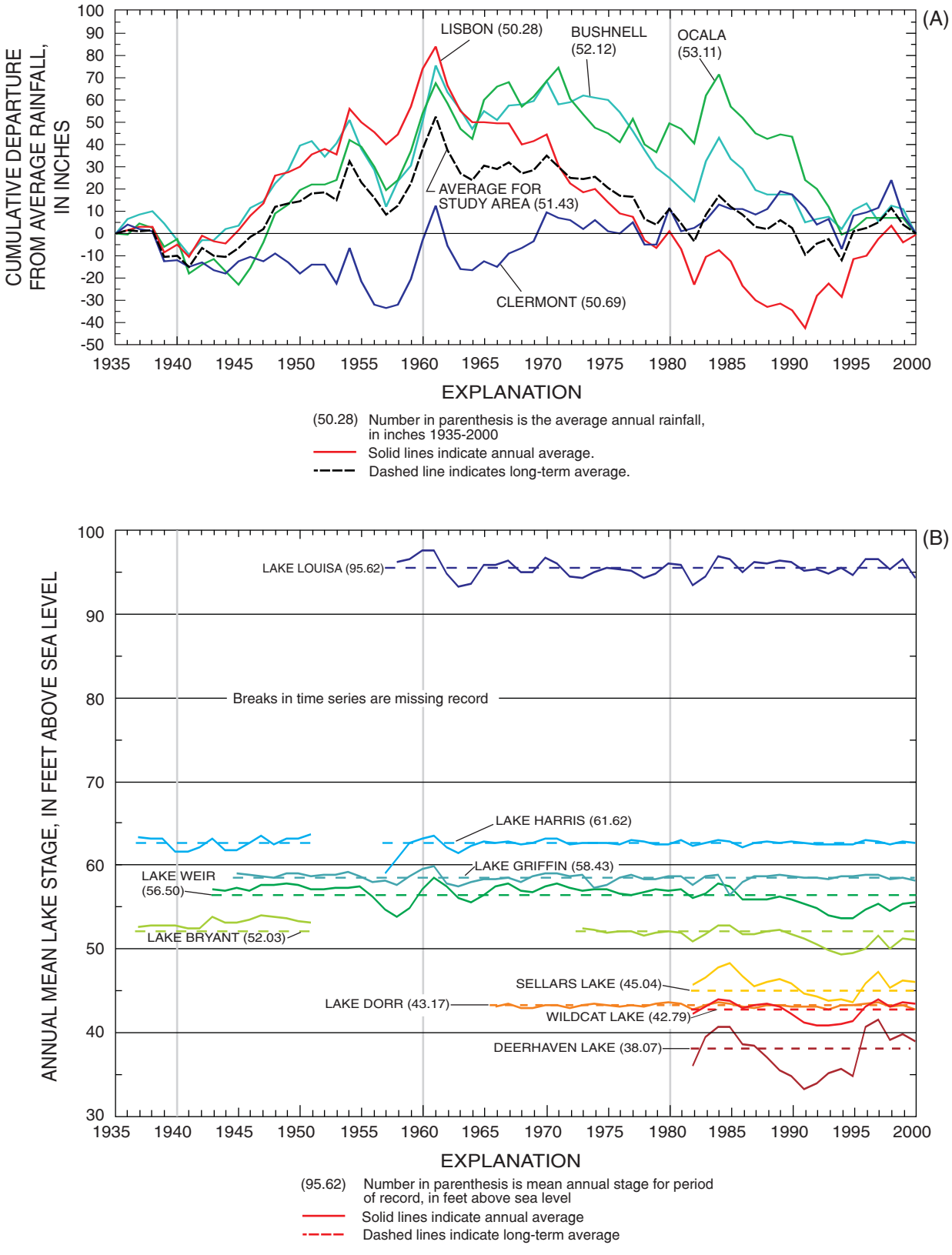

Figure 18. Cumulative departure from average rainfall (A) and lake-stage time series (B) for selected sites in the study area (climatological sites refer to appendix A and lake sites to appendix B).

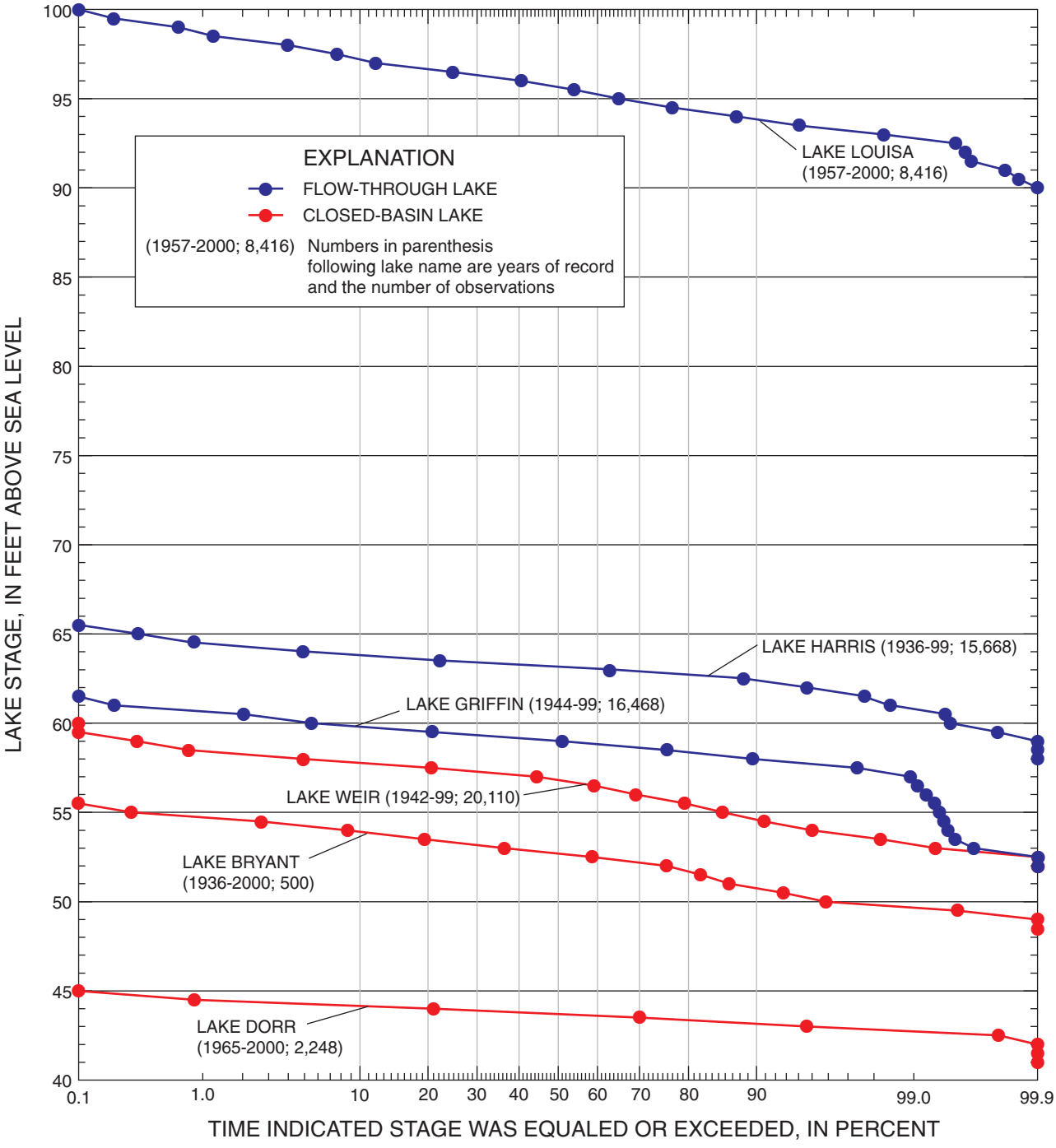

Figure 19. Lake-stage duration for selected lakes.

Ground-Water Levels

Water levels measured in SAS and UFA wells respond to rainfall variations in the same manner that lake stages respond. Daily mean water levels for eight continuous-record wells in the study area for the period 1935-2000 are shown in figure 20A. Continuous water-level data were available prior to 1960 only for well 291115081592501 (Sharpes Ferry Marion DOT5). The daily mean water level for 1936-2000 at the Sharpes Ferry well is 47.96 ft above sea level and ranges from 43.20 ft in 1957 to 55.42 ft above sea level in 1960.

The daily mean water levels in wells with continuous record from September 1997 through 1998 (field data-collection period for this study) are shown in figure 20B. Except for well 291204081564801 (Ocala NF SAS well near Lynne), which reached a maximum during early October 1998, water levels in SAS and UFA wells reached maximums during March 1998 following an unusually wet (El Niño) winter.

Rainfall events, particularly during the (El Niño) winter of 1997-98, generally caused short-term peaks in the hydrographs of SAS wells and more subdued and delayed peaks in the hydrographs of UFA wells (fig. 20B). Water levels in SAS wells located where the unsaturated zone is relatively thin respond quickly to rainfall events, generally peaking within a day or two following the event. In areas where the unsaturated zone is thick (100 ft or more), water levels in SAS wells can take weeks before responding to rainfall events. Persistent, longer-term rainfall events over a period of months are needed to rewet surficial sands sufficiently to allow water to move downward to recharge the SAS, and ultimately, the UFA. Water-level rises in wells tapping the UFA will occur first as a response to increased pressure resulting from the addition of infiltrating water to the overlying water table. The amount of time for recharge water to reach the UFA can be long, particularly if the ICU has a small vertical hydraulic conductivity, large thickness, or both. In the study area, water levels in the UFA can take up to several weeks to respond to rainfall events, but generally water levels respond within a few days of a rainfall event where the UFA is near the land surface, unconfined or thinly confined, and recharge rates are high (for example, in well 283204081544901 at Mascotte in western Lake County). Water-level fluctuations in the UFA are greatest in recharge areas, generally about 5 ft during 1997-98. Periodic measurements of the UFA potentiometric surface in high recharge areas of Sumter and western Lake Counties indicated a range as much as 15-20 ft during 1997-98, which possibly was a result of nearby pumping or rerouting of surface water for mining that would have otherwise recharged the aquifer locally.

Upper Floridan Aquifer Springs

Sixty-five springs that discharge water from the UFA were inventoried during the study (table 1). Springflow occurs at discrete points (vents and boils) or as diffuse ground-water discharge over broader areas where the potentiometric surface of the UFA is above land surface and where the ICU overlying the Floridan aquifer has been breached.

Total calculated springflow for the study area in 1998 was 1,979 ft^3/s (1,279 Mgal/d). In Lake County during 1998, 22 springs accounted for a total springflow of 258 ft^3/s (167 Mgal/d); and in the Ocala NF, 14 springs accounted for a total springflow of 348 ft^3/s (225 Mgal/d). The overlap area contains three springs with a total springflow of 112 ft^3/s (72.6 Mgal/d). Diffuse ground-water discharge, estimated using stream base flow measurements made by the USGS in 1981 and 1997, is about 102 ft^3/s (66.0 Mgal/d) along Juniper and Alexander Creeks. Diffuse ground-water discharge estimated by using a 30-day sliding average of minimum flows, is about 27 ft^3/s (17.4 Mgal/d) in Lake Ocklawaha. Diffuse ground-water discharge also is likely in the St. Johns River, south of Lake George, but the discharge rate is indeterminate because of nearly flat gradients and a large storage capacity of the river in and downstream of the lake.

Springs are categorized by their long-term mean discharges: first-magnitude springs have mean discharges of 100 ft^3/s or more, second-magnitude springs have mean discharges of greater than 10 to 100 ft^3/s, and third-magnitude springs have mean discharges of greater than 1 to 10 ft^3/s (Rosenau and others, 1977). The study area has 4 first-magnitude, 18 second-magnitude, and 43 third-magnitude or less springs.

The largest (first-magnitude) springs, based on long-term discharge (1931-2000), are Silver Springs in Marion County, Blue Springs in Volusia County, Silver Glen Springs in the Ocala NF in Marion County, and Alexander Springs in the Ocala NF in Lake County. Together these springs account for 1,152 ft^3/s (745 Mgal/d), or about 59 percent of the total springflow in the study area (fig. 21).

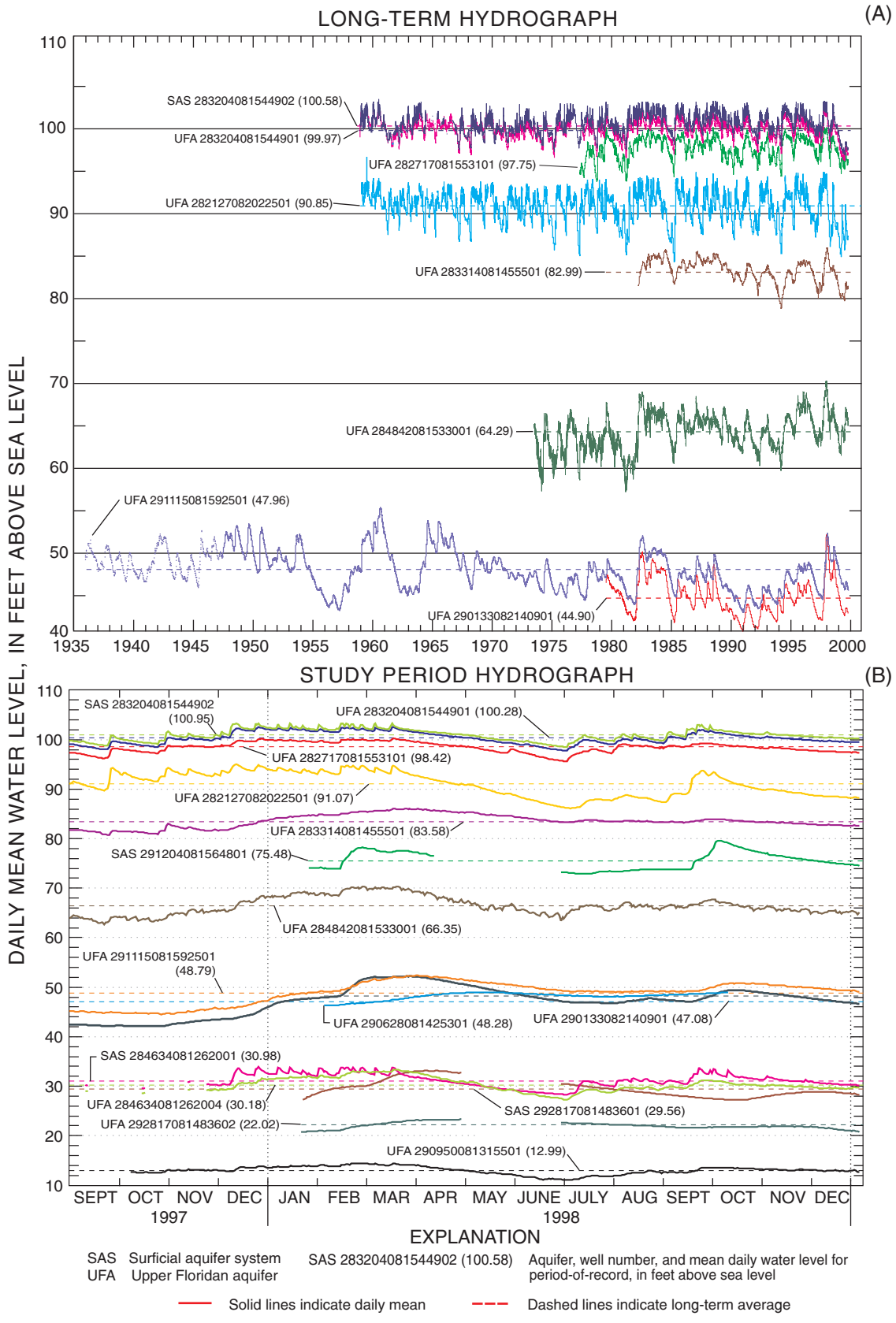

Figure 20. Long-term and 1997-98 water levels in selected wells tapping the surficial and the Upper Floridan aquifer systems in the study area (well sites referenced in appendixes B and C).

Table 1. Summary statistics of springflows

[ft^3/s, cubic foot per second; NA, not available. Abbreviation for accuracy of annual springflow: E, estimate determined from measurements not made during 1998 or derived from baseflow of receiving stream; G, estimate based on reconnaissance; M, measurements made during 1998]

USGS site identification number	Station name	County	Date of first measurement	Mean springflow for period of record (ft^3/s)	Mean springflow for 1998 (ft^3/s)	Accuracy of springflow measurements
283400081405100	Apopka (Gourd Neck) Spring near Oakland	Lake	1971	38	33	M
283844081422300	Wolf's Head Spring along railroad grade near Astatula	Lake	1997	.1	.1	E
283903081430100	Bear Spring near Astatula	Lake	NA	NA	2	G
284038081443201	Double Run Road Seepage (into Little Lake Harris) near Astatula	Lake	1997	2.0	2.4	E
284047081441501	Seepage Run (into Little Lake Harris), County Road 561 near Astatula	Lake	1997	.1	.1	E
02237400	Holiday Springs at Yalaha	Lake	1946	3.8	4.5	M
284437081491700	Sun Eden Spring near Yalaha	Lake	1997	.2	.2	E
284452081495400	Mooring Cove Springs near Yalaha	Lake	1997	.4	.4	E
284455081494100	Blue Springs, Park Drive near Yalaha	Lake	1972	3.0	2.8	M
02237322	Bugg Spring near Okahumpka	Lake	1943	11	12	M
284740081251701	Wekiva Falls Resort flowing borehole	Lake	1975	20	20	E
284922081250300	Island Spring, Wekiva River	Lake	1982	6.4	6.6	E
284940081303800	Droty Springs near Sorrento	Lake	1997	.7	.8	E
285038081270100	Palm Springs, Seminole State Forest	Lake	1997	.5	.6	E
02235250	Seminole Springs near Sorrento	Lake	1931	35	40	E
285102081263900	Blueberry Spring, Seminole State Forest	Lake	1997	.1	.1	E
285105081263800	Moccasin Springs, Seminole State Forest	Lake	1997	.3	.3	E
02235255	Messant Spring near Sorrento	Lake	1946	15	18	E
285224081262400	Shark's Tooth Spring, Seminole State Forest	Lake	1997	.1	.2	E
285318081295200	Blackwater Springs near Cassia	Lake	NA	NA	.2	G
285702081322400	Camp La-No-Che Springs near Paisley	Lake	1954	.9	1.1	E
290220081260400	Mosquito Springs Run, Alexander Springs Wilderness	Lake	1997	1.9	2.3	M
02236095	Alexander Springs	Lake	1931	106	104	M
291136081381000	Juniper Creek South Tributary Seepage near Astor	Lake	1980	6.1	6.1	E
02236160	Silver Glen Springs near Astor	Marion	1931	102	102	M
02236132	Fern Hammock Springs near Ocala	Marion	1935	13	13	M
02236130	Juniper Springs near Ocala	Marion	1931	10	11	M
02236152	Morman Branch (Upper), State Road 19	Marion	1929	2.8	2.8	E
291200081390601	Morman Branch Seepage (into Juniper Creek) near Astor	Marion	1980	4.6	4.6	E
02239500	Silver Springs near Ocala	Marion	1932	788	930	M
02236147	Sweetwater Springs along Juniper Run	Marion	1980	13	14	M
02236205	Salt Springs	Marion	1929	81	84	M
292521081551200	Wells Landings Springs	Marion	1999	9.9	5.0	E
292540081552400	Tobacco Patch Landing Spring Group 1a (Group 1 run inflow)	Marion	1999	.7	.5	E
292542081552600	Tobacco Patch Landing Spring Group 1	Marion	1999	2.8	.5	E

Table 1. Summary statistics of springflows--Continued

[ft^3/s, cubic foot per second; NA, not available. Abbreviation for accuracy of annual springflow: E, estimate determined from measurements not made during 1998 or derived from baseflow of receiving stream; G, estimate based on reconnaissance; M, measurements made during 1998]

USGS site identification number	Station name	County	Date of first measurement	Mean springflow for period of record (ft^3/s)	Mean springflow for 1998 (ft^3/s)	Accuracy of springflow measurements
293021081570600	Camp Seminole Spring, Girl Scout Camp, Orange Springs	Marion	1999	.8	1.0	E
293038081563800	Orange Spring near Orange Springs	Marion	1972	4.8	2.5	E
02243550	Blue Springs near Orange Springs	Marion	1935	5.7	.5	E
284241081281800	Barrel Springs, Wekiwa Springs State Park	Orange	1997	.2	.2	M
02234600	Wekiwa Springs, Wekiwa Springs State Park	Orange	1932	69	66	M
02234620	Witherington Springs, Wekiwa Springs Park near Apopka	Orange	1945	3.9	4.7	E
02234610	Rock Springs near Apopka	Orange	1931	60	58	M
284612081303401	Sulphur (Camp) Springs near Mt. Plymouth	Orange	1995	.6	.7	E
292618081412100	Croaker Hole Spring near Welaka	Putnam	1981	86	94	M
02236220	Beecher Springs near Fruitland	Putnam	1960	9.9	12	M
292725081393500	Forest Springs near Welaka	Putnam	1972	.4	.4	E
292735081394500	Mud Spring near Welaka	Putnam	1972	1.9	1.7	E
02244022	Welaka Spring	Putnam	1972	1.0	1.0	E
02244020	Nashua Spring near Welaka	Putnam	1946	.3	.5	E
293159081403600	Satsuma Spring near Satsuma	Putnam	1956	1.5	1.3	E
02234991	Sanlando Springs near Longwood	Seminole	1941	20	22	M
02234996	Palm Springs near Longwood	Seminole	1941	7.2	5.3	M
02234997	Starbuck Spring near Longwood	Seminole	1944	14	15	M
02234650	Miami Springs near Longwood	Seminole	1945	4.9	5.1	M
284515082050100	Shady Brook Spring #5 (South Panasoffkee Spring Group) near Lake Panasoffkee	Sumter	NA	NA	3.0	E
284612082042000	Shady Brook Spring #4 (South Panasoffkee Spring Group) near Lake Panasoffkee	Sumter	NA	NA	3.0	E
284646082023800	Shady Brook Spring #3 (South Panasoffkee Spring Group) near Coleman	Sumter	NA	NA	3.0	E
284708082024600	Shady Brook Spring #2 (South Panasoffkee Spring Group) near Coleman	Sumter	NA	NA	3.0	E
284742082021900	Fenney Spring (headspring of Shady Brook to Lake Panasoffkee) near Coleman	Sumter	1946	41	43	E
285011082034900	Little Jones Creek Spring #3 (North Panasoffkee Spring Group) near Wildwood	Sumter	NA	NA	3.0	E
285134082051800	Little Jones Creek Spring #2 (North Panasoffkee Spring Group) near Wildwood	Sumter	NA	NA	5.0	E
285208082054100	Little Jones Creek Headspring (North Panasoffkee Spring Group) near Wildwood	Sumter	NA	NA	8.0	E
285144081183900	Gemini Springs near DeBary	Volusia	1972	11	11	M
02235500	Blue Springs near Orange City	Volusia	1932	156	157	M
02236110	Ponce De Leon Springs near DeLand	Volusia	1929	28	22	M
	Total				**1,979 ft^3/s**	

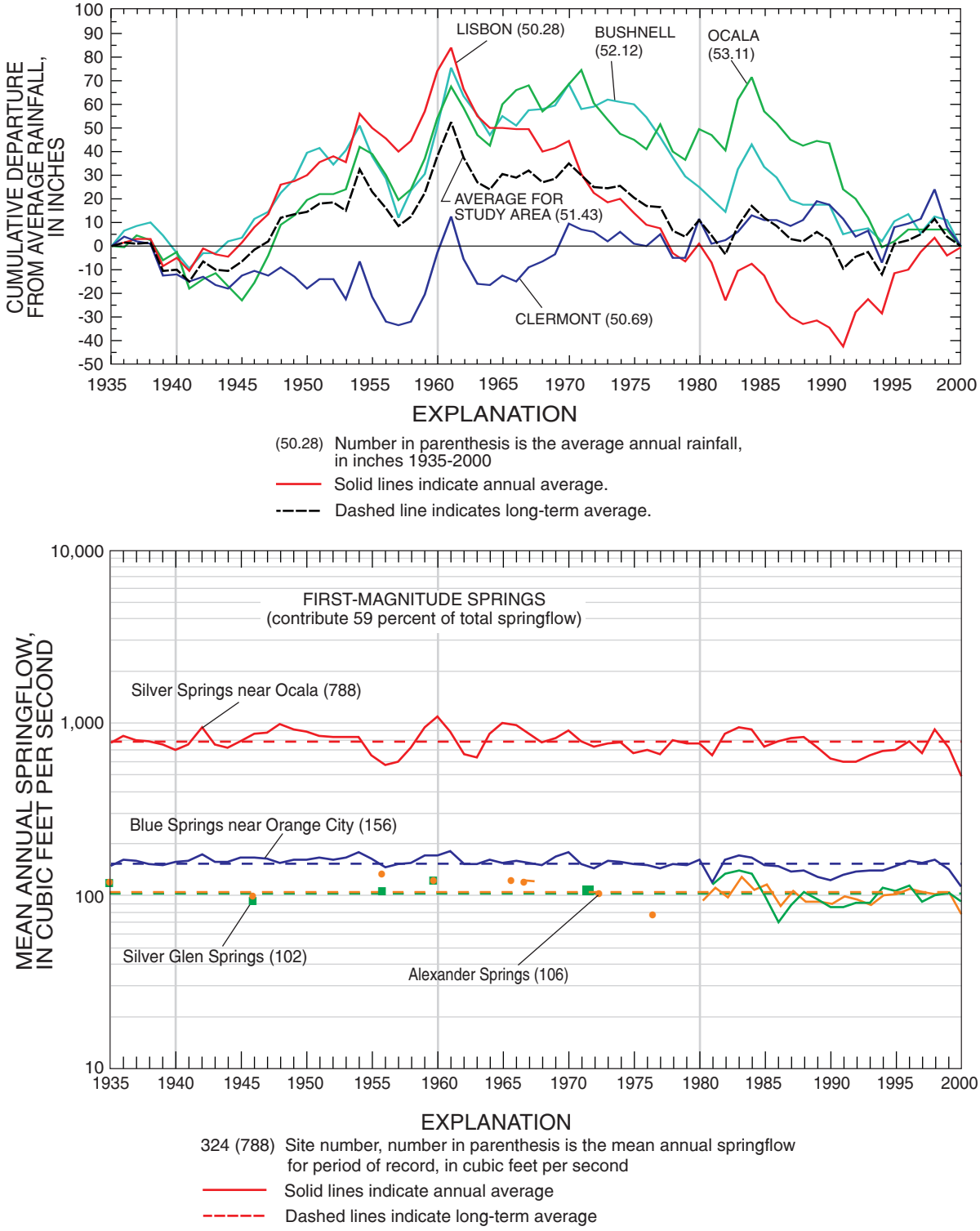

Figure 21. Annual rainfall and springflow of first-magnitude Upper Floridan aquifer springs in the study area, 1935-2000 (spring sites refer to appendix C).

The average discharge from Silver Springs and Blue Springs for 69 years of record is 788 ft^3/s (509 Mgal/d) and 156 ft^3/s (101 Mgal/d), respectively. Long-term trends in spring discharges from Silver Springs and Blue Springs (fig. 21) closely follow trends in rainfall at Ocala (fig. 18A); however, the response of spring discharge from Blue Springs occasionally is suppressed by river stage in the St. Johns River. In the long term, springflows have followed the same slight downward trend as that of most lake stages and ground-water levels, particularly since the early 1960's.

Second- and third-magnitude springs account for about 517 ft^3/s (334 Mgal/d), or 26 percent of the total springflow in the study area—about 142 ft^3/s (92 Mgal/d) in Lake County and 234 ft^3/s (151 Mgal/d) in the Ocala NF, with about 13 ft^3/s (8 Mgal/d) in the overlap area (fig. 22). For convenience, the Lake County total includes the 20 ft^3/s (13 Mgal/d) of discharge from a flowing borehole at the Wekiva Falls Resort. Long-term data for the second- and third-magnitude springs are not as complete as for the first-magnitude springs, but the long-term trends appear to be similar. Many of the second- and third-magnitude springs also are affected by stages in receiving streams, particularly submerged springs located in lakes or streams. For example, spring discharge from Blue Springs (Marion County) and Wells Landing Springs in Lake Ocklawaha are suppressed by regulated stage (elevated 15-18 ft above the natural flow condition) maintained by Rodman Dam at the outlet of Lake Ocklawaha. Spring discharge from Blue Springs was nearly 11 ft^3/s (6.9 Mgal/d) in 1935 before stage regulation. When the regulated stage was lowered by approximately 11 ft in March 1998, discharge was estimated at about 6.0 ft^3/s (3.9 Mgal/d), and when the stage was returned to the regulated 20-ft level in May 1998, discharge was measured at 0.5 ft^3/s (0.3 Mgal/d). The remaining 15 percent of the total springflow is from diffuse ground-water discharge and springs smaller than third-magnitude.

Water Budget

A generalized water-budget analysis of the study (model) area was made for 1998 by using measured or estimated values of rainfall, artificial recharge, springflow, streamflow, pumpage, storage changes, and net boundary leakage. An annual average estimate of ET was calculated as the residual of the water budget. A summary of the water budget is shown in figure 23. This water budget was compiled for comparison to the water budget from the ground-water flow model simulation.

A generalized water-budget equation used for the study area to solve for ET, as shown in figure 23, is:

$$ET = RF + AR - RO - SP - BF - \Delta S - W - BD, \quad (1)$$

where;

$$BF = BF_{FAS} + BF_{SAS},$$

$$\Delta S = \Delta S_{FAS} + \Delta S_{SAS}, \text{ and}$$

ET is evapotranspiration;
RF is rainfall;
AR is artificial recharge from agricultural and golf-course irrigation and reclaimed water application;
RO is overland runoff;
SP is springflow;
BF is total base flow;
BF_{FAS} is base flow from the FAS;
BF_{SAS} is base flow from the SAS;
ΔS is total net change in storage;
ΔS_{FAS} is net change in storage of the FAS;
ΔS_{SAS} is net change in storage of the SAS;
W is total pumpage from the FAS;
BD is net boundary leakage, or net outflow within the FAS crossing study-area boundary;
and all components are in inches.

The largest output component in the water budget, ET, was about 33 in., or about 58 percent of the sum of the rainfall (RF) and artificial recharge (AR) components in 1998. Open-water surface (lake, wetlands, and stream) evaporation, which can be comparable to other estimates of ET, was estimated from pan-evaporation data by applying pan-to-lake coefficients (Sacks and others, 1994), and potential ET from the Gainesville (site 2) and Lisbon (site 24) climatological sites (fig. 5 and app. A). Potential ET for the study area was estimated to be about 51 in. in 1998. The open-water surface area is about 345 mi^2, or about 7 percent of the study area. Partitioning the ET component into lake- and land-evaporation (7 percent lake and 93 percent land coverage) quantities yields a lake-evaporation of about 1.5 in. and a land-evaporation of slightly less than 32 in. for the study area in 1998.

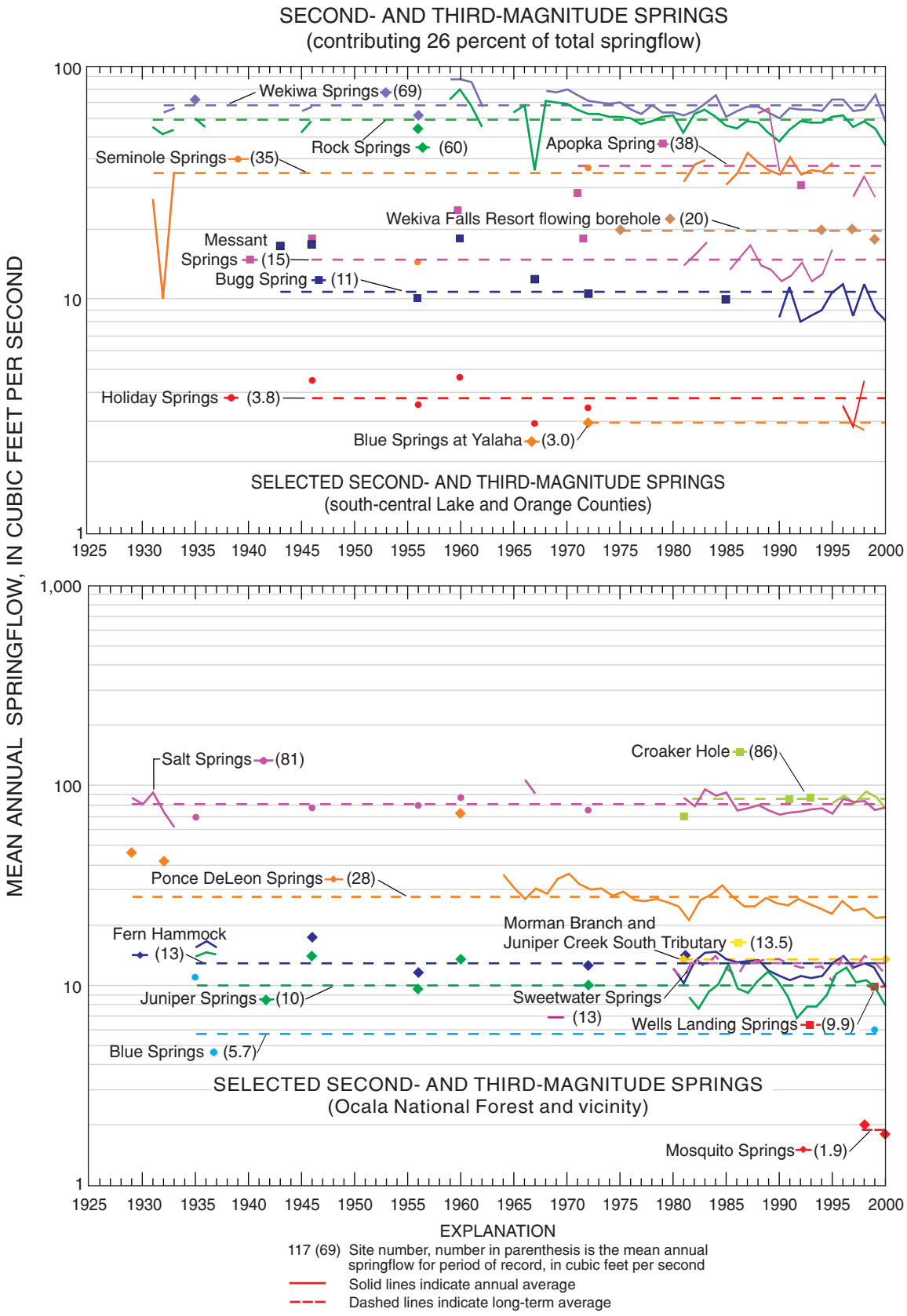

Figure 22. Annual springflow of selected second- and third-magnitude Upper Floridan aquifer springs in the study area, 1929-2000 (spring sites refer to appendix C).

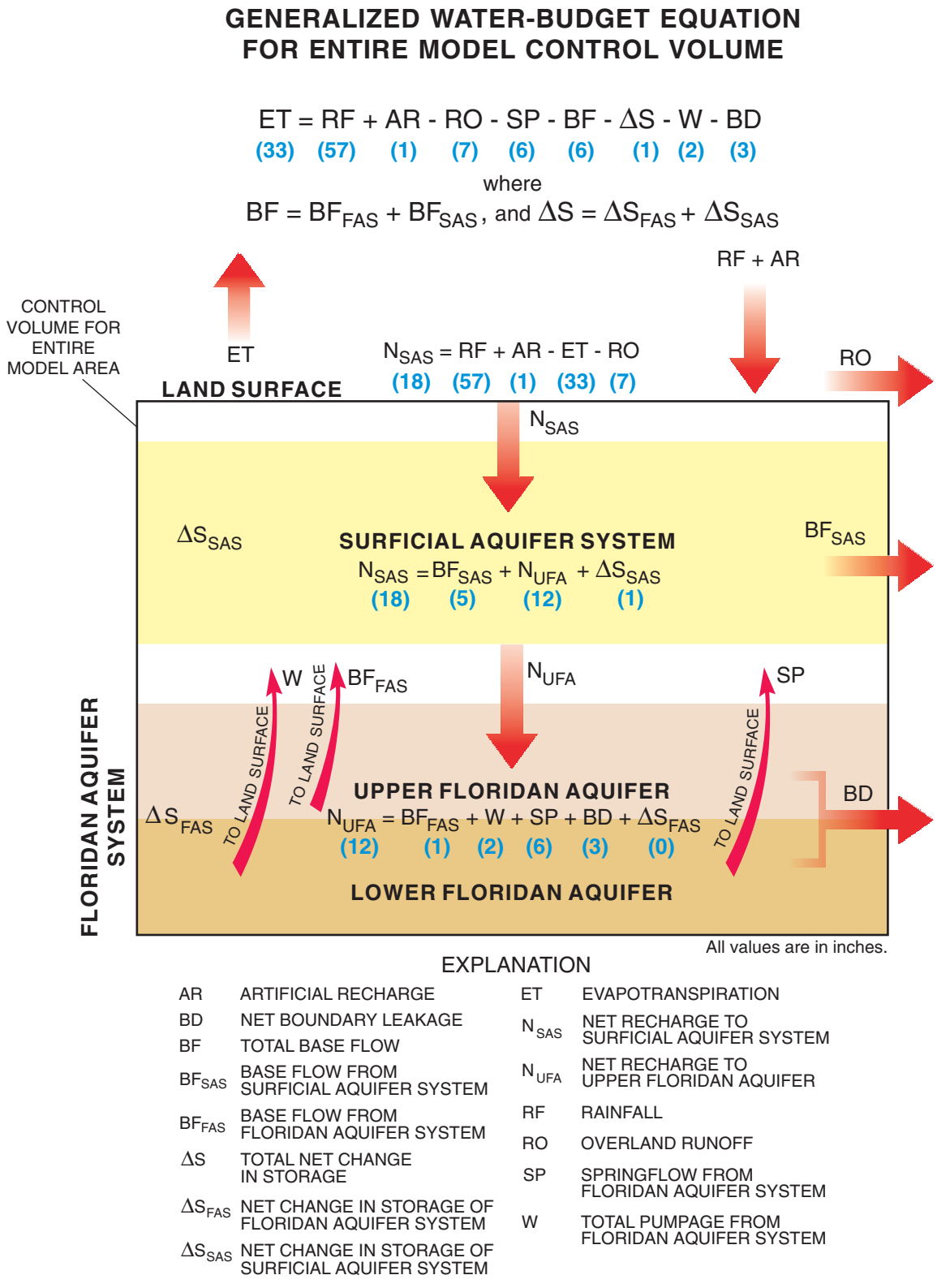

Figure 23. Water budget for Lake County, the Ocala National Forest, and vicinity within the model area, 1998.

Rainfall (RF) and artificial recharge (AR) from agricultural and golf-course irrigation and reclaimed water application were about 57 in. and 1 in., respectively, representing the total available input in 1998. An areal estimate of rainfall was determined using the Theissen method (Fetter, 1980), which adjusts for non-uniform site distribution by applying a weighting factor for each site. This factor was based on the size of the area within an irregular polygon constructed around and closest to each site. Twenty-nine sites (with an average area of 166 mi^2 per site) were used in the analysis. Rainfall varied considerably across the study area, ranging from about 45 in. at Tavares in Lake County to nearly 70 in. at Jumper Lake in the Ocala NF. Rainfall exceeded 60 in. across central Lake County and west-central Ocala NF. Rainfall was less than 50 in. mostly across southern Lake County. AR was estimated using reclaimed water, agricultural, and golf-course water-use data.

Overland runoff (RO) was about 7 in., and was estimated by subtracting the base flow from the net streamflow in the model area (fig. 5). Net streamflow was 18.6 in. in 1998; 11.4 in. of the streamflow was base flow and was estimated from 30-day sliding minimum flows, which included springflow and diffuse ground-water discharge. Net streamflow was computed by subtracting streamflow exiting the study area from streamflow entering the area.

Springflow (SP) was about 6 in. in 1998 and was estimated by using annual mean discharges based on bi-monthly discharge measurements and daily mean discharge data for all springs in the study area. Although springflow contributes to base flow, it was considered as a separate component in this analysis.

Total base flow (BF), excluding measured springflow (SP), was about 6 in. with base flow from the FAS to streams (BF_{FAS}) estimated to be about 1 in. BF_{FAS} was determined by using end-of-dry season base flows (when contribution from the SAS is at a minimum) of contributing tributaries to the St. Johns River and seepage run measurements made in 1981 (Tibbals, 1990) and during this study. Therefore, the base flow from the SAS (BF_{SAS}) was determined to be about 5 in. by subtracting BF_{FAS} from BF.

Total net change in aquifer storage (ΔS) was estimated by adding the net change in storage of the SAS (ΔS_{SAS}) and the net change in storage of the FAS (ΔS_{FAS}). The total net change in storage is zero for a steady-state period; however, a 12-month time period could not be selected so that ΔS would be zero for the study area. Therefore, a 12-month period was selected during which ΔS_{SAS} was minimal and was determined by averaging the changes in lake- and ground-water levels measured bi-monthly. Based on 46 wells measured bi-monthly, water levels in the SAS increased by 0.70 ft on average. Using a specific yield of 0.15, ΔS_{SAS} was computed to be 0.11 ft (1.3 in.). Based on 118 wells measured bi-monthly, water levels in the UFA and LFA increased by 0.12 ft and decreased by 1.29 ft, respectively, on average. Using a specific yield of 0.001, ΔS_{FAS} was computed to be less than 0.01 in. and therefore was assumed to be zero. ΔS was slightly more than zero across eastern Lake County and the Ocala NF, and ranged from a 1-in. loss in southern and central Lake County to a nearly 2-in. gain in south-central and southwestern areas of the Ocala NF.

Total pumpage (W) from the FAS was about 2 in. in 1998 and was estimated from annual water-use data.

Net boundary leakage (BD), or net flow crossing the model boundaries, was estimated to be nearly 3 in. for the FAS (boundary leakage for the SAS was assumed to be negligible.) This estimate was made by constructing flow nets (Fetter, 1980) in areas where water in the UFA crossed the model boundary based on the observed potentiometric surface. This estimate was based on the assumption that horizontal gradients in both the LFA and UFA were the same, as there were no LFA water-level data available. Therefore, the actual boundary leakage could be more or less than 3 in. depending on the horizontal gradients across these boundaries in the LFA.

Net recharge to the SAS in 1998, as shown in figure 23, is:

$$N_{SAS} = RF + AR - ET - RO = 18 \text{ in.}, \quad (2)$$

where;
N_{SAS} is net recharge to the SAS, in inches; and other terms are as previously defined.

A generalized water-budget equation used for the SAS, as shown in figure 23, is:

$$N_{SAS} = BF_{SAS} + N_{UFA} + \Delta S_{SAS} = 18 \text{ in.}, \quad (3)$$

where;
N_{UFA} is net recharge to the FAS, in inches; and
other terms are as previously defined.

Rearranging equation 3 and solving for N_{UFA} yields:

$$N_{UFA} = N_{SAS} - \Delta S_{SAS} - BF_{SAS} = 12 \text{ in.}, \quad (4)$$

where all terms are as previously defined.

A generalized water-budget equation used for the FAS, as shown in figure 23, is:

$$N_{UFA} = BF_{FAS} + W + SP + BD + \Delta S_{FAS} = 12 \text{ in.}, \quad (5)$$

where all terms are as previously defined.

SIMULATION OF GROUND-WATER FLOW

The conceptual model (fig. 8) and hydrologic information presented in the previous sections were used to construct a numerical ground-water flow model of the SAS and FAS. The model simulates steady-state, ground-water flow both for average 1998 conditions (December 1997 to December 1998) and for projected 2020 ground-water withdrawals. For simplicity, conditions during the time period from December 1997 to December 1998 will hereafter be referred to as average 1998 conditions. Particle-tracking analyses were used to identify the areas that contribute recharge to selected springs and well fields under both average 1998 and projected 2020 conditions.

Model Design

The USGS three-dimensional ground-water flow model code MODFLOW-2000 (version 1.1) was used to simulate the flow system (Harbaugh and others, 2000). MODFLOW-2000 incorporates significant revisions over previous versions (McDonald and Harbaugh, 1988; and Harbaugh and McDonald, 1996), most notably the capability to solve other types of equations in addition to the ground-water flow equation. One of the additional capabilities used in this study is the inverse model component that uses formal sensitivity and parameter estimation methods to facilitate model calibration (Hill and others, 2000). For simplicity, MODFLOW-2000 will hereafter be referred to as "MODFLOW."

Model Layers and Grid

Vertical discretization of the model was based on hydrogeologic maps (figs. 10-15). Three layers were used to represent the SAS, UFA, and LFA (fig. 8). The resistance to flow between adjacent layers was assumed to be controlled by the leakance of the intervening ICU or MSCU/MCU (fig. 8). The leakance of a confining unit is calculated as the vertical hydraulic conductivity of the unit divided by its thickness. The large contrast in hydraulic conductivity between the confining units and adjacent aquifers, typically at least one-hundred times less in the confining unit, indicates that flow is nearly vertical in the confining units. Therefore, the confining units were simulated by using their respective vertical hydraulic conductivities and thicknesses, rather than as separate layers. Where the ICU does not exist (fig. 11), the thickness of the unit was assumed to be 1 ft and the base of the SAS was specified at an altitude 1 ft above the top of the UFA. Likewise, where the MSCU/MCU does not exist (fig. 14), the thickness was assumed to be 1 ft and the base of the UFA was specified at an altitude of -499 ft, which is the approximate altitude of the midpoint of the MSCU/MCU in adjacent areas where the unit does exist. Conceptualization of the MSCU/MCU can be difficult because of the existence of two distinct and disconnected confining units that collectively represent the MSCU/MCU in the model (figs. 8 and 9). For modeling purposes, the MSCU/MCU was assumed to extend from the top of the shallower confining unit, the MSCU (middle confining unit I as described by Miller (1986, p. B56)), to the bottom of the deeper confining unit, the MCU (middle confining unit II as described by Miller (1986, p. B56)) (fig. 14).

Horizontal discretization of each layer was oriented along a north-south axis and consisted of 220 rows and 140 columns with a uniform cell size of 2,500 by 2,500 ft (fig. 24). Of the 60,487 active cells, 19,855 represented the SAS; 21,414 represented the UFA; and 19,218 represented the LFA (fig. 24). The active model area represented a surface area of approximately 4,800 mi^2.

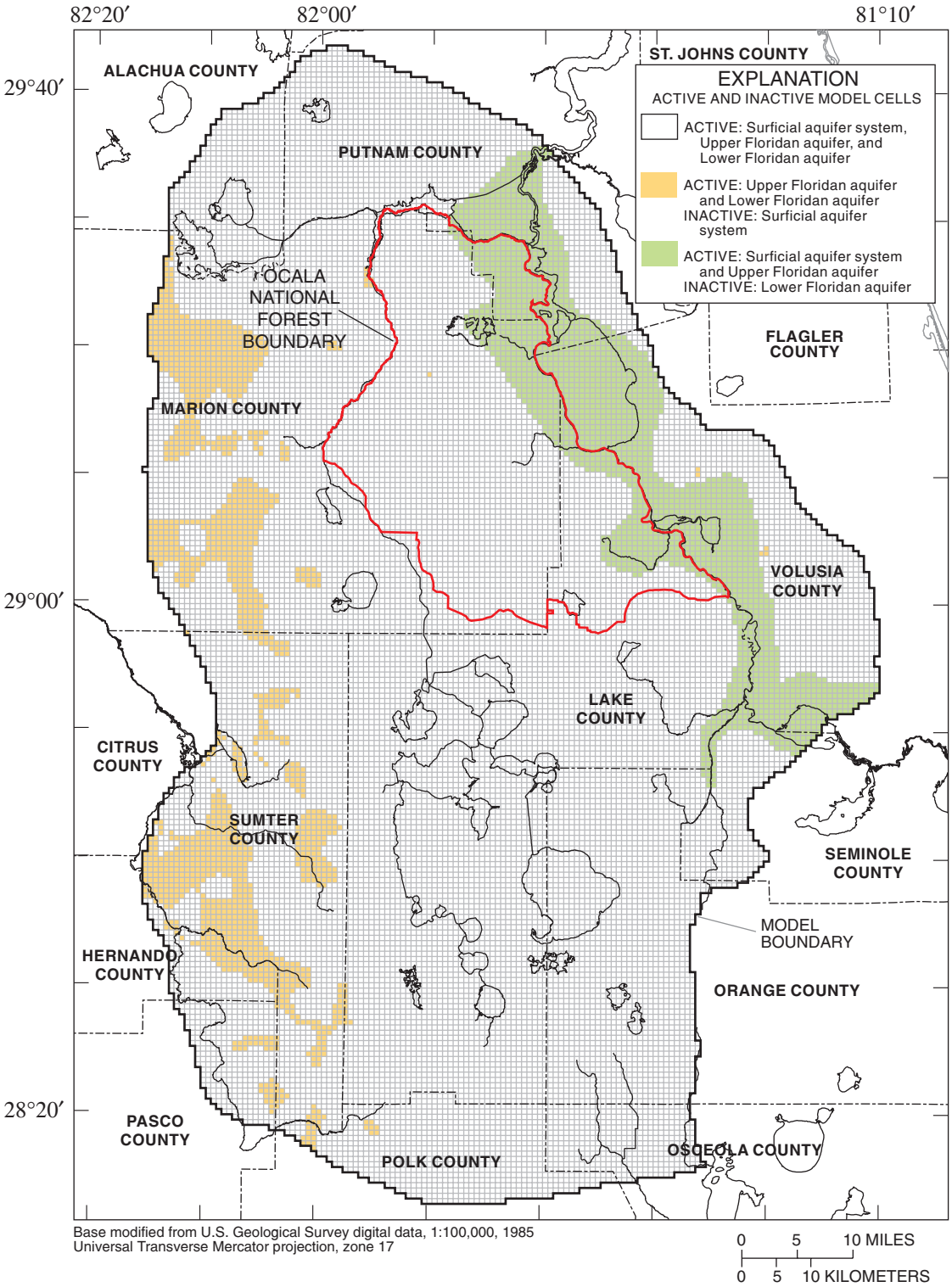

Figure 24. Finite-difference grid showing active and inactive model cells.

Boundary Conditions

Vertical boundaries were based on the geologic, water-quality, and flow-system characteristics of the aquifer system in the model area. A combination of specified fluxes and head-dependent boundaries representing net recharge served as the upper boundary condition, which was located at the altitude of the water table; how net recharge was simulated by the model is described in more detail in a later section. The lower boundary condition was specified as no-flow. The very low permeability of the sub-Floridan confining unit functions as a physical barrier to ground-water flow. However, highly mineralized water exists within the FAS above the sub-Floridan confining unit (fig. 9). If the transition from fresh to mineralized water and the consequent density disparity occurs abruptly and in the absence of any large nearby stress such as a pumping well, the interface between the freshwater and mineralized water flow systems can be approximated as a no-flow boundary (Reilly, 2001, p. 11). The altitude at which the chloride concentration of water is equal to 5,000 mg/L generally can be assumed to be the base of the freshwater flow system in east-central Florida based on the following reasoning: (1) the 5,000 mg/L chloride concentration approximately represents the boundary between moderately brackish water and very brackish to saline water; and (2) the thickness of the transition zone between the 5,000 and 10,000 mg/L chloride concentrations is relatively small (McGurk and Presley, in press). Therefore, the no-flow lower boundary condition for the model was established by the location of the 5,000 mg/L chloride concentration (fig. 16) or the top of the sub-Floridan confining unit (base of the FAS, fig. 15), whichever occurred at a shallower depth.

Lateral boundary conditions for each model layer were based on the geologic, water-quality, and flow-system characteristics of each aquifer, as well as the need to locate boundaries relatively far from the areas of interest (Lake County and the Ocala NF). In the SAS, a no-flow condition was specified along all lateral boundaries because relatively little regional lateral flow occurs in the SAS, based on reported values of hydraulic conductivity and aquifer thickness, and the SAS is thin or absent in parts of the model area. In areas where the SAS and ICU are thin or absent, the UFA probably functions as an unconfined aquifer. For modeling purposes, model cells in the SAS were specified as inactive where the saturated thickness of the SAS was less than 20 ft and the ICU was less than 5 ft thick (fig. 24). In the areas where the SAS was inactive, interaction of the ground-water system with the surface environment, such as stream leakage or net recharge, was applied to the UFA.

Lateral boundary conditions for the UFA and LFA consisted of no-flow and specified-head boundaries. No-flow lateral boundaries for the UFA (fig. 25) were established perpendicular to potentiometric contour lines from the May 1998 UFA potentiometric-surface map (fig. 2). No-flow lateral boundaries for the LFA were coincident with those of the UFA (fig. 25) based on the assumption that the LFA potentiometric surface is similar in configuration to that of the UFA. Specified-head boundaries were established from southwestern Marion to west-central Sumter Counties and across central Orange County (fig. 25). All specified-head cells were simulated using the MODFLOW Time-Variant Specified-Head Package (Leake and Prudic, 1991). Specified-head values for the UFA from southwestern Marion to west-central Sumter Counties and across central Orange County and for the LFA in central Orange County were interpolated from an arithmetic average of data collected in May and September 1998. No water-level data were available for the LFA from southwestern Marion to west-central Sumter Counties; consequently, specified-head values were estimated based on the overlying UFA water levels and an assumed head difference. Aucott (1988) indicated that the area along the Withlacoochee River downstream of State Road 48, including Lake Panasoffkee, is a discharge area for the UFA (fig. 1). Along the model boundary in this area the specified-head values for the LFA were assumed to be 1 ft above those of the UFA and 2 ft below those of the UFA elsewhere along the boundary. Additional no-flow boundaries were specified for the LFA at the interface of freshwater and water with chloride concentrations greater than 5,000 mg/L. A model cell was specified as inactive if less than 3 percent of the layer thickness was above the freshwater/saltwater interface. The small criterion of 3 percent was chosen so the thinning of the aquifer between the point where the freshwater/saltwater interface rises above the bottom of the aquifer to the point where the interface intersects the top of the aquifer (fig. 8) would be accurately represented in the model. Numerous LFA cells met this criterion, generally in the vicinity of the St. Johns River, functioning as a no-flow boundary for the adjacent active LFA and overlying UFA cells (fig. 24).

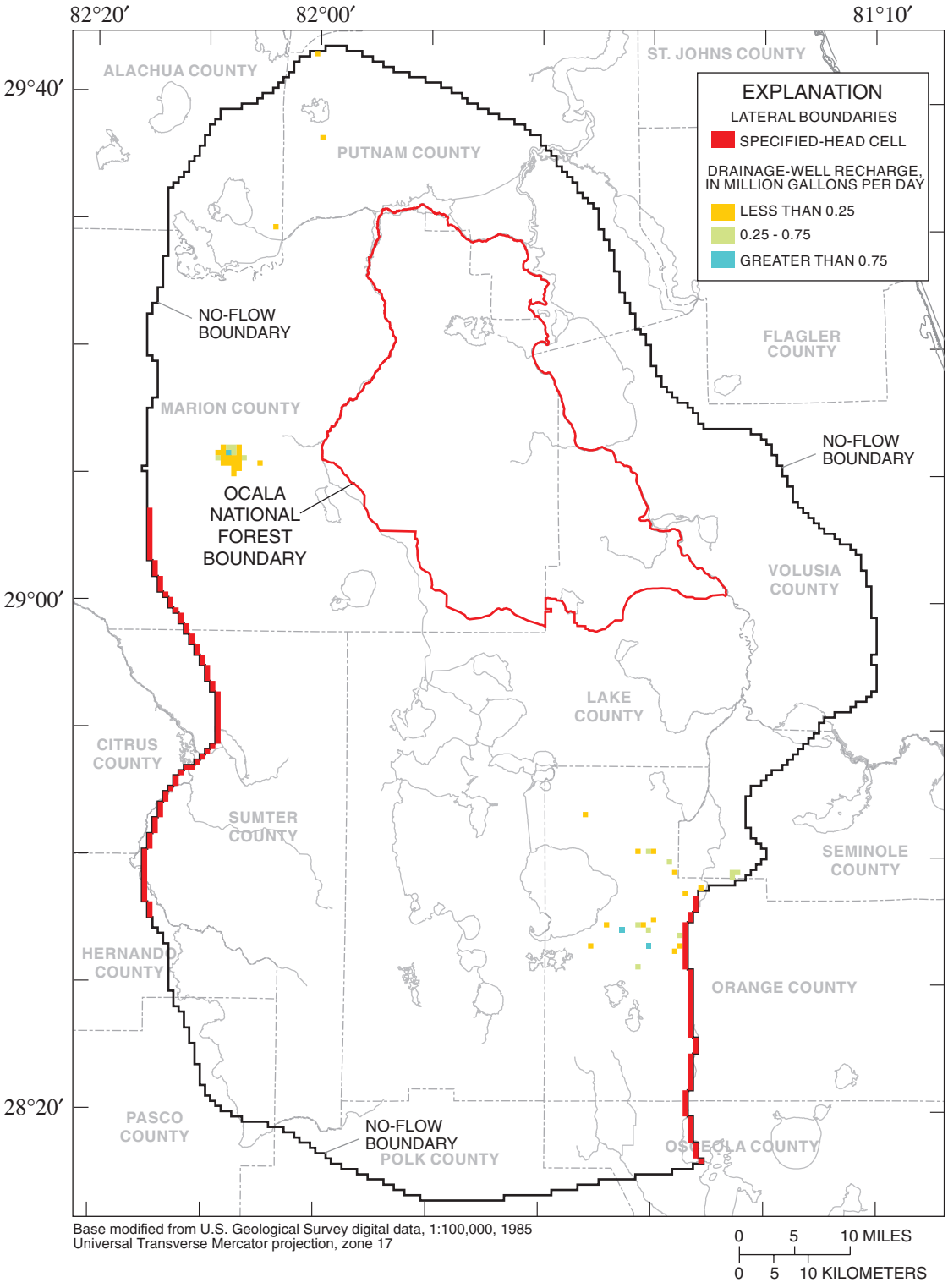

Figure 25. Lateral boundary conditions for the Upper and Lower Floridan aquifers and drainage-well recharge rates for the Upper Floridan aquifer.

Internal boundary conditions were established to represent interaction of the ground-water system with streams, lakes, or wetlands (figs. 26 and 27) because MODFLOW does not simulate surface-water flow. Streams, flow-through lakes, and wetlands were simulated using the MODFLOW River Package, as described in more detail in a later section. Closed-basin lakes were simulated as variable-head cells in the SAS where the area of the lake exceeded 50 percent that of the cell. In order to effectively represent the absence of aquifer materials in these lakes, the hydraulic conductivity of the SAS was specified to be 1,000 times that of the surrounding SAS. This value was of sufficient magnitude to allow the simulation of a flat water table across a lake; likewise, other investigators have reported favorable results using high hydraulic conductivity nodes to represent closed-basin lakes (Lee, 1996; O'Reilly, 1998, p. 37; and Anderson and others, 2002). Although closed-basin lakes are surface-water features, MODFLOW is able to simulate closed-basin lakes because the lack of surface-water flow makes them a surface expression of the ground-water system (Reilly, 2001, p. 6).

Aquifer and Confining Unit Properties

In order to be generally consistent with the known hydrogeology in the model area, the SAS was simulated as an unconfined aquifer and both the UFA and LFA were simulated as confined aquifers. A notable exception is the UFA, which is unconfined in some areas where the water level is below the top of the aquifer and the ICU does not exist. Simulation of the UFA as confined in these areas can result in a calculated transmissivity that is too large. The error resulting from this simplifying assumption is small because the simulated water level averages only 11 ft below the specified top of the aquifer in these areas, which is only 3 percent of the average thickness of the UFA.

Initial values of the horizontal hydraulic conductivity of each aquifer were based on data collected during this study, data reported by previous investigators, or both. All cells in the SAS initially were assigned a horizontal hydraulic conductivity of 6 ft/d with the exception of cells representing closed-basin lakes, which were assigned a value of 6,000 ft/d. The value of 6 ft/d represents the geometric mean of results from 30 slug tests performed in the SAS for this study and reported results of 30 additional slug tests or aquifer performance tests (CH2M Hill, 1989; Szell, 1993; and Spechler and Halford, 2001, p. 16). The initial distribution of horizontal hydraulic conductivity of the UFA was based on data from previous models. As a part of a regional modeling effort covering most of peninsular Florida, Sepúlveda (2002) compiled a grid consisting of square 5,000-ft cells representing transmissivity values for the UFA from 14 different models. The cells of that grid are coincident with the cells of the present model: one 5,000-ft cell of the transmissivity grid covers exactly four 2,500-ft model cells. The portion of the transmissivity grid that is within the boundary of the present model contains data from previously calibrated models by Grubb and Rutledge (1979); Ryder (1985); Tibbals (1990); Blanford and Birdie (1993); Motz (1995); and Murray and Halford (1996). Where previously calibrated models overlap, the value of transmissivity used is the value from the model that provided the best fit between measured and simulated water levels (Sepúlveda, 2002, p. 64). The horizontal hydraulic conductivity of the UFA was calculated by dividing the values in the transmissivity grid by the thickness of the aquifer for each model cell (fig. 28). The initial value of horizontal hydraulic conductivity of the LFA was specified as a uniform value of 200 ft/d, based on an approximate average of transmissivities from previous models and 10 aquifer tests conducted in Orange County (Spechler and Halford, 2001, p. 26) and the approximate aquifer thickness in the model area.

Relatively few data exist on aquifer anisotropy in the model area. Vertical anisotropy is defined as the ratio of horizontal to vertical hydraulic conductivity. Vertical anisotropy is common in many rocks and unconsolidated sediments, and vertical anisotropy of 5 or 10 is not unusual (Bouwer, 1978, p. 56). Camp Dresser and McKee, Inc. (1984) and Sumner and Bradner (1996, p. 21) reported horizontal and vertical hydraulic conductivities with vertical anisotropy values of 1 to 3 for the SAS in western Orange County. Results of a long-term aquifer performance test indicate a vertical anisotropy of 39 for the SAS in eastern Orange County (Bush, 1979, p. 32). Available data based on analyses of rock cores from the FAS indicate highly variable vertical anisotropy values of 0.002 to 267 for the Ocala Limestone and 0.9 to 8 for the Avon Park Formation in Hillsborough County (Robinson, 1995, p. 16) and 0.5 to 38 for the Avon Park Formation and 1.2 for the Oldsmar Formation in north-central Polk County (Navoy, 1986, p. 29). Based on these disparate results, a uniform initial value of 10 for vertical anisotropy was assigned to the SAS, UFA, and LFA.

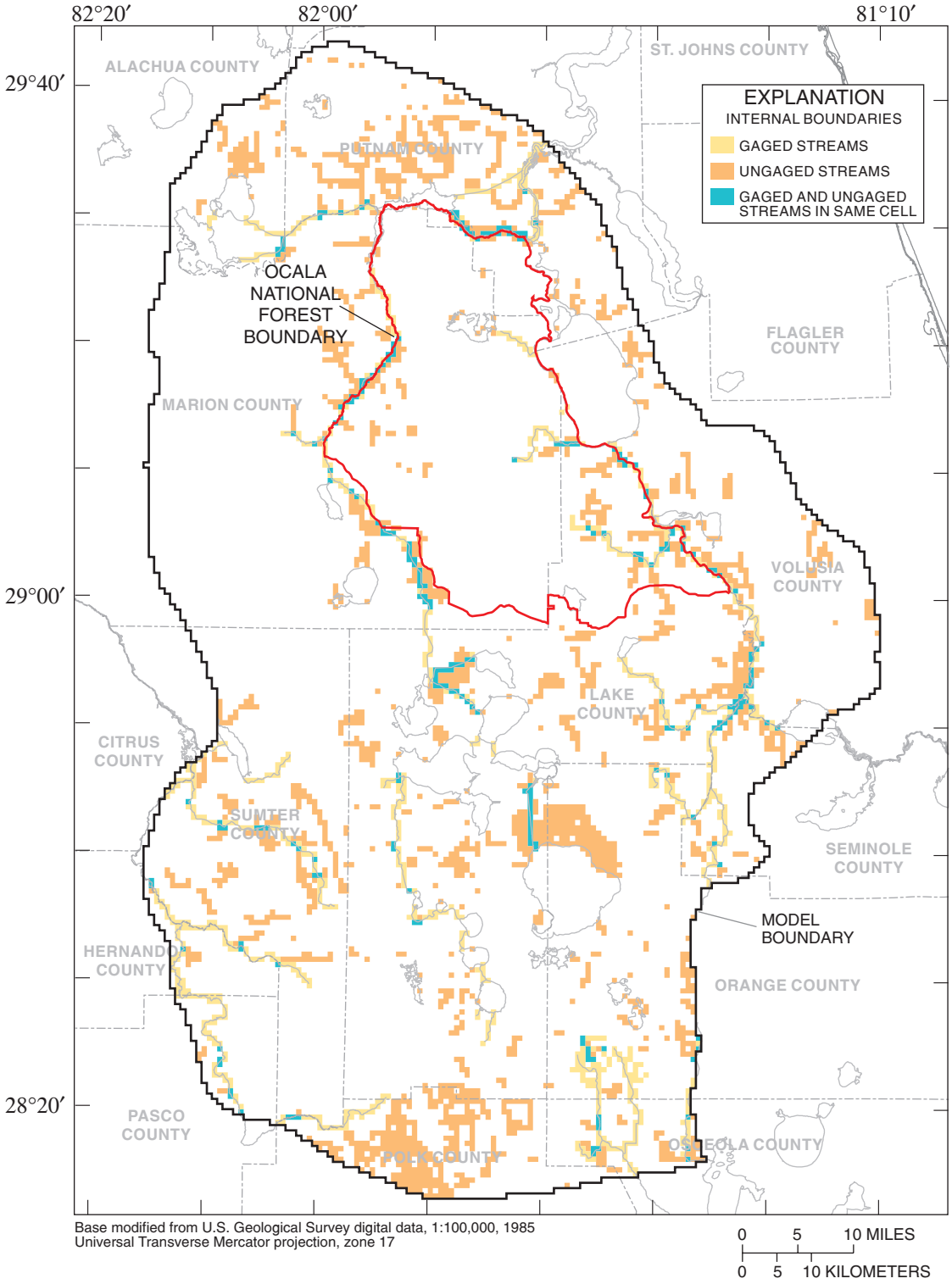

Figure 26. Internal boundary conditions representing streams (boundary conditions are applied to the SAS except where the SAS is inactive, in which case they are applied to the UFA).

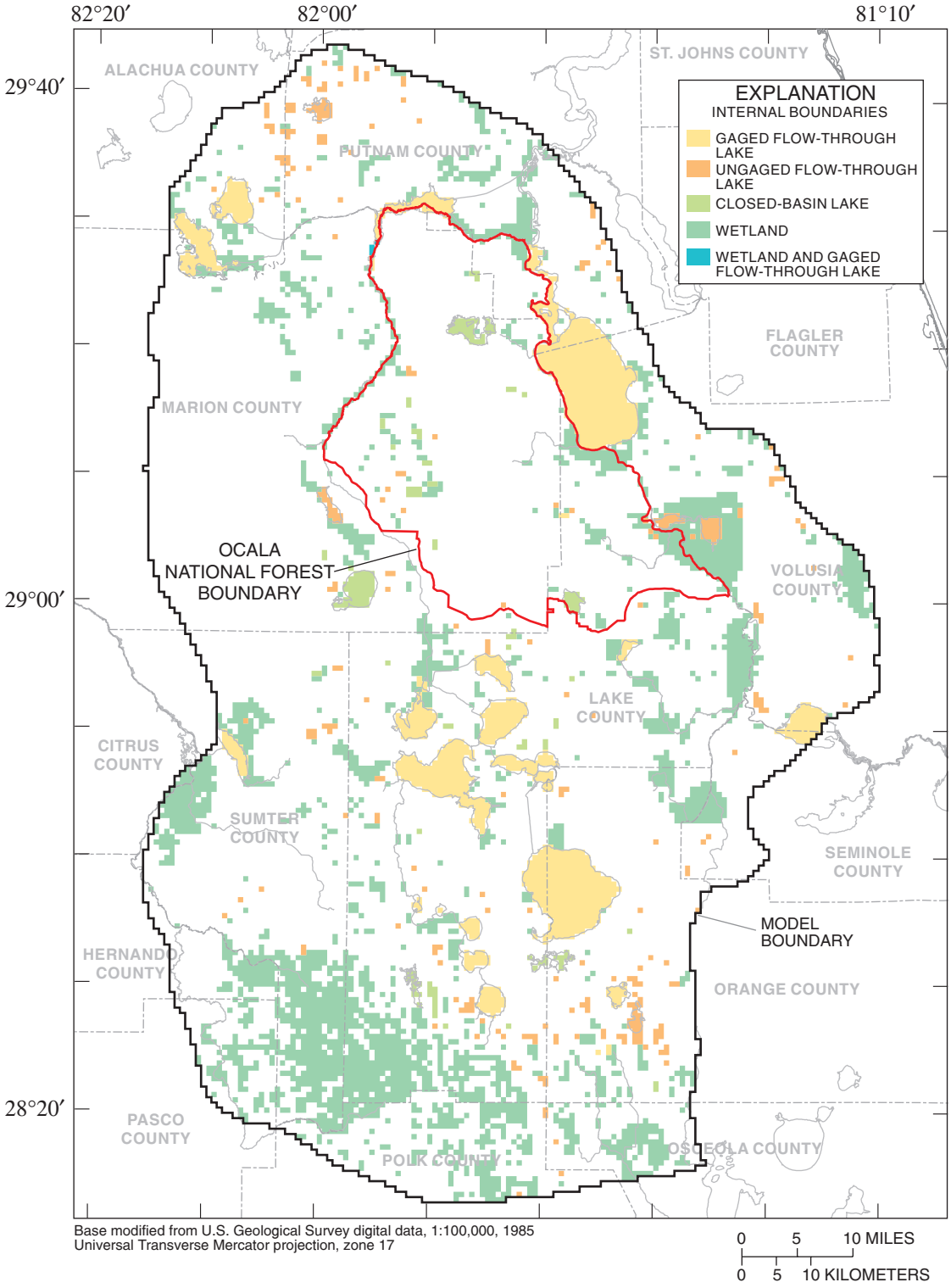

Figure 27. Internal boundary conditions representing lakes or wetlands (boundary conditions are applied to the SAS except where the SAS is inactive, in which case they are applied to the UFA).

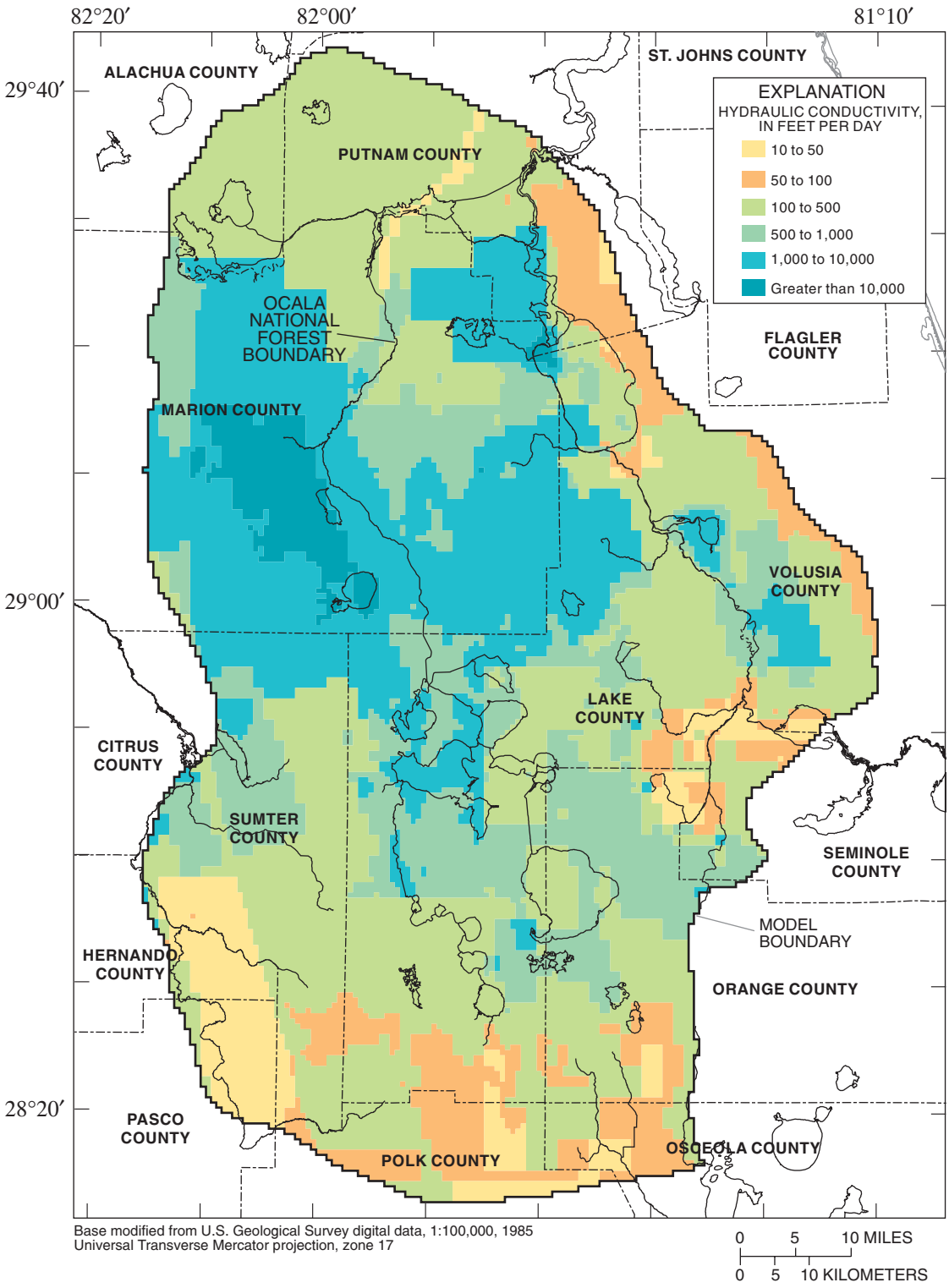

Figure 28. Horizontal hydraulic conductivity of the Upper Floridan aquifer used to initiate model calibration (final values from calibrated model are 20 percent higher).

Horizontal anisotropy is defined in MODFLOW as the ratio of hydraulic conductivity along model columns to that along model rows, because the model grid is assumed to be aligned with the principal directions of hydraulic conductivity (Harbaugh and others, 2000, p. 39). Although some investigators have postulated that fractures and displacements may affect the regional flow of ground water in the FAS (Faulkner, 1973, p. 43), no data are available within the model area to define horizontal anisotropy. Therefore, a horizontal anisotropy of 1 was assigned to the SAS, UFA, and LFA.

Limited data exist for the vertical hydraulic conductivity of the confining units in the model area. Available data based on analyses of cores from the ICU indicate highly variable vertical hydraulic conductivity values of 0.01 to 0.53 ft/d in Lake County (Knochenmus and Hughes, 1976) and $3.2x10^{-6}$ to $4.0x10^{-1}$ ft/d from various locations in the SJRWMD (Boniol and others, 1993). An initial value of 0.02 ft/d was used for the vertical hydraulic conductivity of the ICU. Estimates of the vertical hydraulic conductivity of the MSCU are available from aquifer performance tests conducted in the vicinity of the model area and include values of: 1 to 3 ft/d in south-central Orange County (Boyle Engineering Corp., 1995); less than 0.05 ft/d in eastern Orange County (Phelps and Schiffer, 1996, p. 31); and 0.02 to 2 ft/d in central Osceola County (Post, Buckley, Schuh, and Jernigan, Inc., 1990). The only data available for the vertical hydraulic conductivity of the MCU are those reported by Navoy (1986, p. 29) from laboratory analyses of rock cores obtained from a test well in north-central Polk County: vertical hydraulic conductivities ranged from $2.4x10^{-5}$ to 0.81 ft/d, with a geometric mean of $5.5x10^{-3}$ ft/d, based on samples from 12 different depths. These data, combined with lithologic considerations, indicate that the vertical hydraulic conductivity of the MCU probably is considerably less than that of the MSCU. Therefore, it was necessary to account for this large difference in hydraulic conductivities between the two units, despite the fact that the MSCU and the MCU are represented in the model by only one confining unit. A vertical hydraulic conductivity of 0.07 ft/d for the MSCU/MCU initially was assigned to all cells. This value was modified by a multiplier unique to each model cell to account for the spatial variations in vertical hydraulic conductivity as follows.

- Where only the MSCU exists, a multiplier of 1 was used so the initial value of vertical hydraulic conductivity was 0.07 ft/d.
- Where only the MCU exists, a multiplier of 0.01 was used because field data indicate that, on average, the vertical hydraulic conductivity of the MCU is about one-hundredth that of the MSCU. Therefore, the initial value of vertical hydraulic conductivity was $7x10^{-4}$ ft/d.
- Where both the MSCU and the MCU exist, the multiplier was calculated as $0.01(B/B_{mcu})$ where B is the thickness of the MSCU/MCU specified in the model (extending from the top of the MSCU to the bottom of the MCU) and B_{mcu} is the thickness of the MCU. This effectively means that only the thickness of the MCU is considered when MODFLOW calculates the vertical conductance between the UFA and LFA. This is an acceptable simplification because the vertical hydraulic conductivity of the MCU is much less than that of either the MSCU or the permeable zone between the two units.
- Where neither the MSCU nor the MCU exist, a multiplier of 100 was used so the initial value of vertical hydraulic conductivity was 7 ft/d. This combined with a specified thickness of 1 ft effectively provides no resistance to flow between the UFA and LFA in such areas.

Aquifer Stresses

Aquifer stresses were estimated for calibration of a steady-state model to simulate average 1998 conditions. Where data were available at discrete times during 1998, average annual values were calculated as an arithmetic average of these data.

Recharge and Evapotranspiration

The aquifer system is recharged when sufficient water is applied to overcome evapotranspirative losses and capillary effects in the unsaturated zone and remaining water percolates across the water table. When precipitation or artificial recharge rates exceed the infiltration capacity of the soil, some water continues to move downward, while excess water is rejected and becomes overland runoff. Of the water that reaches the water table, recharge is the fraction that is not quickly extracted by ET and that moves downgradient. However, other processes also can contribute recharge to the aquifer system. In a karst environment,

such as exists in the study area, closed-basin lakes are common and precipitation falling on these lakes must either evaporate or recharge the aquifer. In a karst environment the possibility exists that some fraction of overland runoff provides recharge. Overland runoff to a surface-water body other than a closed-basin lake does not recharge the ground-water system; whereas overland runoff to a closed-basin lake provides water to the lake, which might subsequently recharge the aquifer. In addition, overland runoff that is captured by a land-surface depression, such as might be created by a sinkhole, can subsequently infiltrate and percolate toward the water table. Lastly, water released from storage in aquifer pore spaces or in closed-basin lakes as a result of a falling water level in the aquifer or lake can be mathematically represented as a flux occurring over the time period during which the drop in water table or lake level was measured. Considering all these factors, recharge to the aquifer system was simulated as a net recharge (N) in the model as described by

$$N = P + R_a + O_{cbl} - ET - O_s - \Delta S_{al}, \qquad (6)$$

$$\Delta S_{al} = S_y \Delta H, \qquad (7)$$

where

P is precipitation, [L/T];
R_a is artificial recharge, [L/T];
O_{cbl} is overland runoff to a closed-basin lake, [L/T];
ET is evapotranspiration, [L/T];
O_s is overland runoff to a surface-water body other than a closed-basin lake, [L/T];
ΔS_{al} is change in storage in the aquifer in which the water table is located and in closed-basin lakes, [L/T];
S_y is the specific yield of the aquifer in which the water table is located or equal to 1 for a closed-basin lake, [dimensionless];
ΔH is change in water-table altitude or closed-basin lake level, [L/T]; and

L and T denote length and time units, respectively. Conceptually, the inclusion of ΔS_{al} as a component of net recharge can be interpreted as follows: (1) an increase in storage is equivalent to a reduction in net recharge because a rise in the water-table or closed-basin lake level is produced by water that otherwise would have been available to move downgradient through the aquifer or out of the closed-basin lake or (2) a decrease in storage is equivalent to an increase in net recharge because a drop in the water-table or closed-basin lake level releases water that can move downgradient through the aquifer or out of the closed-basin lake. Because of the small storage coefficients typical of confined aquifers, the change in storage in the confined FAS during 1998 was assumed negligible; therefore, a correction for storage changes was not considered for either the UFA (where it is confined) or the LFA. Net recharge was applied to the SAS, except where the SAS was inactive (fig. 24), in which case it was applied to the UFA.

On an average annual basis, net recharge might not be greatly affected by spatial variations in precipitation, because ET and overland runoff probably have some moderating effect on net recharge. That is, ET and overland runoff probably are greater where precipitation is greater, and ET and overland runoff probably are smaller where precipitation is smaller; therefore, net recharge could be of similar magnitude in both situations. Sumner (2001, p. 46) reported data for Tiger Bay watershed in central Volusia County that might help support this hypothesis, but on a temporal basis; the ratio of annual ET to annual precipitation was 0.74 and 0.77 for 1998 and 1999, respectively, even though precipitation in 1998 was 12 percent less than that in 1999. Based on the results reported by Sumner (2001, p. 46) and the lack of data concerning the actual spatial distribution of ET or overland runoff, model-wide average values were used to estimate several terms in equation 6, as will be discussed later in this section.

The complex process through which net recharge occurs was greatly simplified in the model. Net recharge (eq. 6) was assumed to be divisible into two components: natural net recharge and artificial net recharge. Natural net recharge is net recharge that results from precipitation; whereas artificial net recharge is net recharge from artificial means.

Natural net recharge can occur at the water table or a closed-basin lake. Natural net recharge at the water table (N_n) can be defined by noting that O_{cbl} and R_a of equation 6 will be zero:

$$N_n = P - ET_n - O_{sn} - \Delta S_{aq}, \qquad (8)$$

$$ET_n = ET_{n,min} - ET_{n,ex}, \qquad (9)$$

$$O_{sn} = O_{sn,min} - O_{sn,ex}, \qquad (10)$$

where

ΔS_{aq} is change in storage in the aquifer in which the water table is located, [L/T];

ET_n is natural evapotranspiration, which is evapotranspiration in the absence of artificial recharge, [L/T];

$ET_{n,min}$ is minimum natural evapotranspiration, [L/T];

$ET_{n,ex}$ is excess natural evapotranspiration exceeding $ET_{n,min}$, [L/T];

O_{sn} is natural overland runoff, which is overland runoff in the absence of artificial recharge, to a surface-water body other than a closed-basin lake, [L/T];

$O_{sn,min}$ is minimum natural overland runoff, [L/T]; and

$O_{sn,ex}$ is excess natural overland runoff exceeding $O_{sn,min}$, [L/T].

Substituting equations 9 and 10 into equation 8 and rearranging yields:

$$N_n = P - [ET_{n,min} + O_{sn,min}] - [ET_{n,ex} + O_{sn,ex}] - \Delta S_{aq}. \quad (11)$$

ET and overland runoff are not well known and are difficult to account for in MODFLOW; therefore, the components of ET_n and O_{sn} will be considered together as denoted by the brackets in equation 11. This acknowledges the difficulty in differentiating the individual effects of ET or overland runoff on net recharge. Equation 11 was applied at each model cell of the SAS, or the UFA where the SAS was inactive (fig. 24), except at cells representing closed-basin or flow-through lakes (fig. 27). However, four of the terms of equation 11 (P, $ET_{n,min}$, $O_{sn,min}$, and ΔS_{aq}) were assumed not to vary spatially and model-wide average values were used. In addition, some of the terms of equation 11 will be assumed to be zero depending on whether the simulated water table is above or below the extinction depth. Extinction depth is the maximum depth below land surface from which water contributing to ET can be extracted and is dependent primarily on plant root depth and soil hydraulic characteristics. Areas of the model where the simulated water table is below the extinction depth are referred to as upland zones, and areas of the model where the simulated water table is equal to or above the extinction depth are referred to as transitional zones. Extinction depth was specified to be 13 ft (Tibbals, 1978, p. 10; Tibbals, 1990, p. 10) in all model cells. Lichtler and others (1968, p. 86) reported that the maximum depth of tree roots in Orange County is about 15 ft, which is in reasonable agreement with an extinction depth of 13 ft.

High rates of net recharge often have been considered to exist in areas where the water table is deep, the water table is below the root zone of the local vegetation, and the surficial sands are very permeable (Lichtler and others, 1968, p. 86; Knochenmus and Hughes, 1976, p. 32; and Yobbi, 1996, p. 22). In an upland zone, therefore, ET and overland runoff probably are near their minimum values, and natural net recharge probably is at its maximum value. Therefore, $ET_{n,ex}$ and $O_{sn,ex}$ in equation 11 can be set equal to zero, which yields an expression defined as maximum natural net recharge ($N_{n,max}$):

$$N_{n,max} = P - [ET_{n,min} + O_{sn,min}] - \Delta S_{aq}. \quad (12)$$

$ET_{n,min}$ is assumed to be 27 in/yr based on a value of ET reported by Sumner (1996, p. 30) for nonirrigated, herbaceous vegetation with a deep water table (below the root zone). Knochenmus and Hughes (1976, p. 32) reported that annual overland runoff for the Lake Wales Ridge in Lake County (fig. 3) is 0 to 4 inches; $O_{sn,min}$ was assumed to be zero for the purposes of an initial estimate of $N_{n,max}$. ΔS_{aq} was considered to be negligible because the average change in water level measured in 79 SAS wells during 1998 was only 1.0 inch. Therefore, in an upland zone natural net recharge initially was specified to be a uniform value of 30 in/yr (P = 57 in/yr and $ET_{n,min}$ = 27 in/yr) and was simulated using the MODFLOW Recharge Package.

In a transitional zone, ET and overland runoff are assumed to exceed their minimum values by an amount represented by $ET_{n,ex}$ and $O_{sn,ex}$, respectively. Excess ET is assumed to occur as a result of a shallower water table (equal to or above the extinction depth) in the transitional zone than in the upland zone, and thus water is more accessible to plant roots and direct evaporation. Excess overland runoff is assumed to occur as the simulated water table rises above the extinction depth. The capacity to store water in the unsaturated soil pores decreases as the thickness of the unsaturated zone decreases, and the presence of the fully saturated capillary fringe further reduces this storage capacity. In the ground-water flow model, only

the depth of the water table below the average land surface can be simulated for each model cell. In reality, the simulated water table could be above land surface in some fraction of a model cell and below land surface in the remainder of the model cell, because land surface altitude can vary considerably within a single model cell. If this situation occurred, overland flow should be greater than if the water table were below land surface throughout the model cell. Therefore, the assumption that overland runoff likely will increase as the water table rises above the extinction depth probably is reasonable.

Natural net recharge in a transitional zone is defined by combining equations 11 and 12:

$$N_n = N_{n,max} - [ET_{n,ex} + O_{sn,ex}]. \quad (13)$$

Therefore, natural net recharge always is less in a transitional zone than in an upland zone. The quantity in brackets in equation 13 represents the combined effects of excess ET and excess overland runoff; this quantity was simulated by using the MODFLOW Evapotranspiration Package. The important premise is that the sum of excess ET and excess overland runoff can be approximated as a linear function of water-table altitude; however, either excess ET or excess overland runoff may not individually follow this linear relation. This approximation is believed to be reasonable because both excess ET and excess overland runoff are assumed to be proportional to water-table altitude. The validity of this approximation was tested during model calibration. Substituting the mathematical function used by the Evapotranspiration Package (McDonald and Harbaugh, 1988) for the term $[ET_{n,ex} + O_{sw,ex}]$ of equation 13 yields the following expression for natural net recharge in a transitional zone:

$$N_n = N_{n,max} - R_{ex,max}\left[1 - \frac{z_{ls} - h}{D_e}\right], \quad (14)$$

$$(z_{ls} - D_e \le h \le z_{ls}),$$

where

$R_{ex,max}$ is maximum rate of combined excess ET and excess overland runoff, [L/T];

z_{ls} is mean land-surface altitude in model cell, [L];

h is simulated water-table altitude, [L]; and

D_e is extinction depth, [L].

The minimum rate of natural net recharge ($N_{n,min}$) occurs in a transitional zone when the simulated water-table is above land surface:

$$N_{n,min} = N_{n,max} - R_{ex,max}. \quad (15)$$

$N_{n,max}$ of equations 14 and 15 is identical to that specified for an upland zone; therefore, $N_{n,max}$ was calculated using equation 12 for model cells in transitional zones as well as upland zones and was simulated using the MODFLOW Recharge Package. The initial value of the maximum rate of excess ET was estimated to be 24 in/yr (potential ET of 51 in/yr based on 1998 pan evaporation data minus $ET_{n,min}$ of 27 in/yr). The maximum rate of excess overland runoff is unknown; its initial value was assumed to be equal to the average rate of total overland runoff of 7 in/yr (*RO*, eq. 1 and fig. 23). Therefore, the initial value of $R_{ex,max}$ was specified to be a uniform value of 31 in/yr in all model cells. The altitude at which the maximum rate of ET was simulated by the Evapotranspiration Package was set equal to mean land-surface altitude in each model cell (z_{ls}, eq. 14). Mean land-surface altitude was determined from a digital elevation model interpolated from 5-ft topographic contours from USGS 7.5-minute quadrangles. Therefore, in a transitional zone initial values of natural net recharge varied from -1 to 30 in/yr, depending on the position of the simulated water table.

Figure 29 graphically depicts how equations 12, 14, and 15 and the Recharge and Evapotranspiration Packages were used to simulate natural net recharge at the water table. Where the simulated water table is above land surface, natural net recharge is at its minimum value (eq. 15); where the simulated water table is below the extinction depth, natural net recharge is at its maximum value (eq. 12); and between these two extremes, natural net recharge varies linearly (eq. 14). Using the combined fluxes simulated by the Recharge and Evapotranspiration Packages to simulate natural net recharge eliminates the need to delineate upland and transitional zones. Whether a model cell is in an upland or transitional zone depends only on the simulated position of the water table relative to the specified extinction depth. Furthermore, this allows the model to simulate possible future changes in natural net recharge that might occur as a result of a change in stress, such as future increases in ground-water withdrawals. In addition, changes in the spatial distribution of natural net recharge can be easily effected by adjusting only three parameters in the model: $N_{n,max}$, $R_{ex,max}$, and D_e (fig. 29).

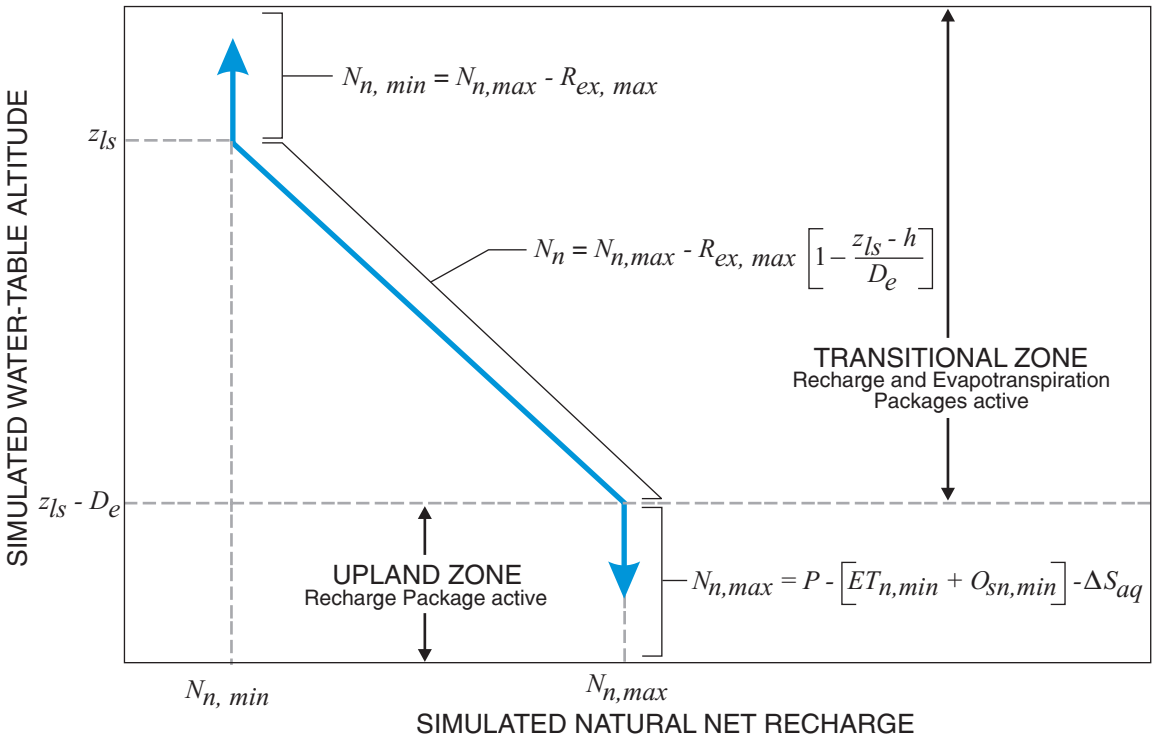

EXPLANATION

D_e	Extinction depth
$ET_{n,min}$	Minimum natural evapotranspiration (that is, evapotranspiration in the absence of artificial recharge)
h	Simulated water-table altitude
N_n	Natural net recharge
$N_{n,max}$	Maximum natural net recharge
$N_{n,\,min}$	Minimum natural net recharge
$O_{sn,min}$	Minimum natural overland runoff (that is, overland runoff in the absence of artificial recharge) to a surface-water body other than a closed-basin lake
P	Precipitation
$R_{ex,\,max}$	Maximum rate of combined excess evapotranspiration and excess overland runoff
ΔS_{aq}	Change in storage in the aquifer in which the water table is located
z_{ls}	Mean land surface altitude in model cell

Figure 29. Simulated natural net recharge at the water table as a function of simulated water-table altitude.

Net recharge was specified at closed-basin lakes (fig. 27) because water levels in these lakes were simulated by the model; net recharge was specified at zero at all flow-through lakes (fig. 27) because these lakes were simulated by internal boundary conditions. Net recharge at a lake is equivalent to natural net recharge because artificial recharge is assumed to be zero at lakes. Net recharge at a closed-basin lake (N_{cbl}) can be defined as follows (based on eq. 6):

$$N_{cbl} = P + O_{cbl} - E_l - \Delta S_{cbl}, \quad (16)$$

where

E_l is lake evaporation, [L/T]; and

ΔS_{cbl} is change in closed-basin lake storage, [L/T].

Because closed-basin lakes generally are located in areas where the surficial sands are permeable, the infiltration capacity of the soil probably is relatively great and overland runoff probably is correspondingly small. Therefore, overland runoff to closed-basin lakes was assumed to be very small and was set equal to zero. Annual lake evaporation in central Florida often has been reported to be slightly less than annual precipitation and is commonly based on pan-evaporation data (Lichtler and others, 1968; Knochenmus and Hughes, 1976; O'Reilly, 1998). Farnsworth and others (1982) reported a value of 48 in. for annual free-water surface evaporation in peninsular Florida, which closely approximates lake evaporation from a shallow lake with negligible heat storage. A study by Swancar and others (2000), however, indicates that annual lake evaporation for a closed-basin lake can actually exceed annual precipitation. Swancar and others (2000) reported that annual lake evaporation (measured by the energy-budget method from August 1996 through July 1998) at Lake Starr, a 134-acre closed-basin lake in central Polk County, exceeded annual precipitation by 13 percent the first year (E_l = 57.08 in. and P = 50.68 in.) and 3 percent the second year (E_l = 55.88 in. and P = 54.04 in.). Actual measurements of lake evaporation were not available for any lakes in the model area in 1998; consequently, lake evaporation was assumed to be equal to potential ET (51 in/yr) estimated from 1998 pan-evaporation data. The change in closed-basin lake storage was estimated to be 5 in/yr, which was the average change in lake level measured at 90 lakes in the model area. Therefore, net recharge at closed-basin lakes initially was specified to be 1 in/yr (P = 57, E_l = 51, and ΔS_{cbl} = 5 in/yr) and was simulated using the MODFLOW Recharge Package.

Artificial recharge applied above the water table consisted of land application of reclaimed water from wastewater treatment plants and effluent leakage from septic tanks. The fraction of artificial recharge that actually percolates to the water table is referred to as artificial net recharge. Artificial net recharge (N_a) can be defined based on equation 6 and noting that P and O_{cbl} are zero, and assuming that artificial recharge causes a negligible change in aquifer storage:

$$N_a = R_a - ET_a - O_{sa}, \quad (17)$$

where

R_a is artificial recharge, [L/T];

ET_a is evapotranspiration extracted from artificial recharge before the water percolates to the water table, [L/T]; and

O_{sa} is overland runoff to a surface-water body as a result of artificial recharge, [L/T]; overland runoff to a closed-basin lake as a result of artificial recharge is assumed to be zero.

Reclaimed water can be applied at the land surface by rapid infiltration basins, spray fields, or some other form of irrigation (agricultural, golf course, or landscape irrigation). Artificial recharge rates were based on 1998 gaged or estimated reclaimed water flow rates (D. Boniol, St. Johns River Water Management District, written commun., 2000). Artificial net recharge from rapid infiltration basins was assumed to be 100 percent of the gaged or estimated flow to the basin. Because the basins are small in area and generally have a high infiltration capacity, it is reasonable to assume a negligible amount of water is lost to ET; also, the nature of basin design and operation ensures that no water is lost to overland runoff. The other forms of reclaimed water application involve irrigation over relatively large areas. As a result of the increase in available water from irrigation, ET will be greater than ET_n (eq. 8) in irrigated areas, resulting in a significant reduction in the amount of water that reaches the water table. In addition, overland runoff from irrigation can occur if the application rate exceeds the infiltration capacity of the soil. The magnitude of overland runoff is unknown, but can occur as a result of, for example, excessive landscape irrigation. Average reclaimed water application rates for 1998 at spray fields, agricultural crops, golf courses, and landscaped

areas were 84, 20, 32, and 24 in/yr, respectively. Because of the relatively small agricultural, golf course, and landscape irrigation rates, all of the reclaimed water was assumed to be lost to increases in ET and overland runoff. However, the large application rates typical at spray fields precluded this assumption, and artificial net recharge at these locations was assumed equal to the application rate reduced by the quantity of water representing the increase in ET. This additional ET resulting from spray-field application of reclaimed water (ET_a, eq. 17) was assumed to equal the difference between potential ET (51 in/yr) and minimum ET (27 in/yr), or 24 in/yr. This assumes that the spray field was located in an upland zone where ET previously was at its minimum value. Likewise, the assumption that most agricultural, golf course, and landscape irrigation is lost to ET_a also is primarily based on the assumption that the irrigation occurs in an upland zone. If reclaimed water irrigation facilities were located in a transitional zone, where ET is simulated to exceed its minimum value, ET_a should be less than 24 in/yr. This possible discrepancy was not formally accounted for in the model for three reasons: (1) the delineation of upland and transitional zones was based on the simulated depth of the water table relative to extinction depth, and assignment of a reclaimed water irrigation facility to one zone or the other and the calculation of ET_a would have to be performed in an iterative manner; (2) overland runoff could account for some fraction of the discrepancy; and (3) the total amount of reclaimed water applied in the model area by irrigation is only 0.2 in/yr averaged over the model area, which is very small compared to other water budget components (fig. 23). Artificial net recharge at rapid infiltration basins and spray fields was simulated using the MODFLOW Well Package (fig. 30). The areal distribution of individual spray fields was unknown; therefore, artificial net recharge at these locations was evenly distributed over a circular area based on the reported acreage and location of each spray field.

Artificial recharge resulting from septic tank leakage was estimated from domestic self-supplied ground-water withdrawal rates. Artificial recharge resulting from septic tank leakage is equivalent to the rate of leakage from septic tank drain fields for the following two reasons: (1) ET induced by the additional water provided by septic tank drain fields (ET_a, eq. 17) is assumed to be negligible, because a septic tank drain field probably would increase the moisture content of the unsaturated zone only in the immediate vicinity of the drain field and probably would not significantly increase the amount of soil moisture available to be lost to ET; and (2) overland runoff (O_{sa}, eq. 17) is zero because septic tank drain fields are located below land surface. Domestic self-supplied withdrawals represent ground-water withdrawn by individual households and small commercial, industrial, and public supply systems with a daily average pumpage of less than 0.01 Mgal/d or fewer than 400 users (Marella, 1999, p. 17). Domestic self-supplied withdrawals and septic tank leakage were assumed to occur only in land-use areas classified as low- or medium-density residential that were not served by a public water supply utility (fig. 31). Domestic self-supplied withdrawal rates generally are compiled by county, and average 1998 withdrawal rates for each county in the model area (table 2) were estimated from 1995 data provided by R.L. Marella (U.S. Geological Survey, written commun., 2000).

Table 2. Domestic self-supplied ground-water withdrawal rates and septic tank leakage rates, average 1998 and projected 2020 conditions

[mi^2, square miles; Mgal/d, million gallons per day; in/yr, inches per year]

County	Area[1] (mi^2)	Domestic self-supplied withdrawals[2] (Mgal/d)		Septic tank leakage (in/yr)	
		1998	2020	1998	2020
Alachua	5.0	0.65	0.71	1.6	1.8
Hernando	3.3	.51	.76	1.9	2.9
Lake	41	11.2	2.0	3.4	.60
Marion	103	22.3	29.8	2.7	3.6
Orange	5.8	6.7	7.3	15	16
Osceola	1.3	.38	.56	3.6	5.4
Pasco	1.5	.33	.38	2.9	3.3
Polk	.67	.10	.13	1.9	2.4
Putnam	35	6.9	6.2	2.5	2.2
Seminole	.00095	.0010	.00066	13	8.8
Sumter	15	3.8	5.7	3.2	4.7
Vousia	5.1	2.0	2.0	4.9	5.0

[1]This represents only the portion of the county within the model area where domestic self-supplied withdrawals and septic tank leakage are estimated to occur.

[2]This represents only the withdrawals that are estimated to occur in the portion of the county within the model area, that is, the county-wide withdrawal rate is greater than this value if the county does not lie completely within the model area.

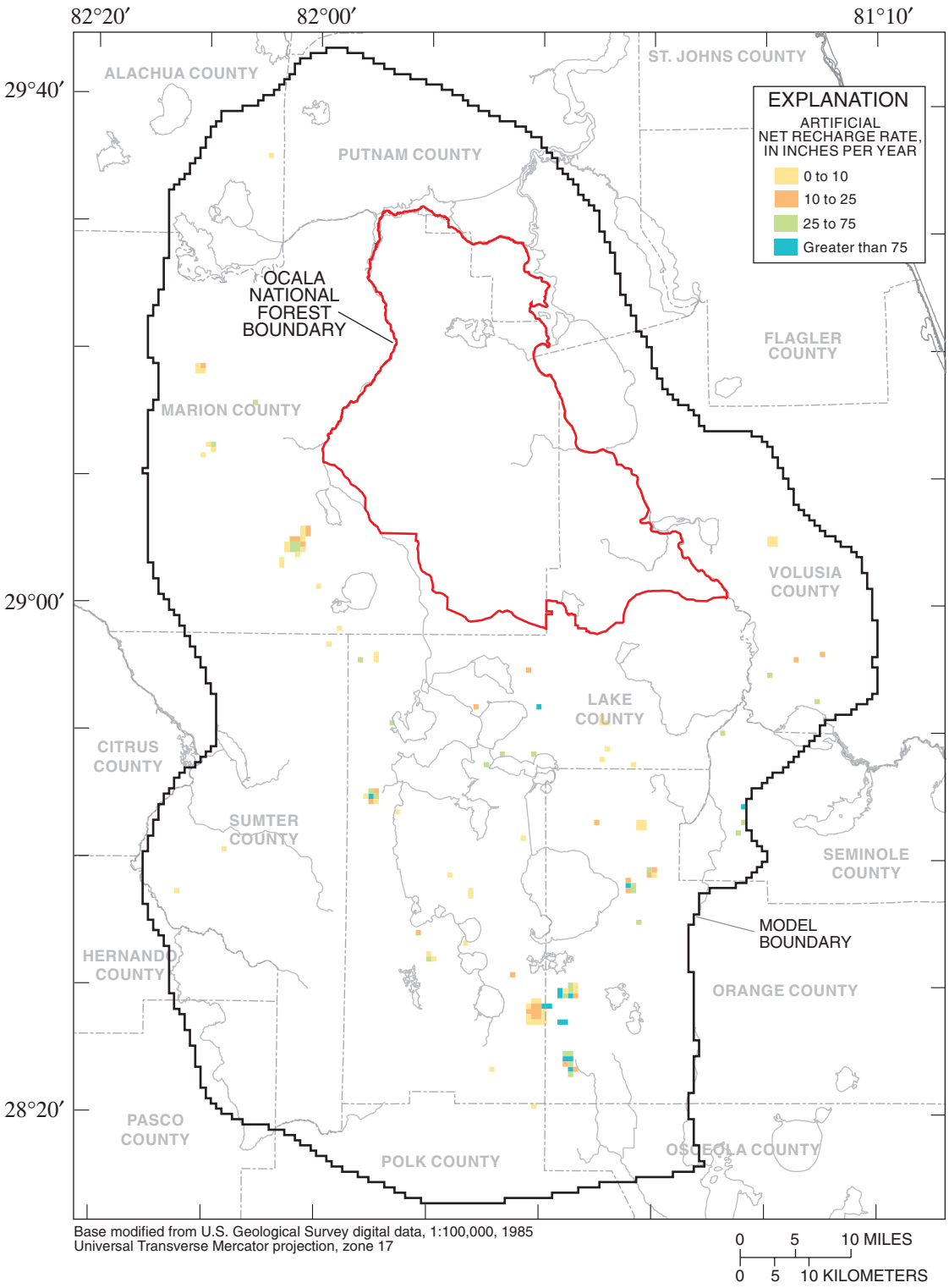

Figure 30. Artificial net recharge rates from rapid infiltration basins and spray fields, average 1998 conditions.

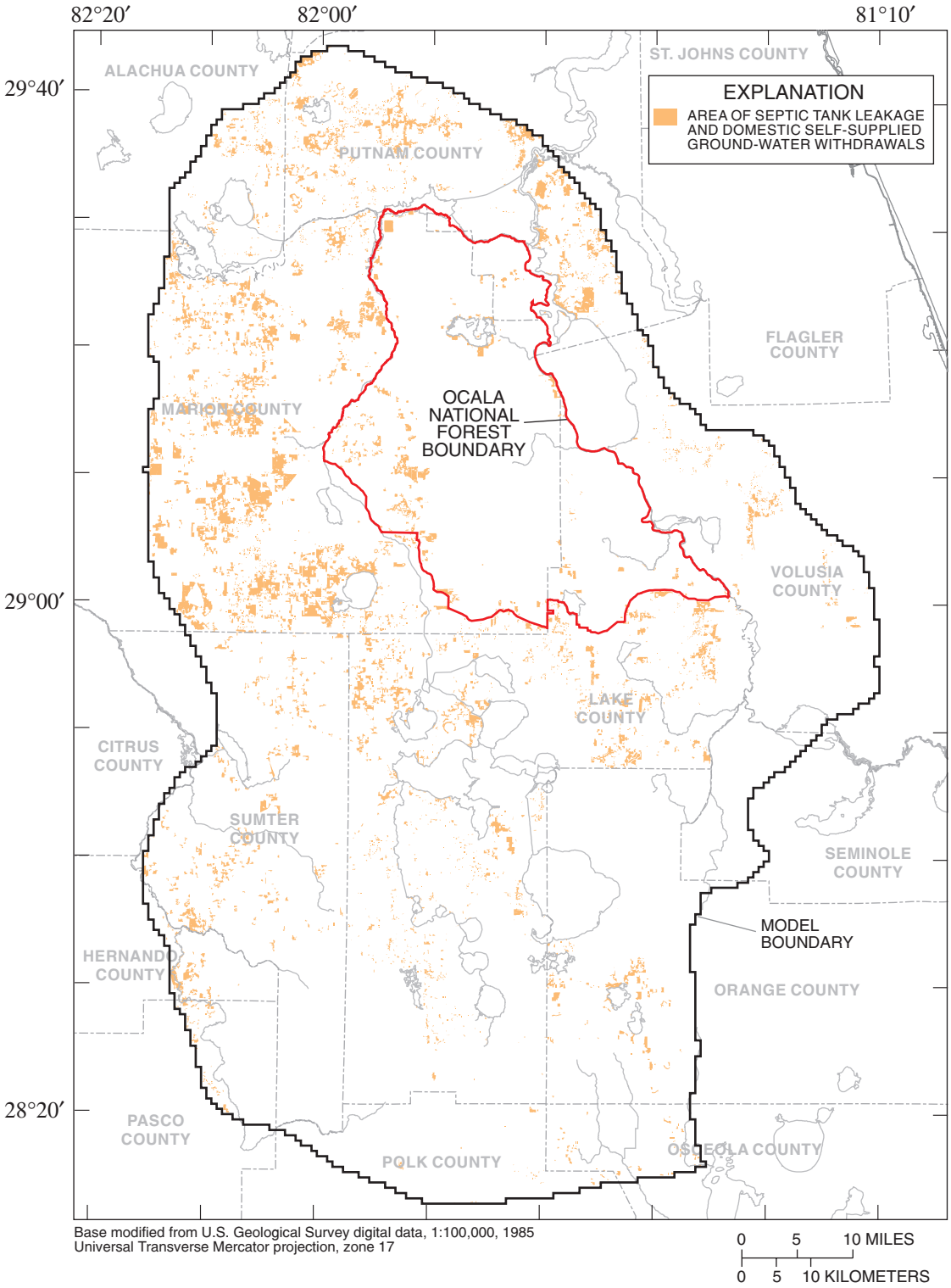

Figure 31. Areas in which septic tank leakage and domestic self-supplied ground-water withdrawals from the Upper Floridan aquifer were estimated to occur (septic tank leakage rates and domestic self-supplied ground-water withdrawal rates are listed in table 2).

Septic tank leakage as a percentage of domestic self-supplied withdrawals was estimated to range from 33 to 140 percent, with an average of approximately 60 percent, for the counties in the model area (R.L. Marella, U.S. Geological Survey, written commun., 2000). Because of the difficulty in accurately estimating these data, average 1998 septic tank leakage for each county was assumed to equal 60 percent of the respective domestic self-supplied withdrawal rate. Using these estimated septic tank leakage rates, a flux was calculated based on the area of each county where domestic self-supplied withdrawals and septic tank leakage were assumed to occur (fig. 31). This yields an average flux representing the artificial recharge resulting from septic tank leakage for each county (table 2). Artificial recharge resulting from septic tank leakage was simulated using the MODFLOW Well Package.

Streams and Lakes

Leakage of water from the ground-water system to streams and lakes, or from streams and lakes to the ground-water system (figs. 26 and 27), was simulated by using the MODFLOW River Package. Only flow-through lakes were simulated by using the River Package. Closed-basin lakes were simulated as variable-head cells. Streams and lakes simulated with the River Package were in hydraulic connection with the SAS, except where the SAS was inactive (fig. 24); streams and lakes in such areas were simulated to be in hydraulic connection with the UFA. Flow between an aquifer and a stream or lake is simulated by the River Package using the following equations (McDonald and Harbaugh, 1988):

$$Q_{riv} = C_{riv}(H_{riv} - h), \quad h > z_{bot}, \tag{18}$$

$$Q_{riv} = C_{riv}(H_{riv} - z_{bot}), \quad h \le z_{bot}, \tag{19}$$

$$C_{riv} = \frac{K_{v,riv}A}{m}, \tag{20}$$

where

Q_{riv} is volumetric flow rate simulated by the River Package, [L^3/T];

C_{riv} is conductance of sediments constituting the riverbed specified in the River Package, [L^2/T];

H_{riv} is stream or lake water-level altitude specified in the River Package, [L^2/T];

h is simulated water-table altitude, [L];

z_{bot} is altitude of the bottom of sediments constituting the riverbed specified in the River Package, [L];

$K_{v,riv}$ is vertical hydraulic conductivity of sediments constituting the riverbed, [L/T];

A is area of sediments constituting the riverbed, [L^2]; and

m is thickness of sediments constituting the riverbed, [L].

Under typical conditions, the flow between an aquifer and a stream or lake is dependent on the head difference between the aquifer and the stream or lake (eq. 18). However, if the simulated water table is below the bottom of the streambed or lakebed, then flow between an aquifer and a stream or lake is no longer dependent on the altitude of the simulated water table: a constant flow to the aquifer is simulated because an unsaturated zone now exists under the stream or lake (eq. 19). Gaged streams and lakes were treated slightly differently than those that were ungaged because additional data existed to better simulate the gaged stream or lake.

For gaged streams, streambed conductance (eq. 20) was based on an estimated vertical hydraulic conductivity for streambed material of 0.3 ft/d, the product of streambed width measured during discharge measurements and total stream length in the model cell (A, eq. 20), and an assumed streambed thickness of 1 ft. No measurements of the vertical hydraulic conductivity of streambed material were available and the spatial variability is unknown; therefore, only a single value of vertical hydraulic conductivity was used. The initial value of 0.3 ft/d was calculated as one-half the vertical hydraulic conductivity of the SAS (horizontal hydraulic conductivity of 6 ft/d and vertical anisotropy of 10). Streambed conductance for gaged streams was adjusted during model calibration by varying $K_{v,riv}$ (eq. 20). Values of stream water level, streambed width, and streambed bottom altitude were assigned by linear interpolation based on measured values at gaging stations using the RIVGRID program developed by Leake and Claar (1999).

No data existed for ungaged streams except their locations, which were obtained from USGS 1:100,000-scale topographic quadrangle maps. Each ungaged stream generally is relatively small. Considered collectively, however, ungaged streams can have a significant impact on the ground-water system because they are a significant surface-water feature in many parts of the model area (fig. 26). Whether all ungaged streams perennially contain water is not known; in particular, some small streams and the headwaters of some streams may have been dry during 1998. Therefore, streambed bottom altitude was set equal to stream water level so the river nodes representing ungaged streams would never be recharging the SAS or UFA (Q_{riv} equals zero when the simulated water table is less than or equal to streambed bottom altitude, eq. 19). Ungaged stream water level was estimated by adding 3 ft to the median land-surface altitude along the stream. Median land-surface altitude along each stream in each model cell was obtained by using a geographic information system to: (1) delineate a 200-ft buffer polygon around all ungaged streams; (2) intersect this polygon with a digital elevation model; and (3) calculate the median land-surface altitude of all digital elevation model nodes that fell within the buffer polygon for each model cell. Because little is known about ungaged streams, the stream water level and streambed bottom altitude were specified at values such that the river nodes representing ungaged streams do not become active until the simulated water table is well above (3 ft) the likely stream water level. At this higher water level, ungaged streams probably are more likely to contain water and flow. Streambed conductance was based on an initial streambed material vertical hydraulic conductivity of 0.3 ft/d, the area of the 200-ft buffer polygon contained in the model cell, and an assumed streambed thickness of 1 ft. Streambed conductance for ungaged streams was adjusted during model calibration by varying $K_{v,riv}$ (eq. 20).

For flow-through lakes, lakebed conductance was based on an initial lakebed material vertical hydraulic conductivity of 0.3 ft/d, the area of the lake contained in the model cell, and an assumed lakebed thickness of 1 ft. Lakebed conductance was adjusted during model calibration by varying $K_{v,riv}$ (eq. 20). Lake stage was obtained from field measurements for gaged flow-through lakes. The water level for each ungaged flow-through lake was estimated from a digital elevation model to be the median value of all digital elevation model nodes that fell within the shoreline of the lake. The water level that had been assigned to lakes in the digital elevation model was equal to the lowest interpolated land-surface altitude along the lake shore; this approximately represents the lake water level depicted on the USGS 7.5-minute topographic quadrangles. A comparison of water levels estimated from the digital elevation model with water levels obtained from field measurements for 27 flow-through lakes indicated that the digital elevation model provided a reasonably accurate estimate of lake water level: water levels estimated from the digital elevation model averaged 0.7 ft less than gaged lake water levels and varied from 2.2 ft less than to 3.2 ft greater than gaged lake water level. Most lakes in the model area are relatively shallow. Danek and others (1991) reported average depths from 7 to 19 ft for Lakes Harris, Beauclair, Dora, Eustis, Yale, Griffin, and Weir. Lakebed bottom altitude was uniformly specified to be 15 ft below the lake water level to reflect the relatively shallow depth assumed for all lakes in the model area.

Wetlands

The numerous wetlands within the model area typically have perennial water levels that are above or very near land surface. Many wetlands are adjacent to streams; consequently, ground-water discharge to wetlands can augment stream flow if the water level in the wetland rises above land surface and overland flow to the stream occurs. Because of this important ground-water and surface-water interaction, wetlands were included in the model (fig. 27) and were simulated using the MODFLOW River Package (eqs. 18, 19, and 20). Wetlands were simulated to be in hydraulic connection with the SAS, except where the SAS was inactive (fig. 24); wetlands in these areas were simulated to be in hydraulic connection with the UFA. Only wetlands that occupied greater than 50 percent of a model cell were included. Conductance of the sediments representing the bed materials of the wetland was based on an initial vertical hydraulic conductivity of 0.3 ft/d, the area of the wetland contained in the model cell, and a thickness of 1 ft. Conductance was adjusted during model calibration by varying $K_{v,riv}$ (eq. 20). The water level in the wetland was estimated using the digital elevation model and adding 3 ft to the median land-surface altitude of the portion of the wetland in each model cell. This water level was used as the river

node stage. The altitude of the riverbed bottom was set equal to the river node stage so the river nodes representing wetlands would never be recharging the SAS or UFA (Q_{riv} equals zero when the simulated water table is less than or equal to riverbed bottom altitude, eq. 19). Using this formulation means that river nodes representing wetlands are inactive except where the simulated water table is greater than 3 ft above the median land-surface altitude in the wetland. The important assumptions are (1) on an average annual basis, a wetland will receive a net gain of water from the ground-water system; and (2) if the water level in a wetland were 3 ft deep, overland flow to nearby streams would occur, representing a loss of water from the ground-water system. These assumptions probably are not always valid, but the use of river nodes to represent wetlands as described above is a reasonable approximation and preferable to not explicitly simulating any ground-water interaction with wetlands.

Springs

All 65 UFA springs documented for this study were included in the model (fig. 7 and table 1), representing a total springflow of 1,279 Mgal/d (about 5.6 in/yr averaged over the model area). During model calibration each spring was simulated with a single UFA well discharging an amount of water equal to the measured or estimated 1998 springflow (table 1). The flow from some springs is derived in part from zones of saline water in the UFA. Some of these zones might contain water with chloride concentrations exceeding 5,000 mg/L; consequently, some fraction of the springflow would be derived from the saline water flow system, which is not simulated by the model. However, no adjustments were made to the springflows specified in the model to account for this possibility because of the lack of data available to make this determination. The MODFLOW Drain Package was used to simulate the springs in the final calibrated model. This allowed simulated springflow to vary as the head difference between the specified spring pool altitude and the simulated UFA water level changed during predictive simulations.

Based on the assumption that the hydraulic properties of the FAS are constant and that spring pool altitude will change relatively little over time, impacts on springflow from future stresses on the ground-water system primarily are a function of changes in the UFA water level at the spring. The change in flow at a spring simulated by the Drain Package is largely dependent on the initial simulated head difference at the spring. For example, if the actual head difference at a spring is 10 ft and the simulated head difference is 5 ft, a simulated 1 ft drawdown at the spring would result in a 20 percent decrease in simulated springflow. However, if the initial simulated head difference were equal to its actual value of 10 ft, the simulated decrease in springflow would be only 10 percent for the same 1 ft drawdown. Considering this reasoning when converting spring "wells" to "drains," a drain elevation (representing an adjusted spring pool altitude) was calculated so that the simulated 1998 head difference was equal to the measured or estimated head difference. The head difference at each spring was calculated as the altitude of the average UFA water level in the model cell containing the spring (interpolated from May 1998 (fig. 2) and September 1998 (Bradner, 1999) potentiometric maps) minus the measured or estimated 1998 spring pool altitude. Spring pool altitudes measured during 1998 were available for 18 springs, representing 83 percent of total spring flow; spring pool altitudes for the remaining 47 springs were estimated from land-surface altitudes obtained from USGS 7.5-minute topographic quadrangles. The spring conductance was calculated as the 1998 spring discharge divided by the head difference. This formulation acknowledges the fact that in any calibration effort discrepancies exist between simulated and measured water levels. By forcing the simulated head difference at each spring to equal its measured or estimated value, a change in springflow from 1998 conditions as a result of projected future conditions will not be affected by an incorrectly simulated 1998 head difference.

Pumping and Drainage Wells

Average 1998 ground-water withdrawals for the FAS from pumping wells within the model area were estimated to total approximately 470 Mgal/d (about 2.1 in/yr averaged over the model area). This total included water used for public supply, agriculture, commercial or industrial purposes, recreation, and domestic self-supply. Ground-water withdrawals from the SAS, if occurring, are small and were not included

in the model. Pumping rates for 1998 were available for wells in the SWFWMD (Jim Waylon, Southwest Florida Water Management District, written commun., 1999); however, 1998 rates were not available for many wells in the SJRWMD and the South Florida Water Management District (SFWMD), and, therefore, were estimated based on 1995 rates obtained from Brian McGurk (St. Johns River Water Management District, written commun., 2000) and L.H. Motz (University of Florida, written commun., 1999). County-wide average pumping rates for 1998 were acquired from R.L. Marella (U.S. Geological Survey, written commun., 2000), and were used to estimate 1998 pumping rates for individual wells by using the percent change in the county-wide average pumping rate from 1995 to 1998 (for wells with reported rates) for each water-use category. Estimated 1998 pumping rates for individual wells were calculated so that the total pumpage in each county, including wells with reported 1998 pumping rates, equaled the 1998 county-wide pumpage provided by R.L. Marella (U.S. Geological Survey, written commun., 2000). Reported 1998 pumping rates represented approximately 35 percent of the total pumpage in the model area; the remaining 65 percent of the total pumpage was estimated from 1995 data. Well location and construction data were obtained from Brian McGurk (St. Johns River Water Management District, written commun., 2000), Jim Waylon (Southwest Florida Water Management District, written commun., 1999), and L.H. Motz (University of Florida, written commun., 1999), with the exception of domestic self-supply wells.

Where available, total well depth and well casing depth were used in combination with hydrogeologic maps to determine whether a well was withdrawing water from either the UFA or LFA or both. Where no well construction data were available, 100 percent of the well pumpage was assigned to the UFA. Where well construction data indicated a well was withdrawing water from both the UFA and LFA, total well pumpage was divided between the two aquifers based on the thickness of each aquifer open to the well and an assumed ratio of UFA to LFA horizontal hydraulic conductivity of 0.5. The ratio of 0.5 is based on an average transmissivity of 80,000 ft^2/d for the UFA and 500,000 ft^2/d for the LFA, based on results of aquifer performance tests reported by Szell (1993) and Spechler and Halford (2001, p. 24 and 26), and an average aquifer thickness of 400 ft for the UFA and 1,300 ft for the LFA, calculated from aquifer and confining unit base altitudes specified in the model. Very few wells withdraw water from both the UFA and LFA, and pumping from these wells represents less than 3 percent of total ground-water withdrawals in the model; therefore, the error resulting from this approximation probably has little impact on model results. The final distribution of ground-water withdrawal rates, excluding domestic self-supplied withdrawals, for average 1998 conditions used in the model for the UFA and LFA are shown in figures 32 and 33, respectively.

Domestic self-supplied ground-water withdrawals were based on estimated 1998 rates (table 2) and distributed evenly county-by-county over low- and medium-density residential land-use areas that were not served by a public water supply utility (fig. 31). The 1998 estimate of domestic self-supplied water use was 20 percent greater than the 1995 values provided by R.L. Marella (U.S. Geological Survey, written commun., 2000), and was based on the 20 percent increase in total public-supply water-use change over the same time period (1995-1998). All domestic self-supply wells were assumed to be withdrawing from only the UFA. All pumping wells were simulated using the MODFLOW Well Package.

Average 1998 recharge rates from drainage wells within the model area were estimated to total approximately 13 Mgal/d (about 0.06 in/yr averaged over the model area). Average drainage-well recharge rates for a particular period of time are strongly correlated to the amount of precipitation during that period (Sepúlveda, 2002, p. 34). Sepúlveda (2002, p. 34-35) estimated average drainage-well recharge rates for the period August 1993 through July 1994 based on a reanalysis of data reported by CH2M Hill (1997) and Bradner (1996) for wells in the Orlando metropolitan area, and extrapolated these data to wells outside the Orlando metropolitan area. Estimated drainage-well recharge rates specified in the present model (fig. 25) were based on those reported by Sepúlveda (2002, p. 34-35), but those estimates were adjusted to reflect 1998 conditions by multiplying by the ratio of precipitation during 1998 to that during the period August 1993 through July 1994. All drainage wells were simulated using the MODFLOW Well Package.

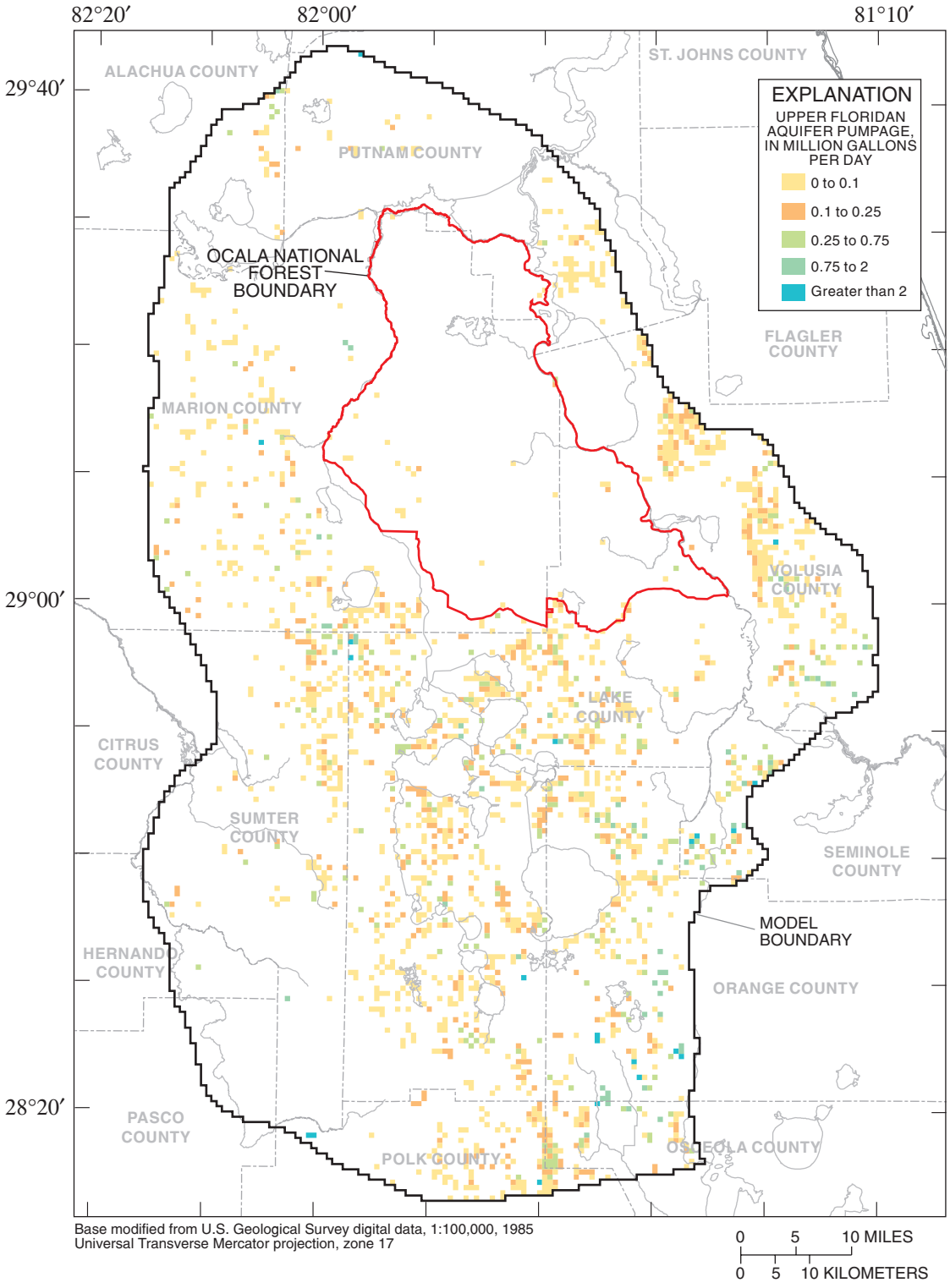

Figure 32. Ground-water withdrawal rates for the Upper Floridan aquifer specified in the model, average 1998 conditions.

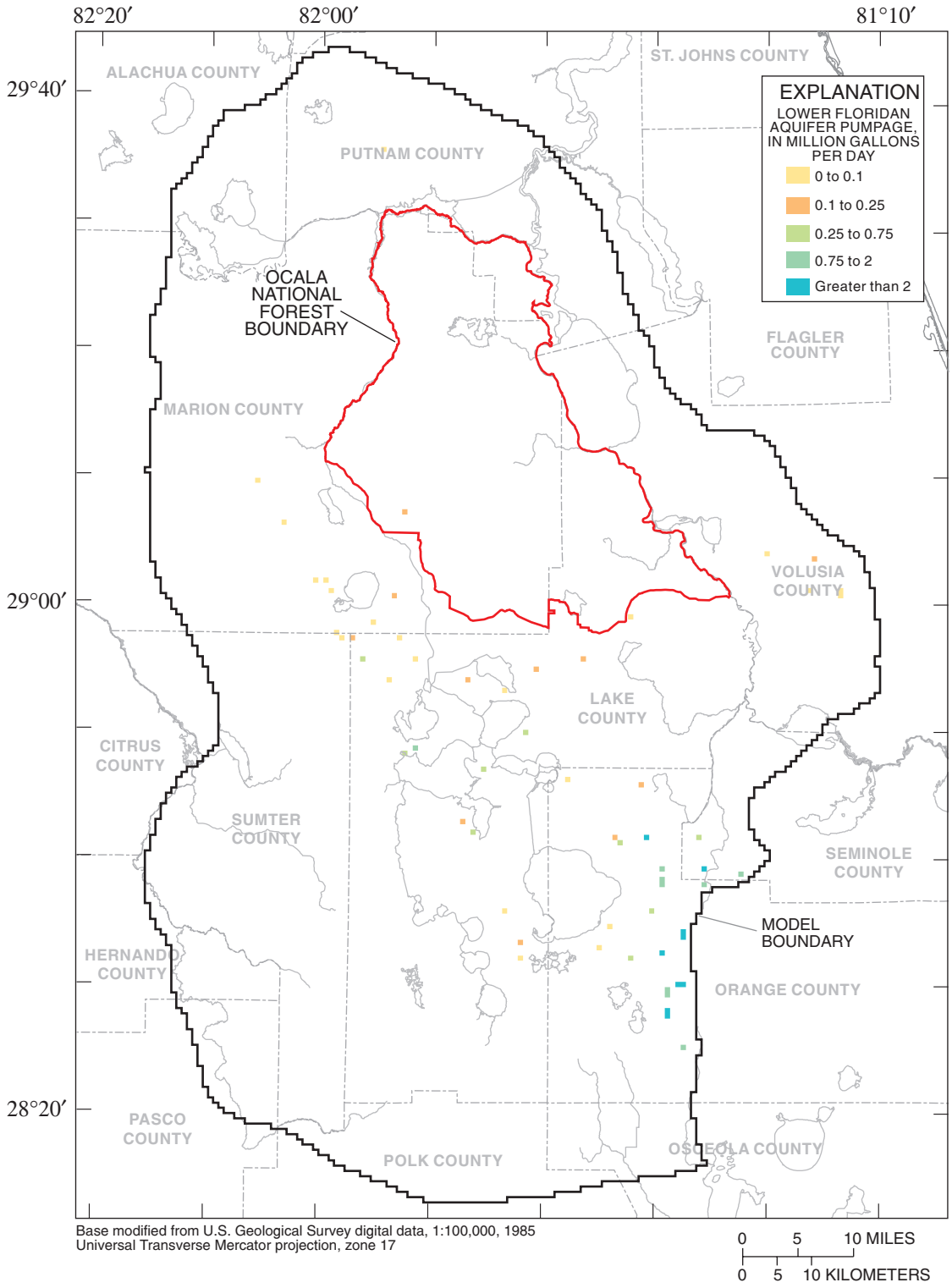

Figure 33. Ground-water withdrawal rates for the Lower Floridan aquifer specified in the model, average 1998 conditions.

Calibration

Calibration is the attempt to reduce the difference between model results and observed data by adjusting model hydrologic parameters within reasonable ranges. In MODFLOW, a parameter is defined as "a single value that is given a name and determines the value of a variable used in the finite-difference ground-water flow equation at one or more model cells" (Harbaugh and others, 2000, p. 4). For the purposes of the present model, the numerical value of a parameter is defined as a "parameter value;" the model cell or group of model cells to which the parameter applies is defined as a "parameter zone;" and the areal distribution of parameter zones for all parameters is defined as the "parameter zonation" of the model. Simulated values usually depart from observed values, even after a diligent calibration effort. The differences between model results and observations usually result from the simplifications inherent in the conceptual model, grid scale, and the difficulty in obtaining sufficient measurements to account for all of the spatial variation in hydrologic properties and stresses throughout the model area.

The steady-state ground-water flow model was calibrated to water-level and flow data collected from December 1997 to December 1998 (average 1998 conditions). The rationale for developing the steady-state calibration to average 1998 conditions was as follows: model results will be used to ascertain the long-term hydrologic effects of future ground-water withdrawals, not the relatively short-term transient variations that may occur as a result of, for example, a period of below-average precipitation. The SAS is strongly influenced by temporal variations in precipitation, ET, and the movement of water in the unsaturated zone. However, sufficient data do not exist to simulate unsaturated-zone hydraulics on a regional scale. In addition, a transient simulation would have introduced at least three more variables, SAS, UFA, and LFA storage coefficients, which are not well known. December 1997 to December 1998 was the longest period during the 16 months of data collection for this study that the SAS and FAS were considered reasonably near steady-state based on measured water levels. Calibration to historical data (that is, data collected prior to the data-collection period for this study) was not feasible because relatively few data existed prior to this study, especially for the SAS. Finally, the bimonthly frequency of data collection during the study period was sufficient for calculation of representative annual average values.

Inverse Model

Model calibration was facilitated by using the Observation, Sensitivity, and Parameter Estimation Processes of MODFLOW (Hill and others, 2000). These capabilities of MODFLOW, which use nonlinear, least-squares regression and associated statistics, constitute the inverse model that was used to automatically calculate parameter values that produce the smallest differences, or residuals, between observed water levels and flows, or observations, and simulated water levels and flows. The fit between observed and simulated water levels and flows is quantified by the following weighted least-squares objective function (Hill, 1998, p. 4), the value of which is referred to as the sum of squared, weighted residuals (*SSWR*):

$$SSWR = \sum_{k=1}^{no} w_k (y_k - \hat{y}_k)^2, \qquad (21)$$

where

y_k is kth observed water level, [L], or flow, [L^3/T];

$\hat{y}_k$ is kth simulated water level, [L], or flow, [L^3/T];

w_k is the weight for the kth water level, [L^{-2}], or flow, [$(L^3/T)^{-2}$]; and

no is the number of water-level and flow observations.

The weights in equation 21 account for measurement errors incurred in acquiring the observation in the field and normalize the residuals to account for the difference in units between water-level and flow observations. The best fit between observed and simulated values, and therefore, the set of optimal parameter values, is achieved by minimizing the objective function (eq. 21). The minimum of the objective function generally is considered to be attained at the iteration when the greatest change in any parameter value is less than 1 percent (Hill and others, 2000, p. 79); this was the convergence criterion used in the present model.

Parameter values estimated by an inverse model are optimal only for the given conceptual model, parameter zonation, and observations. That is, different conceptual models, parameter zonations, or observations could yield a different set of optimal parameter values. Observations generally will not change for a given calibration effort once errors (for example, a water-level observation assigned to the incorrect

aquifer) have been identified and resolved. Therefore, the primary focus of model calibration with an inverse model is to identify the conceptual model and parameter zonation that best match the available observations. A statistic that can be used to compare various conceptual models and parameter zonations is the standard error of the regression (*SE*):

$$SE = \sqrt{\frac{SSWR}{no - np}}, \qquad (22)$$

where *np* is number of estimated parameters and the other variables are as defined in equation 21. A smaller value of *SE* is preferred because it generally indicates a model that both more closely matches the observations and has fewer parameters. Other qualities of a more accurate model include: reasonable parameter values; narrower confidence intervals on the estimated parameters; weighted residuals that are independent and normally distributed; and weighted residuals that exhibit no consistent spatial patterns or trends (Hill, 1998, p. 49 and 53). An inverse model can provide the statistics to make these evaluations. Testing alternative conceptual models and parameter zonations is a trial-and-error process that can be significantly guided by the use of an inverse model and its related statistics, but this process must be constrained by more qualitative hydrologic knowledge and actual field data. Additional details on the theory and application of inverse modeling to ground-water flow problems are presented by Carrera and Neuman (1986a, 1986b, 1986c), Yeh (1986), Cooley and Naff (1990), Poeter and Hill (1997), Hill and others (1998), and Hill (1998).

Observations

The inverse model included water-level observations from 54 closed-basin lakes (assumed to be representative of the SAS water table), 79 SAS wells, 251 UFA wells, and 20 LFA wells. Multiple measurements for a well or lake were reduced to a single representative 1998 water-level measurement by calculating an arithmetic average.

The inverse model also included one flow observation representing the total ground-water discharge, or base flow, (excluding spring discharge) to all streams and all lakes and wetlands that drain to streams in the model area. This quantity was independently estimated for the entire model area by examining 1998 discharge records of gaging stations located where major streams entered or exited the model area. Base flow was estimated by applying a 30-day sliding minimum to the total gaged discharge record; this is similar to the sliding-interval method described by Sloto and Crouse (1996), except the width of the sliding interval used by Sloto and Crouse (1996) is dependent on stream drainage area. This analysis resulted in an estimate of approximately 7.2 in/yr for overland runoff and 11.4 in/yr for base flow. Of this 11.4 in/yr, 5.6 in/yr is springflow, which leaves 5.8 in/yr (1.78×10^8 ft^3/d) of base flow that was used as an observation. This method of estimating base flow is simple and may contain considerable error, but it is believed to be a reasonable approximation considering the large degree of uncertainty inherent in all streamflow hydrograph-separation techniques. Measured or estimated springflows were not included in the inverse model as observations because the conductance term is poorly known and typically has to be individually estimated for each spring. In addition, most large springs are believed to have reliable flow measurements for 1998 (90 percent of total springflow was based on measurements made in 1998 as shown in table 1); therefore, specifying these flows with the MODFLOW Well Package is less problematic than if considerable error were known to exist in these measurements.

The weight (w_k of equation 21) assigned to each observation was equal to the inverse of the variance of the estimated measurement error (Hill, 1998, p. 45). The measurement errors for each observation were assumed to be normally distributed. For water-level observations, it was assumed that there was a 95-percent probability that the true water level was within ±2 ft of the observed water level; this yields a standard deviation of measurement error of 1 ft and a weight of 1 ft^{-2}. For the flow observation, it was assumed that there was a 95-percent probability that the true base flow was within ±20 percent of the estimated base flow; this yields a coefficient of variation of measurement error of 10 percent and a weight of approximately 3.1×10^{-15} (ft^3/d)$^{-2}$. The large error specified for the flow observation acknowledges the large uncertainty in this observation. Assignment of weights is subjective, although Hill (1998, p. 48) states that the method described above generally works well in practice. In addition, the inverse model was relatively insensitive to the weights used; for example, increasing the weights for all water-level observations to 4 ft^{-2} resulted in relatively little change in the final parameter values estimated by the inverse model.

Calibration Procedure

A three-step iterative procedure was used to calibrate the model:

1. Adjust parameter values to minimize the differences between observed data and the corresponding simulated values for a given conceptual model and parameter zonation. For example, change net recharge to better match observed water levels in an aquifer.
2. Adjust the parameter zonation, followed by repeating step 1 for a given conceptual model. For example, assume that the hydraulic conductivity of an aquifer in the western part of a model area is different from that in the eastern part and estimate separate values for each.
3. Adjust the conceptual model, followed by repeating step 1 and, possibly, step 2. For example, simulate the possible presence of a confining unit not included in the original conceptual model.

Step 1 was performed automatically by the inverse model, and steps 2 and 3 were performed in a trial-and-error manner. This three-step procedure was continued until a combination of a conceptual model, parameter zonation, and parameter values were attained that best matched both the quantitative observed data and the modeler's qualitative knowledge of the hydrologic system.

The calibration procedure relied heavily upon the principal of parsimony. Hill (1998, p. 37) explains that, "Using the principal of parsimony, the model is kept as simple as possible while still accounting for the system processes and characteristics evident in the observations and while respecting other information about the system." Hill (1998, p. 38) further states that use of a simple model generally will produce a well-posed inverse model that will converge to an optimal set of parameter values, given reasonable starting parameter values. Using the inverse model and the principal of parsimony, the three-step model calibration procedure was continued until a model was obtained that best met the following criteria: small standard error; narrow confidence intervals on estimated parameter values; weighted residuals that were random, independent, and normally distributed; and realistic parameter values. This process is an objective analysis of the information provided by the observations.

Calibration started with a very simple model and complexity was added as warranted by statistics calculated by the inverse model. Composite scaled sensitivity and parameter correlation coefficient are two statistics that are particularly useful for determining which parameters could likely be uniquely estimated with the available observations (Hill and others, 1998, p. 523). The composite scaled sensitivity for a parameter is a measure of the total amount of information provided by all the observations for the estimation of that parameter. The larger the composite scaled sensitivity, the more sensitive the model is to that parameter. The inverse model generally will have difficulty converging if the composite scaled sensitivity for any parameter is less than 0.01 times the largest composite scaled sensitivity (Hill, 1998, p. 38). The parameter correlation coefficient is a measure of the linear dependence of one parameter on another. Two parameters with a correlation coefficient exceeding 0.95 generally cannot be uniquely estimated (Hill and others, 1998, p. 523).

During the calibration process the simulated water level in the SAS was below the bottom of the aquifer in some areas, primarily in western Marion and northern Sumter Counties. For the purposes of this model, the altitude of the base of the SAS was adjusted to maintain a minimum aquifer thickness of 20 ft throughout the model area. The altitudes of the bases of all the underlying confining units and aquifers also were adjusted to maintain their original thicknesses. This was reasoned to be an acceptable solution to this problem, as opposed to adjusting parameter values in the immediate vicinities of these isolated areas, for the following reasons: First, no SAS wells, lakes, or streams exist in these areas to provide data on the altitude of the water table that could be used to guide the adjustment of parameter values in these areas. Also, regional interpolation of lithologic data collected only at isolated locations might have led to the erroneous interpretation that an areally continuous SAS exists in these areas. Faulkner (1973, p. 35) and Phelps (1994, p. 5) reported that the Hawthorn Group has been removed by erosion in western Marion County and any remnants commonly form isolated caps on hilltops. This degree of detail generally was not portrayed on the lithologic maps compiled for this study (figs. 10 and 11), which depict a more generalized lithology. Therefore, additional areas where the SAS possibly should have been simulated as inactive could not be delineated because of the lack of more detailed lithologic data. Finally, nearly all the net recharge applied at the water table in these areas reaches the UFA as leakage through the ICU, because

very little lateral flow is simulated in the SAS in these areas. This is essentially equivalent to specifying the SAS as inactive in these areas and applying net recharge directly to the UFA, as was done in areas where the SAS was known to be absent. Therefore, the error introduced by actively simulating the SAS in these isolated areas, where perhaps the SAS does not exist, probably is negligible. After adjustments were made to the aquifer and confining unit base altitudes, additional calibration was performed to attain the final calibrated model.

Parameter Values from Calibrated Model

Thirteen parameters constitute the parameter zonation used in the final model and collectively define the hydrologic properties of the ground-water flow system in the model area (table 3). Zonation of the model into areas of homogeneous hydrologic properties (each zone characterized by one constant parameter value) minimizes nonuniqueness problems, which commonly are caused by estimating too many parameters. A nonunique solution is not desirable because it indicates that different sets of parameters can be estimated from the same set of observations (Carrera and Neuman, 1986b, p. 212). All parameters representing hydraulic conductivity or anisotropy were log-transformed in MODFLOW using the natural logarithm; this can promote convergence of the inverse model by making the ground-water flow equation less nonlinear and prevent actual parameter values from becoming negative (Carrera and Neuman, 1986b, p. 214).

Eight parameters were estimated with the inverse model for the final calibrated model (table 3). The remaining five parameters were specified in the ground-water flow model but were not estimated using the inverse model (table 3). The sensitivity of the model to the various parameters did not change greatly during the calibration process, as evidenced by the generally similar composite scaled sensitivities between the initial and final parameter values (fig. 34).

Table 3. Initial parameter values specified in the model and final parameter values estimated with the inverse model to calibrate the model

[ET, evapotranspiration; in/yr, inches per year; ft/d, foot per day; ≤, less than or equal to; >, greater than; --, not applicable]

Parameter description	Parameter symbol	Initial value	Final value
Maximum rate of natural net recharge for entire model area excluding lakes (in/yr)	$N_{n,max}$	30	27
Net recharge at closed-basin lakes[1] (in/yr)	N_{cbl}	1.0	--
Maximum rate of combined excess ET and excess overland runoff[1] (in/yr)	$R_{ex,max}$	31	--
Horizontal hydraulic conductivity (ft/d):			
Surficial aquifer system	$K_{h,sa}$	6.0	22
Lower Floridan aquifer	$K_{h,lf}$	200	66
Multiplier for horizontal hydraulic conductivity of Upper Floridan aquifer (dimensionless)	$K_{h,uf}$	10 [2,3]	12 [2,3]
Vertical anisotropy (dimensionless):			
Surficial aquifer system[1]	VAN_{sa}	10	--
Upper Floridan aquifer[1]	VAN_{uf}	10	--
Lower Floridan aquifer[1]	VAN_{lf}	10	--
Vertical hydraulic conductivity (ft/d):			
Riverbed	$K_{v,riv}$	.30	.084
Intermediate confining unit, ≤ 50 ft thick	$K_{v,ic1}$	.020	.028
Intermediate confining unit, > 50 ft thick	$K_{v,ic2}$	.020	.0060
Multiplier for vertical hydraulic conductivity of middle semiconfining unit and middle confining unit (dimensionless)	$K_{v,ms}$	.070 [2]	.56 [2]

[1]This parameter was specified and not estimated with the inverse model.

[2]The value of the hydraulic property represented by this parameter is the product of the unique value assigned to each model cell (representing the spatial variability of the hydraulic property) and this parameter value.

[3]The spatially variable values of horizontal hydraulic conductivity of the Upper Floridan aquifer (fig. 28) were decreased by a factor of 10 in order to ensure that $K_{h,uf}$ would not equal 1. The composite scaled sensitivity of a log-transformed parameter is calculated as zero by the inverse model when the parameter equals 1.

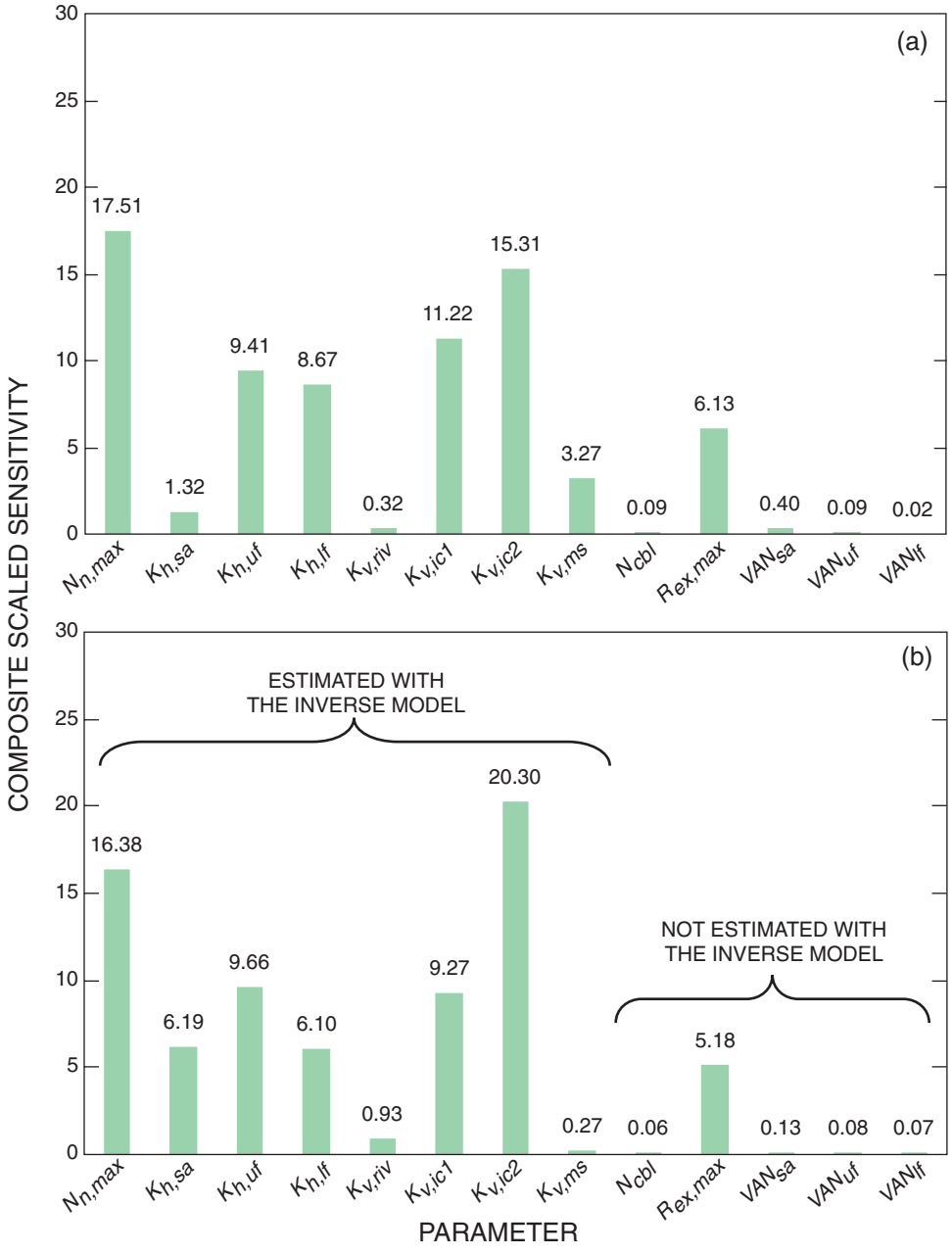

Figure 34. Composite scaled sensitivities for (a) initial and (b) final parameter values.

The calibrated model was most sensitive to the vertical hydraulic conductivity of the ICU where the ICU is greater than 50 ft thick ($K_{v,ic2}$), maximum rate of natural net recharge ($N_{n,max}$), multiplier for horizontal hydraulic conductivity of the UFA ($K_{h,uf}$), and vertical hydraulic conductivity of the ICU where the ICU is less than or equal to 50 ft thick ($K_{v,ic1}$); moderately sensitive to the horizontal hydraulic conductivity of the SAS ($K_{h,sa}$), horizontal hydraulic conductivity of the LFA ($K_{h,lf}$), and maximum rate of combined excess ET and excess overland runoff ($R_{ex,max}$); and relatively insensitive to the vertical hydraulic conductivity of the riverbed ($K_{v,riv}$), multiplier for vertical hydraulic conductivity of the MSCU/MCU ($K_{v,ms}$), vertical anisotropy of the SAS (VAN_{sa}), vertical anisotropy of the UFA (VAN_{uf}), vertical anisotropy of the LFA (VAN_{lf}), and net recharge at closed-basin lakes (N_{cbl}) (fig. 34). Parameter correlation coefficients were similar between the initial and final parameter values, the largest of which was only 0.75 for the final values of parameter pairs $K_{v,ms}$ and VAN_{lf} and $N_{n,max}$ and $R_{ex,max}$. Composite scaled sensitivities and correlation coefficients can vary significantly among different parameter values as a result of the effects of model nonlinearity and scaling by the parameter value (Hill, 1998, p. 41-42). This was not the case for the present model, and these statistics were well suited for testing alternative conceptual models and parameter zonations.

Natural net recharge was represented by three parameters in the calibrated model (table 3): $N_{n,max}$, N_{cbl}, and $R_{ex,max}$. Simulated values of natural net recharge at the water table were adjusted by varying the values of parameters $N_{n,max}$ and $R_{ex,max}$ and the extinction depth (fig. 29). Net recharge to closed-basin lakes was directly simulated by the value of N_{cbl}. The large composite scaled sensitivity for $N_{n,max}$ allowed this parameter to be estimated with the inverse model (fig. 34). The small composite scaled sensitivity for N_{cbl} precluded the estimation of this parameter with the inverse model (fig. 34); N_{cbl} was held constant at its initial value of 1 in/yr, which is consistent with independent evidence. $R_{ex,max}$ has a composite scaled sensitivity of moderate magnitude (fig. 34), but this parameter was not estimated with the inverse model for reasons that will be discussed later in this section.

In upland zones (areas where the simulated water table is below the extinction depth), natural net recharge is equal to $N_{n,max}$ and its value from the calibrated model is 27 in/yr. This value represents the highest natural net recharge flux simulated in the model area and is consistent with independent evidence discussed in a previous section. The 3-in/yr discrepancy between the initial and final values of $N_{n,max}$ may be explained by the fact that minimum natural overland runoff ($O_{sn,min}$, eq. 12) probably is not zero as was initially assumed; also, this discrepancy may be explained by errors in the initially estimated values of precipitation, minimum natural ET, or change in aquifer storage (P, $ET_{n,min}$, and ΔS_{aq}, respectively, eq. 12) or in the specified value of $R_{ex,max}$.

In transitional zones (areas where the simulated water table is equal to or above the extinction depth), natural net recharge is equal to the sum of the fluxes simulated by the MODFLOW Recharge Package (equal to $N_{n,max}$) and Evapotranspiration Package. The flux simulated by the Evapotranspiration Package represents the combined effects of excess ET and excess overland runoff, and is determined by the simulated water-table altitude, $R_{ex,max}$, and the extinction depth (fig. 29). $R_{ex,max}$ was specified at its initial value of 31 in/yr for the calibrated model; therefore, in transitional zones natural net recharge simulated by the calibrated model equals -4 in/yr where the simulated water table is above land surface and linearly varies from -4 in/yr, where the simulated water table is equal to land surface, to 27 in/yr, where the simulated water table is equal to the extinction depth.

As previously mentioned, $R_{ex,max}$ could not be estimated with the inverse model even though the ground-water flow model was fairly sensitive to this parameter. The inverse model was unable to converge to the specified convergence criterion when attempts were made to estimate $R_{ex,max}$ in addition to the other eight parameters. When a larger convergence criterion was specified, the inverse model converged with a smaller standard error (eq. 22), but with unrealistic values for $N_{n,max}$ (42 in/yr) and $R_{ex,max}$ (92 in/yr). Many different conceptual models and parameter zonations were tested in an attempt to devise a method to estimate natural net recharge with the inverse model that did not require the specification of $R_{ex,max}$, such as dividing $N_{n,max}$ into two parameters based on suspected areas of low or high overland runoff. However, no alternative models yielded both a good fit to the observations and realistic parameter values. Therefore, the current conceptual model and parameter zonation were considered to be the most appropriate because both yielded a reasonably good fit to the observations; parameter values were realistic and could be supported by independent evidence; and six of the parameters to which the model is most sensitive were estimated with the inverse model (the seventh being $R_{ex,max}$, fig. 34). In addition, all alternative models fit the observations

only slightly better (standard error was no more than 4 percent smaller), had one or more unrealistic parameter values, and had more complex parameter zonations.

MODFLOW does not allow for the incorporation of extinction depth as a parameter to be estimated with the inverse model, but the value specified for extinction depth does affect how natural net recharge is simulated with the model (fig. 29). Therefore, the sensitivity of the model to extinction depth and the possible optimum value of extinction depth were investigated in a trial-and-error manner. Eleven simulations of the inverse model were performed using the same parameter zonation as the calibrated model; one of the following extinction depths was used for each simulation: 3, 6, 9, 13, 16, 20, 25, 30, 35, 40, and 45 ft. Parameter values from the calibrated model (table 3) were used as the initial values for each inverse model simulation. The standard error (eq. 22) varied over a small range from 8.87 to 9.12 among the 11 simulations; the minimum standard error occurred for an extinction depth of 35 ft and gradually increased for depths above and below this value. These results indicate that the model was relatively insensitive to the value of extinction depth; consequently, the optimum value of extinction depth cannot be determined with much confidence using results from only the present model. An extinction depth of 13 ft was specified for the calibrated model because this represents the extinction depth with the smallest standard error for which supporting independent evidence also exists.

The values of 31 in/yr for $R_{ex,max}$ and 13 ft for extinction depth also can be justified based on a comparison of the combined rate of ET and overland runoff simulated by the Evapotranspiration Package and that estimated for the independent water budget (fig. 23). First, natural ET (ET_n, eq. 9) is assumed to be equal to the rate of ET from land surface areas (excluding about 7 percent of the model area which is lakes or streams) because ET extracted from artificial recharge (ET_a, eq. 17) is very small on a model-wide average basis. ET from land surface areas was estimated to be about 32 in/yr based on the independent water budget, as described in a previous section. Next, natural overland runoff (O_{sn}, eq. 10) is assumed to be equal to the rate of overland runoff because overland runoff resulting from artificial recharge (O_{sa}, eq. 17) is very small on a model-wide average basis. Overland runoff was estimated to be 7 in/yr based on the independent water budget (fig. 23). Therefore, the combined rate of ET and overland runoff estimated for the independent water budget is 39 in/yr and is equal to the sum of natural ET and natural overland runoff. Finally, the same quantity (sum of ET_n and O_{sn}) can be calculated based on results from the calibrated model. The combined rate of excess ET and excess overland runoff ($ET_{n,ex}$ (eq. 9) and $O_{sn,ex}$ (eq. 10), respectively) simulated by the Evapotranspiration Package was 12.5 in/yr. The combined rate of minimum ET and minimum overland runoff ($ET_{n,min}$ (eq. 9) and $O_{sn,min}$ (eq. 10), respectively) was assumed to be 27 in/yr, as described in a previous section. Therefore, the combined rate of ET and overland runoff simulated by the model is 40.3 in/yr. The combined rate of ET and overland runoff simulated by the model is only 1.3 in/yr greater than that estimated for the independent water budget; this is within the error expected for these data. In conclusion, the values of 31 in/yr for $R_{ex,max}$ and 13 ft for extinction depth produce simulated fluxes in good agreement with fluxes based on observed data.

The final value of $K_{h,sa}$ was 22 ft/d, larger than its initially estimated value but well within the range of reported values from slug tests and aquifer performance tests. In fact, an examination of a histogram of 60 measurements of horizontal hydraulic conductivity, within or in the vicinity of the model area, indicate that the largest number of values (19 measurements) are in the range 2.5 to 6.3 ft/d but the second largest number of values (13 measurements) are in the range 16 to 40 ft/d. In addition, 10 of the 60 measurements have values less than or equal to 1 ft/d, and probably can be excluded because they are not regionally representative values based on the typical lithology of the SAS.

The parameter $K_{h,uf}$ is a multiplier for the spatially variable distribution of values representing the horizontal hydraulic conductivity of the UFA (table 3). The final value of this parameter indicates that the horizontal hydraulic conductivity of the UFA is 20 percent greater than its initial estimate in all model cells. Transmissivity was calculated as the product of horizontal hydraulic conductivity from the calibrated model and UFA thickness to facilitate comparison with results from previous models and aquifer performance tests. Transmissivity ranges from 5,900 to 11,000,000 ft^2/d with a geometric mean of 160,000 ft^2/d (fig. 35). Because the initial distribution of the horizontal hydraulic conductivity of the UFA was based on results from previous models (fig. 28), the final UFA transmissivity matches the trends depicted in previous models, but generally is slightly greater in magnitude. A meaningful comparison with results from aquifer performance tests is more difficult because relatively few tests have been performed within the model area.

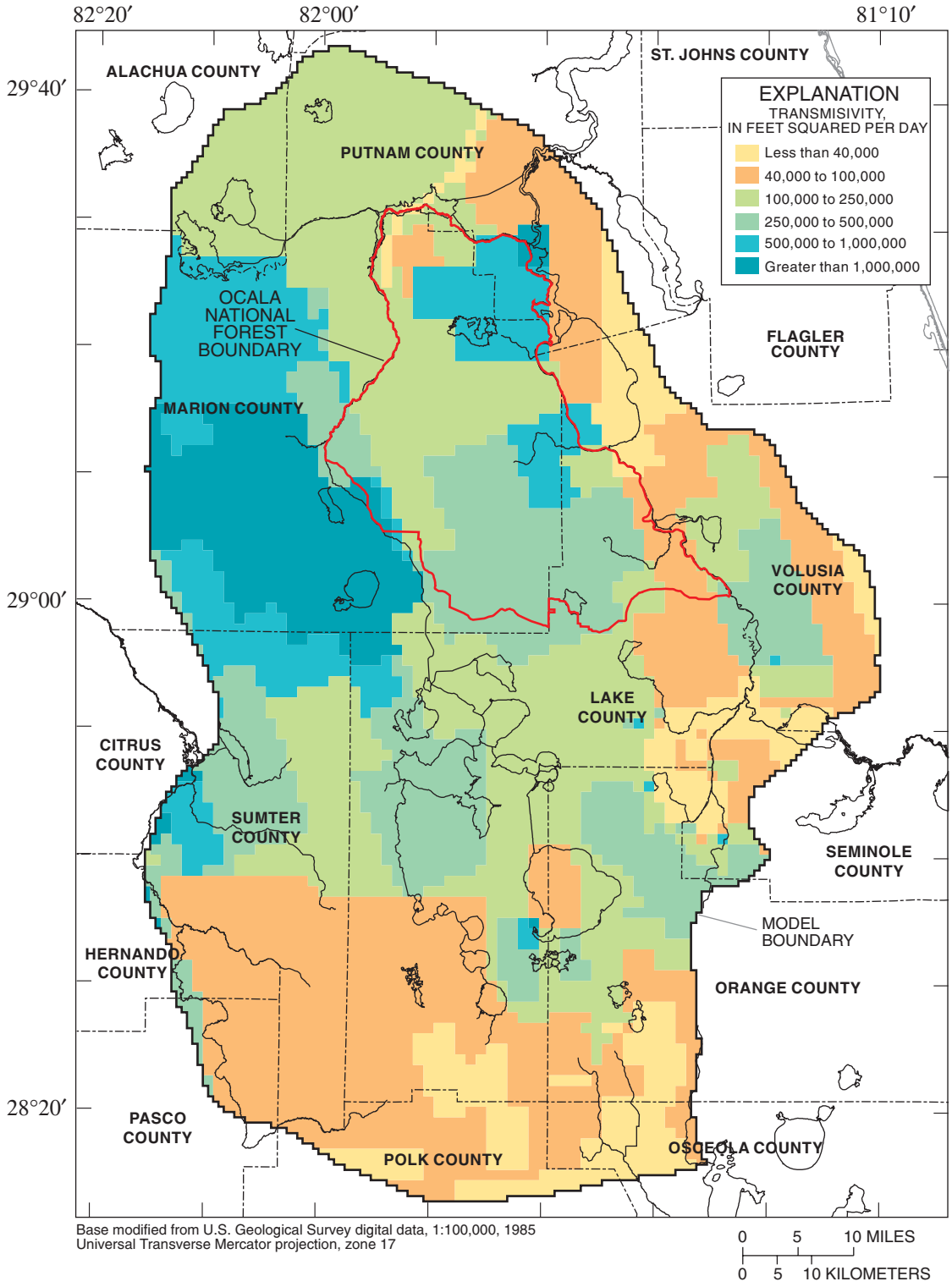

Figure 35. Transmissivity of the Upper Floridan aquifer based on aquifer thickness and horizontal hydraulic conductivity from the calibrated model.

Results from 126 aquifer performance tests with reported values for UFA transmissivity were compiled for this study (Szell, 1993; Spechler and Halford, 2001, p. 24). One-half of these lie outside, but still in the vicinity of, the model boundaries. Of the 63 tests performed in the model area, only 10 were in Lake County and none in the Ocala NF. Significant discrepancies exist between model-derived and aquifer performance test-derived values of transmissivity—in some instances greater than two orders of magnitude. However, transmissivity values derived from model calibration were greater than those from 54 of the 63 aquifer performance tests. Many factors may explain this trend, but two of the more likely explanations are: (1) most of the wells used in the aquifer performance tests do not fully penetrate the UFA and consequently the calculated transmissivity may be underestimated (of the 49 tests where well construction data were available, 65 percent of the wells were open to less than 50 percent of the full aquifer thickness); and (2) model-derived transmissivity probably is more representative of a regional value that takes into account larger scale features, such as fractures and dissolution features, which contribute to a larger transmissivity than would be measured at the smaller scale of an aquifer performance test.

Because the hydraulic properties and potentiometric surface of the LFA are not well known, the horizontal hydraulic conductivity of the LFA was represented by one constant parameter $K_{h,lf}$ (table 3). Transmissivity, calculated as the product of horizontal hydraulic conductivity from the calibrated model and LFA thickness, ranges from 2,300 to 99,000 ft^2/d with a geometric mean of 56,000 ft^2/d. The smallest values are the result of a thinner aquifer caused by the presence of water containing 5,000 mg/L chloride concentration. These values are less than transmissivity values derived from aquifer performance tests in Orange County (Spechler and Halford, 2001, p. 26), but generally are comparable in average magnitude to transmissivity values from previous models (Tibbals, 1990; Motz, 1995; and Murray and Halford, 1996). The spatial distribution of LFA transmissivity is considerably different in the present model compared to the previous models. However, the spatial distribution of LFA transmissivity based on $K_{h,lf}$ fit the observations better than using LFA transmissivity values from previous models.

The vertical anisotropy of each of the three aquifers (SAS, UFA, and LFA) was specified at a value of 10 and not estimated with the inverse model. The composite scaled sensitivities of the vertical anisotropy parameters were very small (less than one hundredth of that for the parameter with the largest composite scaled sensitivity) for both the initial and final sets of parameters values (fig. 34). Therefore, sufficient information was not present in the observations to justify adjustment of these parameters during model calibration.

The parameter $K_{v,riv}$ represents the vertical hydraulic conductivity of sediments constituting the riverbed simulated by the MODFLOW River Package (table 3). River nodes are used to simulate streams, flow-through lakes, and wetlands; the conductance of the bed material for each of these features was formulated such that conductance is proportional to the area of the bed material. Therefore $K_{v,riv}$ functions as a multiplier that uniformly adjusts the spatially variable values of riverbed conductance. In interpreting the value of $K_{v,riv}$, it is important to realize that while $K_{v,riv}$ is conceptualized to represent vertical hydraulic conductivity, its final value could be compensating for errors in the specified riverbed area, the assumed riverbed thickness of 1 ft, or the scale of the model grid. Nevertheless, the final value of 0.084 ft/d for $K_{v,riv}$ probably is a reasonable value, because $K_{v,riv}$ generally would be expected to be less than the measured horizontal hydraulic conductivity of SAS sediments (the smallest of which was 0.2 ft/d).

Composite scaled sensitivities indicate that the model is quite sensitive to the vertical hydraulic conductivity of the ICU (parameters $K_{v,ic1}$ and $K_{v,ic2}$, fig. 34), but very little information exists on which to base a logical parameter zonation. Field measurements of leakance or vertical hydraulic conductivity are sparse and detailed descriptions of the lithology of the ICU, while more abundant, probably are fewer than would be required to represent the heterogeneity in confining unit properties. Heterogeneity in aquifer and confining unit properties is expected in any geologic environment. In the mantled karst environment common in the model area, however, a large degree of heterogeneity in hydrologic properties, resulting from, for example, sinkhole activity, is typical rather than exceptional. Results from previous models can have limited transfer value because for a given leakage rate between two aquifers, leakance is inversely and completely correlated with the simulated head difference between the aquifers. That is, if the head difference between the SAS and the UFA is simulated incorrectly, the leakance could be adjusted during calibration to compensate for this error. A large error in simulated head difference is likely because the altitude of the SAS water table is unknown in many areas and can vary considerably over small distances.

Considering all of these uncertainties, numerous parameter zonations of the vertical hydraulic conductivity of the ICU were tested, taking into account such things as total thickness of overburden (depth to the top of the UFA below land surface) and surface geology (Scott and others, 2001). The final parameter zonation used two parameters, $K_{v,ic1}$ and $K_{v,ic2}$, to represent the vertical hydraulic conductivity of the ICU where the unit is less than or equal to 50 ft thick and greater than 50 ft thick, respectively (table 3). This was based on the reasoning that the confining unit is more likely to be discontinuous or breached by sinkhole activity where it is relatively thin. Consequently, the average vertical hydraulic conductivity of the ICU in such areas would be greater than in areas where it is relatively thick and less prone to sinkhole activity. This difference in vertical hydraulic conductivity is evident in the final parameter values: $K_{v,ic1}$ is nearly 5 times larger than $K_{v,ic2}$, and both values are within the range of previously reported values. Leakance of the ICU (fig. 36) was calculated based on vertical hydraulic conductivity from the calibrated model and confining unit thickness (fig. 11). Leakances of the ICU generally agree, on average, with those from previous models, although some variations in spatial distribution are present. Considerable error might exist in the leakances derived from this model, especially at a local scale, but the simple parameter zonation presented here was determined to be the most suitable given the regional scale of this model and the available data.

The parameter $K_{v,ms}$ is a multiplier for the spatially variable distribution of values representing the vertical hydraulic conductivity of the MSCU/MCU (table 3). The spatial variability accounts only for the different lithology between the MSCU and the MCU. More specifically, vertical hydraulic conductivity is a uniform value equal to $K_{v,ms}$ where only the MSCU exists; vertical hydraulic conductivity is a uniform value equal to one-hundredth of $K_{v,ms}$ where only the MCU exists and where the MSCU and the MCU overlap; and vertical hydraulic conductivity is a uniform value equal to one hundred times $K_{v,ms}$ where no MSCU exists. The final value of $K_{v,ms}$ of 0.56 ft/d is consistent with previously reported values for the MSCU. The final vertical hydraulic conductivity of the MCU is 0.0056 ft/d, which also is consistent with previously reported values. Leakance of the MSCU/MCU (fig. 37) was calculated based on vertical hydraulic conductivity from the calibrated model and confining unit thickness (fig. 14). To be consistent with the assumption that the MCU is much less leaky than the MSCU, only the thickness of the MCU was used to calculate leakance where the MSCU and the MCU overlap. The final leakances of the MSCU generally are greater than those from previous models; whereas final leakances of the MCU generally are less than those from previous models.

Parameter Uncertainty

The parameter variance-covariance matrix calculated by the inverse model was used to quantify the reliability of parameter estimates. Parameter coefficients of variation and confidence intervals on parameter values can be useful for comparing the reliability of different parameters from the same run of the inverse model (Hill, 1992, p. 58). Coefficients of variation and linear 95-percent confidence intervals on parameter values were calculated for the parameters estimated with the inverse model (table 4). Parameters $N_{n,max}$, $K_{h,uf}$, $K_{v,ic1}$, and $K_{v,ic2}$ have relatively small coefficients of variation and narrow confidence intervals (when considered as a fraction of the respective final parameter value), indicating they are estimated more reliably than parameters $K_{h,sa}$, $K_{h,lf}$, $K_{v,riv}$, and $K_{v,ms}$. This is because the observations contain more information from which these parameters can be estimated, as indicated by their larger composite scaled sensitivities (fig. 34); however, the linear 95-percent confidence intervals in table 4 should be interpreted only as rough measures of parameter uncertainty because the model is nonlinear and weighted residuals are not normally distributed. Nevertheless, linear 95-percent confidence intervals indicate the relative reliability of the final parameter values (Yager and others, 2001, p. 52-53).

Table 4. Coefficients of variation and linear 95-percent confidence intervals for the parameters estimated with the inverse model

Parameter[1]	Final value	Coefficient of variation	Linear 95-percent confidence interval	
			Lower limit	Upper limit
$N_{n,max}$	27	0.051	24	30
$K_{h,sa}$	22	.43	11	48
$K_{h,uf}$	12 [2]	.16	8.7 [2]	16 [2]
$K_{h,lf}$	66	.43	31	140
$K_{v,riv}$	.084	14	.0033	2.1
$K_{v,ic1}$	.028	.23	.018	.043
$K_{v,ic2}$	.0060	.18	.0043	.0084
$K_{v,ms}$	.56 [2]	2.2	.077 [2]	4.1 [2]

[1]See table 3 for parameter symbol definition.

[2]The value of the hydraulic property represented by this parameter is the product of the unique value assigned to each model cell (representing the spatial variability of the hydraulic property) and this parameter value.

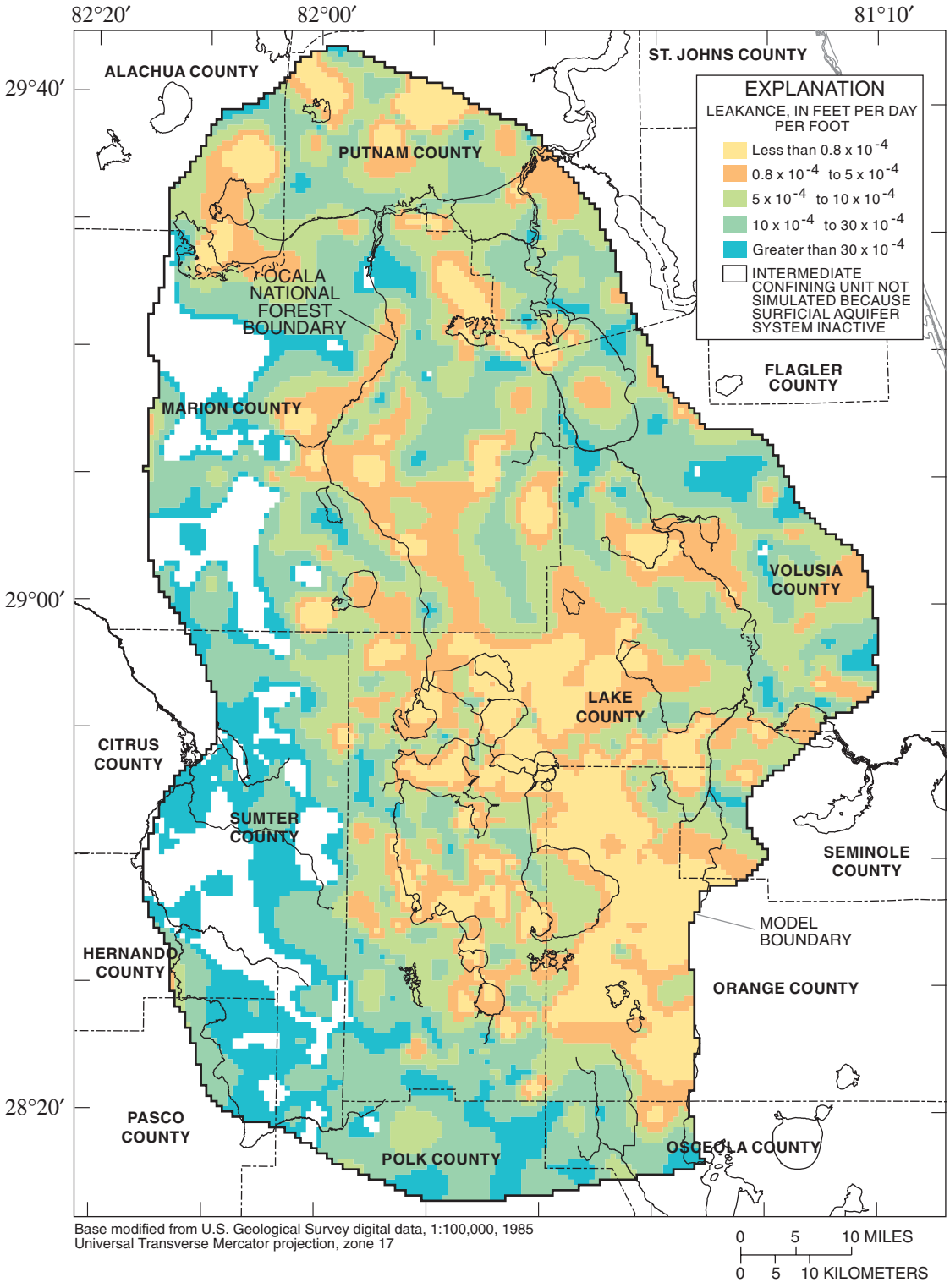

Figure 36. Leakance of the intermediate confining unit based on confining unit thickness and vertical hydraulic conductivity from the calibrated model.

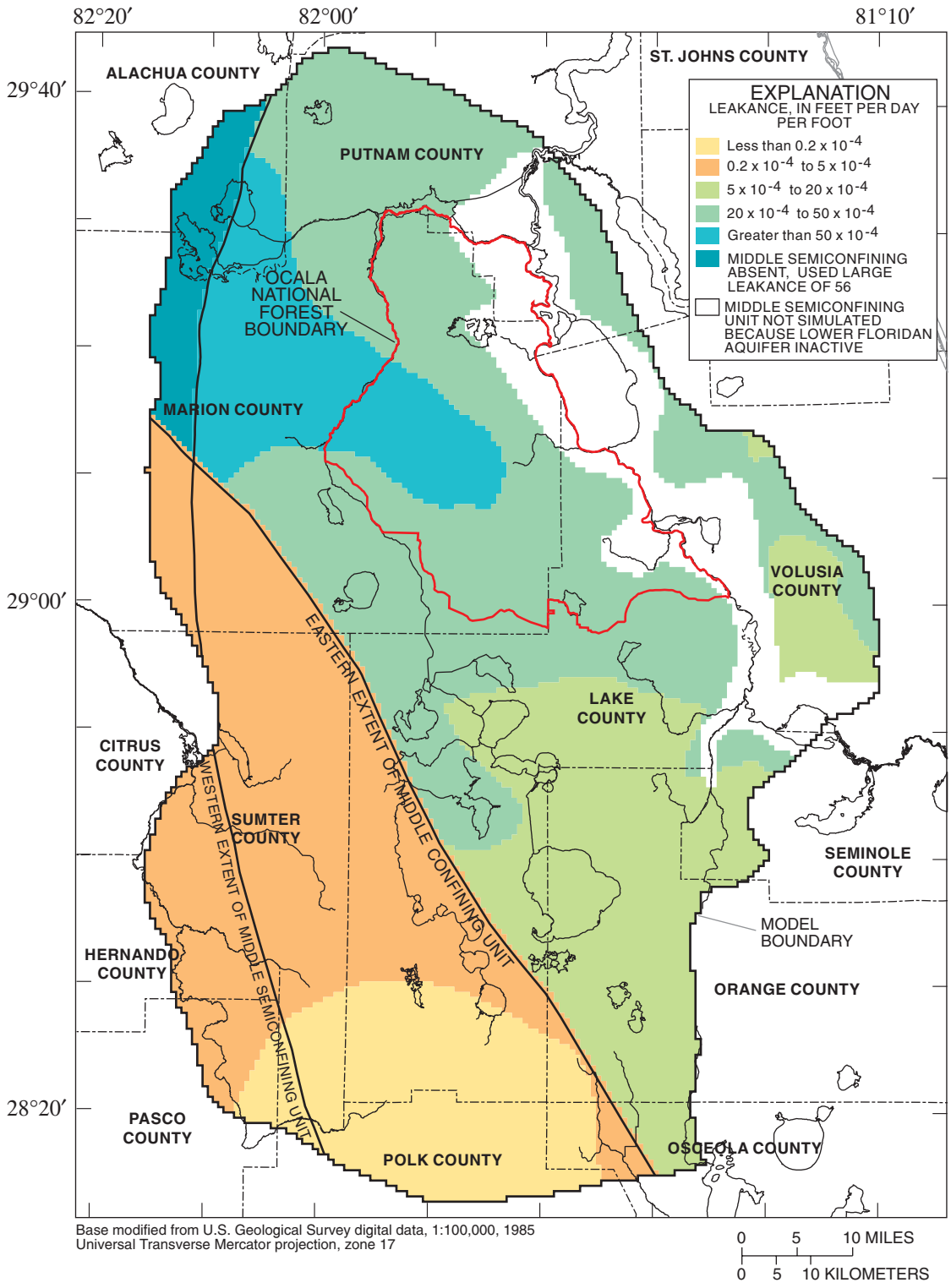

Figure 37. Leakance of the middle semiconfining and middle confining units based on confining unit thickness and vertical hydraulic conductivity from the calibrated model.

A parameter might be precisely estimated based on its confidence interval, but still not represent its true value as a result of parameter correlation or local minima in the objective function. Correlation coefficients indicate that all 13 parameters are not highly correlated. A test was performed to determine if the eight final parameter values for the calibrated model were the result of a global, rather than local, minimum in the objective function as suggested by Hill and others (2000, p. 18). The inverse model was run twice, using a different set of initial parameter values for each run: the lower and upper limits of the linear 95-percent confidence intervals (table 4). Final parameter values from each of these two runs were very close to those for the calibrated model, with the exception of $K_{h,sa}$ and $K_{v,riv}$. Using the upper limit of the linear 95-percent confidence intervals from the final calibrated model as the initial parameter values, the values estimated by the inverse model for $K_{h,sa}$ and $K_{v,riv}$ were 13 and 0.10 ft/d, respectively, and linear 95-percent confidence intervals were 5.6 and 30 ft/d for $K_{h,sa}$ and 0.0030 and 3.6 ft/d for $K_{v,riv}$. These linear 95-percent confidence intervals significantly overlap the confidence intervals on the corresponding final values for the calibrated model (table 4). Therefore, the eight final parameter values for the calibrated model can be considered unique for the observations used in the inverse model.

Model Fit

An evaluation of the model fit was made for the calibrated model using statistics and results generated by the inverse model in order to determine how well simulated water levels and flows matched observed values. The calibrated model has a standard error (eq. 22) of 8.95, which is less than or only slightly greater than the value for each of the alternative models tested during calibration. The standard error will equal 1 if the model fit is consistent with the weights assigned to the observations, but typically will exceed 1 as a result of model error, such as discretization effects (Poeter and Hill, 1997, p. 254). An examination of water-level residuals grouped by aquifer indicated that the majority of the model error is associated with the SAS (table 5). In fact, the root-mean-square error (*RMSE*) is nearly three times larger for the SAS water-level observations than for the UFA or LFA observations. The calculation of *RMSE* is identical to that for standard error except the number of estimated parameters is excluded from equation 22 and only water-level observations and no weights are included in the calculation of *SSWR* (eq. 21). Even though *RMSE* does not account for the number of estimated parameters, this is of no consequence when comparing results from models with the same parameter zonation. Even though the water-level residuals are quite large for the SAS, these errors are a relatively small percentage of total model response because the *RMSE* is less than 9 percent of the simulated head range in the aquifer (table 5). In addition, the SAS water table is a more complex surface than the potentiometric surface of either the UFA or LFA, and, therefore, a more accurate simulation of the SAS water table would require a smaller grid size than is reasonable for the present regional-scale model. Simulated base flow in streams and in lakes and wetlands that drain to streams closely matches observed base flow, considering the error inherent in

Table 5. Water-level residual statistics for the calibrated model

[RMSE, root mean square error; ft, feet; %, percent]

Aquifer	Number of water-level observations	Minimum residual[1] (ft)	Maximum residual[1] (ft)	Average residual[1] (ft)	RMSE (ft)	RMSE as percent of head range[2] (%)
Surficial aquifer system	133	-46.70	50.50	-1.78	13.9	8.9
Upper Floridan aquifer	251	-14.90	17.10	.53	4.72	3.0
Lower Floridan aquifer	20	-4.00	9.99	2.33	4.60	2.9
Entire model	**404**	**-46.70**	**50.50**	**-.14**	**8.87**	**5.7**

[1]Residual is observed minus simulated value.

[2]Head range is the maximum simulated water level minus the minimum simulated water level for all active model cells in each aquifer.

estimating actual base flow. Simulated base flow is 4.5 in/yr, 1.3 in/yr less than the value used as an observation, and its weighted residual is quite small. Considering the 404 water-level observations and the 1 flow observation, the correlation coefficient between the weighted observations and the weighted simulated values is 0.95, indicating that most of the weighted simulated values are close to the weighted observations.

Weighted residuals should be randomly distributed about a value of zero for all weighted, simulated values (Hill, 1994, p. 3), and they should be independent and normally distributed (Hill, 1994, p. 6). The weighted residuals for the calibrated model do not show any trend with weighted simulated values and the average weighted residual is -0.14 (fig. 38). However, the weighted residuals are not independent and normally distributed, because the plotted values do not fall along a straight line on a normal probability plot (fig. 39); this is particularly true for SAS observations. Additional analysis indicated that the curvilinear nature of the normal probability plot (fig. 39) probably can be attributed to the nonlinearity of the ground-water flow model. Most of the nonlinear functions (for example, the MODFLOW River and Evapotranspiration Packages) used in the model are applied to the SAS, with some applied to the UFA. The weighted residuals for the LFA water levels do appear to be normally distributed (fig. 39).

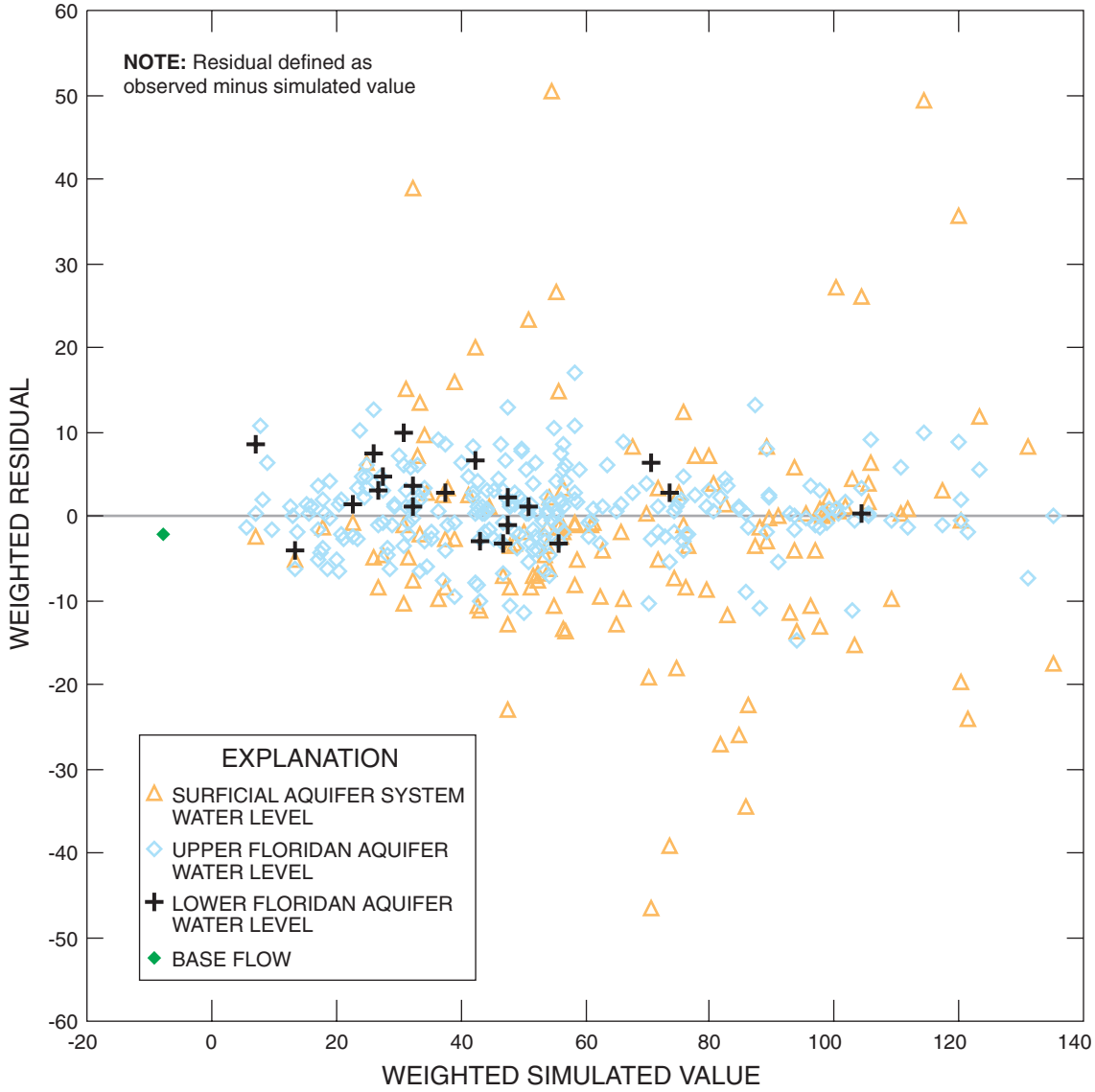

Figure 38. Comparison of weighted residuals to weighted simulated values.

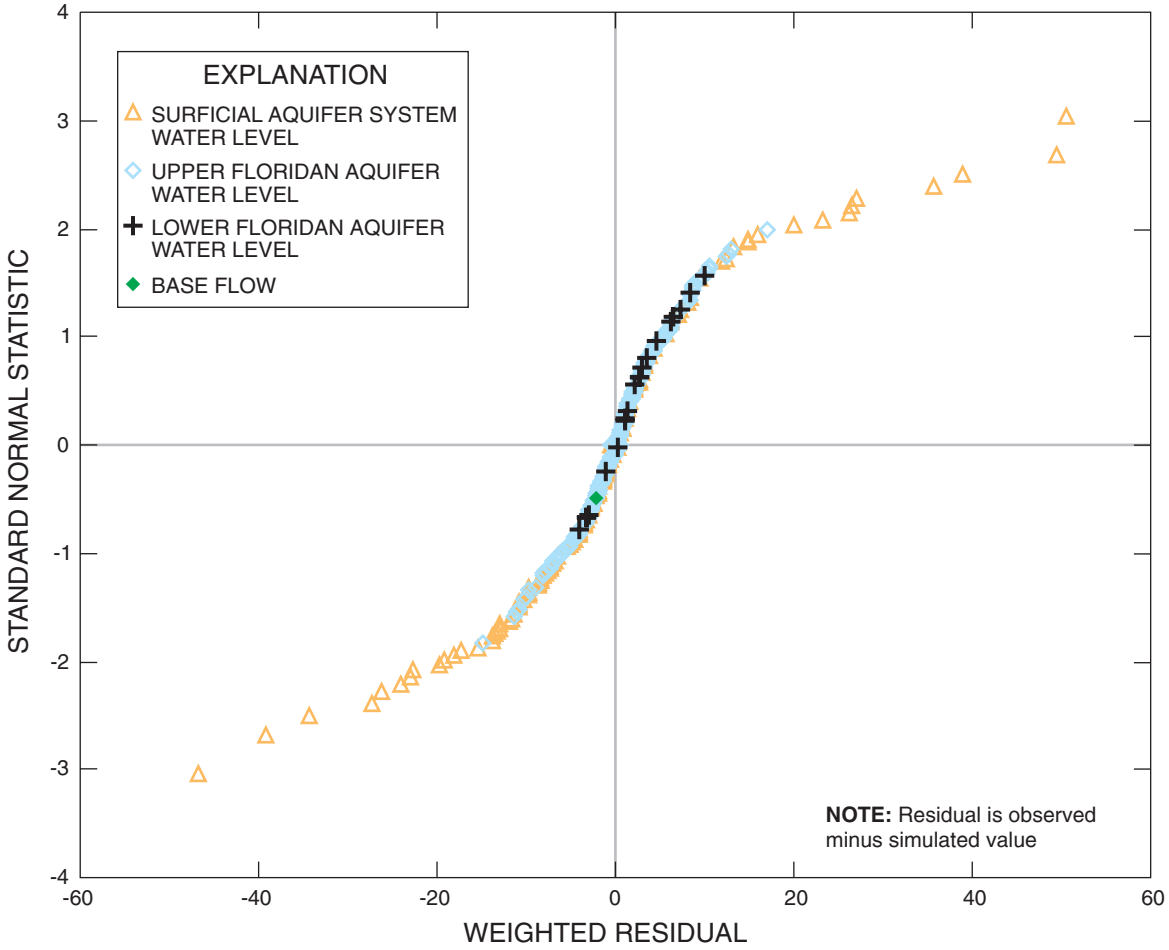

Figure 39. Normal probability plot of weighted residuals.

Model linearity was tested by calculating a statistic referred to as the modified Beale's measure (Hill, 1994, p. 45) using BEALE-2000 (Hill and others, 2000), a post-processing program for MODFLOW-2000. The modified Beale's measure for the calibrated model is 0.53, with critical values of 0.045 and 0.50. If the modified Beale's measure is less than the smaller critical value, the model is effectively linear for parameter values close to the final parameter values; if the modified Beale's measure is greater than the larger critical value, the model is highly nonlinear for parameter values close to the final parameter values. Therefore, the calibrated model is highly nonlinear. A closer examination reveals that parameter $K_{v,riv}$ causes most of the nonlinearity: the modified Beale's measure for the calibrated model excluding $K_{v,riv}$ is 0.24, which is midway between the two critical values, 0.043 and 0.48, indicating that the model is only moderately nonlinear. Head-dependent flow boundaries, such as simulated by the MODFLOW River Package and $K_{v,riv}$, can be a major source of nonlinearity when the simulated water level fluctuates above and below the specified riverbed bottom altitude (eqs. 18 and 19). The fact that the model is nonlinear and that the weighted residuals are not normally distributed have important implications for interpretation of some statistics calculated by the inverse model, such as linear confidence intervals (table 4). Linear confidence intervals on estimated parameter values, predicted water levels, and predicted flows can be valuable indicators of uncertainty. However, when the model is nonlinear and weighted residuals are not normally distributed, linear confidence intervals must be considered only as rough measures of simulation uncertainty.

Another important characteristic of an accurate model is the spatially random distribution of weighted residuals (Poeter and Hill, 1997, p. 254). Model-wide trends in the spatial distribution of water-level residuals for each aquifer are not apparent (figs. 40, 41, and 42).

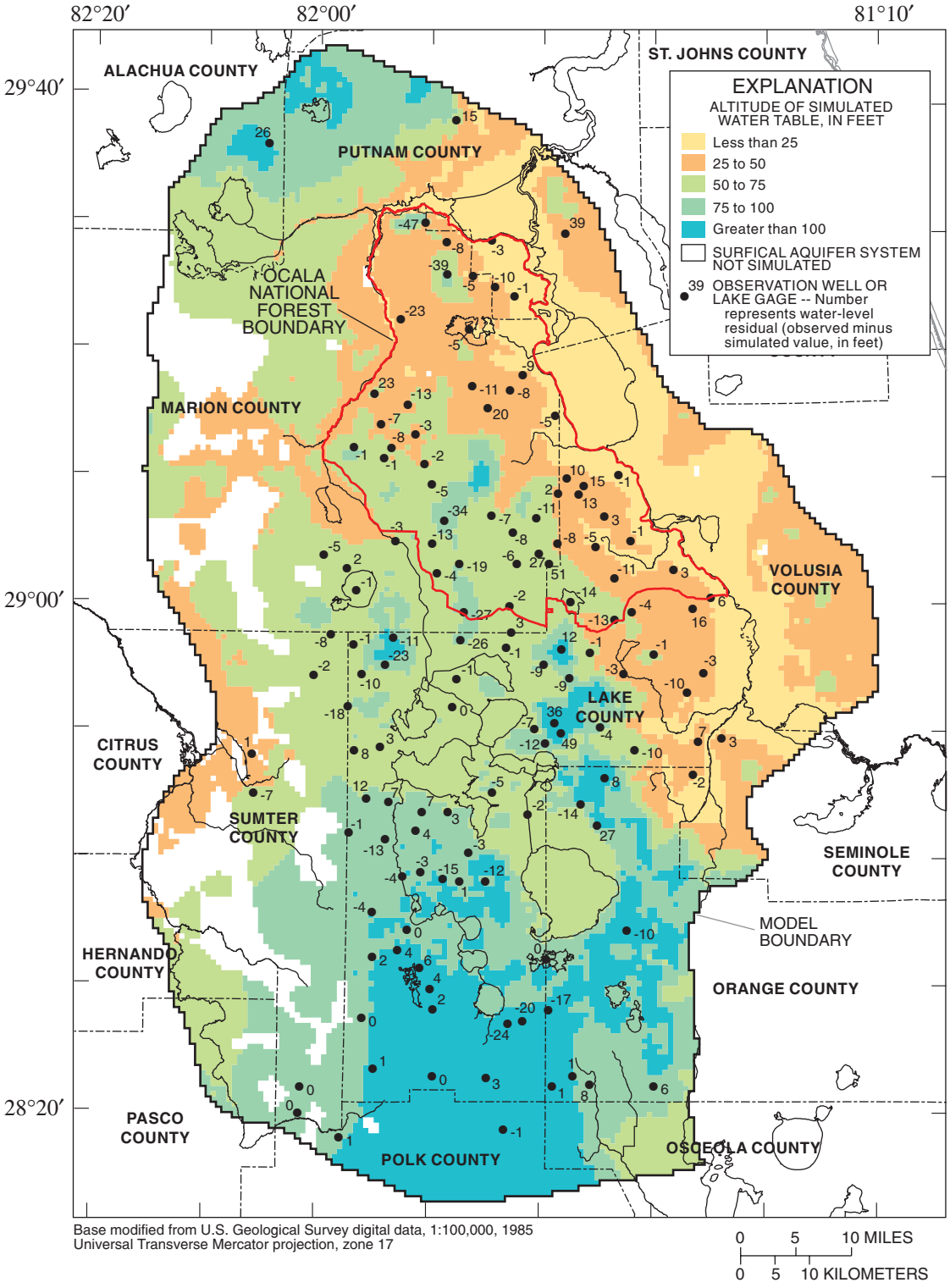

Figure 40. Simulated water table and water-level residuals for the surficial aquifer system, average 1998 conditions.

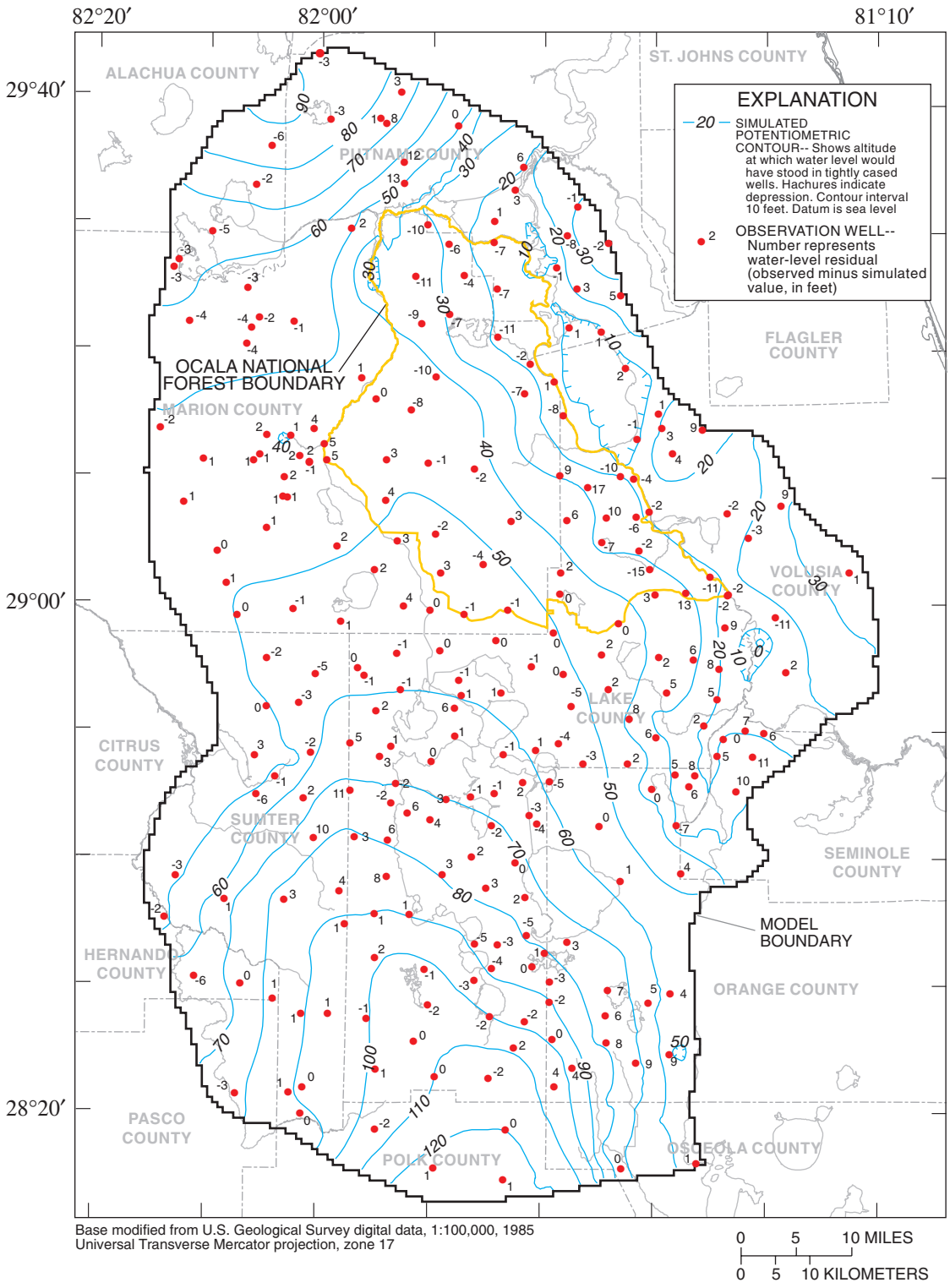

Figure 41. Simulated potentiometric surface and water-level residuals for the Upper Floridan aquifer, average 1998 conditions.

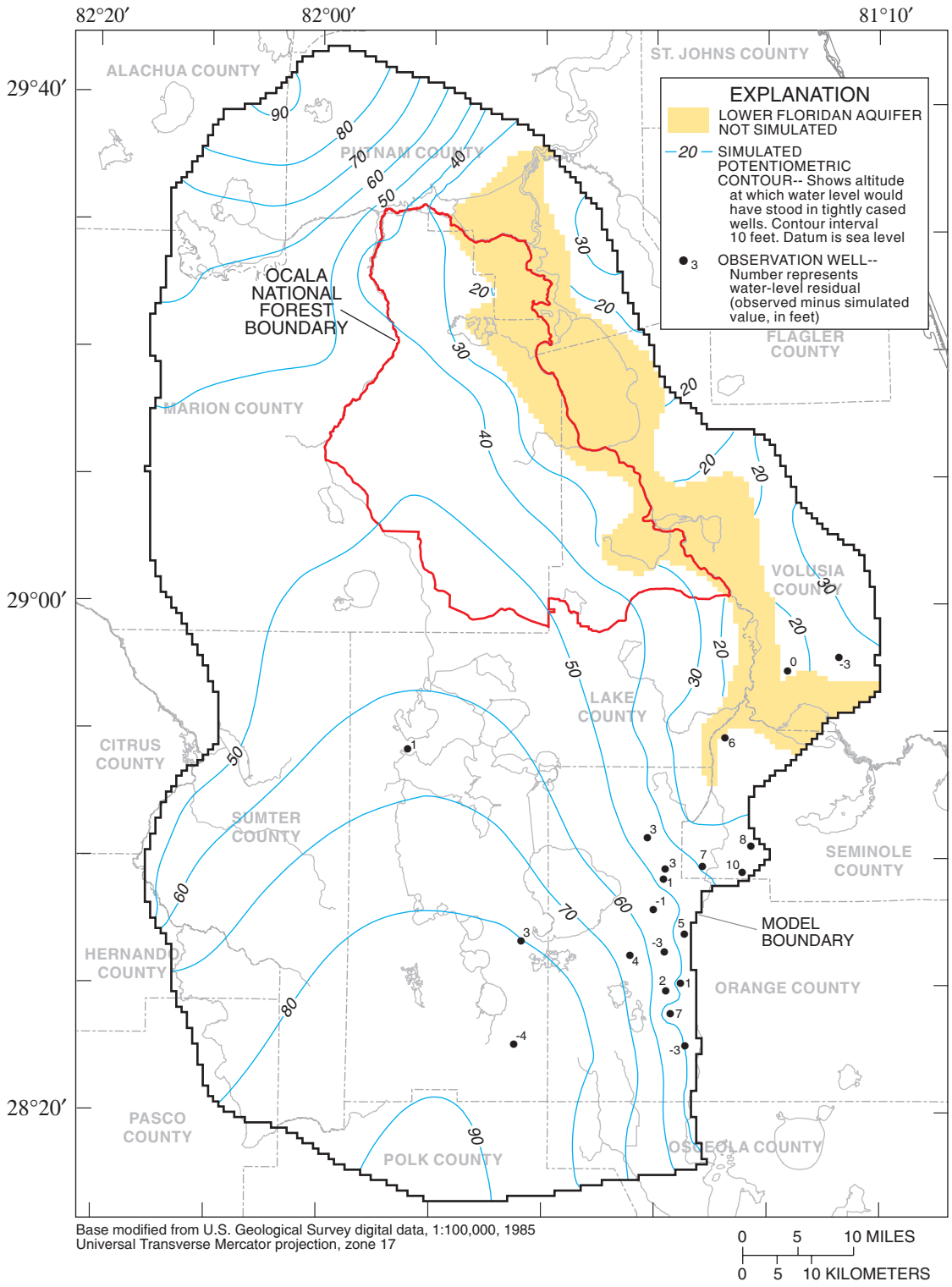

Figure 42. Simulated potentiometric surface and water-level residuals for the Lower Floridan aquifer, average 1998 conditions.

Groupings of positive or negative water-level residuals do exist on a more local scale, however, such as within the Ocala NF (fig. 40). The "runs statistic" (Hill, 1998, p. 22), calculated by the MODFLOW Observation Process, can be used to indicate the presence of groupings of residuals or lack of randomness. A "run" is defined as a sequence of numbers of the same sign, and the runs statistic is a measure of the number of runs, or changes in sign, in the set of residuals. The number of runs in a given set of residuals is dependent on the order in which the residuals are listed. Water-level observations were ordered by layer, row, and column in the MODFLOW Head-Observation Package input file; that is, for each model layer, water-level observations were listed in order according to their spatial location: from north to south (increasing row number) and from west to east (increasing column number). Because the water-level observations were in a logical spatial order, the runs statistic for the calibrated model can be used as a measure of the spatial randomness of the residuals. The value of the runs statistic approaches zero as the actual number of runs approaches the expected number of runs. The runs statistic value of -2.4 indicates there are too few runs in the water-level residuals, indicating spatial groupings of residuals of the same sign exist in the same aquifer; consequently, the residuals are less randomly distributed than would be ideal. This is in agreement with the groupings of residuals as previously noted on maps of water-level residuals (figs. 40, 41, and 42). More randomly distributed residuals possibly could be obtained by adjusting parameter values at a more local scale or on a node-by-node basis, but this would add considerable complexity to the model that is not likely to be justified by the existing data. The present parameter zonation is considered to be an acceptable compromise between possibly greater model accuracy achieved through more complex parameter zonations and generally greater reliability (that is, less model uncertainty) resulting from more parsimonious parameter zonations.

Simulated 1998 Water Levels and Flows

The simulated water table of the SAS (fig. 40) is considerably different than the observed water table. The largest residuals (table 5 and fig. 38) and the least normal (fig. 39) and least random distributions of residuals (fig. 40) all occur in the SAS. Reasons for the relatively poor match between simulated and observed water levels are as follows: (1) the hydrogeology of the SAS is very heterogeneous; (2) large spatial variations in ET directly affect net recharge (the largest stress on the aquifer); (3) large variations in the leakance of the ICU directly affect the exchange of water with the UFA (the second largest stress on the SAS); and (4) the SAS generally is in direct hydraulic connection with numerous surface-water features (streams, lakes, and wetlands), resulting in complex interactions between ground water and surface water than can vary significantly from one surface-water feature to another. In addition, the SAS is much more affected than the FAS by the slow dissipation of transient effects, which are not accounted for by a steady-state simulation, because of the relatively small diffusivity of the SAS (the ratio of transmissivity to storage coefficient). All these factors are responsible for the complex configuration of the water table and are some of the least well known characteristics of the SAS. Additionally, the model grid resolution probably is not fine enough to duplicate the complex water-table surface. A relatively large amount of error was accepted for the SAS in order to use a simpler parameter zonation that reflects this lack of information, while still representing what is known about the aquifer on a more regional scale.

The simulated water table of the SAS (fig. 40) generally reflects the regional trend of the UFA potentiometric surface (fig. 41), with generally higher altitudes in the northern and southern parts of the model area and lower altitudes along the S. Johns River. However, mounds in the SAS water table occur in many areas, particularly along the Mount Dora Ridge (figs. 3 and 40), creating flow systems that are more local than those in the UFA. The direct interaction of the SAS with the surface environment and the relatively low horizontal hydraulic conductivity of the SAS contribute to the formation of numerous local flow systems. In addition, the configuration of the SAS water table and, in particular, the locations of water-level mounds are strongly influenced by variations in the leakance of the ICU (compare figures 36 and 40).

The simulated potentiometric surface of the UFA (fig. 41) generally conforms to observed data (fig. 2). The water-level residuals for the UFA generally are small (fig. 38), have a *RMSE* of 4.72 ft (table 5), and are fairly normally distributed (fig. 39). The runs statistic for the 251 UFA observations is -0.56, indicating that relatively few spatial trends exist

in water-level residuals (fig. 41). The observed potentiometric surface of the UFA can be reproduced by the model more accurately than the water table of the SAS, because the spatial variation of the UFA potentiometric surface is more regional in scale and a relatively large amount of data is available describing its configuration. The largest water-level residuals in the UFA generally are in northern Lake County near the St. Johns River, where water-level observations indicate very steep hydraulic gradients (fig. 2). These gradients may be the result of local areas of low transmissivity, or perhaps they are the result of vertical variations in water level in the UFA. Most large residuals were relatively isolated and no attempt was made to adjust hydrologic properties on a node-by-node basis to produce a closer match to these observations. Large mounds in the simulated potentiometric surface of the UFA do not exist where they are present in the simulated water-table surface for the SAS. This is the result of the high transmissivity of most of the UFA (fig. 35), which allows water to move very easily through the aquifer (compared to the SAS) to points of discharge, such as springs and wells.

The water-level residuals for the LFA generally are small (fig. 38), have a RMSE of 4.60 ft (table 5), are normally distributed (fig. 39), and show few spatial trends (fig. 42). The most noticeable deficiency regarding the simulation of the LFA is the lack of data. In most of the model area, no LFA observations are available (fig. 42). The majority of observations are in Orange and Seminole Counties; many of these are near the specified-head boundary in Orange County (fig. 25), which reduces the sensitivity of the model to these observations. The lack of information leads to a simple parameter zonation. The simulated potentiometric surface of the LFA (fig. 42) closely resembles that of the UFA (fig. 41). The most notable exception is in the southwestern part of the model area where the MCU exists. In extreme southern Lake County and northern Polk County, the simulated water level in the LFA is greater than 25 ft below that of the UFA. This large head difference is the direct result of the low leakance simulated for the MCU (fig. 37).

A comparison was made between the independent water budget compiled for the model area (fig. 23) and the simulated water budget (fig. 43). Average annual quantities that can be obtained from the independent water budget and that are directly comparable to simulated values are natural net recharge at the water table, net recharge to the UFA, base flow, springflow, and boundary leakage. Base flow is accounted for as an observation in the inverse model and springflow was specified during calibration. Boundary leakage was not formally included as an observation in the inverse model because of the large uncertainty involved with the independent estimation of this quantity. Natural net recharge at the water table and net recharge to the UFA could not be formally included as observations in the inverse model, but were checked during calibration to ensure reasonable simulated values. Natural net recharge at the water table, which excludes artificial recharge and includes storage effects, was estimated to be approximately 16 in/yr in 1998 (the sum of precipitation (57 in/yr), ET (-33 in/yr), overland runoff (-7 in/yr), and net change in storage (-1 in/yr)) from the independent water budget (fig. 23); whereas natural net recharge at the water table is simulated to be 12.6 in/yr (the sum of the recharge and ET components for the SAS and UFA, fig. 43). Net recharge to the UFA was estimated to be approximately 12 in/yr in 1998 (fig. 23); simulated net recharge to the FAS was 8.9 in/yr (the sum of the recharge and ET components for the UFA and net leakage through the ICU, fig. 43). The discrepancies of about 3 in/yr between the estimated and simulated values primarily are the result of boundary leakage for the FAS, which is simulated to be about 2 in/yr less than its estimated value. Considering the margin of error within which boundary leakage and other components of the water budget can be independently estimated, the simulated water budget agrees reasonably well with the independent water budget.

An examination of the simulated water budget reveals some important characteristics of the groundwater flow system in the model area. The total flow through the SAS and FAS together is 13.3 in/yr, which is equal to the sum of inflows to or outflows from the entire aquifer system (fig. 43). However, in calculating the total flow, the net differences between the recharge and ET components (fig. 43) were counted as net inflows because they collectively represent natural net recharge. Accordingly, natural net recharge for the SAS is 11.4 in/yr, averaged over the entire model area, or 12.3 in/yr averaged over only the 19,855 active SAS model cells (fig. 24); natural net recharge for the UFA is 1.2 in/yr, averaged over the entire model area, or 16.5 in/yr averaged over only the 1,559 model cells where the UFA is active and the SAS is inactive (fig. 24).

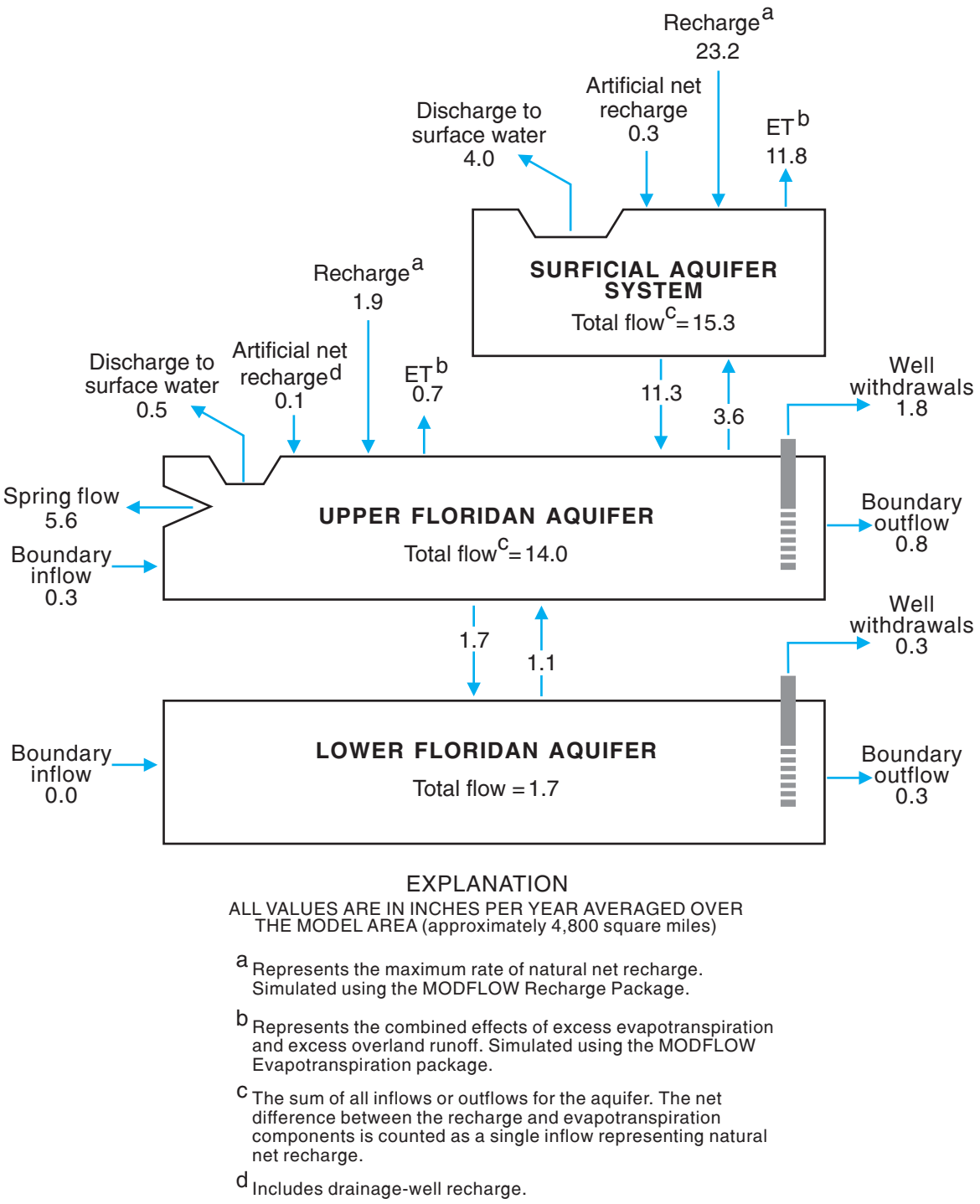

Figure 43. Simulated volumetric water budget for the aquifer system in the model area, average 1998 conditions.

Natural net recharge is the source of about 95 percent of the 13.3 in/yr of total flow through the SAS and FAS; the remaining 5 percent comes from boundary inflow and artificial recharge. Most of the 13.3 in/yr circulated through the SAS and the UFA rather than the LFA. In addition, simulated net leakage through the ICU was 7.7 in/yr downward, representing 50 and 55 percent of the total flows in the SAS and the UFA, respectively. These results are in agreement with the high leakance characteristics of the ICU. Consequently, hydrologic conditions in the SAS can have relatively significant effects on conditions in the UFA; likewise, hydrologic conditions in the UFA can have relatively significant effects on conditions in the SAS. A limited amount of flow from the UFA reaches the LFA (about 12 percent of the total flow in the UFA). Outflows from the LFA are relatively small, so the ground-water flow system in the LFA generally is relatively sluggish in comparison to the UFA.

The ground-water flow system can be characterized as relatively vigorous in the SAS and the UFA; however, the scale of the flow systems differs greatly between the two aquifers. That is, the SAS is characterized by local flow systems with some water moving laterally from recharge areas to nearby surface-water features, but with most water moving from recharge areas vertically downward as leakage to the UFA. Nearly three times the amount of water leaks downward to the UFA as discharges to surface-water features in the SAS (fig. 43). A comparison of the simulated spatial distributions of net recharge at the water table (fig. 44) and leakage through the ICU (fig. 45) shows numerous similarities, which further indicates that water primarily moves vertically in the SAS. The UFA is characterized by more regional flow systems, with water generally moving laterally from recharge areas (sometimes over great distances) to discharge areas, such as springs, well fields, and areas of upward leakage to the SAS. Springflow, well withdrawals, boundary outflow, and discharge to surface-water features account for 62 percent of the total outflow from the UFA; these budget components are partially responsible for inducing lateral flow in the aquifer.

The distribution of net recharge or discharge at the water table (fig. 44) was calculated from the fluxes simulated by the MODFLOW Recharge and Evapotranspiration Packages (fig. 29) and the artificial recharge fluxes (eq. 17) specified in the MODFLOW Well Package. Simulated discharge occurs in areas where the simulated water table is just below land surface or above land surface, because parameter $R_{ex,max}$ is greater than $N_{n,max}$ (table 3; fig. 29). This simulated discharge generally occurs in the vicinity of streams (fig. 44) and can be considered as representing additional base flow that might actually be occurring in riparian areas, but is not otherwise accounted for in the model. The spatial variation in net recharge at the water table primarily is the result of the varying depth of the simulated water table below land surface. Therefore, simulated net recharge generally is greatest in the ridge areas, where the simulated water table typically is far below land surface, and lowest in valleys or plains, where the simulated water table typically is near land surface (compare figs. 3 and 44). This distribution of net recharge is consistent with the conceptual model of the aquifer system. Net recharge can exceed 30 in/yr (fig 44) where artificial recharge occurs; these high rates generally occur at rapid infiltration basins or spray fields.

The spatial distribution of leakage through the ICU varies considerably (fig. 45), depending on the leakance of the ICU and the head difference between the SAS and UFA. A good example of this variation occurs in an area of the Ocala NF just west of Juniper Springs (site number 311, fig. 7), where the simulated leakance of the ICU is low, but adjacent to areas where the simulated leakance is high (fig. 36). A mound in the SAS water table ranging in altitude from 50 to 100 ft exists in this area (fig. 40); however, the UFA potentiometric surface drops only about 10 ft across the area of the SAS mound (fig. 41), indicating a large variation in head difference between the two aquifers. Leakage is low where the product of leakance and head difference is low, such as near the center of the mound where leakage varies from 0 to 10 in/yr; leakage is high where the product of leakance and head difference is high, such as along the "toe" of the mound where leakage rates exceed 30 in/yr. Leakage rates through the ICU can exceed net recharge at the water table in the SAS. Most leakage rates exceeding 30 in/yr (fig. 45) are supported by lateral flow in the SAS, generally from areas of lower leakance such as described in the preceding example. This lateral flow generally occurs over relatively short distances, thus supporting local rather than regional flow systems. Numerous areas of high leakance exist, perhaps even more than are simulated in the model. In addition, lateral flow that is not intercepted by areas of high leakance is likely to discharge at local surface-water features or to be extracted by ET before forming regional flow systems in the SAS.

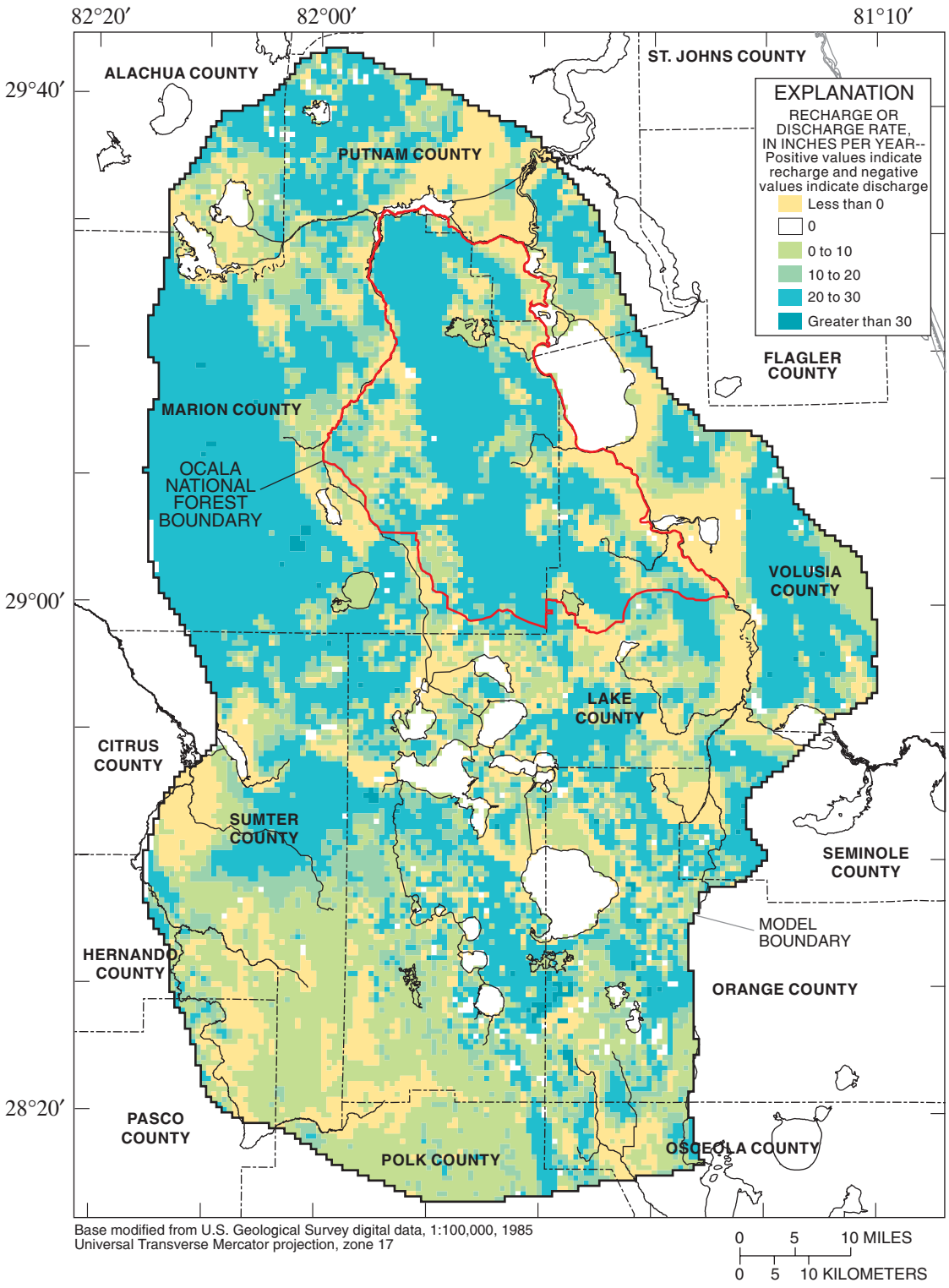

Figure 44. Simulated rate of net recharge or discharge at the water table, average 1998 conditions.

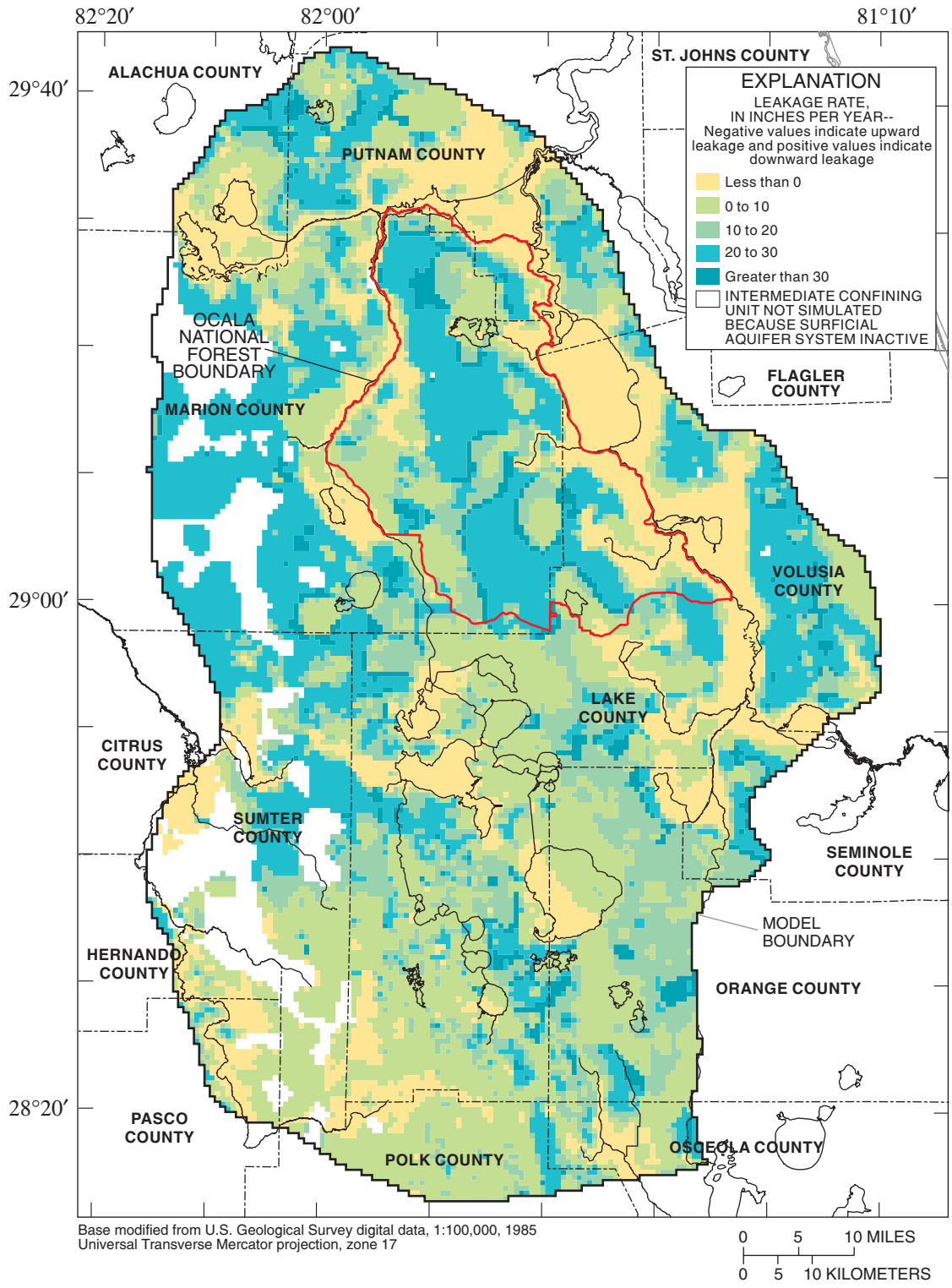

Figure 45. Simulated rate of leakage through the intermediate confining unit, average 1998 conditions.

The leakage of water between the UFA and LFA is determined by the leakance of the MSCU/MCU and the head difference between the aquifers. The presence of the MCU and its low simulated leakance have important implications concerning recharge to the LFA. The LFA is recharged only by leakage of water from the overlying UFA. In the portion of the model area where the MCU exists, the average simulated rate of leakage to the LFA is 0.8 in/yr; whereas in the remainder of the model area where only the MSCU exists or both confining units are absent, the average simulated rate of leakage to the LFA is 4.2 in/yr. Therefore, the majority of water in the LFA in the model area originates as leakage from the UFA east of the eastern extent of the MCU.

Effects of Projected 2020 Ground-Water Withdrawals

The ground-water flow model simulated the SAS and FAS water levels and flows under average 1998 conditions reasonably well. This calibrated model was used to evaluate the potential effects of projected ground-water withdrawals in 2020 on steady-state water levels and flows in the aquifer system. Particle-tracking analyses were used to identify the areas that contribute recharge to selected springs and well fields under both average 1998 and projected 2020 conditions. Finally, the effects of parameter uncertainty on model predictions were examined.

Projected Boundary Conditions

Boundary conditions specified in the calibrated model were based on average 1998 conditions and might not be valid under future conditions. Most boundary conditions were not changed for the predictive simulations. The net recharge upper boundary condition was not changed because the objective of predictive simulations was to evaluate the effects of future withdrawals rather than changes in climatic conditions, such as a drought, which might affect net recharge. Internal boundary conditions representing streams or flow-through lakes (figs. 26 and 27) were left unchanged because any change in ground-water discharge to these features likely would have very little impact on their stage, which generally is primarily controlled by the surface-water flow system. Internal boundary conditions representing wetlands (fig. 27) were not changed because the MODFLOW River Package was formulated to allow the simulation of potential decreases in ground-water discharge to wetlands (where the simulated water table is greater than 3 ft above the median land-surface altitude in the wetland) and the simulation of potential drawdown of the water table in wetlands. The lateral no-flow boundary condition in the SAS was not changed because the SAS probably will continue to be dominated by downward leakage to the UFA and by local flow systems. The lateral no-flow boundary conditions for the UFA and LFA (fig. 25) were not changed because the general configuration of their respective potentiometric surfaces is not expected to change significantly. Historical maps of the UFA potentiometric surface indicate that this probably is a good assumption. The UFA potentiometric surface generally has decreased in altitude more or less uniformly over large areas as withdrawals have increased; this is consistent with a high-transmissivity aquifer, for which drawdowns tend to be relatively small and spread over relatively large areas. No attempt was made to account for movement of the interface between the freshwater and mineralized water flow systems that might occur under future conditions.

The specified-head boundaries in the UFA and LFA (fig. 25) were revised because the average 1998 water levels at these boundaries are not valid under future conditions. The specified-head boundaries in Marion and Sumter Counties are less problematic because projected increases in withdrawals are relatively small in this area; although some of the largest increases in withdrawals are projected to occur in Orange County and are expected to have a relatively large effect at the model boundary in this area. All specified-head boundaries were converted to specified flow for predictive simulations as follows: simulated flows into or out of the specified-head cells were extracted from the calibrated model; specified-head cells were converted to variable-head cells; the MODFLOW Well Package was used to input the corresponding specified flows into each of the former specified-head cells; and a comparison between model results for the specified-head and specified-flow boundaries indicated that the largest discrepancy in simulated water level was only 0.001 ft. A specified-flow boundary is equivalent to assuming that the hydraulic gradient at the boundary will remain

unchanged between average 1998 and projected future conditions. Although this formulation is an approximation of the unknown future boundary, it probably is relatively good: in Orange County where the largest drawdowns are expected, future withdrawals are projected to increase east of the model boundary in a pattern similar to that specified in the model west of the boundary, thereby maintaining a hydraulic gradient probably similar to that for average 1998 conditions. Furthermore, any error that might be caused by the approximation of future boundary conditions will be of lesser magnitude in the area of interest (Lake County and the Ocala NF) than near the model boundaries.

Projected Water Use

Withdrawals from the FAS within the model area in 2020 are projected to be 704 Mgal/d (about 3.1 in/yr averaged over the model area), a 50 percent increase from 1998 rates. Nearly all of this increase is attributed to additional water withdrawn for public supply (fig. 4).

Pumping rates at existing wells and projected future wells in 2020 were provided by Brian McGurk (St. Johns River Water Management District, written commun., 2000), Jim Waylon (Southwest Florida Water Management District, written commun., 1999), and L.H. Motz (University of Florida, written commun., 1999). Domestic self-supplied ground-water withdrawals in 2020 (table 2) were estimated in a manner identical to that for 1998 rates based on projected rates of increase or decrease reported by SJRWMD (1998), SFWMD (1998), SWFWMD (1998), and Suwannee River Water Management District (1998). Additional uncertainty exists in projected domestic self-supplied withdrawals because the future locations of these withdrawals are unknown and were assumed to be at the same locations as in 1998. Withdrawals from UFA wells (fig. 46) are projected to increase from 1998 to 2020 by 44 percent to 576 Mgal/d. Withdrawals from LFA wells (fig. 47) are projected to increase from 1998 to 2020 by 73 percent to 128 Mgal/d.

Artificial recharge resulting from septic tank leakage in 2020 (table 2) was estimated to be 60 percent of the projected 2020 rates for domestic self-supplied withdrawals in order to be consistent with the assumptions used in the calibrated model. This resulted in only a 1 percent increase in septic tank leakage from average 1998 conditions for the model area as a whole, but more significant changes were projected for individual counties (table 2). Facilities involved in the land application of reclaimed water probably will discharge at higher rates and will increase in number in the future, but these rates and locations are not well known. Therefore, artificial recharge from rapid infiltration basins and spray fields was assumed constant at 1998 rates. Recharge to the UFA by drainage wells was assumed constant at 1998 rates because the objective of the predictive simulations was not to evaluate changes in climatic conditions that would affect drainage-well recharge rates.

The changes in simulated water levels and flows indicated by predictive simulations are unique to a particular set of pumping locations and rates. If actual 2020 well locations or pumping rates differ from those described above, then corresponding simulations would be required to evaluate the revised 2020 conditions.

Predicted Water Levels and Flows

The predicted water levels and flows for projected 2020 conditions demonstrate the effects of changes in withdrawals from the FAS and artificial recharge from septic tank leakage. Septic tank leakage generally has a small impact on the results of predictive simulations because the magnitude of and change in septic tank leakage is relatively small (table 2) and the total volume of water resulting from septic tank leakage is a small component of the water budget (about 0.14 in/yr averaged over model area). Therefore, in the following discussion the differences in simulated water levels and flows between 1998 and 2020 can be attributed almost entirely to changes in the amount of ground water withdrawn from the FAS.

Drawdowns were calculated for all three aquifers (SAS, UFA, and LFA) by subtracting the simulated water level for average 1998 conditions from the predicted 2020 conditions (figs. 48, 49 and 50). Drawdowns generally were smallest in magnitude and areal extent in the SAS and greatest in the LFA. Average and maximum drawdowns in Lake County, the Ocala NF, and the entire model area are listed in table 6. The largest simulated drawdowns in each aquifer occurred in Orange County, where withdrawals generally are greatest in both the UFA and LFA. Significant drawdowns were simulated in Lake County, but in the Ocala NF drawdowns were relatively small.

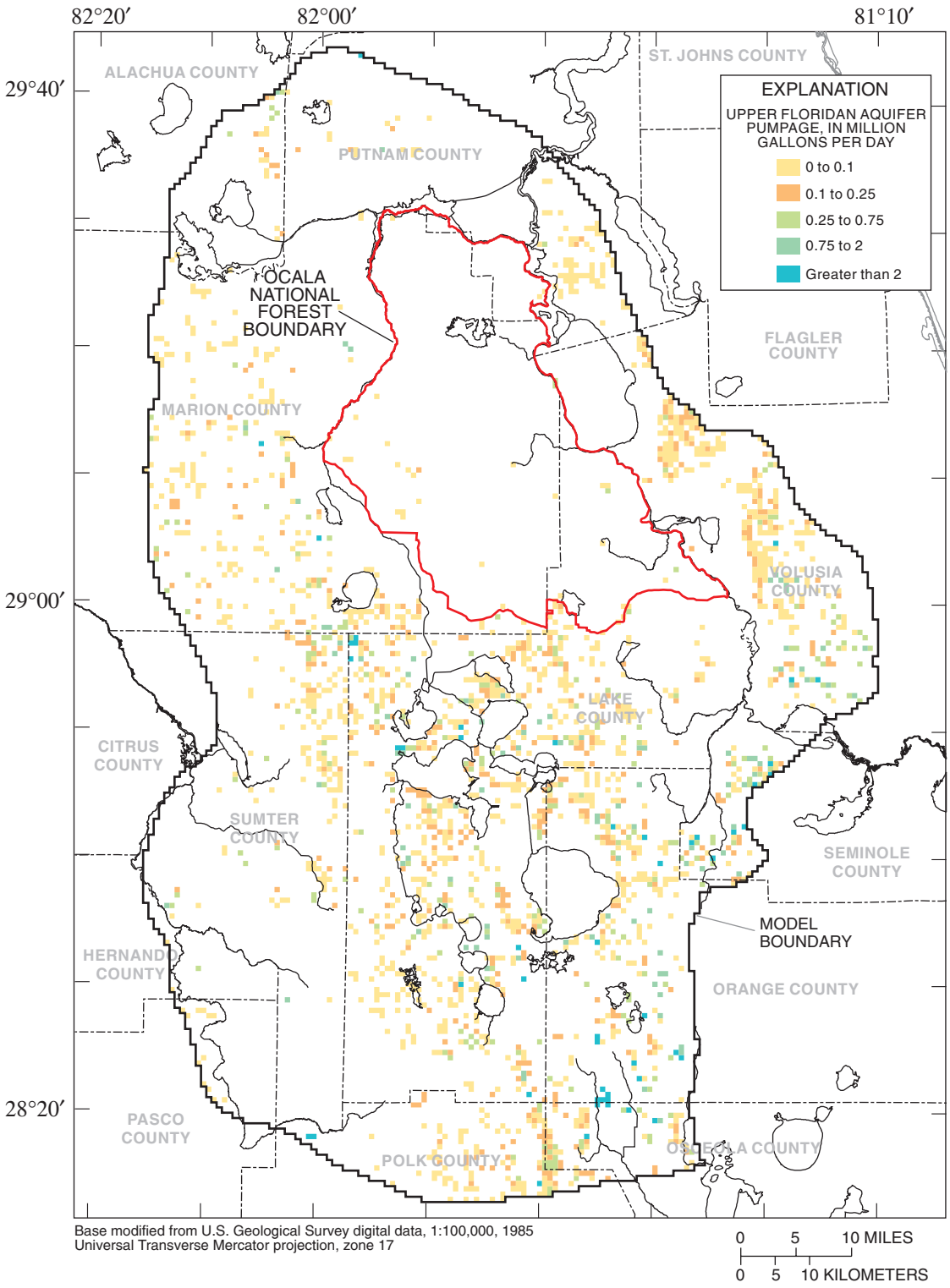

Figure 46. Ground-water withdrawal rates for the Upper Floridan aquifer specified in the model, projected 2020 conditions.

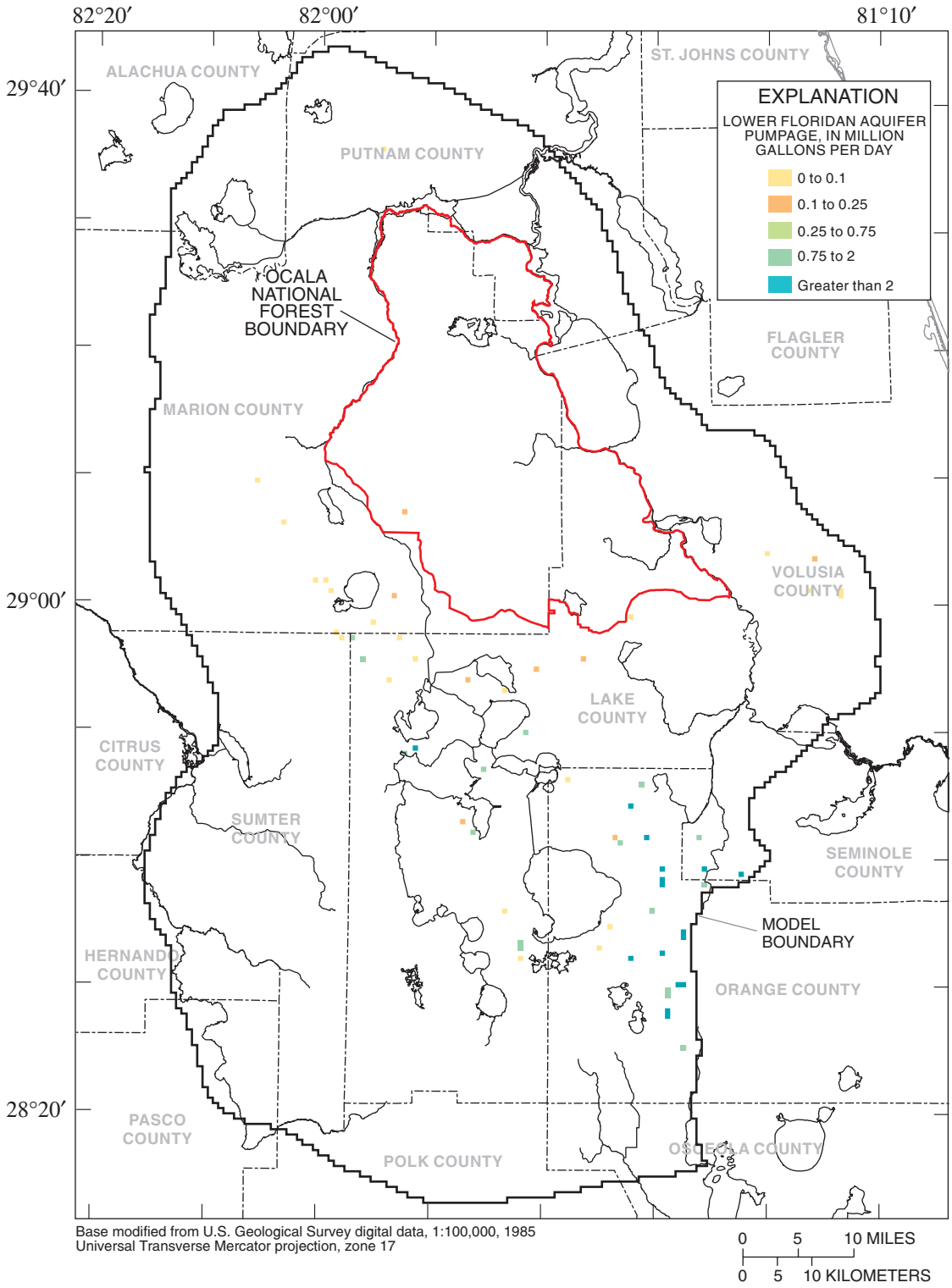

Figure 47. Ground-water withdrawal rates for the Lower Floridan aquifer specified in the model, projected 2020 conditions.

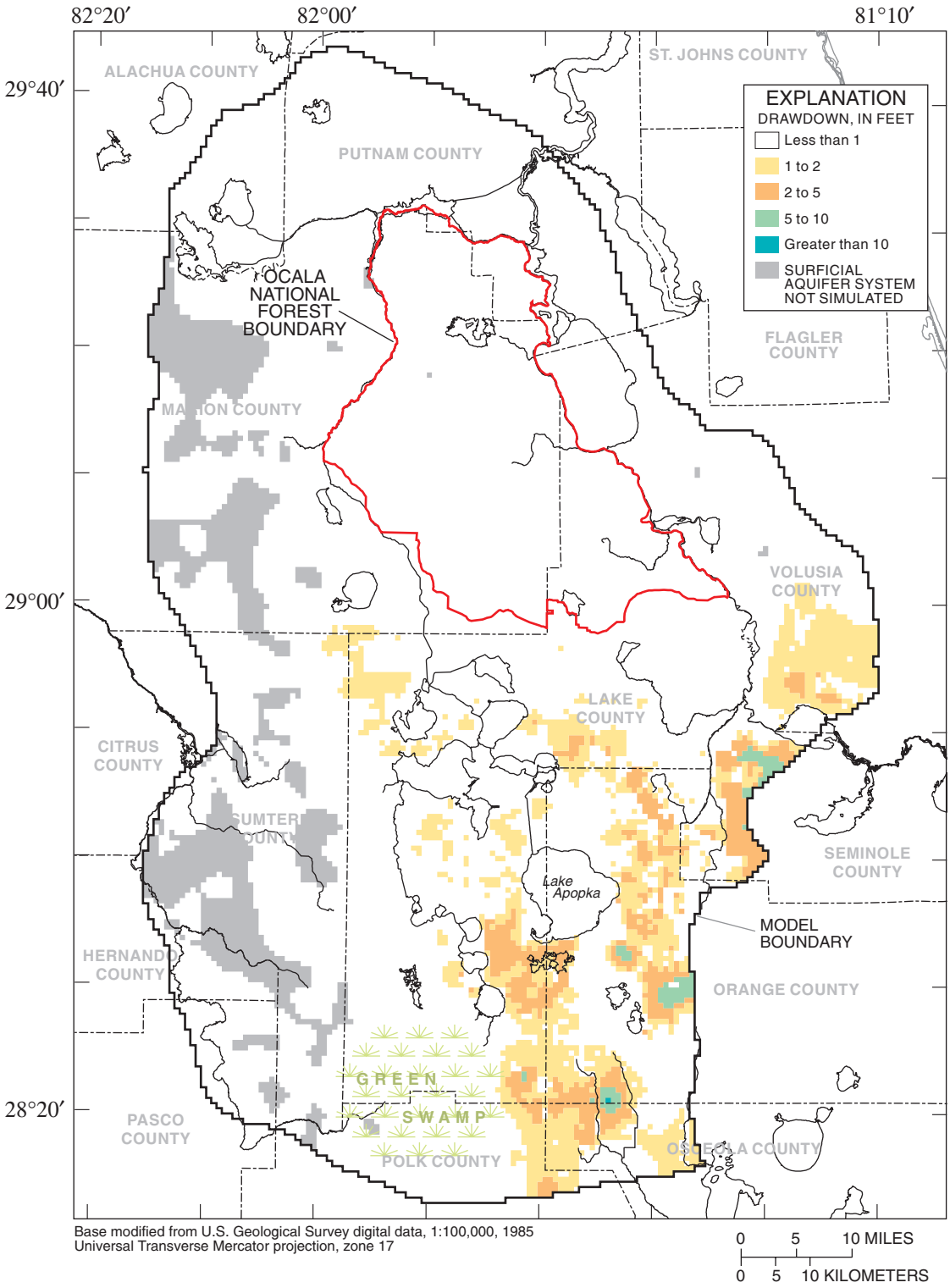

Figure 48. Simulated drawdown in the surficial aquifer system from average 1998 conditions as a result of projected 2020 conditions.

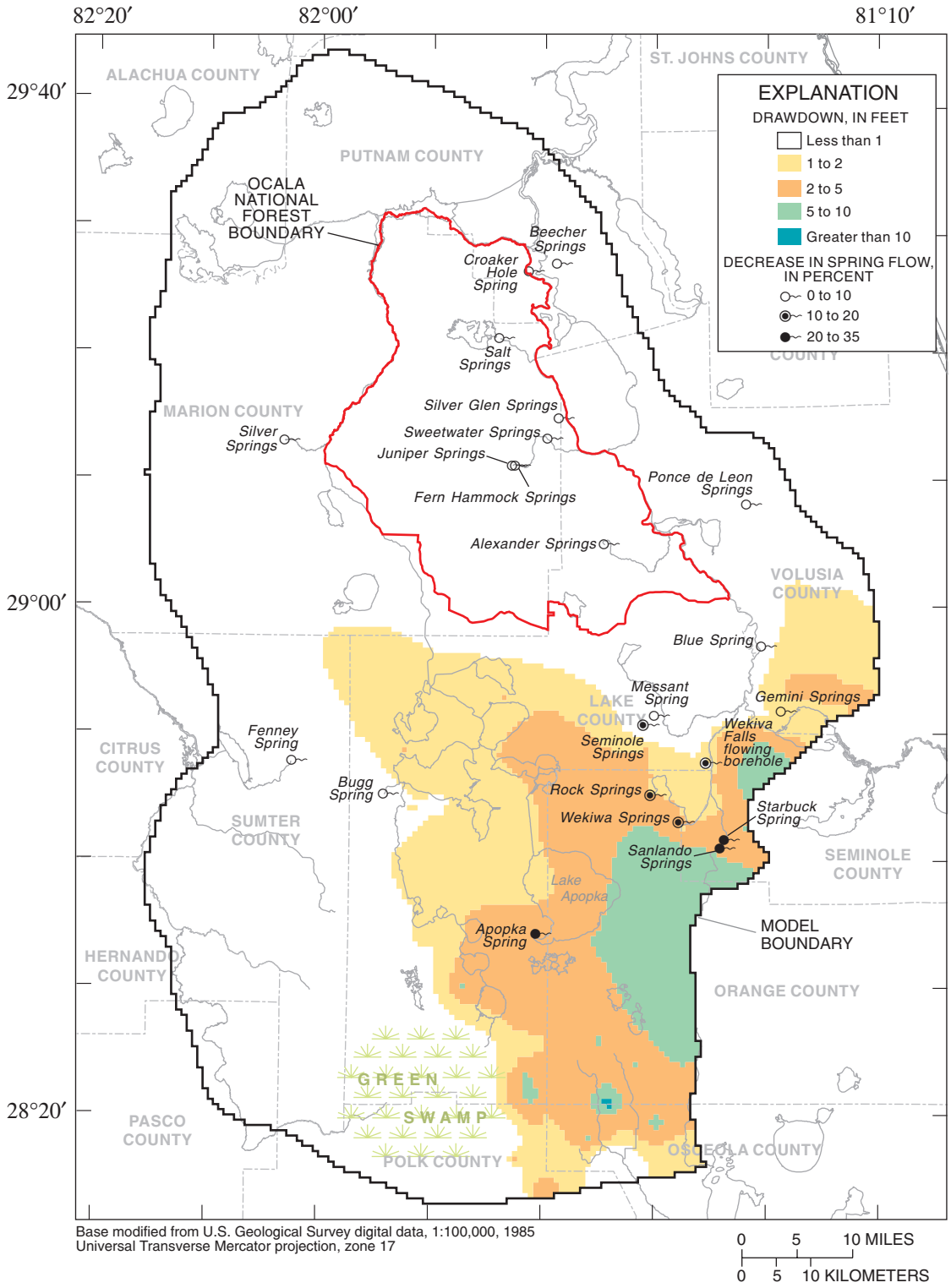

Figure 49. Simulated drawdown in the Upper Floridan aquifer and simulated decrease in flow from selected Upper Floridan aquifer springs from average 1998 conditions as a result of projected 2020 conditions.

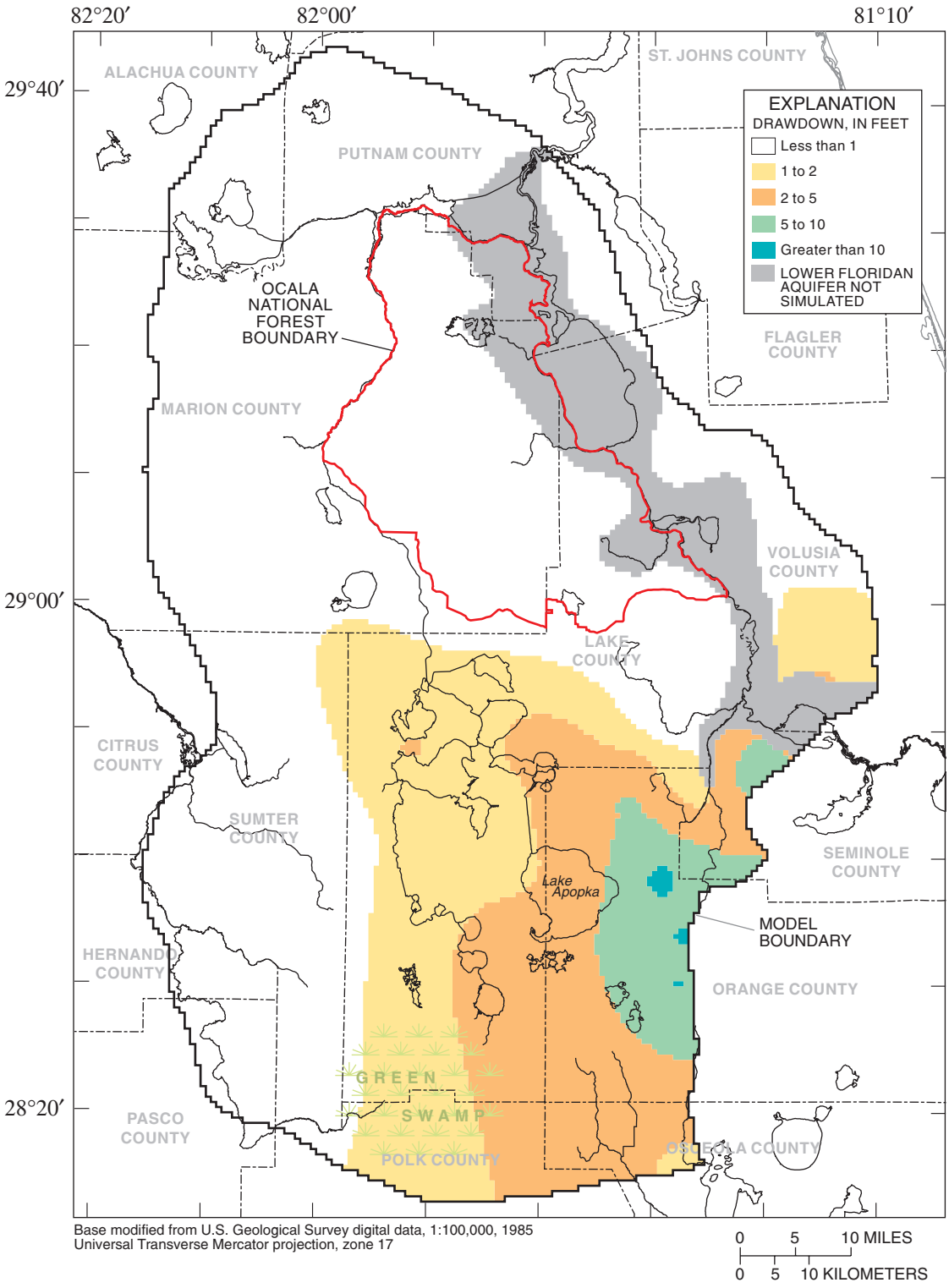

Figure 50. Simulated drawdown in the Lower Floridan aquifer from average 1998 conditions as a result of projected 2020 conditions.

Table 6. Average and maximum drawdowns from average 1998 conditions as a result of projected 2020 conditions for two predictive scenarios simulated by the model

[ft, feet; NF, National Forest; SAS, surficial aquifer system; UFA, Upper Floridan aquifer; LFA, Lower Floridan aquifer]

Area	Aquifer	Predictive scenario			
		Ground-water withdrawals and septic tank leakage adjusted to projected 2020 values in entire model area		Ground-water withdrawals and septic tank leakage adjusted to projected 2020 values in Lake County and Ocala NF only	
		Average drawdown (ft)	Maximum drawdown (ft)	Average drawdown (ft)	Maximum drawdown (ft)
Lake County	SAS	0.5	5.7	0.3	5.1
	UFA	1.1	7.6	.7	6.8
	LFA	1.4	4.3	.7	2.9
Ocala NF	SAS	.1	1.0	.1	.9
	UFA	.2	.8	.1	.5
	LFA	.3	.8	.2	.5
Entire model	SAS	.4	10.3	.1	5.1
	UFA	.9	11.8	.3	6.8
	LFA	1.2	19.1	.3	2.9

The simulated drawdown in the SAS (fig. 48) primarily is a function of the depth of the simulated water table below land surface, the leakance of the ICU (fig. 36), and the simulated drawdown in the UFA (fig. 49). In areas where the 1998 simulated water table is shallower than the specified extinction depth, drawdown will be smaller than if the simulated water table were below the extinction depth, because natural net recharge actually increases by an amount equal to the reduction in flux simulated by the MODFLOW Evapotranspiration Package (fig. 29). For example, in Orange County east of Lake Apopka the simulated drawdown of the water table varies spatially even though the leakance of the ICU is relatively uniform (fig. 36) and the variation in drawdown in the UFA is fairly small (fig. 49). Greater drawdown occurs in areas where the 1998 simulated water table was below the extinction depth, such as in ridge areas (compare figure 48 with areas where land-surface altitude exceeds 150 ft shown in figure 3); smaller drawdown occurs where the 1998 simulated water table was between land surface and the extinction depth. The degree to which drawdown in the UFA is propagated to the SAS is controlled by the leakance of the ICU. Drawdown in the SAS (fig. 48) most closely matches that in the UFA (fig. 49) where the leakance of the ICU is greatest (fig. 36). This clearly demonstrates the importance of the ICU on the hydrology of the SAS.

Drawdowns simulated in the UFA (fig. 49) primarily are a function of the magnitude of the increase in ground-water withdrawals from the UFA (compare figures 32 and 46), the transmissivity of the UFA (fig. 35), the leakance of the MSCU (fig. 37), and the simulated drawdowns in the LFA (fig. 50). Drawdowns will be relatively large where the UFA transmissivity is small and the projected increase in withdrawals is large, such as in the southeastern corner of Lake County (fig. 49). However, drawdowns will be relatively small if transmissivity is large even though the projected increase in withdrawals is large, such as in the northwestern corner of Lake County (fig. 49). Drawdown in the LFA can significantly impact the UFA in areas where the leakance of the MSCU is large. In Orange County east of Lake Apopka, moderate increases in withdrawals from the UFA are projected to occur, but even greater increases in withdrawals are expected from the LFA; therefore, the large drawdowns in the LFA (fig. 50) resulting from increased pumping from the LFA and the large leakance of the MSCU produce relatively large drawdowns in the UFA (fig. 49). Transmissivity controls not only the magnitude of drawdown, but also the spatial distribution of drawdown. The effects of pumping at a well will propagate further from the well if the transmissivity of the aquifer is greater; likewise, drawdown will be confined closer to the well if the

transmissivity of the aquifer is small. The relatively low transmissivity of the UFA in southern Lake County is the primary reason why drawdown from withdrawals in southeastern Lake County does not extend further west into the Green Swamp (fig. 49).

Drawdowns simulated in the LFA (fig. 50) primarily are a function of the magnitude of the increase in ground-water withdrawals from the LFA (compare figures 33 and 47), the transmissivity of the LFA, the leakance of the MSCU (fig. 37), and the simulated drawdown in the UFA (fig. 49). Spatial variation in LFA transmissivity is relatively small because the aquifer's horizontal hydraulic conductivity is assumed to be constant. Drawdown in the LFA generally matches, in a qualitative manner, the distribution and magnitude of the increase in withdrawals from the aquifer. Drawdown in the UFA can significantly impact the LFA in areas where the leakance of the MSCU is large. For example, in northwestern Seminole County significant drawdowns in the LFA are simulated to occur even though there are no withdrawals from the LFA aquifer in this area. Increases in withdrawals from the UFA reduce the rate of downward leakage through the MSCU or even reverse the direction of leakage, resulting in drawdowns in the LFA. A similar situation exists in southern Lake County, but the driving mechanism is somewhat different. The majority of the drawdown within this area is caused by eastward lateral flow in the LFA induced by the larger drawdowns in Orange County. The low leakance of the MCU (fig. 37) precludes much leakage between the UFA and LFA in southern Lake County.

The simulated water budget for the entire model area for projected 2020 conditions indicates that withdrawals from the FAS increased by 1 in/yr, or 50 percent, compared to average 1998 conditions. Because all predictive simulations were for steady-state conditions, any increase in withdrawals must be balanced by an equal increase in inflow from or decrease in outflow to other budget components. Comparing simulated 2020 budget components to those for average 1998 conditions (fig. 43), the 1 in/yr increase in well withdrawals can be accounted for as follows: outflow to ET nodes representing the combined effects of excess ET and excess overland runoff decreased 0.4 in/yr; inflow from river nodes representing streams or flow-through lakes increased 0.1 in/yr, while outflow to river nodes representing streams, flow-through lakes, or wetlands decreased 0.2 in/yr, for a net decrease of 0.3 in/yr in base flow; and outflow to drain nodes representing springflow decreased 0.3 in/yr.

Simulated water budgets for average 1998 and projected 2020 conditions also were compiled for Lake County and for the Ocala NF (figs. 51 and 52, respectively). The flow needed to meet projected 2020 conditions in Lake County is expected to increase 1.3 in/yr from that for average 1998 conditions as follows: withdrawals from the FAS are projected to increase 1.1 in/yr, artificial recharge resulting from septic tank leakage is projected to decrease 0.1 in/yr, and boundary inflow is simulated to decrease 0.1 in/yr because of increases in withdrawals from outside of Lake County. This 1.3 in/yr is simulated to be balanced by the following changes in other budget components (fig. 51): outflow to ET nodes representing the combined effects of excess ET and excess overland runoff decreases 0.5 in/yr; inflow from river nodes representing streams or flow-through lakes increases 0.1 in/yr while outflow to river nodes representing streams, flow-through lakes, or wetlands decreases 0.3 in/yr for a net decrease of 0.4 in/yr in base flow; outflow across county boundaries decreases 0.1 in/yr; and outflow to drain nodes representing springflow decreases 0.3 in/yr. Simulated flow changes in the Ocala NF are minimal because changes in withdrawals from the FAS in the Ocala NF are negligible. The Ocala NF is slightly affected by withdrawals from surrounding areas. Boundary inflow decreases 0.2 in/yr from average 1998 to projected 2020 conditions; this is simulated to be balanced by a 0.1 in/yr decrease in outflow to ET nodes representing the combined effects of excess ET and excess overland runoff and a 0.1 in/yr decrease in outflow to drain nodes representing springflow (fig. 52).

The decrease in springflow from average 1998 to projected 2020 conditions that is simulated to occur partially accounts for the additional water removed from the ground-water flow system by increased withdrawals from the FAS. Spring pool altitudes were assumed not to change as a result of projected 2020 conditions. The percent change in flow for any individual spring is equal to the percent change in the head difference (aquifer water level minus spring pool altitude) at the spring. For example, if the simulated head difference under 1998 conditions were 2 ft and the drawdown in the UFA 1 ft, simulated springflow would decrease 50 percent; however, if the simulated head difference were 10 ft the simulated springflow would decrease only 10 percent for the same 1 ft drawdown.

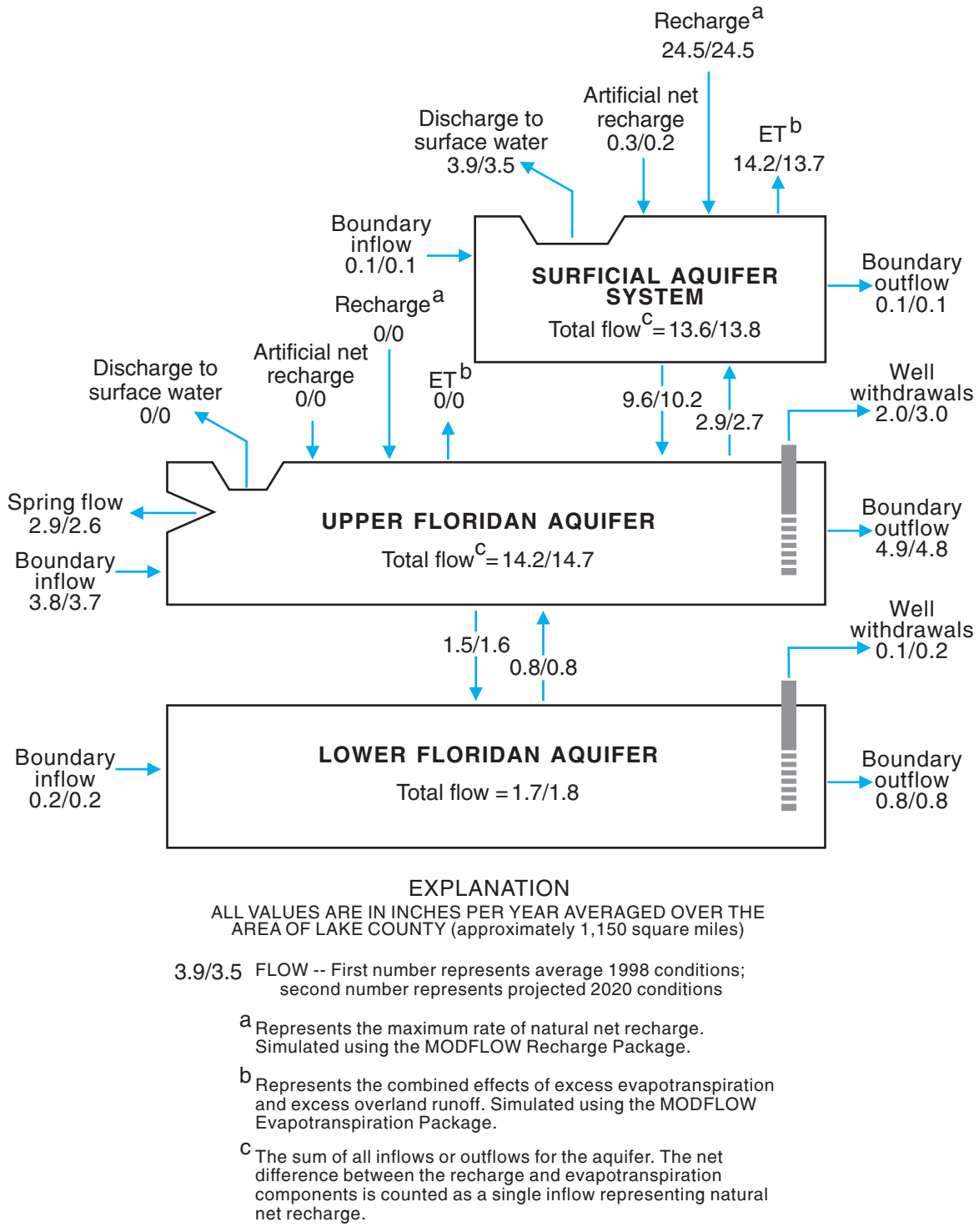

Figure 51. Simulated volumetric water budget for the aquifer system in Lake County, average 1998 and projected 2020 conditions.

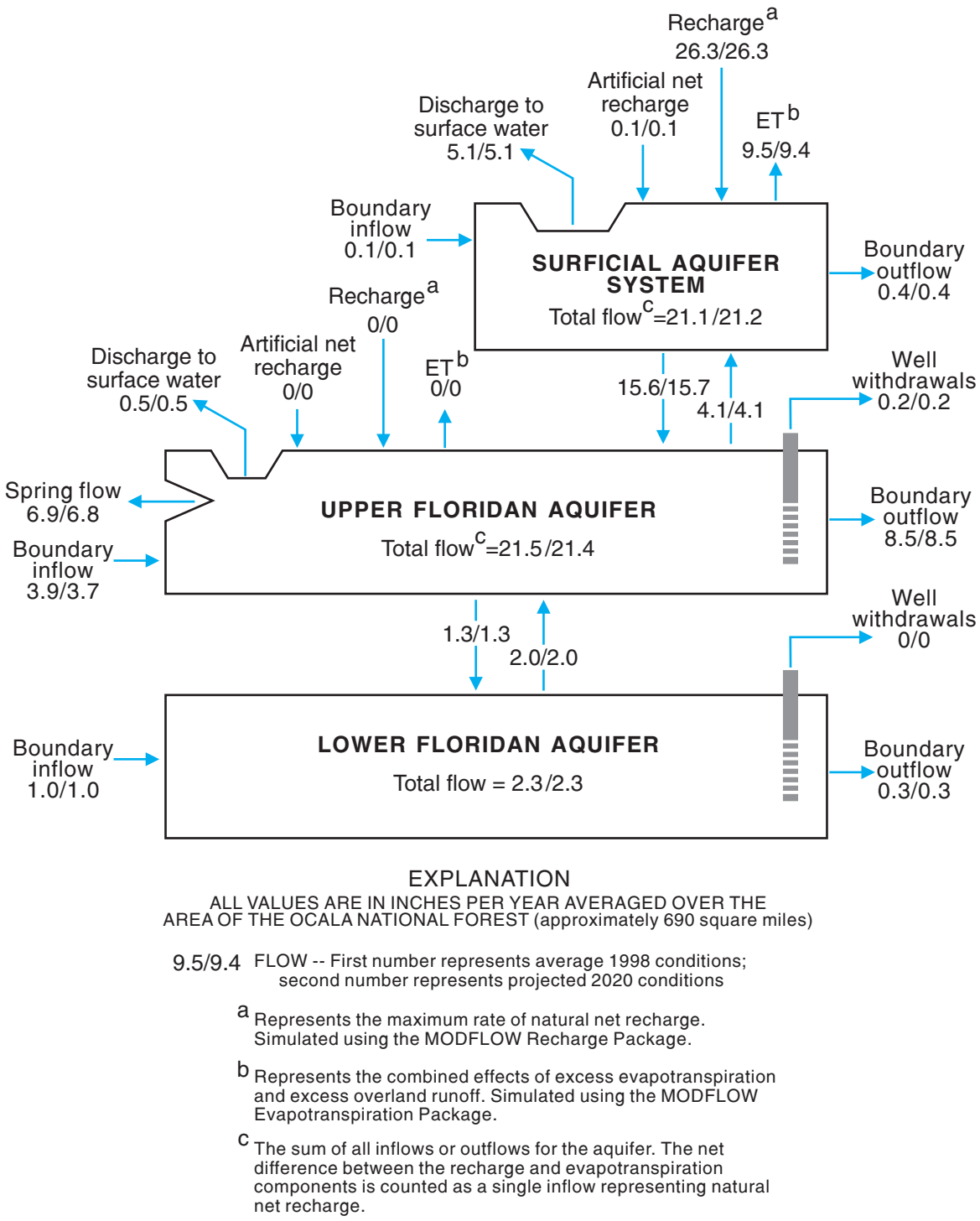

Figure 52. Simulated volumetric water budget for the aquifer system in the Ocala National Forest, average 1998 and projected 2020 conditions.

Simulated percent decreases in springflow vary considerably among the springs in the model area. The simulated 2020 flows for all first, second, and third-magnitude springs are shown in table 7, and the range in percent decreases in flow of all first- and second-magnitude springs is shown in figure 49. The greatest decreases occurred for springs having small head differences (table 7) and located in areas with large drawdowns in the UFA (fig. 49). Of all the first- or second-magnitude springs, each of the following springs had a simulated flow decrease greater than 10 percent: Seminole, Rock, Wekiwa, Starbuck, Sanlando, and Apopka (fig. 49 and table 7). Of these six springs, Starbuck, Apopka, and Sanlando Springs had the largest simulated decreases in flow of 25, 28, and 33 percent, respectively. The largest simulated flow decreases for first- or second-magnitude springs in Lake County were at Bugg (9 percent), Seminole (12 percent), and Apopka Springs (28 percent). The largest simulated flow decreases for first- or second-magnitude springs in the Ocala National Forest were at Alexander (1 percent), Fern Hammock (1 percent), and Juniper Springs (4 percent). Some third-magnitude and smaller springs experienced larger percentage decreases in springflow; for example, simulated springflow at Bear and Holiday Springs in Lake County decreased 44 and 69 percent, respectively (table 7).

Ground-water levels within Lake County and the Ocala NF are affected by ground-water withdrawals in adjacent areas. More than one-half of the total increase in withdrawals from 1998 to 2020 conditions is projected to occur in Orange, Seminole, and Marion Counties. The effects of this pumping propagate into Lake County, the Ocala NF, and surrounding counties. An additional predictive simulation was performed by adjusting ground-water withdrawals and septic tank leakage to projected 2020 conditions only in Lake County and the Ocala NF. All other stresses in the remainder of the model area were maintained at average 1998 levels. Average and maximum drawdowns resulting from this predictive scenario are listed in table 6 and can be compared to drawdowns simulated under the first predictive scenario. Drawdowns in the SAS in Lake County generally were similar in spatial distribution to those in figure 48 but were smaller in magnitude. Drawdowns in the UFA in Lake County exceeded 2 ft in the vicinity of Clermont and in the southeastern corner of the County. Drawdowns in the LFA in Lake County exceeded 1 ft in the vicinities of Lady Lake, Leesburg, Eustis, Mount Dora, and Clermont. Drawdowns were relatively small in the Ocala NF (table 6). All these drawdowns are less than those considering projected 2020 withdrawals within the entire model area (figs. 48, 49, and 50; and table 6). These results demonstrate the regional scale of ground-water flow in the FAS and the importance of considering the regional ground-water system surrounding the area of interest when assessing the effects of future water-use needs.

Lake and Wetland Water Levels

The interaction between lakes or wetlands and the ground-water flow system is quite complex and difficult to simulate. The response of a lake or wetland to hydrologic stresses can be significantly affected by local hydrologic and lithologic conditions. Such variations can be large in the mantled karst environment that exists throughout much of the model area. Using high-resolution seismic-reflection data, Tihansky and others (1996) confirmed the sinkhole origin of four lakes along the Lake Wales Ridge in Polk and Highlands Counties. They concluded that the lithology and distribution of geologic materials under and in the immediate vicinity of a lake can be highly variable, yet important in determining the response of the lake to changes in stress. Most of the lakes in the model area probably are similar to these four lakes; likewise, wetlands where the water level is above land surface probably behave similarly to these lakes. Therefore, the effects of increased withdrawals from the FAS can differ considerably between any two lakes or wetlands, even those in close proximity to each other.

The hydrologic behavior of individual lakes cannot be accurately simulated by a regional-scale model, such as the one presented in this report. The present model should be used only in a more qualitative manner to determine areas where lakes are more likely to be affected by increased withdrawals from the FAS. A qualitative interpretation of lake-level declines in closed-basin lakes can be estimated from figure 48. Because net recharge at closed-basin lakes (parameter N_{cbl}, table 3) is assumed to remain constant from average 1998 to projected 2020 conditions, simulated drawdown of closed-basin lake levels primarily is controlled by the leakance of the ICU and the simulated drawdown in the UFA.

Table 7. Simulated discharge from selected Upper Floridan aquifer springs, projected 2020 conditions

[USGS, U.S. Geological Survey; ft, feet; cfs, cubic feet per second]

USGS site identification number	Station name	County	Head difference at spring[1] (ft)	Simulated discharge, 2020 (cfs)	Percent change in discharge, 1998 - 2020
284740081251701	Apopka (Gourd Neck) Spring near Oakland	Lake	7.5	24	-28
284612081303401	Bear Spring near Astatula	Lake	3.0	1.1	-44
02234620	Double Run Road Seepage (into Little Lake Harris) near Astatula	Lake	2.2	1.2	-51
02236205	Holiday Springs at Yalaha	Lake	1.0	1.4	-69
02243550	Blue Springs, Park Drive near Yalaha	Lake	5.2	2.3	-17
285224081262400	Bugg Spring near Okahumpka	Lake	6.3	11	-9.5
285038081270100	Wekiva Falls Resort flowing borehole	Lake	2.4	16	-18
291136081381000	Island Spring, Wekiva River	Lake	9.8	6.1	-7.2
02237322	Seminole Springs near Sorrento	Lake	2.2	35	-12
02235250	Messant Spring near Sorrento	Lake	11.0	18	-2.7
292725081393500	Camp La-No-Che Springs near Paisley	Lake	8.8	1.0	-5.4
02234610	Mosquito Springs Run, Alexander Springs Wilderness	Lake	0.7	2.0	-14
283903081430100	Alexander Springs	Lake	9.5	103	-1.1
02236160	Juniper Creek South Tributary Seepage near Astor	Lake	15.4	6.1	-.7
284038081443201	Silver Glen Springs near Astor	Marion	5.4	102	-.5
02235255	Fern Hammock Springs near Ocala	Marion	6.7	13	-1.3
285702081322400	Juniper Springs near Ocala	Marion	2.0	11	-4.3
284241081281800	Morman Branch Headwater Seepage at SR19	Marion	1.0	2.5	-11
02236147	Morman Branch Seepage (into Juniper Creek) near Astor	Marion	11.5	4.6	-.8
283400081405100	Silver Springs near Ocala	Marion	3.7	889	-3.4
285105081263800	Sweetwater Springs along Juniper Run	Marion	9.1	14	-.8
02237400	Salt Springs	Marion	7.9	84	-.3
291112081400400	Wells Landings Springs	Marion	7.9	5.0	-.3
292735081394500	Camp Seminole Spring, Girl Scout Camp, Orange Springs	Marion	6.9	1.0	-.8
02234600	Orange Spring near Orange Springs	Marion	17.6	2.5	-.3
284437081491700	Wekiwa Springs, Wekiwa Springs State Park	Orange	11.3	55	-17
02239500	Witherington Springs, Wekiwa Springs Park near Apopka	Orange	9.6	3.1	-33
284452081495400	Rock Springs near Apopka	Orange	8.0	45	-19
284047081441501	Croaker Hole Spring near Welaka	Putnam	7.3	94	-.1
285318081295200	Beecher Springs near Fruitland	Putnam	11.4	12	.0
292618081412100	Mud Spring near Welaka	Putnam	7.2	1.7	-.2
02244022	Welaka Spring	Putnam	11.7	1.0	-.1
02236220	Satsuma Spring near Satsuma	Putnam	17.2	1.3	.1
284922081250300	Sanlando Springs near Longwood	Seminole	9.4	15	-33
02236132	Palm Springs near Longwood	Seminole	13.2	4.0	-24
285102081263900	Starbuck Spring near Longwood	Seminole	13.1	11	-25
02236130	Miami Springs near Longwood	Seminole	12.7	4.0	-21
292521081551200	Shady Brook Spring #5 (South Panasoffkee Spring Group) near Lake Panasoffkee	Sumter	9.4	3.0	-.7
292540081552400	Shady Brook Spring #4 (South Panasoffkee Spring Group) near Lake Panasoffkee	Sumter	1.5	2.9	-4.1
292542081552600	Shady Brook Spring #3 (South Panasoffkee Spring Group) near Coleman	Sumter	1.0	2.8	-7.2
293021081570600	Shady Brook Spring #2 (South Panasoffkee Spring Group) near Coleman	Sumter	3.0	2.9	-2.7
284455081494100	Fenney Spring (headspring of Shady Brook to Lake Panasoffkee) near Coleman	Sumter	2.0	45	-1.2
293038081563800	Little Jones Creek Spring #3 (North Panasoffkee Spring Group) near Wildwood	Sumter	1.0	2.6	-12
291200081390601	Little Jones Creek Spring #2 (North Panasoffkee Spring Group) near Wildwood	Sumter	1.7	4.5	-9.4
02236095	Little Jones Creek Headspring (North Panasoffkee Spring Group) near Wildwood	Sumter	4.2	7.5	-5.8
290220081260400	Gemini Springs near DeBary	Volusia	17.8	10	-6.0
283844081422300	Blue Spring near Orange City	Volusia	5.8	159	-2.8
284940081303800	Ponce De Leon Springs near DeLand	Volusia	11.7	22	-1.0

[1]Head difference was calculated as the altitude of the average 1998 Upper Floridan aquifer water level (interpolated from May 1998 (fig. 2) and September 1998 (Bradner, 1999) potentiometric maps) in the model cell containing the spring minus the measured or estimated 1998 spring pool altitude.

The most definitive conclusion that can be drawn from the regional-scale model concerning impacts on lake levels caused by withdrawals from the FAS is that lake-level declines are more likely to be greater in areas where the magnitude of the drawdown in the UFA is greater (fig. 49), the leakance of the ICU is greater (fig. 36), and no surface-water inflow to or outflow from the lake exists. Applying these criteria to the areas of primary interest, Lake County and the Ocala NF, closed-basin lakes are most likely to experience the greatest decreases in lake levels under projected 2020 conditions in the following areas: southern Lake County, generally east and south of the Clermont chain-of-lakes, and east-central Lake County, generally in the vicinity of Mount Dora. However, anywhere the ICU has a high leakance, such as many areas in the Ocala NF, the potential exists for relatively large declines in lake levels if large drawdowns also occur in the UFA.

The effects of projected 2020 ground-water withdrawals on wetlands is simulated differently by the model depending on the position of the simulated water table. Where the simulated 1998 water table is greater than 3 ft above the median land-surface altitude in a wetland, an increase in 2020 withdrawals from the FAS can cause a decrease in simulated ground-water discharge to the wetland. Generally, little drawdown of the simulated water table will occur because the decrease in simulated ground-water discharge to the wetland occurs instead. Where the simulated 1998 water table is less than or equal to 3 ft above the median land-surface altitude in a wetland, an increase in 2020 withdrawals from the FAS can cause drawdown of the simulated water table in the wetland. Because ground-water discharge to the wetland is simulated to be zero in this case, simulated drawdown generally will be larger than if ground-water discharge were simulated to occur. The hydrologic behavior of individual wetlands cannot be accurately simulated by a regional-scale model, such as the one presented in this report. The present model should be used only in a more qualitative manner to determine areas where wetlands are more likely to be impacted by increased withdrawals from the FAS. A qualitative interpretation of water-table declines in the vicinity of wetlands can be estimated from figure 48. Factors affecting the magnitude and location of water-table declines in wetlands are the same as those described for lake levels. Water-table declines in wetlands are more likely to be greater in areas where the magnitude of the drawdown in the UFA is greater (fig. 49), the leakance of the ICU is greater (fig. 36), and no surface-water inflow to or outflow from the wetland exists. Likewise, in the areas of primary interest, Lake County and the Ocala NF, wetlands are most likely to experience the greatest decreases in water levels under projected 2020 conditions in the same areas as those described for closed-basin lakes: southern Lake County, generally east and south of the Clermont chain-of-lakes, and east-central Lake County, generally in the vicinity of Mount Dora. However, anywhere the ICU has a high leakance, such as many areas in the Ocala NF, the potential exists for relatively large water-table declines in wetlands if large drawdowns also occur in the UFA.

Spring and Well-Field Contributing Areas

A contributing area for a spring or discharging well is defined as the surface area that delineates the location of water entering the ground-water system, either at the water table or by induced infiltration from surface-water bodies, that eventually flows to a spring or well and discharges (Reilly and Pollock, 1993, p. 2). Often the objective of defining a contributing area is to delineate areas where regulatory or management measures may be applied to minimize the likelihood of contaminating source water to springs or wells. A contributing area for a spring or well is not the same as its cone of depression: sources of water to a spring or well can be located considerable distances beyond the area of influence of the feature; likewise, source water can originate from only a small area within the area of influence. Consequently, the configuration of a contributing area can be quite complex and generally is best delineated by using a three-dimensional ground-water flow model.

The USGS particle-tracking program MODPATH (Pollock, 1994) was used with ground-water flow model results to delineate contributing areas. Particle-tracking techniques can only simulate the advective transport of solutes and cannot be used to calculate solute concentrations in ground water because these techniques do not consider dispersion, degradation, or retardation processes. Nevertheless, particle-tracking techniques are well suited for defining contributing areas because the configuration of a contributing area is dependent on the hydraulics of the ground-water flow system, not the transport or geochemistry of a solute.

Effective porosity values for each aquifer and confining unit in the model are the only hydrologic data required, in addition to standard MODFLOW input and output, for a steady-state particle-tracking analysis. Effective porosity is the fraction of interconnected pore space in a volume of rock or unconsolidated sediment. An effective porosity value of 0.40 was used for the SAS and ICU and 0.20 was used for the UFA, MSCU/MCU, and LFA. The value of effective porosity only affects particle traveltime and has no effect on particle paths calculated by MODPATH; therefore, error in the values used for effective porosity will not affect the configuration of contributing areas.

Particle starting locations were based on volumetric flow rates; one particle represented approximately 1,000 ft^3/d (7,480 gal/d) of springflow or 100 ft^3/d (748 gal/d) of well discharge. Particles were located on each inflow face of the model cell containing the spring or well; the number of particles were proportional to the simulated flow though each cell face and were distributed in an array proportional to the dimensions of each cell face. For example, if the inflow through the face of a cell containing a spring were 500,000 ft^3/d and the cell face were 2,500 ft wide and 400 ft high, particle starting locations were distributed in an array of 56 particles in the horizontal direction and 9 particles in the vertical direction. Particles moved through the ground-water system in a backward-tracking manner until they stopped at the water table. Because of the proportional arrangement of particle starting locations, the density of particle ending locations at the water table is proportional to the contributing recharge rate. The contributing recharge rate is defined in this report as the flow quantity that represents the amount of net recharge at the water table or induced infiltration from surface-water bodies that eventually flows to the spring or well of interest, as opposed to other downgradient discharge locations. Contributing recharge rates might vary considerably throughout a contributing area; for example, the majority of the water discharged by a spring or well might originate in only a small part of its contributing area.

Two springs and two UFA well fields were selected for particle-tracking analyses. Apopka Spring and Alexander Springs were selected because although both are large-discharge springs, each is affected by different hydrologic stresses. Apopka Spring is located in southern Lake County, where effects from projected 2020 withdrawals are expected to be relatively large; conversely, Alexander Springs is located in the Ocala NF, where effects from projected 2020 withdrawals are expected to be minimal. Several wells in east-central Lake County, collectively referred to as the "Central well field," and several wells in the southeastern corner of Lake County, collectively referred to as the "South well field," were selected because they are located in areas expected to experience significant impacts from projected 2020 withdrawals.

An attempt was made to select springs and well fields that were not located in weak sinks. A weak sink is a model cell that contains internal sinks that do not discharge at a rate large enough to consume all the water entering the cell (Pollock, 1994, p. 2-17); by comparison, a strong sink is a model cell in which all the water entering the cell is discharged by the internal sinks. This problem is exacerbated by large cell size and high transmissivity, both of which are common in regional ground-water flow models of the FAS. Apopka and Alexander Springs and the Central and South well fields are all contained in weak sink cells under average 1998 conditions, projected 2020 conditions, or both. Springs and well fields that were contained in strong sink cells under both average 1998 and projected 2020 conditions and also were located in geographic areas of interest were not available in the present model. The degree to which a weak sink affects the delineation of a contributing area varies and will be discussed in the following paragraphs for each of the selected springs or well fields.

The contributing areas depicted in figures 53 and 54 demonstrate configurations that are typical in a complex hydrogeologic environment. The contributing area for Apopka Spring covers approximately 30 mi^2 based on average 1998 conditions; a flux of approximately 15 in/yr distributed evenly over the contributing area would be required to supply the total springflow of 33 ft^3/s (21 Mgal/d). Most of the water that discharges from Apopka Spring originates as recharge at the water table north of Lake Louisa; a lesser amount originates as recharge at the water table south of Lake Louisa; and a small amount (less than 4 percent) originates as leakage from Lake Louisa and other surface-water bodies (fig. 53). The contributing area for Alexander Springs covers approximately 76 mi^2 based on average 1998 conditions; a flux of approximately 18 in/yr distributed evenly over the contributing area would be required to supply the total springflow of 104 ft^3/s (67 Mgal/d).

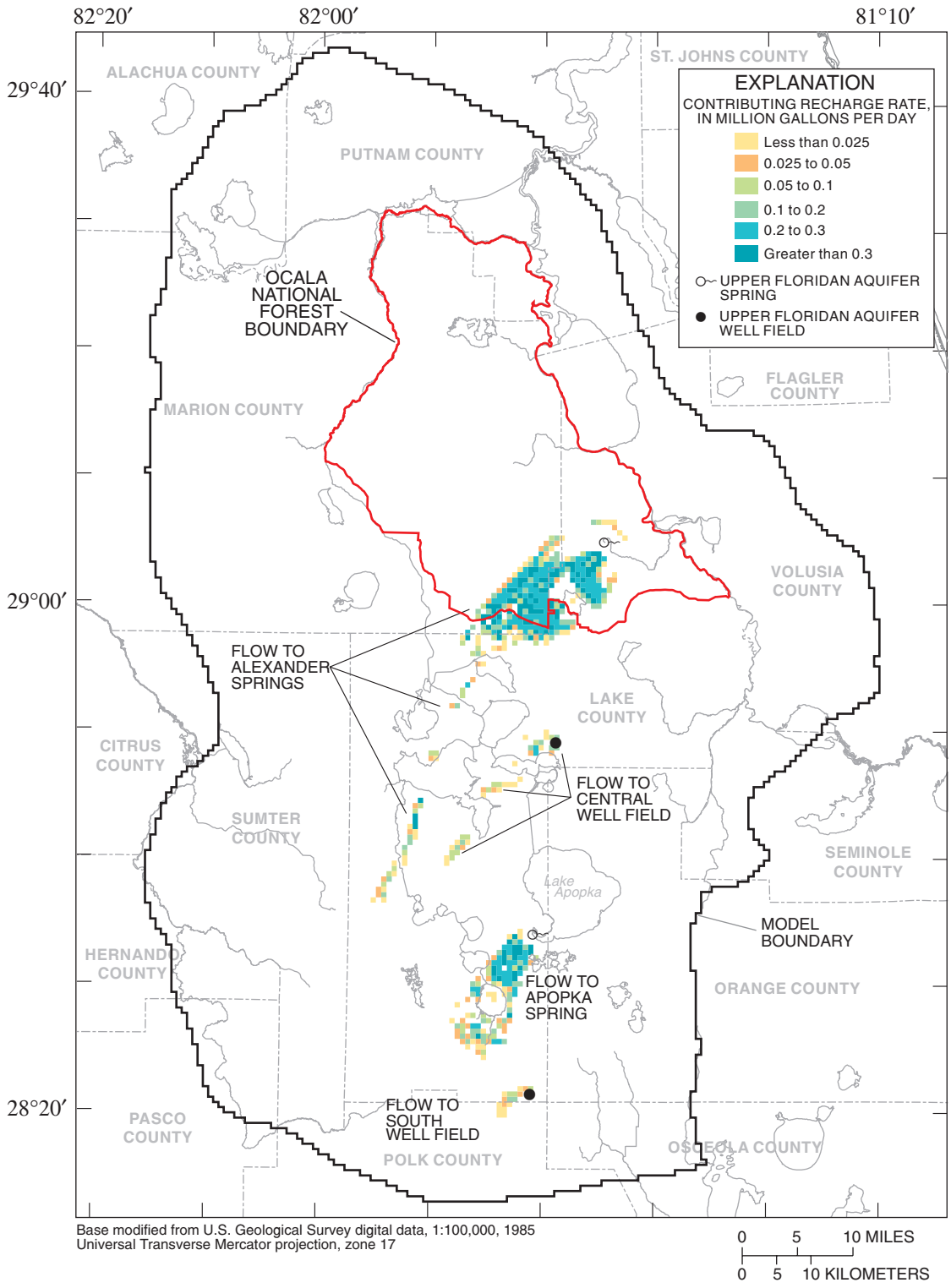

Figure 53. Contributing areas for selected springs and public-supply well fields based on particle-tracking analyses of simulated steady-state 1998 conditions.

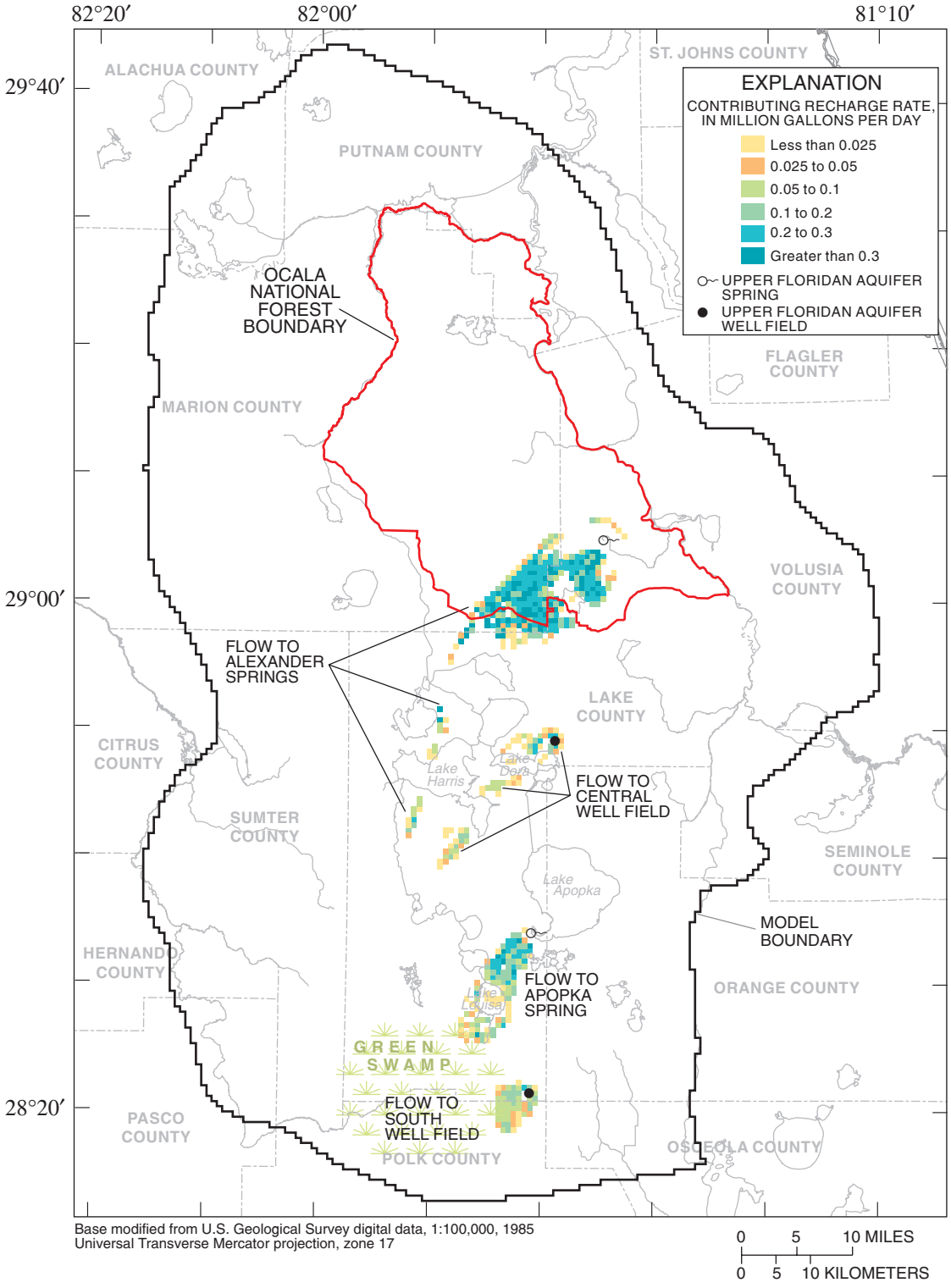

Figure 54. Contributing areas for selected springs and public-supply well fields based on particle-tracking analyses of simulated steady-state projected 2020 conditions.

The majority of water that discharges from Alexander Springs originates as recharge at the water table southwest of the spring in the south-central part of the Ocala NF (fig. 53). Water originating in the part of the contributing area that extends into central Lake County (fig. 53) accounts for less than 6 percent of the total springflow; this source water moves along very long flow paths, with most of the water passing through the LFA before moving back up into the UFA and discharging at the spring. Only Apopka Spring under average 1998 conditions is a strong sink. Apopka Spring under projected 2020 conditions and Alexander Springs under both average 1998 and projected 2020 conditions are weak sinks. However, the effect on contributing areas probably is insignificant because the flow that passes through these weak sinks, as opposed to discharging at the spring, is negligible (less than 0.5 percent of the respective springflow).

Changes in contributing areas from average 1998 to projected 2020 conditions were relatively small for both springs (figs. 53 and 54). This was expected for Alexander Springs because springflow is simulated to decrease only 1 percent to 103 ft^3/s (67 Mgal/d) and relatively little pumping exists in the vicinity of the spring contributing area. However, simulated flow at Apopka Spring under projected 2020 conditions is 24 ft^3/s (16 Mgal/d), a decrease of 28 percent; yet the size of the contributing area decreases a relatively small amount from 30 to 26 mi^2. The decrease in springflow is balanced by decreases in contributing recharge rates in addition to the decrease in contributing area size (figs. 53 and 54). A flux of approximately 13 in/yr distributed evenly over the contributing area would be required to supply the reduced flow from Apopka Spring under projected 2020 conditions.

The configuration of and changes in contributing areas for wells are governed by the same processes as those for springs. The Central well field consists of four wells located within the same model cell. The total pumpage from these wells was 2.4 Mgal/d (3.8 ft^3/s) in 1998; this is projected to nearly double to 4.6 Mgal/d (7.1 ft^3/s) in 2020. The Central well field was simulated as a weak sink under average 1998 conditions, but as a strong sink with the increase in pumping projected under 2020 conditions. A flow of approximately 0.3 Mgal/d (0.5 ft^3/s) passes through the weak sink containing the Central well field and exits from the east face of the cell under average 1998 conditions. Therefore, the contributing area (fig. 53) actually is the contributing area for the model cell, which has a total flow of 2.7 Mgal/d (4.2 ft^3/s); the contributing area for only the Central well field would be smaller, would have lower contributing recharge rates, or both. Nevertheless, the actual contributing area for the Central well field probably is not greatly different from that shown in figure 53. The South well field consists of four wells located in the same model cell. The total pumpage from these wells was only 0.060 Mgal/d (0.1 ft^3/s) in 1998, but this is projected to increase greatly to 4.5 Mgal/d (7.0 ft^3/s) in 2020. Well field pumpage was so small in 1998 (about 9 percent of the total flow in the cell) that the contributing area for the well field is much too small to be delineated with a regional flow model. The contributing area shown in figure 53 is for the 0.7 Mgal/d (1.1 ft^3/s) of total flow in the model cell. Under projected 2020 conditions the South well field is a weak sink because a small amount of downward leakage through the MSCU/MCU is simulated to occur. This downward leakage, however, represents only 0.3 percent of the projected 2020 well field pumpage and is not of sufficient magnitude to have a significant effect on the delineation of the contributing area for the South well field.

Changes in contributing areas from average 1998 to projected 2020 conditions are significant for the Central and South well fields (figs. 53 and 54) because large percentage increases in withdrawals are projected to occur at these wells. For the Central well field, the contributing recharge area increased in size from 9.2 mi^2 to 16 mi^2, although the average contributing recharge flux decreased slightly from 6.3 in/yr to 6.0 in/yr. This is a direct result of the relatively low rates of net recharge at the water table in the vicinity of the Central well field contributing area (fig. 44); consequently, the size of the contributing area must increase in order to capture enough water to meet the increased demand. In fact, approximately 38 percent of the water withdrawn by the Central well field under projected 2020 conditions is simulated to originate as net recharge at the water table south of Lakes Dora and Harris (fig. 54). The South well field is located just east of the Green Swamp where rates of net recharge at the water table also are relatively low (fig. 44). The contributing area for the South well field under projected 2020 conditions covers approximately 13 mi^2 and extends west and southwest into the Green Swamp over a relatively large area. Contributing recharge rates are relatively low in this area (fig. 54), and the average contributing recharge flux is 7.4 in/yr.

Effects of Parameter Uncertainty on Model Predictions

The uncertainty that exists in parameter values from the calibrated model (table 4) also affects the reliability of model results. For example, if the vertical hydraulic conductivity of the MSCU/MCU could have been more accurately estimated during model calibration, then the simulated drawdowns in the UFA and LFA might have been significantly different from those derived from the calibrated model. Additional analyses were performed in order to illustrate the possible effects of parameter uncertainty on model predictions.

Linear 95-percent confidence intervals were calculated for simulated drawdowns using YCINT-2000 (Hill and others, 2000), a post-processing program for MODFLOW-2000. The length of a linear 95-percent confidence interval on a simulated water-level difference, or drawdown, is dependent on the change in sensitivities of the simulated water level with respect to each parameter between a base simulation and a predictive simulation (subject to different hydrologic stresses or boundary conditions) and on the parameter variance-covariance matrix for calibration conditions (Hill, 1994, p. 36). The length of linear 95-percent confidence intervals will be small in areas where the changes in sensitivities are small for the parameters with a small variance and small covariances; simulated drawdowns in such areas should be interpreted as being more reliable. Likewise, the length of linear 95-percent confidence intervals will be large in areas where the changes in sensitivities are large for the parameters with a large variance and large covariances; simulated drawdowns in these areas should be interpreted as being less reliable.

Linear 95-percent confidence intervals were calculated for simulated drawdowns in all 60,487 active model cells; the half-lengths of the confidence intervals are depicted in figures 55, 56, and 57. Because these are linear confidence intervals, the lower and upper limits are symmetric about the simulated drawdown and can be estimated by subtracting from and adding to the simulated drawdown (figs. 48, 49, and 50) the half-length of the linear 95-percent confidence interval. Simultaneous, as opposed to individual, confidence intervals were used to portray uncertainty over the entire model area, rather than just at a few specific locations. All 13 model parameters were considered in the calculation of the linear 95-percent confidence intervals on drawdown. The five parameters that were held constant during inverse modeling (table 3) might be important under predictive conditions, and it is important to acknowledge the uncertainty presented by these parameters.

The mean half-length of linear 95-percent confidence intervals on drawdown is similar among all three aquifers: 7.0 for the SAS, 7.0 for the UFA, and 7.2 ft for the LFA. Throughout most of the model area simulated drawdowns generally are equally reliable, but uncertainty still exists even where simulated drawdowns are small. The half-length of linear 95-percent confidence intervals on drawdown is larger than 6.8 ft in all model cells. This minimum level of uncertainty results from the uncertainty inherent in the parameter values from the calibrated model (table 4), as well as the five parameters held constant during inverse modeling, and from the fact that simulated water levels throughout the model area are sensitive (to some degree) to the increase in ground-water withdrawals projected to occur under 2020 conditions. The simulated drawdowns generally are less reliable in western Orange and western Seminole Counties, where confidence intervals are largest (figs. 55, 56, and 57). The large projected increases in withdrawals from the FAS in these areas contribute to this uncertainty by increasing the sensitivity of simulated water levels to one or more model parameters. For example, withdrawals from the LFA at a well field in northwestern Orange County are projected to increase from 3.1 Mgal/d in 1998 to 21.2 Mgal/d in 2020. Because of such a large change in stress, the simulated LFA water level at the well field is much more sensitive to $K_{h,lf}$ under projected 2020 conditions than under average 1998 conditions: a 100-percent increase in $K_{h,lf}$ results in a 14-ft increase in simulated water level under projected 2020 conditions but only a 2.2-ft increase under 1998 conditions. This large change in sensitivity, coupled with the relatively large variance of the final value of $K_{h,lf}$ (as indicated by the relatively large coefficient of variation for $K_{h,lf}$, table 4), results in a linear 95-percent confidence interval on drawdown with a half-length of 27 ft at the well field (fig. 57). Consequently, simulated drawdown at the well field should be considered less reliable than the simulated drawdown in most other areas.

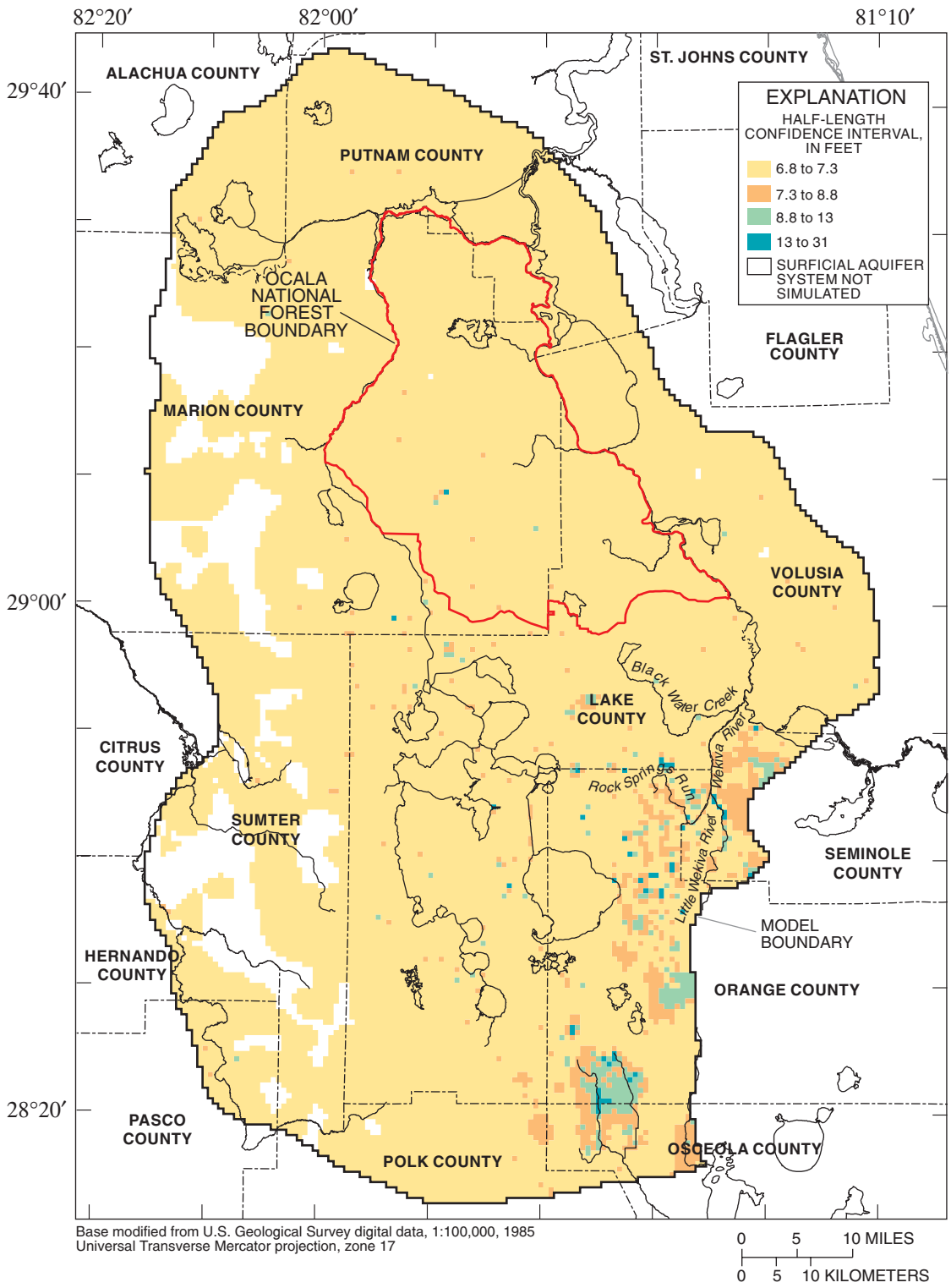

Figure 55. Half-length of linear 95-percent confidence intervals on the simulated drawdown in the surficial aquifer system from average 1998 conditions as a result of projected 2020 conditions.

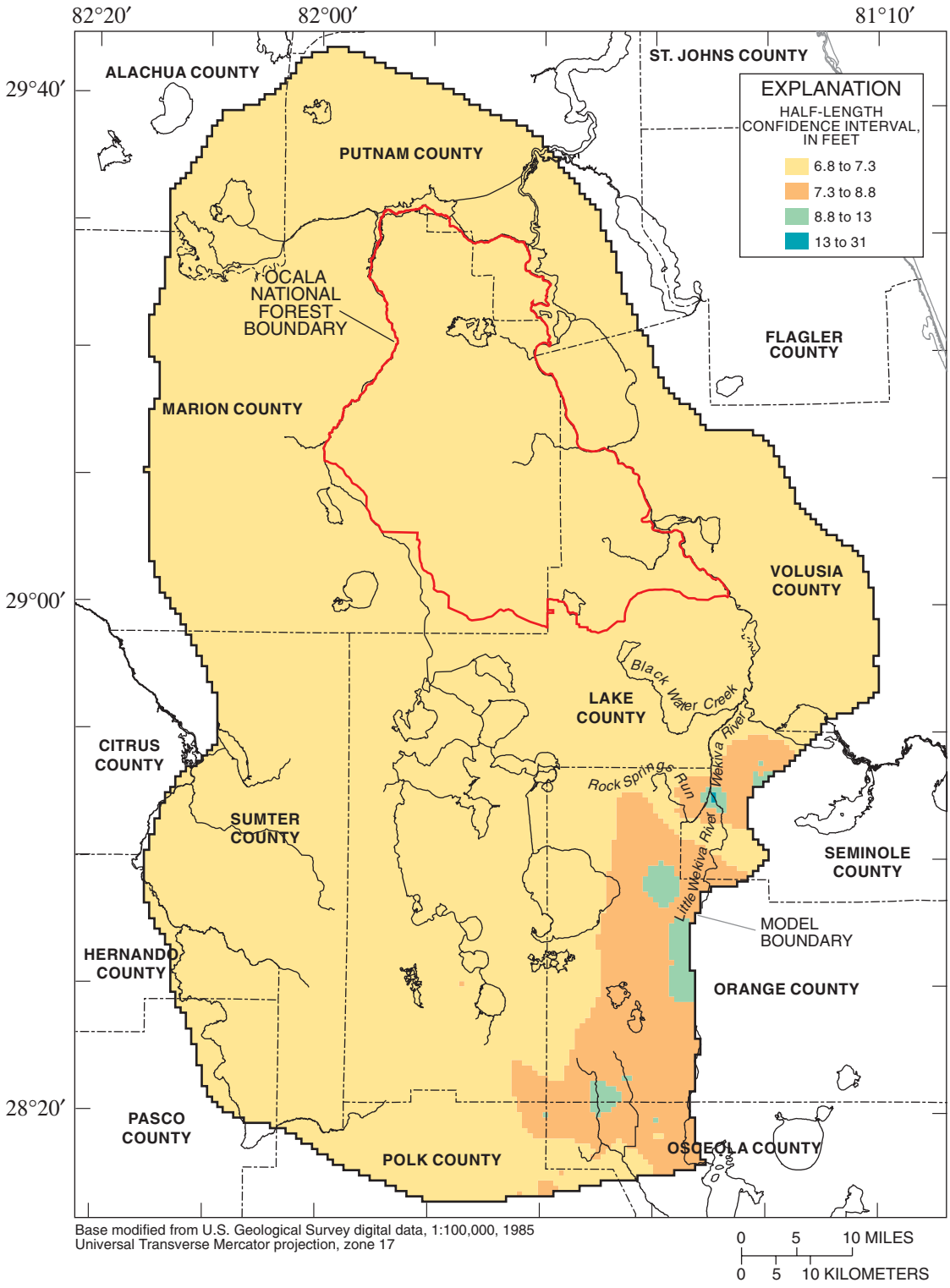

Figure 56. Half-length of linear 95-percent confidence intervals on the simulated drawdown in the Upper Floridan aquifer from average 1998 conditions as a result of projected 2020 conditions.

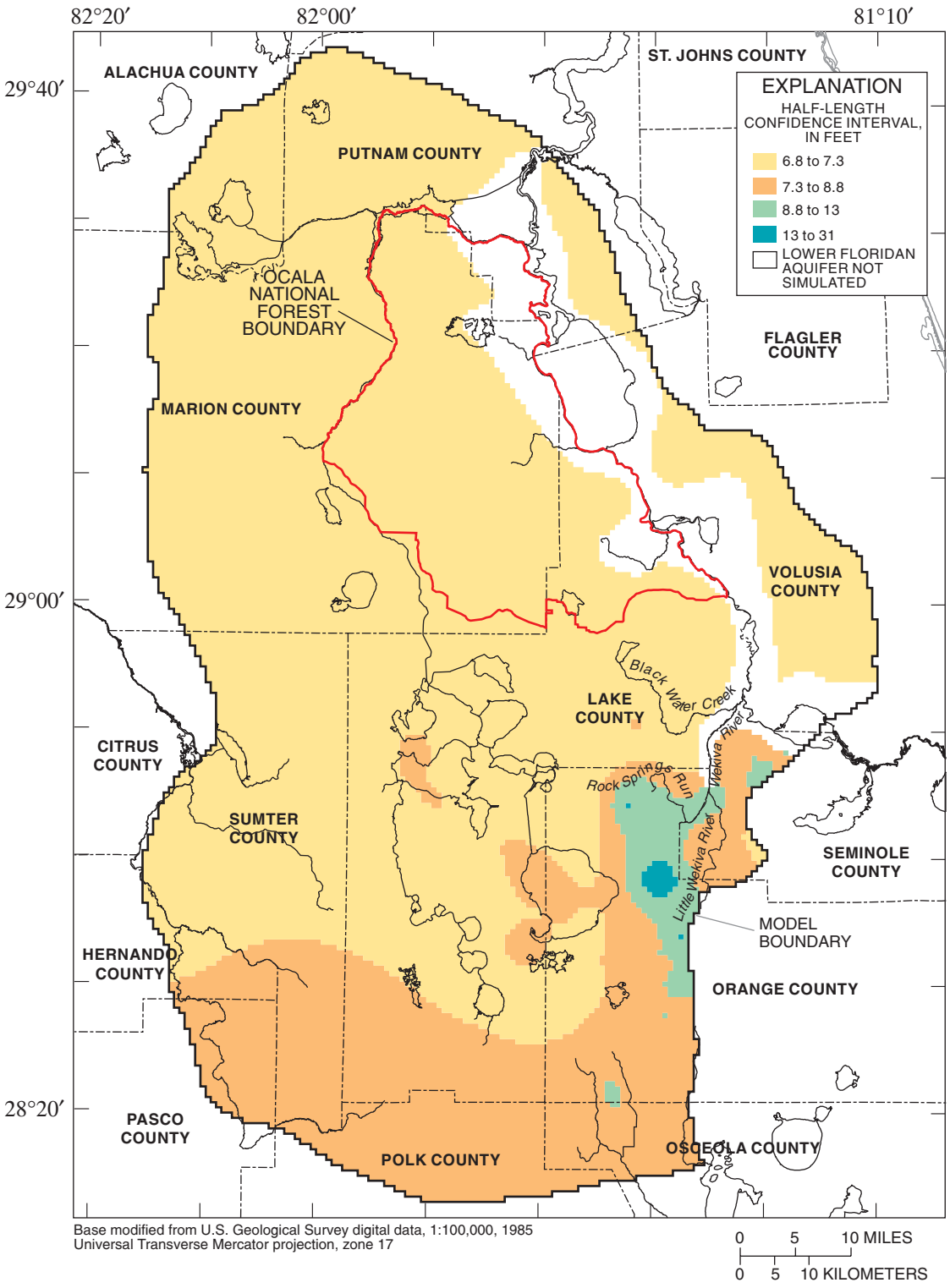

Figure 57. Half-length of linear 95-percent confidence intervals on the simulated drawdown in the Lower Floridan aquifer from average 1998 conditions as a result of projected 2020 conditions.

A large degree of uncertainty in simulated drawdowns does not exist only where large drawdowns also are simulated. Changes in simulated fluxes resulting from changes in ground-water withdrawals also can cause uncertainty in simulated drawdowns, even where drawdowns are relatively small. Simulated base flow to the Little Wekiva River near its confluence with the Wekiva River decreased 33 percent from average 1998 to projected 2020 conditions, leading to a significant increase in the sensitivity of the simulated SAS water level to several model parameters. Linear 95-percent confidence intervals with half-lengths exceeding 13 ft along the lower Little Wekiva River (fig. 55) indicate that the uncertainty in simulated SAS drawdown caused by this decrease in simulated base flow, which itself was caused by the increase in FAS withdrawals, is relatively large. This relatively large degree of uncertainty exists even though drawdowns in each aquifer in the area were smaller than in surrounding areas (figs. 48, 49, and 50). The leakance of the ICU in the area is quite high (fig. 36) and is the mechanism through which pumping from the FAS can have such a large effect on the SAS. Consequently, simulated drawdowns in the UFA in the area also are less reliable (fig. 56) because of a 33-percent decrease in simulated upward leakage through the ICU that occurs along with the 33-percent decrease in simulated base flow, both of which are caused by the increase in FAS withdrawals.

Uncertainty in simulated drawdown can also be caused by nonlinear head-dependent boundaries, such as those simulated by the MODFLOW Evapotranspiration, River, and Drain Packages. Head-dependent boundaries can be nonlinear because the boundary condition can change from head-dependent to specified flux, or specified flux to head-dependent, depending on the simulated head in the model cell containing the boundary. Many cells in this model contain head-dependent boundaries simulated by the MODFLOW Evapotranspiration and River Packages, especially in the SAS. Many of the large linear 95-percent confidence intervals on drawdown in the SAS (fig. 55) are the result of a head-dependent boundary converting between specified flux and head-dependent boundary conditions. Evapotranspiration nodes change from a specified-flux boundary under average 1998 conditions to a head-dependent flux boundary under projected 2020 conditions as the simulated water level declines from above land surface to below land surface. For example, one cell in the Ocala NF has a linear 95-percent confidence interval on drawdown with a half-length of 18 ft (fig. 55). Drawdown of the SAS water table is only 0.12 ft, but this was sufficient to lower the simulated water table under projected 2020 conditions below land surface and change the boundary condition from specified flux to head-dependent flux. The sensitivity of the simulated water table to each model parameter significantly decreased with the head-dependent boundary, resulting in a large linear 95-percent confidence interval on drawdown. River nodes change from a head-dependent flux boundary under average 1998 conditions to a specified-flux boundary under projected 2020 conditions as the water level drops below the riverbed bottom altitude. For example, where a river node converts to a specified-flux boundary with zero flow, which can occur in this model at river nodes representing ungaged streams or wetlands, the simulated SAS water level is no longer constrained by the river node and consequently is much more sensitive to all parameters. Such large changes in sensitivities lead to linear 95-percent confidence intervals on drawdown with half-lengths exceeding 13 ft in eastern Lake County between Blackwater Creek and Rock Springs Run (fig. 55).

The model is nonlinear and the weighted residuals are not normally distributed. Under these circumstances, linear confidence intervals do not accurately portray the true uncertainty in simulated drawdowns. In addition, the confidence intervals presented in this section reflect only the uncertainty of the 13 model parameters, not the additional uncertainty presented by possible alternative conceptual models or parameter zonations. Therefore, the half-length of a linear 95-percent confidence interval should be considered only as a rough indicator of the effect of parameter uncertainty on simulated drawdown, based on the assumption that other aspects of the model accurately depict the true ground-water flow system. Nevertheless, figures 55, 56, and 57 provide an approximate measure of the reliability of model predictions that could be useful when assessing the effects of future water-use needs.

Model Limitations

Results derived in this study are based primarily on ground-water flow model simulations. Consequently, these results are subject to the assumptions and limitations inherent in the model. Model results are limited by simplifications of the conceptual model, grid scale, the lack of sufficient hydrologic data to

account for all of the spatial variation in hydrologic properties and stresses throughout the model area, and the distribution and accuracy of data used for calibration and predictive simulations.

The conceptual model used to construct the ground-water flow model is a highly simplified representation of the true ground-water system. Simplifications in the conceptual model, which are needed to represent extremely complex natural systems, are the most likely source of error in the ground-water flow model. Also, the aquifer systems are neither isotropic nor homogeneous. Varying lithology produces preferential flow zones, and in the FAS these probably are enhanced by dissolution features. The actual relation between the combined effects of excess ET and excess overland runoff and the depth of the water table below land surface probably is more complex than that simulated by using the MODFLOW Evapotranspiration Package; this might affect model results significantly, especially the simulated 2020 drawdowns. Lateral boundaries were located as far outside of Lake County and the Ocala NF as practical because inaccuracies in assigned boundary conditions can adversely affect model results, especially near model boundaries. As a result, the model should not be used for analysis near any of the lateral boundaries. If sufficient data were available, transient calibration and model simulations would have more accurately portrayed the ground-water system; however, steady-state analyses are sufficient for simulating the average long-term effects of future ground-water withdrawals.

The horizontal and vertical discretization required by a finite-difference approximation assumes that hydrologic properties and stresses do not vary within a model cell. Because this rarely is the case in natural hydrologic systems, any variations at the scale of a model cell must be represented by an appropriate average value. The adequacy of the discretization is a function of how well an average value of the property or stress represents the effects of the actual, spatially variable values. Significant variations in hydrologic properties at a scale smaller than the model cell (2,500 by 2,500 ft) are common in the mantled karst environment in the model area. These small-scale variations might significantly affect larger scale average values. In addition, the location of stresses (for example, well withdrawals or artificial recharge) is distorted to some degree by discretization effects. The vertical discretization of one model layer for each aquifer does not allow for simulation of vertical flow within each aquifer. However, most vertical flow within the FAS probably occurs through the MSCU; significant vertical flow may occur within the SAS, but available data are not sufficient for the calibration of a multilayer SAS. In addition, much of the vertical flow that occurs within the SAS probably is associated with local flow systems, which cannot be adequately simulated with a regional-scale model. Consequently, the discretization used in the present model is adequate for fulfilling the objective of modeling ground-water flow on a regional scale.

Because the objective of the model is to simulate ground-water flow on a regional scale, the model should not be used to interpret local-scale phenomena. Site-specific questions are better addressed with a site-specific study. This is particularly true when interpreting the simulated effects of projected 2020 ground-water withdrawals on individual lakes and wetlands.

Parameter values and predictions from the present model differ, to some degree, with results from other models (Spechler and Halford, 2001; Sepúlveda, 2002; and McGurk and Presley, in press). Differences among results from models covering the same area do not necessarily invalidate the respective models. Each model's results are a product of the particular hydrologic data, assumptions, and methodology used in constructing and calibrating the model. Each model is an alternative way of representing the ground-water system that, given the available data, may be equally valid. In complex, natural systems, selecting only one model as superior to all others often is difficult. It may be necessary to accept with equal confidence the range of results provided by the various models.

Parameter values and distributions from the calibrated model are dependent not only on the accuracy of hydrologic data but also on the spatial distribution of those data, which include water levels and flows to which the model was calibrated, as well as stresses such as artificial recharge or well withdrawals. Model results are more likely to be accurate in areas where there are large known stresses and corresponding water-level or flow observations indicating aquifer response to those stresses. Model results should be interpreted cautiously in areas where there was either no stress or a poorly known stress on the aquifer system or no water-level or flow observations. In general, if additional data were available, perhaps collected under different hydrologic conditions, a recalibration of the model might yield significantly different results.

Simulated drawdowns are affected by the accuracy of 2020 water-use projections and are calculated relative to average 1998 conditions, which do not represent long-term average conditions. The magnitude and distribution of future ground-water withdrawals may be different from those based on present-day projections. Error in projected 2020 withdrawals used in the model would have a direct affect on simulated drawdowns: if actual 2020 withdrawals were greater than projected 2020 withdrawals, then actual drawdowns in 2020 would be greater than simulated drawdowns; likewise, if actual 2020 withdrawals were less than projected 2020 withdrawals, then actual drawdowns in 2020 would be less than simulated drawdowns. If simulated drawdowns relative to long-term average conditions, or any condition other than average 1998 conditions, were desired, an additional simulation based on estimated conditions during the desired time period would be required.

Predictive simulations presented in this report pertain primarily to changes in ground-water withdrawals and, to a much lesser degree, changes in septic tank leakage, but not to changes in climatic conditions, such as a drought. Effects of a drought on hydrologic conditions, such as aquifer water levels or springflows, could be of similar or greater magnitude compared to effects from projected 2020 withdrawals. Assessing the affects of changes in climatic conditions on the ground-water flow system in the model area was beyond the scope of this study. However, the predictive simulations do fulfill the model objective of adequately simulating the effects of the major anthropogenic stresses on the hydrologic system.

SUMMARY

The hydrogeology and water resources of Lake County and the Ocala National Forest (Ocala NF) were evaluated during a 5-year study (1995-2000) and the effects of future water-use needs on those resources were simulated. Lake County is predominantly rural, with several widely scattered, but steadily growing urbanized areas. Urban expansion also is steadily expanding into the County, mainly from the Orlando area southeast of Lake County. The Ocala NF remains mostly undeveloped; however, urban expansion in Marion County is steadily moving towards the southwestern and western edges of the Ocala NF.

The study area of about 4,800 square miles (mi^2), which includes Lake County (1,150 mi^2) and the Ocala NF (690 mi^2), was defined by delineating estimated ground-water flow divides of the Upper Floridan aquifer (UFA) around Lake County and the Ocala NF. Lake County and the Ocala NF are drained by surface and subsurface drainage systems. Surface drainage mainly is by the Palatlakaha River, Ocklawaha River, and other tributaries to and including the St. Johns River. Subsurface drainage occurs through karst features in much of the study area. A substantial amount of ground water discharges from the UFA to these drainage basins as base flow to streams or springs and seeps.

The principal hydrogeologic units in Lake County and the Ocala NF are the surficial aquifer system (SAS) and the Floridan aquifer system (FAS). The two aquifer systems generally are separated by the intermediate confining unit (ICU), which contains beds of lower permeability sediments that confine the water in the FAS. The bottom of the freshwater flow system is defined by either the sub-Floridan confining unit, which comprises low permeable limestone, dolomite, and anhydrite, or the depth at which the chloride concentration of the water is greater than 5,000 milligrams per liter (mg/L) in the FAS, whichever is shallower.

The SAS is up to 300 feet (ft) thick where present, unconfined, and composed principally of fine- to coarse-grained quartz sand, silt, and interbedded clay, peat, marl, and shell. The SAS serves as a reservoir and filter bed for purifying water before it recharges the underlying FAS. The base of the SAS was defined by the first occurrence of persistent beds of Miocene or Pliocene age containing at least 50 percent silt, clay, limestone, or dolomite.

The ICU underlies the SAS and generally consists of the Hawthorn Group composed principally of an interbedded mixture of marine sediments including phosphatic sand, clay, and limestone; and low permeable silt and clay beds of younger age. Throughout most of the study area, the ICU restricts the vertical movement of water between the SAS and the UFA (except where breached by sinkholes). Thickness of the ICU is highly variable because of past erosional processes and sinkhole formation; thickness ranges from 0 to 150 ft in the study area.

The FAS is a thick sequence of carbonate rocks that are generally highly permeable and hydraulically connected in varying degrees. The FAS in the study area ranges in thickness from 900 to 2,000 ft and is subdivided on the basis of the vertical occurrence of

two zones of relatively high permeability, the UFA and the Lower Floridan aquifer (LFA), which generally are separated by either the middle semiconfining unit or middle confining unit. The thickness of the UFA averages about 300 ft through most of the study area, and ranges from 200 ft thick or less in the southwestern part of the Ocala NF and in the extreme northwestern part of Lake County to more than 400 ft thick in the extreme northeastern part of the Ocala NF and southwestern Lake County. The LFA averages about 1,400 ft thick throughout most of the study area, ranging from about 1,200 ft in the northern part of the Ocala NF to 1,500 ft or more in western Lake County and much of northern Sumter County.

The FAS is the major source of ground water in the study area. In 1998, about 115 million gallons per day (Mgal/d) were pumped in Lake County and about 5.7 Mgal/d were pumped in the Ocala NF. Agricultural use accounted for nearly 50 percent; municipal, domestic, and recreation use accounted for more than 40 percent; and commercial and industrial use accounted for less than 10 percent of the total water pumped. Total water pumped from the UFA is projected to be about 173 Mgal/d in Lake County by 2020, and is projected to remain at about 5.7 Mgal/d in the Ocala NF.

The UFA in the northern and eastern parts of Lake County and the Ocala NF contains naturally occurring brackish or moderately saline ground water at relatively shallow depths along the St. Johns River and its tributaries. The depth to water containing at least 5,000 mg/L chloride concentration ranges from less than 200 ft along the St. Johns River to nearly 2,500 ft below sea level in southern Sumter and Lake Counties. The thickest section of freshwater in the FAS in the study area is located across much of southern and central Lake County, extending into the southwestern part of the Ocala NF.

Recharge areas of the UFA cover much of the study area and include well-drained and poorly drained soils, swamps, closed-basin lakes, and sinkholes. The UFA is recharged by the downward movement of water through the SAS and, where present, the ICU. Additional recharge also occurs through drainage wells drilled into the UFA to dispose of excess surface water in Ocala and western Orange County. Recharge to the SAS, and consequently to the FAS, is augmented locally by artificial recharge—wastewater land application, rapid-infiltration basins, and septic systems.

Discharge from the UFA generally occurs through numerous springs, a few flowing wells, and as diffuse ground-water discharge along the St. Johns, Wekiva, and Ocklawaha Rivers; the south shore of Lake Harris; and the west shore of Lake Apopka. Total estimated springflow in 1998 was 1,979 cubic feet per second (ft^3/s) (1,279 Mgal/d). Springflow occurs at discrete points (vents and boils) or as diffuse ground-water discharge over broader areas where the potentiometric surface of the UFA is above land surface and where the ICU overlying the FAS has been breached. In Lake County, 22 springs account for a total springflow of 258 ft^3/s (167 Mgal/d); and in the Ocala NF, 14 springs account for a total springflow of 348 ft^3/s (225 Mgal/d).

Fluctuations of lake stage and ground-water levels are highly related to cycles and distribution of rainfall. The most significant rises and declines in water levels follow consecutive years with above-average and below-average rainfall, respectively. The long-term (1940 to 2000) lake and ground-water hydrographs generally show a slight downward trend. After the early 1960's, declines in water levels are more pronounced, which corresponds with the accumulating rainfall deficits and increased ground-water withdrawals. Water levels of closed-basin lakes fluctuate slightly less than those of flow-through lakes; however, the closed-basin lakes (selected based on the longevity of data record) also are located in areas where the downward gradient between the SAS and the UFA is nearly zero. Therefore, these closed-basin lakes may not represent the magnitude of the water-level fluctuations that occur in other closed-basin lakes located where a much larger downward gradient exists between the SAS and the UFA.

A generalized water-budget analysis of the study area for 1998 was performed by using measured values of springflow, streamflow, pumpage, and storage changes. An annual average estimate of evapotranspiration (ET) was calculated as the residual of the water budget. In 1998, total available input was about 58 inches (in.), representing 57 in. of rainfall and 1 in. of artificial recharge; springflow was about 6 in.; streamflow (including overland runoff and base flow without measured springflow) was about 13 in., representing 7 in. of overland runoff and 6 in. of base flow; total pumpage from the FAS was about 2 in.; net change in storage was about 1 in.; boundary leakage was nearly 3 in.; and ET, computed as the residual, was about 33 in.

The USGS three-dimensional ground-water flow model MODFLOW-2000 was used to simulate ground-water flow in the SAS and FAS in Lake County, the Ocala NF, and adjacent areas. A steady-state calibration to average 1998 conditions was facilitated by using the inverse modeling capabilities of MODFLOW-2000. Values of hydrologic properties from the calibrated model were in reasonably close agreement with independently estimated values and results from previous modeling studies. The calibrated model generally produced simulated water levels and flows in reasonably close agreement with measured values and was used to simulate the hydrologic effects of projected 2020 conditions.

Projected 2020 conditions simulated by the model consisted of a 44 and 73 percent average increase in withdrawals from the UFA and LFA, respectively, and a 1 percent average increase in artificial recharge resulting from septic tank leakage. Drawdowns from average 1998 conditions as a result of projected 2020 conditions generally were smallest in magnitude and areal extent in the SAS and greatest in the LFA. The average and maximum drawdowns, respectively, in the model area were 0.4 and 10.3 ft in the SAS, 0.9 and 11.8 ft in the UFA, and 1.2 and 19.1 ft in the LFA. Significant drawdowns were simulated in Lake County: the average and maximum drawdowns, respectively, were 0.5 and 5.7 ft in the SAS, 1.1 and 7.6 ft in the UFA, and 1.4 and 4.3 ft in the LFA. The largest drawdowns in Lake County were simulated in the southeastern corner of the County and in the vicinities of Clermont and Mount Dora. Closed-basin lakes and wetlands are more likely to be affected by future pumping in these large drawdown areas, as opposed to other areas of Lake County. However, within the Ocala NF, drawdowns were relatively small: the average and maximum drawdowns, respectively, were 0.1 and 1.0 ft in the SAS, 0.2 and 0.8 ft in the UFA, and 0.3 and 0.8 ft in the LFA. Projected 2020 withdrawals from the FAS caused decreases from average 1998 conditions in the following simulated flows: combined rates of excess evapotranspiration and excess overland runoff (which represent evapotranspiration and overland runoff that occur in excess of their assumed minimum rates); ground-water discharge to streams, lakes, and wetlands; and springflow.

Simulated percent decreases in springflow from average 1998 to projected 2020 conditions vary considerably among the springs in the model area. The greatest decreases occurred for springs that had small differences between simulated UFA water levels and spring pool altitudes in 1998 and were in close proximity to large drawdowns in the UFA. Of all the first- or second-magnitude springs, each of the following springs had a simulated flow decrease greater than 10 percent: Seminole, Rock, Wekiwa, Starbuck, Sanlando, and Apopka. The largest simulated flow decreases for first- or second-magnitude springs in Lake County were at Apopka Springs (28 percent), Seminole (12 percent), and Bugg (9 percent). The largest simulated flow decreases for first- or second-magnitude springs in the Ocala NF were at Juniper Springs (4 percent), Alexander (1 percent), and Fern Hammock (1 percent). Some third-magnitude and smaller springs experienced percentage decreases in simulated springflow exceeding 33 percent.

The USGS particle-tracking program MODPATH was used with ground-water flow model results to delineate areas that contribute recharge to selected springs and well fields under both average 1998 and projected 2020 conditions. The contributing area for Apopka Spring covers approximately 30 mi^2 and has an average contributing recharge flux of 15 inches per year (in/yr) based on average 1998 conditions. The contributing area for Alexander Springs covers approximately 76 mi^2 and has an average contributing recharge flux of 18 in/yr based on average 1998 conditions. The contributing area for Alexander Springs changed little as a result of projected 2020 conditions because relatively little pumping exists in the vicinity of the spring's contributing area. However, the size of the contributing area for Apopka Spring decreased to 26 mi^2 and the average contributing recharge flux decreased to 13 in/yr because a significant decrease in flow from Apopka Spring was simulated for projected 2020 conditions.

Changes in contributing areas from average 1998 to projected 2020 conditions are significant for the two selected well fields because large percentage increases in pumping rates are projected to occur at these wells. For the well field in east-central Lake County, the contributing recharge area increased in size from 9.2 to 16 mi^2, while the average contributing recharge flux decreased slightly from 6.3 to 6.0 in/yr. The pumping rate from the well field in southeast Lake County was small in 1998, but the contributing area for the well field under projected 2020 conditions covered approximately 13 mi^2 with an average contributing recharge flux of 7.4 in/yr.

Linear 95-percent confidence intervals were calculated for simulated drawdowns using YCINT-2000, a post-processing program for MODFLOW-2000, in order to evaluate the effects of parameter uncertainty on model predictions. Uncertainty in simulated drawdowns results from the uncertainty present in all parameter values and from the fact that all simulated water levels are sensitive (to some degree) to the increase in ground-water withdrawals projected for 2020 conditions. Simulated drawdowns generally are equally reliable throughout most of the model area; however, simulated drawdowns generally are less reliable in western Orange and western Seminole Counties. The large increases in withdrawals from the FAS in these areas contribute to this uncertainty by increasing the sensitivity of simulated water levels to one or more model parameters.

Results derived in this study were based primarily on ground-water flow model simulations. Consequently, these results are subject to the assumptions and limitations inherent in the model. Oversimplification of the conceptual model used to construct the ground-water flow model, which is needed to represent extremely complex natural systems, probably is the most likely source of error. However, the hydrologic properties and simulation results derived from the ground-water flow model and particle-tracking analyses were within realistic and previously referenced limits.

SELECTED REFERENCES

Adamski, J.C., 1998, Potentiometric surface of the Upper Floridan aquifer in the St. Johns River Water Management District and vicinity, Florida, May 1998: U.S. Geological Survey Open File Report 98-648, 1 sheet.

Adamski, J.C., and Knowles, Leel, Jr., 2001, Ground-water quality of the surficial aquifer system and the Upper Floridan aquifer, Ocala National Forest and Lake County, Florida, 1990-99: U.S. Geological Survey Water-Resources Investigations Report 01-4008, 51 p.

Anderson, M.P., Hunt, R.J., Krohelski, J.T., and Chung, Kuopo, 2002, Using high hydraulic conductivity nodes to simulate seepage lakes: Ground Water, v. 40, no. 2, p. 117-122.

Anderson, M.P., and Woessner, W.M., 1992, Applied groundwater modeling: Simulation of flow and advective transport: San Diego, Ca., Academic Press, Inc., 381 p.

Anderson, Warren, 1971, Hydrologic considerations in draining Lake Apopka--A preliminary analysis, 1970, Florida: U.S. Geological Survey Open-File Report FL-71004, 41 p.

Anderson, Warren, and Hughes, G.H., 1977, Hydrologic considerations in dewatering and refilling Lake Carlton, Orange and Lake Counties, Florida: U.S. Geological Survey Water-Resources Investigations 76-131 (PB-266 304/AS), 31 p.

Aucott, W.R., 1988, Areal variation in recharge to and discharge from the Floridan aquifer system in Florida: U.S. Geological Survey Water-Resources Investigations Report 88-4057, 1 sheet.

Blanford, T.N., and Birdie, T.R., 1993, Development of wellhead protection areas for the major supply wells in Hernando County, Florida: Herndon, Va., HydroGeoLogic, 90 p.

Boniol, D., Munch, D., and Williams, M., 1993, Mapping recharge to the Floridan aquifer using a Geographic Information System: St. Johns River Water Management District Technical Publication SJ93-5.

Bouwer, Herman, 1978, Groundwater Hydrology: New York, McGraw-Hill, 480 p.

Boyle Engineering Corporation, 1995, Hydrogeologic report--Orange County southern regional wellfield: Prepared for the Board of County Commissioners, Orange County, Florida, 59 p.

Bradner, L.A., 1996, Estimation of recharge through selected drainage wells and the potential effects from well closure, Orange County, Florida: U.S. Geological Survey Open-File Report 96-316, 30 p.

———1999, Potentiometric surface of the Upper Floridan aquifer, St. Johns River Water Management District, September 1998: U.S. Geological Survey Open-File Report 99-100, 1 sheet.

Bush, P.W., 1972, A hydrologic description of Lake Minnehaha at Clermont, Florida: Florida Bureau of Geology Map Series 69, 1 sheet.

———1979, Connector well experiment to recharge the Floridan aquifer, east Orange County, Florida: U.S. Geological Survey Water-Resources Investigations Report 78-73, 40 p.

Camp Dresser and McKee, Inc., 1984, Design development report for southwest Orange County regional wastewater treatment facilities water conservation project: For the Board of County Commissioners, Orange County, Fla., technical report and two appendices.

Carrera, Jesus, and Neuman, S.P., 1986a, Estimation of aquifer parameters under transient and steady state conditions: 1. Maximum likelihood method incorporating prior information: Water Resources Research, v. 22, no. 2, p. 199-210.

———1986b, Estimation of aquifer parameters under transient and steady state conditions: 2. Uniqueness, stability, and solution algorithms: Water Resources Research, v. 22, no. 2, p. 211-227.

———1986c, Estimation of aquifer parameters under transient and steady state conditions: 3. Application to synthetic and field data: Water Resources Research, v. 22, no. 2, p. 228-242.

CH2M Hill, 1989, Wastewater management program for the 1,000-acre site: Prepared for Reedy Creek Improvement District, Lake Buena Vista, Fla.

———1997, Artificial recharge of the Floridan aquifer through drainage or injection wells in Orange and Seminole Counties: Prepared for St. Johns River Water Management District, 103 p.

Cooke, C.W., 1945, Geology of Florida: Florida Geological Survey Bulletin 29, 339 p.

Cooley, R.L., and Naff, R.L., 1990, Regression modeling of ground-water flow: U.S. Geological Survey Techniques of Water-Resources Investigations, book 3, chapter B4, 232 p.

Danek, L.J., Barnard, T.A., and Tomlinson, M.S., 1991, Bathymetric and sediment thickness analysis of seven lakes in the upper Oklawaha River basin: St. Johns River Water Management District Special Publication SJ91-SP14.

Farnsworth, R.K., Thompson, E.S., and Peck, E.L., 1982, Evaporation atlas for the contiguous 48 United States: National Oceanic and Atmospheric Administration Technical Report NWS 33, 26 p., and 4 sheets.

Faulkner, G.L., 1973, Geohydrology of the Cross-Florida Barge Canal area with special reference to the Ocala vicinity: U.S. Geological Survey Water-Resources Investigations 1-73 (PB-244 669/AS), 117 p.

Fetter, C.W., Jr., 1980, Applied Hydrogeology: Columbus, Oh., Charles E. Merrill Publishing Co., 488 p.

Grubb, H.F., 1978, Potential for downward leakage to the Floridan aquifer, Green Swamp area, central Florida: U.S. Geological Survey Water-Resources Investigations 77-71, 1 sheet.

Grubb, H.F., Chappelear, J.W., and Miller, J.A., 1978, Lithologic and borehole geophysical data, Green Swamp area, Florida: U.S. Geological Survey Open-File Report 78-574, 270 p.

Grubb, H.F., and Rutledge, A.T., 1979, Long-term water supply potential, Green Swamp area, Florida: U.S. Geological Survey Water-Resources Investigations Report 78-99, 76 p.

Harbaugh, A.W., Banta, E.R., Hill, M.C., and McDonald, M.G., 2000, MODFLOW-2000, The U.S. Geological Survey modular ground-water flow model—user guide to modularization concepts and the ground-water flow process: U.S. Geological Survey Open-File Report 00-92, 121 p.

Harbaugh, A.W., and McDonald, M.G., 1996, User's documentation for MODFLOW-96, an update to the U.S. Geological Survey modular finite-difference ground-water flow model: U.S. Geological Survey Open-File Report 96-485, 56 p.

Healy, H.G., 1978, Appraisal of uncontrolled flowing artesian wells in Florida: U.S. Geological Survey Water-Resources Investigations 78-95, 26 p.

Heath, R.C., and Conover, C.S., Hydrologic Almanac of Florida: U.S. Geological Survey Open-File Report 81-1107, 239 p.

Hill, M.C., 1992, A computer program (MODFLOWP) for estimating parameters of a transient, three-dimensional, ground-water flow model using nonlinear regression: U.S. Geological Survey Open-File Report 91-484, 358 p.

———1994, Five computer programs for testing weighted residuals and calculating linear confidence and prediction intervals on results from the ground-water parameter-estimation computer program MODFLOWP: U.S. Geological Survey Open-File Report 93-481, 81 p.

———1998, Methods and guidelines for effective model calibration: U.S. Geological Survey Water-Resources Investigations Report 98-4005, 90 p.

Hill, M.C., Banta, E.R., Harbaugh, A.W., and Anderman, E.R., 2000, MODFLOW-2000, the U.S. Geological Survey modular ground-water flow model—user guide to the observation, sensitivity, and parameter-estimation processes and three post-processing programs: U.S. Geological Survey Open-File Report 00-184, 209 p.

Hill, M.C., Cooley, R.L., and Pollock, D.W., 1998, A controlled experiment in ground water flow model calibration: Ground Water, v. 36, no. 3, p. 520-535.

Knochenmus, D.D., 1969, A reconnaissance of the quality of water in Lake Dicie and West Crooked Lake near Eustis, Florida: U.S. Geological Survey Open-File Report FL-69003, 10 p.

Knochenmus, D.D., and Hughes, G.H., 1976, Hydrology of Lake County, Florida: U.S. Geological Survey Water-Resources Investigations 76-72, 100 p.

Knochenmus, L.A., and Robinson, J.L., 1996, Descriptions of anisotropy and heterogeneity and their effect on ground-water flow and areas of contribution to public supply wells in a karst carbonate aquifer system: U.S. Geological Survey Water-Supply Paper 2475, 47 p.

Knowles, Leel, Jr., 1996, Estimation of evapotranspiration in the Rainbow Springs and Silver Springs basins in north-central Florida: U.S. Geological Survey Water-Resources Investigations Report 96-4024, 37 p.

Lamonds, A.G., 1974, Chemical and biological quality of Lake Dicie at Eustis, Florida: U.S. Geological Survey Water-Resources Investigations Report 36-74, 61 p.

Leake, S.A., and Claar, D.V., 1999, Procedures and computer programs for telescopic mesh refinement using MODFLOW: U.S. Geological Survey Open-File Report 99-238, 53 p.

Leake, S.A., and Prudic, D.E., 1991, Documentation of a computer program to simulate aquifer-system compaction using the modular finite-difference ground-water flow model: U.S. Geological Survey Techniques of Water-Resources Investigations, book 6, chapter A2, 68 p.

Lee, T.M., 1996, Hydrogeologic controls on the groundwater interactions with an acidic lake in karst terrain, Lake Barco, Florida: Water Resources Research, v. 32, no. 4, p. 831-844.

Lee, T.M., and Swancar, A., 1997, Influence of evaporation, ground water, and uncertainty in the hydrologic budget of Lake Lucerne, a seepage lake in Polk County, Florida: U.S. Geological Survey Water-Supply Paper 2439, 61 p.

Lichtler, W.F., 1972, Appraisal of water resources in the east central Florida region: Florida Bureau of Geology Report of Investigations no. 61, 52 p.

Lichtler, W.F., Anderson, Warren, and Joyner, B.F., 1968, Water resources of Orange County, Florida: Florida Division of Geology Report of Investigations no. 50, 150 p.

Locker, S.D., Brooks, G.R., and Doyle, L.J., 1988, Results of a seismic reflection investigation and hydrogeologic implications for Lake Apopka, Florida: Consultant's report prepared for the St. Johns River Water Management District, Special Publication SJ88-SP5.

Lohman, S.W., 1972, Ground-water hydraulics: U.S. Geological Survey Professional Paper 708, 70 p.

Marella, R.L., 1992, Water withdrawals, use, and trends in Florida, 1990: U.S. Geological Survey Water-Resources Investigations Report 92-4140, 38 p.

———1999, Water withdrawals, use, discharge, and trends in Florida, 1995: U.S. Geological Survey Water-Resources Investigations Report 99-4002, 90 p.

McDonald, M.G., and Harbaugh, A.W., 1988, A modular three-dimensional finite-difference ground-water flow model: U.S. Geological Survey Techniques of Water-Resources Investigations, book 6, chapter A1, 576 p.

McGurk, Brian, and Presley, P., in press, Simulation of the effects of groundwater withdrawals on the Floridan aquifer system in east-central Florida: Model expansion and revision: St. Johns River Water Management District, Palatka, Florida.

McGurk, Brian, Toth, David, and Burger, Patrick, 1998, An examination of changes in salinity with depth within the Floridan aquifer system in the St. Johns River Water Management District, Florida: delineation of the elevations of the 250, 1000, and 5000 mg/L isosurfaces [abs.] *in* Annual Water Resources Conference of the American Water Resources Association, Point Clear, Alabama, 1998: Middleburg, Va., American Water Resources Association.

Miller, J.A., 1986, Hydrogeologic framework of the Floridan aquifer system in Florida and in parts of Georgia, Alabama, and South Carolina: U.S. Geological Survey Professional Paper 1403-B, 91 p., 33 pl.

Motz, L.H., 1995, North-central Florida regional ground-water investigation and flow model: St. Johns River Water Management District Special Publication SJ95-SP7, 225 p.

Murray, L.C., Jr., and Halford, K.J., 1996, Hydrogeologic conditions and simulations of ground-water flow in the Greater Orlando Metropolitan Area, east-central Florida: U.S. Geological Survey Water-Resources Investigations Report 96-4181, 100 p.

National Oceanic and Atmospheric Administration, 1935-99, Climatological Data Annual Summary, Florida, vols. 39-103, no. 13, Asheville, N.C., variously paged.

———2000, Climatological Data, Florida, v. 104, nos. 1-12, Asheville, N.C., published monthly, variously paged.

Navoy, A.S., 1986, Hydrogeologic data from a 2,000-foot deep core hole at Polk City, Green Swamp area, central Florida: U.S. Geological Survey Water-Resources Investigations Report 84-4257, 89 p.

O'Reilly, A. M., 1998, Hydrogeology and simulation of the effects of reclaimed-water application in west Orange and southeast Lake Counties, Florida: U.S. Geological Survey Water Resources Investigations Report 97-4199, 91 p.

O'Reilly, A.M., Spechler, R.S., and McGurk, B.E., 2002, Hydrogeology and water-quality characteristics of the Lower Floridan Aquifer in east-Central Florida: U.S. Geological Survey Water-Resources Investigations Report 02-4193, 60 p.

Phelps, G.G., 1985, Recharge and discharge areas of the Floridan aquifer in the St. Johns River Water Management District and vicinity, Florida; U.S. Geological Survey Water-Resources Investigations Report 82-4058, 1 sheet.

———1994, Hydrogeology, water quality, and potential for contamination of the Upper Floridan aquifer in the Silver Springs ground-water basin, central Marion County, Florida: U.S. Geological Survey Water-Resources Investigations Report 92-4159, 69 p., 5 pl.

Phelps, G.G., and Schiffer, D.M., 1996, Geohydrology and potential for upward movement of saline water in the Cocoa well field, east Orange County, Florida: U.S. Geological Survey Open-File Report 95-736, 38 p.

Pirkle, E.C., and Brooks, H.K., 1959, Origin and hydrology of Orange Lake, Sante Fe Lake, and Levys Prairie Lakes of north-central peninsular Florida: The Journal of Geology, v. 67, no. 3, p. 302-317.

Poeter, E.P., and Hill, M.C., 1997, Inverse models: A necessary next step in ground-water flow modeling: Ground Water, v. 35, no. 2, p. 250-260.

Pollock, D.W., 1994, User's guide for MODPATH/MODPATH-PLOT, version 3: A particle tracking post-processing package for MODFLOW, the U.S. Geological Survey finite-difference ground-water flow model: U.S. Geological Survey Open-File Report 94-464, 6 ch.

Post, Buckley, Schuh, and Jernigan, Inc., 1990, Floridan aquifer testing and analysis, Bull Creek wildlife management area, Osceola County: Prepared for South Brevard Water Authority, Melbourne, Florida, 2 volumes.

Pride, R.W., Meyer, F.W., and Cherry, R.N., 1966, Hydrology of Green Swamp area in Central Florida: Florida Geological Survey Investigations Report 42, 137 p.

Puri, H.S., and Vernon, R.O., 1964, Summary of the geology of Florida and a guidebook to the classic exposures: Florida Geological Survey Special Publication 5, 312 p.

Reilly, T.E., 2001, System and Boundary Conceptualization in Ground-Water Flow Simulation: U.S. Geological Survey Techniques of Water-Resources Investigations, book 3, chapter B8, 29 p.

Reilly, T.E., and Pollock, D.W., 1993, Factors affecting areas contributing recharge to wells in shallow aquifers: U.S. Geological Survey Water-Supply Paper 2412, 21 p.

Robinson, J.L., 1995, Hydrogeology and results of tracer tests at the old Tampa well field in Hillsborough County, with implications for wellhead-protection strategies in west-central Florida: U.S. Geological Survey Water-Resources Investigations Report 93-4171, 63 p.

Rosenau, J.C., Faulkner, G.L., Hendry, C.W., Jr., and Hull, R.W., 1977, Springs of Florida: Florida Bureau of Geology Bulletin No. 31 (revised), 461 p.

Rutledge, A.T., 1985, Use of double-mass curves to determine drawdown in a long-term aquifer test in north-central Volusia County, Florida: U.S. Geological Survey Water-Resources Investigations Report 84-4309, 29 p.

Rutledge, A.T., and Grubb, H.F., 1978, Hydrogeologic maps of a flood detention area proposed by Southwest Florida Water Management District, Green Swamp area, Florida: U.S. Geological Survey Open-File Report 78-460, 7 sheets.

Ryder, P.D.,1985, Hydrology of the Floridan aquifer system in west-central Florida: U.S. Geological Survey Professional Paper 1403-F, 63 p., 1 sheet.

Sacks, L.A., Lee, T.M., and Radell, M.J., 1994, Comparison of energy-budget evaporation losses from two morphometrically different Florida seepage lakes: Journal of Hydrology, v. 156, p. 311-334.

Scott, T.M., Campbell, K.M., Rupert, F.R., Arthur, J.D., Missimer, T.M., Lloyd, J.M., Yon, J.W., and Duncan, J.G., 2001, Geologic map of the State of Florida: Florida Geological Survey Map Series 146, 1 sheet.

Sepúlveda, Nicasio, 2002, Simulation of ground-water flow in the intermediate and Floridan aquifer systems in peninsular Florida: U.S. Geological Survey Water-Resources Investigations Report 02-4009, 130 p.

Sloto, R.A., and Crouse, M.Y., 1996, HYSEP: A computer program for streamflow hydrograph separation and analysis: U.S. Geological Survey Water-Resources Investigations Report 96-4040, 46 p.

Smith, S.K., and Nogle, June, 1999, Projections of Florida population by county 1998-2020; Gainesville, University of Florida, College of Business Administration, Bureau of Economic and Business Research, v. 32, no. 2, Bulletin no. 123, 8 p.

South Florida Water Management District, 1998, Districtwide water supply assessment: West Palm Beach, Florida, 249 p.

Southwest Florida Water Management District, 1998, Water supply assessment 1995 - 2020: Brooksville, Florida, 48 p.

Spechler, R.M., and Halford, K.J., 2001, Hydrogeology, water quality, and simulated effects of ground-water withdrawals from the Floridan aquifer system, Seminole County and vicinity, Florida: U.S. Geological Survey Water-Resources Investigations Report 01-4182, 116 p.

Sprinkle, C.L., 1989, Geochemistry of the Floridan aquifer system in Florida and in parts of Georgia, South Carolina, and Alabama: U.S. Geological Survey Professional Paper 1403-I, 105 p.

St. Johns River Water Management District, 1998, Water supply assessment 1998: St. Johns River Water Management District Technical Publication SJ98-2, 96 p.

Sumner, D.M., 1996, Evapotranspiration from successional vegetation in a deforested area of the Lake Wales Ridge, Florida: U.S. Geological Survey Water-Resources Investigations Report 96-4244, 37 p.

———2001, Evapotranspiration from a cypress and pine forest subjected to natural fires, Volusia County, Florida, 1998-99: U.S. Geological Survey Water-Resources Investigations Report 01-4245, 56 p.

Sumner, D.M., and Bradner, L.A., 1996, Hydraulic characteristics and nutrient transport and transformation beneath a rapid infiltration basin, Reedy Creek Improvement District, Orange County, Florida: U.S. Geological Survey Water-Resources Investigations Report 95-4281, 51 p.

Suwannee River Water Management District, 1998, SRWMD Water supply assessment: Live Oak, Florida, 31 p.

Swain, E.D., 1993, Documentation of a computer program (Streamlink) to represent direct-flow connections in a coupled ground-water and surface-water model: U.S. Geological Survey Water-Resources Investigations Report 93-4011, 62 p.

Swancar, Amy, Lee, T.M., and O'Hare, T.M., 2000, Hydrogeologic setting, water budget, and preliminary analysis of ground-water exchange at Lake Starr, Polk County, Florida: U.S. Geological Survey Water-Resources Investigations Report 00-4030, 65 p.

Szell, G.P., 1993, Aquifer characteristics in the St. Johns River Water Management District, Florida: St. Johns River Water Management District Technical Publication SJ93-1, 495 p.

Taylor, G.F., 1984, Distribution and occurrence of total coliform bacteria in Floridan aquifer wells, west Lake County, Florida: U.S. Geological Survey Water-Resources Investigations Report 84-4130, 28 p.

Tibbals, C.H., 1975, Aquifer tests in the Summit reach of the proposed Cross-Florida Barge Canal near Ocala, Florida: U.S. Geological Survey Water-Resources Investigations 28-75, 42 p.

———1978, Effects of paved surfaces on recharge to the Floridan aquifer in east-central Florida—a conceptual model: U.S. Geological Survey Water-Resources Investigations 78-76, 42 p.

———1981, Computer simulation of the steady-state flow system of the Tertiary limestone (Floridan) aquifer system in east-central Florida: U.S. Geological Survey Water-Resources Investigations Open-File Report 81-681, 31 p., 9 sheets.

———1990, Hydrology of the Floridan aquifer system in east-central Florida: U.S. Geological Survey Professional Paper 1403-E, 98 p.

Tihansky, Ann B., 1999, Sinkholes, West-central Florida; *in* Land Subsidence in the United States: U. S. Geological Survey Circular 1182, p. 121-140.

Tihansky, A.B., Arthur, J.D., and Dewitt, D.W., 1996, Sublake geologic structure from high-resolution seismic-reflection data from four sinkhole lakes in the Lake Wales Ridge, central Florida: U.S. Geological Survey Open-File Report 96-224, 71 p.

University of Florida, 1976, Florida estimates of population, July 1, 1975; Gainesville, University of Florida, College of Business Administration, Bureau of Economic and Business Research, 51 p.

———1996, Florida estimates of population, 1995; Gainesville, University of Florida, College of Business Administration, Bureau of Economic and Business Research, 809 p.

Wallace, John M., and Hobbs, Peter V., 1977, Atmospheric science, an introductory survey: Academic Press, Inc., 467 p.

White, W.A., 1970, The geomorphology of the Florida peninsula: Florida Department of Natural Resources, Bureau of Geology Geological Bulletin, no. 51, 164 p.

Winsberg, Morton D., 1990, Florida Weather: University of Central Florida Press, Orlando, Florida, 171 p.

Yager, R.M., Miller, T.S., and Kappel, W.M., 2001, Simulated effects of salt-mine collapse on groundwater flow and land subsidence in a glacial outwash aquifer system, Livingston County, New York: U.S. Geological Survey Professional Paper 1611, 85 p.

Yeh, W. W-G., 1986, Review of parameter identification procedures in groundwater hydrology: The inverse problem: Water Resources Research, v. 22, no. 2, p. 95-108.

Yobbi, D.K., 1996, Analysis and simulation of groundwater flow in Lake Wales Ridge and adjacent areas of central Florida: U.S. Geological Survey Water-Resources Investigations Report 94-4254, 81 p.

Appendixes

Appendix A. Index to stream-gaging and climatological data-collection sites

[Site numbers refer to figure 5. Abbreviation for data type: D, stream stage and discharge; E, evaporation; R, rainfall; S, stream stage. Abbreviation for frequency: C, daily; M, monthly or bimonthly; W, weekly. Abbreviation for source of data: LCWA, Lake County Water Authority; NOAA, National Oceanographic and Atmospheric Administration; SJRWMD, St. Johns River Water Management District; USFS, U.S. Forest Service; USGS, U.S. Geological Survey]

Site number	USGS site identification number	Station name	Data type	Frequency	Source of data
1	294500081320001	Federal Point near Palatka	R	C	NOAA
2	294100082160001	Gainesville Municipal Airport	R, E	C	NOAA
3	02244040	St. Johns River, Buffalo Bluff near Satsuma	D	C	USGS
4	02243000	Orange Creek, Orange Springs	D	C	USGS
5	02243960	Ocklawaha River, Rodman Dam	D	C	USGS
6	292600081310001	Crescent City	R	C	NOAA
7	292403081482201	Ocala Sand Pine Seed Orchard, Ocala NF near Kerr City	R	C	USFS
8	02240500	Ocklawaha River, Eureka	D	C	USGS
9	291311081514301	Jumper Lake, Ocala NF, private boat ramp	R	W	USFS
10	02240000	Ocklawaha River near Conner	D	C	USGS
11	02239500	Silver Springs, Silver River near Ocala	D	C	USGS
12	291200082050001	Ocala	R	C	NOAA
13	02236125	St. Johns River, Astor	D	C	USGS
14	290633081375201	Camp Ocala, Ocala NF	R	C	USFS
15	02238500	Ocklawaha River DSS, Moss Bluff	S	C	USGS
16	02238499	Ocklawaha River USS, Moss Bluff	D	C	USGS
17	290100081180001	DeLand 1 SSE	R	C	NOAA
18	290047081382801	Pittman Work Center near Altoona, Ocala NF	R	C	USFS
19	02236000	St. Johns River near DeLand	D	C	USGS
20	285503081550601	Lady Lake	R	C	LCWA
21	02235200	Black Water Creek near Cassia	D	C	USGS
22	02238001	Haines Creek DSS, Lisbon	S	C	USGS
23	02238000	Haines Creek USS, Lisbon	D	C	USGS
24	285200081470001	Lisbon	R, E	C	NOAA
25	02234500	St. Johns River near Sanford	D	C	USGS
26	02312720	Withlacoochee River Wysong Dam, Carlson	D	C	USGS
27	02312700	Lake Panasoffkee Outlet River at Panacoochee Retreats	D	C	USGS
28	02235000	Wekiva River near Sanford	D	C	USGS
29	284809081441401	Tavares, LCWA Office	R	C	LCWA
30	284800081140001	Sanford Experimental Station	R	C	NOAA
31	284749081353901	Round Lake near Sorrento	R	C	LCWA
32	02237734	Wolf Branch at FCRR near Mt. Dora	D	C	USGS
33	022349993	Wekiva River RXR Bridge near Sanford	D	C	USGS
34	284725081320001	Musselburg, CR 435, Mt. Plymouth	R	C	LCWA
35	02312667	Shady Brook Creek	D	C	USGS
36	02312600	Withlacoochee River near Floral City	D	C	USGS
37	02237293	Palatlakaha River at M-1 near Okahumpka	D	C	USGS
38	284439081522202	M-1 Structure near Okahumpka	R	C	LCWA
39	02237701	Apopka-Beauclair Canal DSS near Astatula	S	C	USGS
40	02237700	Apopka-Beauclair Canal USS near Astatula	D	C	USGS
41	02237207	Palatlakaha River DSS M-4 near Okahumpka	S	C	USGS
42	02237206	Palatlakaha River USS M-4 near Okahumpka	S	C	USGS
43	02234998	Little Wekiva River near Longwood	D	C	USGS
44	02312640	Jumper Creek	D	C	USGS
45	284122081534401	Groveland Tower, SR 33 south of Okahumpka	R	C	SJRWMD
46	02237051	Palatlakaha River DSS M-5 near Okahumpka	S	C	USGS
47	02237050	Palatlakaha River USS M-5 near Okahumpka	S	C	USGS
48	284000082050001	Bushnell 2 E	R	C	NOAA

Appendix A. Index to stream-gaging and climatological data-collection sites--Continued

[Site numbers refer to figure 5. Abbreviation for data type: D, stream stage and discharge; E, evaporation; R, rainfall; S, stream stage. Abbreviation for frequency: C, daily; M, monthly or bimonthly; W, weekly. Abbreviation for source of data: LCWA, Lake County Water Authority; NOAA, National Oceanographic and Atmospheric Administration; SJRWMD, St. Johns River Water Management District; USFS, U.S. Forest Service; USGS, U.S. Geological Survey]

Site number	USGS site identification number	Station name	Data type	Frequency	Source of data
49	02237011	Palatlakaha River DSS M-6 near Mascotte	S	C	USGS
50	02237010	Palatlakaha River USS M-6 near Mascotte	S	C	USGS
51	283654081515601	Villa City	R	C	LCWA
52	283544081505001	Lake Lucy near Groveland	R	C	SJRWMD
53	02312500	Withlacoochee River, Croom	D	C	USGS
54	02236900	Palatlakaha River USS Cherry Lake near Groveland	D	C	USGS
55	02236901	Palatlakaha River DSS Cherry Lake near Groveland	S	C	USGS
56	283439081345701	Winter Garden Street	R	C	SJRWMD
57	02312200	Little Withlacoochee River, Rerdell	D	C	USGS
58	283400081321201	Starke Lake near Ocoee	R	W	SJRWMD
59	283355081411701	Site 38 Turnpike, Waits Junction	R	C	SJRWMD
60	02312180	Little Withlacoochee River near Tarrytown	D	C	USGS
61	02312000	Withlacoochee River at Trilby	D	C	USGS
62	282837081511101	Erie Lake near Groveland	R	C	SJRWMD
63	02236700	Little Creek near Clermont	D	C	USGS
64	02312140	Bayroot Slough Headwaters near Bay Lake	D	M	USGS
65	282700081450001	Clermont 7 S	R	C	NOAA
66	282700081190001	Orlando WSO McCoy	R	C	NOAA
67	02236500	Big Creek near Clermont	D	C	USGS
68	02266291	Lateral 405, S-405A near Dr. Phillips	D	C	USGS
69	02263869	South Lake Outlet at S-15 near Vineland	D	C	USGS
70	02266025	Reedy Creek at S-46 near Vineland	D	C	USGS
71	02266205	Whittenhorse Creek at S-411 near Vineland	D	C	USGS
72	02264000	Cypress Creek, Vineland	D	C	USGS
73	02264003	Cypress Creek Canal at S-103A near Vineland	D	C	USGS
74	02311700	Dade City Canal near Dade City	D	M	USGS
75	02266200	Whittenhorse Creek near Vineland	D	C	USGS
76	02264051	Black Lake Outlet at S-101A, Buena Vista	D	C	USGS
77	02264060	Lateral 101 at S-101 near Buena Vista	D	C	USGS
78	282207081413801	CR 474, 0.5 mi. west of US 27	R	C	LCWA
79	02266295	Lateral 410 at S-410 near Vineland	D	C	USGS
80	282127082022501	Cumpressco Ranch ROMP-89, RNF 308 near Tarrytown	R	C	SWFWMD
81	02311500	Withlacoochee River near Dade City	D	C	USGS
82	02264100	Bonnet Creek near Vineland	D	C	USGS
83	02266300	Reedy Creek near Vineland	D	C	USGS
84	02263130	C-2 Canal near Vineland	D	C	USGS
85	02310947	Withlacoochee River near Cumpressco	D	C	USGS
86	281841081544301	ROMP 88 near Rock Ridge	R	C	SWFWMD
87	02236350	Green Swamp Run near Eva	D	C	USGS
88	02263800	Shingle Creek at Airport near Kissimmee	D	C	USGS
89	281709081461401	Brown Shinn near Polk City	R	C	LCWA
90	02311000	Withlacoochee-Hillsborough Overflow near Richland	D	C	USGS
91	02266480	Davenport Creek near Loughman	D	C	USGS
92	02266500	Reedy Creek near Loughman	D	M	USGS
93	02234990	Little Wekiva River near Altamonte Springs	D	M	USGS

Appendix B. Index to lake-gaging and surficial aquifer system well data-collection sites

[Site numbers refer to figure 6. Abbreviation for data type: Gs, surficial aquifer system well water level; Ls, lake stage; Q, water quality. Abbreviation for frequency: C, daily; M, monthly or bimonthly; Q, quarterly; S, semiannual; W, weekly. Abbreviation for source of data: FLDEP, State of Florida Department of Environmental Protection; LCWA, Lake County Water Authority; PBG&S, Parsons Brinckerhoff; SJRWMD, St. Johns River Water Management District; SSC, Silver Springs Citrus; SWFWMD, Southwest Florida Water Management District; USFS, U.S. Forest Service; USGS, U.S. Geological Survey]

Site number	USGS site identification number	Station name	Data type	Frequency	Source of data
1	281440081431701	USGS 6” shallow, Sweet Hill Road, 1.95 mi S of Dean Still Road	Gs	S	USGS
2	281753081574001	Hart Hammock 2” near Rock Ridge	Gs	M	USGS
3	281836081430401	Green Bay Ranch Cabin 2”	Gs	M	USGS
4	281951082012001	Green Swamp LLMS	Gs	M	USGS
5	02263776	Lake Bryan near Vineland	Ls	Q	USGS
6	282152082011201	Green Swamp L11KS near Dade City	Gs	M	USGS
7	282202081384601	Lake Oliver 4” near Vineland	Gs	C	USGS
8	282210081352601	Disney 6”, Tree Farm near Vineland	Gs	C	USGS
9	282241081443901	Sand Mine (L-0050) near Horsehead Pond	Gs	M	SJRWMD
10	282245081492601	Eva 6”	Gs	M	USGS
11	282249081365601	RIBS II 4”, Hartzog Road near Whittenhorse Creek	Gs	M	USGS
12	282318081544003	Hayes Grubb 2” (LK756W)	Gs	M	USGS
13	02263868	South Lake near Vineland	Ls	C	USGS
14	02263850	Bay Lake near Vineland	Ls	C	USGS
15	282507081423001	Keene Lake near Clermont	Ls	C	SJRWMD
16	282650081475701	Kirkland Lake near Clermont	Ls	W	SJRWMD
17	02266239	Trout Lake near Clermont	Ls	W	USGS
18	282706081412601	RCID 4”	Gs	M	USGS
19	282710081490901	Pretty Lake near Clermont	Ls	D	SJRWMD
20	282717081554401	USGS 2”, SWFWMD (former Warden’s House site) near Bay Lake	Gs	M	USGS
21	282740082012101	Green Swamp L12BS 2” near Bay Lake	Gs	M	USGS
22	282801081390802	Conserv II, RIBS V Piez 8004 WNW of Avalon Lookout Tower	Gs	W	PBG&S
23	282837081511101	Erie Lake near Groveland	Ls	D	SJRWMD
24	282911081493701	Pine Island Lake, Florida Boy’s Ranch Road	Ls	M	LCWA
25	02263900	Lake Butler, Windermere	Ls	W	USGS
26	282949081440201	Lake Louisa near Clermont	Ls	C	SJRWMD
27	283114081503701	Bernard DuFrene 4” (L-0697), SR 33 S of Groveland	Gs	M	USGS
28	283204081544902	Mascotte 6” near Mascotte (L-0041)	Gs	C	USGS
29	02237540	Johns Lake, Oakland	Ls	W	USGS
30	283238081470501	Lake Minnehaha, Clermont	Ls	C	SJRWMD
31	283239081523502	Florida Select Citrus West Sprayfield 2” (MW-8) near Groveland	Gs	Q	FLDEP
32	283355081411702	Site 38 Turnpike, Waits Junction 4” (L-0044)	Gs	C	USGS
33	283400081321201	Starke Lake near Ocoee	Ls	W	SJRWMD
34	02312670	Lake Catherine, Groveland	Ls	W	USGS
35	283436081351301	Lake Apopka, Winter Garden	Ls	C	SJRWMD
36	02236900	Cherry Lake, Palatlakaha River near Groveland	Ls	C	USGS
37	283534081460801	Lake Minneola, Clermont	Ls	C	SJRWMD
38	283537081545201	USGS 4” (L-0693), Tuscanooga Road 1.4 mi N of SR 50	Gs	M	USGS
39	283544081505001	Lake Lucy near Groveland	Ls	C	SJRWMD
40	02236860	Apshawa Lake near Minneola	Ls	C	USGS
41	283624081434401	Camp Lake Abandoned 4”	Gs	M	USGS
42	283713081303601	Trout Lake near Clarcona	Ls	W	SJRWMD
43	283804081470601	Clerbrook RV Resort 2” (MW-3)	Gs	Q	FLDEP
44	283806081444801	S. Duncan 4”, CR561, Quail Hollow Arabian Farms near Horseshoe Lake	Gs	M	USGS

Appendix B. Index to lake-gaging and surficial aquifer system well data-collection sites--Continued

[Site numbers refer to figure 6. Abbreviation for data type: Gs, surficial aquifer system well water level; Ls, lake stage; Q, water quality. Abbreviation for frequency: C, daily; M, monthly or bimonthly; Q, quarterly; S, semiannual; W, weekly. Abbreviation for source of data: FLDEP, State of Florida Department of Environmental Protection; LCWA, Lake County Water Authority; PBG&S, Parsons Brinckerhoff; SJRWMD, St. Johns River Water Management District; SSC, Silver Springs Citrus; SWFWMD, Southwest Florida Water Management District; USFS, U.S. Forest Service; USGS, U.S. Geological Survey]

Site number	USGS site identification number	Station name	Data type	Fre-quency	Source of data
45	283817081483502	Sunshine Parkway, STP (MW-1)	Gs	Q	FLDEP
46	283825081521101	Sand Mine 2", M-6A Structure Road near Palatlakaha River	Gs	M	USGS
47	02237370	Church Lake near Groveland	Ls	W	USGS
48	02237660	Lake Francis near Plymouth	Ls	M	USGS
49	284020081461901	T. McCormack 4" near Howey in the Hills	Gs	M	USGS
50	284122081534402	Groveland Tower 4" (L-0096), SR 33 S of Okahumpka	Gs	C	SJRWMD
51	284147081512301	Turkey Lake, US 27, 7 mi SE of Leesburg	Ls	M	LCWA
52	284149081570001	Sunshine Peat 2" (Claypit), 4 mi N of Center Hill	Gs	M	USGS
53	284230081345301	Plymouth Tower 4" (OR0107)	Gs, Q	M	SJRWMD
54	284322081410301	Apopka Lock (Field Station) 4" (L-0287)	Gs	M	USGS
55	284329081502901	Silver Springs Citrus 2" Background NW-8, New Sprayfield near Yalaha	Gs	W	SSC
56	284330081481002	Silver Springs Citrus 2" Background P-2, Old Sprayfield near Howey in the Hills	Gs	W	SSC
57	284409081361201	Lake Maggiore near Zellwood	Ls	W	SJRWMD
58	284418081532801	Ogden Martin Systems (MW-4) 2", Okahumpka	Gs	Q	FLDEP
59	284430081552701	(City of) Leesburg, Plantation at SR 470 Spraysite #2, 2" (MW-2A) near Okahumpka	Gs	Q	FLDEP
60	284456082053102	ROMP LP-5 Avon Park	Gs	M	SWFWMD
61	284504081441501	Astatula 1 Landfill 4" (8A)	Gs	Q	USGS
62	284617081341001	Smith Lake near Bay Ridge	Ls	W	SJRWMD
63	284634081262004	Rock Springs Run State Reserve Cluster 4" (OR0650), Shell Mound Road	Gs	C	USGS
64	284733081362401	Wolf Sink (LCWA) 6"	Gs	M	USGS
65	284746081383901	Lake Dora, Mt. Dora	Ls	C	SJRWMD
66	284756081514901	Lake Harris, Leesburg	Ls	C	SJRWMD
67	284759082054102	ROMP LP-6 2", Coleman	Gs	M	SWFWMD
68	284817081563501	Zeb Teeter 2", Flying Bar Z Ranch near Airstrip, S Whitney Road near Leesburg	Gs	M	USGS
69	284819081413001	Lake Saunders near Eustis	Ls	C	SJRWMD
70	284827081541801	Dyches Lake, Leesburg	Ls	W	SJRWMD
71	284828081393801	Lake Gertrude, Heim Road near Mt. Dora	Ls	W	LCWA
72	02235260	Mt. Plymouth Lake, Mt. Plymouth	Ls	W	USGS
73	02312698	Lake Panasoffkee	Ls	C	USGS
74	284908081255001	Bear Pond, Seminole State Forest	Ls	M	USGS
75	284914081540602	Allied Universal Corp 2" (MW-1), Leesburg	Gs	Q	FLDEP
76	284923081234802	Yankee Lake 4" (S-1310)	Gs	M	USGS
77	284943081382601	Loch Leven, Loch Leven Dr., Mt. Dora	Ls	M	LCWA
78	02237753	West Crooked Lake near Eustis	Ls	W	USGS
79	285009081384701	Lake Joanna, Eustis	Ls	C	SJRWMD
80	285012081343801	Cardinal Ln. (Extension) R/W 4" (L-0701)	Gs	M	USGS
81	285106081412901	Lake Eustis, Eustis	Ls	C	SJRWMD
82	285144081475001	Leesburg Fire Tower 4" (L-0289)	Gs	M	USGS
83	285147081571001	Lake Co School Board 4" (L-0700), CR 466A near Fruitland Park	Gs	M	USGS
84	285148081513101	Lake Griffin, Picciola Island Trailer Park	Ls	C	SJRWMD
85	285208081354101	Lake Seneca near Eustis	Ls	D	SJRWMD

Appendix B. Index to lake-gaging and surficial aquifer system well data-collection sites--Continued

[Site numbers refer to figure 6. Abbreviation for data type: Gs, surficial aquifer system well water level; Ls, lake stage; Q, water quality. Abbreviation for frequency: C, daily; M, monthly or bimonthly; Q, quarterly; S, semiannual; W, weekly. Abbreviation for source of data: FLDEP, State of Florida Department of Environmental Protection; LCWA, Lake County Water Authority; PBG&S, Parsons Brinckerhoff; SJRWMD, St. Johns River Water Management District; SSC, Silver Springs Citrus; SWFWMD, Southwest Florida Water Management District; USFS, U.S. Forest Service; USGS, U.S. Geological Survey]

Site number	USGS site identification number	Station name	Data type	Frequency	Source of data
86	02238200	Lake Yale, Grand Island	Ls	C	USGS
87	285300081265302	Boggy Creek Gang 2" (MW-1), Cassia	Gs	Q	FLDEP
88	285357081472801	Cabbage Hammock 4" (L-0703)	Gs	M	USGS
89	285416081555701	Lady Lake Landfill 4" (LLC7D)	Gs	S	USGS
90	285422081371701	Lake Dalhousie, Recreation Area near Umatilla	Ls	M	USGS
91	285422082001801	Lake Miona (STA 253) Boat Ramp near Oxford	Ls	M	SWFWMD
92	285425081323401	USGS 2" (L-0378), Lake Norris Road	Gs	M	USGS
93	285444081251601	Gaiter Lake near Pine Lakes	Ls	D	SJRWMD
94	02312694	Lady Lake near Lady Lake	Ls	M	USGS
95	02237865	Lake Umatilla, Umatilla	Ls	W	USGS
96	285554081294301	Gourd Lake, Dragonwood Farms near Pine Lakes	Ls	M	USGS
97	285605081353501	Coates Tree Farm 2", NE corner of CR 439 & Will Murphy Road near Umatilla	Gs	M	USGS
98	02238180	Holly Lake near Umatilla	Ls	W	USGS
99	285618081380801	Umatilla Landfill 2" (C-2)	Gs	S	USGS
100	285643081563601	Paradise Lake, Residential Park near Lady Lake	Ls	M	USGS
101	285658081321601	Lake Norris near Paisley	Ls	D	SJRWMD
102	285659081470901	USGS 4" (L-0699), Emeralda Road & CR 452 near Lake Yale	Gs	M	USGS
103	285703081394701	South Twin Lake near Umatilla	Ls	D	SJRWMD
104	285703081425001	Ella Lake near Umatilla	Ls	C	SJRWMD
105	285709081530801	USGS 4" (L-0696), Marion County Road near Lady Lake	Gs	M	USGS
106	285725081584301	Spruce Creek South Perc Pond (MW-3) 2"	Gs	Q	FLDEP
107	285841081331601	Clearwater Lake, Ocala NF near Paisley	Ls	M	USFS
108	285909081314601	Lake Lulu, Paisley	Ls	D	SJRWMD
109	02238330	Big Bass Lake, Ocala NF near Campground	Ls	M	USFS
110	285934081262502	LCFD (District 2 Station 2) 4" (L-0695), Lack Mack Rd	Gs	M	USGS
111	02238170	Nicotoon Lake near Altoona	Ls	D	SJRWMD
112	02235150	Lake Dorr near Altoona	Ls	W	USGS
113	290025081244801	Ocala NF 2" near River Forest (pumphouse), FSR 541	Gs, Q	M	USGS
114	290155081332401	Bunch Ground Pond 4" (L-0702), Paisley Road & Shockley Cemetery Road, Ocala NF	Gs, Q	M	USGS
115	02238830	Bowers Lake near Ocklawaha	Ls	D	SJRWMD
116	02238800	Lake Weir, Ocklawaha	Ls	W	SJRWMD
117	290224081491801	Doe Lake Camp, Ocala NF	Ls	M	USFS
118	290236081280701	Deerhaven Lake, Ocala NF	Ls	M	USFS
119	290300081391801	Ocala NF 2", FSR 573, 1.1 mi W of SR 19	Gs, Q	M	USGS
120	290300081420901	Ocala NF 2", FSR 573, 0.4 mi E of FSR 566	Gs, Q	M	USGS
121	290300081471701	Ocala NF 2", FSR 573, 0.8 mi W of FSR 523	Gs, Q	M	USGS
122	02238820	Smith Lake near Candler	Ls	W	SJRWMD
123	290350081401101	Blue Sink, Ocala NF	Ls	M	USFS
124	290423081495801	Lake Mary, Ocala NF boat ramp	Ls	M	USFS
125	290425081350801	Ocala NF 2" near Alexander Springs, Paisley Road	Gs, Q	M	USGS
126	290436081383101	Railroad Grade Road 2", FSR 550	Gs, Q	M	USGS
127	290447081530101	Moss Bluff Field Station 4" (M-0377)	Gs, Q	M	USGS
128	290452081320001	Ocala NF 2", FSR 552 & 552A & 552B near Alexander Springs Wilderness	Gs, Q	M	USGS

Appendix B. Index to lake-gaging and surficial aquifer system well data-collection sites--Continued

[Site numbers refer to figure 6. Abbreviation for data type: Gs, surficial aquifer system well water level; Ls, lake stage; Q, water quality. Abbreviation for frequency: C, daily; M, monthly or bimonthly; Q, quarterly; S, semiannual; W, weekly. Abbreviation for source of data: FLDEP, State of Florida Department of Environmental Protection; LCWA, Lake County Water Authority; PBG&S, Parsons Brinckerhoff; SJRWMD, St. Johns River Water Management District; SSC, Silver Springs Citrus; SWFWMD, Southwest Florida Water Management District; USFS, U.S. Forest Service; USGS, U.S. Geological Survey]

Site number	USGS site identification number	Station name	Data type	Frequency	Source of data
129	290531081423101	Ocala NF 4" (M-0412), FSR 566/595, S of US Naval Bombing Range	Gs, Q	M	USGS
130	290615081402801	Farles Lake Prairie, Ocala NF Recreation Area Boat Ramp	Ls	M	USFS
131	290624081483901	Ocala NF 4" (M-0411), FSR 595/579	Gs	M	USGS
132	290636081375201	Sellers Lake, Camp Ocala near Alexander Springs	Ls	C	SJRWMD
133	290646081442801	Ocala NF 2", FSR 584 W of US Bombing Range	Gs, Q	M	USGS
134	290647081342101	Alexander Springs 4" (L-0456)	Gs, Q	M	SJRWMD
135	290802081371001	South Grasshopper Lake, Ocala NF boat ramp near Astor Park	Ls	M	USFS
136	02240200	Lake Bryant near Silver Springs	Ls	M	SJRWMD
137	290835081383001	Ocala NF 2", FSR 562-1 & FSR 524 near US Naval Tracking Station	Gs, Q	M	USGS
138	290914081361101	Crooked Lake, Camp McQuarrie near Astor Park	Ls	M	USFS
139	290932081491801	Halfmoon Lake, Ocala NF near Lynne	Ls	M	USFS
140	291002081330603	Astor 4" (L-0460)	Gs, Q	M	SJRWMD
141	291011081373801	Wildcat Lake, Ocala NF Boat Ramp	Ls	M	USFS
142	02240210	Mill Dam Lake near Lynne	Ls	M	USFS
143	291117081540502	Redwater Lake 4" (M-0045)	Gs, Q	M	SJRWMD
144	291150081532701	Redwater Lake, Ocala NF near Lynne	Ls	M	USFS
145	291204081564801	Ocala NF 2", NE125 Terr Road (cemetary) near Ocala NF Boundary	Gs, Q	M	USGS
146	291311081514301	Jumper Lake, Ocala NF, private boat ramp	Ls	M	USFS
147	291335081543101	Lake Charles, Ocala NF boat ramp	Ls	M	USFS
148	291440081384801	Ocala NF 2", SR19 entrance to Silver Glen Springs	Gs, Q	M	USGS
149	291514081445001	Hughes Island Sink, Ocala NF	Ls	M	USFS
150	291519081515501	Lake Eaton, Recreation Area dock	Ls	M	USFS
151	291621081550401	Fore Lake, Ocala NF Recreation Area	Ls	M	USFS
152	291628081413801	Hopkins Prairie near Salt Springs	Ls	M	USFS
153	291657081461501	Ocala NF 4" (M-0408), FSR 88B & FSR 88	Gs, Q	M	USGS
154	02236210	Lake George near Salt Springs	Ls	C	USGS
155	291751081414301	Ocala NF 4" (M-0413), FSR 90 1.5 mi W of SR 19	Gs, Q	M	USGS
156	02236200	Lake Kerr, Ocala NF near Salt Springs	Ls	C	SJRWMD
157	292139081512501	Ocala NF 4" (M-0409), FSR 97A08 (former Eureka Lookout Tower site)	Gs	M	USGS
158	292210081524001	Ft. McCoy	Gs	M	USGS
159	292403081422901	Ocala NF 2", FSR 47 & FSR 43	Gs, Q	M	USGS
160	292447081441402	SR 19 near Frontier 6" (P-0820)	Gs	M	SJRWMD
161	292515081455401	Lake Delancy, Ocala NF, private dock	Ls	C	SJRWMD
162	02242450	Orange Lake, Orange Lake	Ls	C	SJRWMD
163	292543081483201	Ocala NF 2", FSR 75 & FSR 88	Gs, Q	M	USGS
164	292817081483601	Ocala NF 2", FSR 88 & FSR 31	Gs, Q	M	USGS
165	292824081443301	Johnson's Field 4" (P-0473) near Welaka	Gs, Q	S	USGS
166	292948081503002	USGS (P-0738), Road 77 & 77-G	Gs	M	SJRWMD
167	02242400	Lochloosa Lake, Lochloosa	Ls	C	SJRWMD
168	02243958	Lake Ocklawaha near Orange Springs	Ls	C	USGS
169	293556082043401	Hawthorne Tower 4" (A-0436)	Gs	M	SJRWMD
170	293733081474801	Hollister Workctr 4" (P-0511)	Gs	M	SJRWMD

Appendix C. Index to Floridan aquifer system well and spring data-collection sites

[Site numbers refer to figure 7. Abbreviation for hydrologic unit: LFA, Lower Floridan aquifer; UFA, Upper Floridan aquifer; SP, Upper Floridan aquifer spring. Abbreviation for data type: D, ground-water discharge; Q, water quality; W, ground-water level; --, no data. Abbreviation for frequency of flow and water-level data: C, daily; I, intermittently; IA, currently inactive; M, monthly or bimonthly; Q, quarterly; S, semiannual; W, weekly. Abbreviation for source of data: FLDEP, State of Florida Department of Environmental Protection; LC, Lake County; LO, Land Owner, PBG&S, Parsons Brinckerhoff; SJRWMD, St. Johns River Water Management District; SWFWMD, Southwest Florida Water Management District; USGS, U.S. Geological Survey]

Site number	USGS site identification number	Station name	Hydrologic unit	Data type	Frequency of flow and water-level data	Source of data
1	281440081431701	USGS 6", Sweet Hill Road	UFA	Q, W	S	USGS
2	281532081493001	USGS (PK7410) 6" near Polk City	UFA	W	S	USGS
3	281536081324801	Florida Power 6" (SRK01) near Intercession City	UFA	W	S	USGS
4	281559081260701	Shingle Creek 4" at SR 531A	UFA	W	S	USGS
5	281835081552201	Green Swamp Check Station 4", Main Grade (Tanic Road)	UFA	Q	I	USGS
6	281836081430401	Green Bay Ranch Cabin 4"	UFA	W	M	USGS
7	281841081544301	ROMP 88 8" near Rock Ridge	UFA	Q, W	C	SWFWMD, USGS
8	281951082012001	Green Swamp L11MD	UFA	W	M	SWFWMD, USGS
9	282121082071101	Cummer Office	UFA	W	S	USGS
10	282127082022501	Cumpressco Ranch ROMP-89 near Tarrytown	UFA	Q, W	C	SWFWMD, USGS
11	282152082011201	Green Swamp L11KD near Dade City	UFA	W	M	SWFWMD, USGS
12	282202081384601	Lake Oliver 6" (OR0072) near Vineland	UFA	W	C	USGS
13	282221082103001	Collura #1 6"	UFA	W	S	USGS
14	282241081443901	Sand Mine (L-0051) near Horsehead Pond	UFA	Q, W	M	SJRWMD, USGS
15	282245081492601	Eva 6"	UFA	Q, W	M	USGS
16	282318081544003	(L-0555) Green Swamp 4" (Hayes Grubb-LK751W/ LK7425)	UFA	Q, W	M	USGS
17	282331081370801	USGS 4" (OR0009), Hartzog Road near Whittenhorse Creek	UFA	Q, W	S	USGS
18	282354081313001	RCID Obs 4" #1, Disney World Buena Vista Blvd	UFA	Q, W	S	USGS
19	282434081283102	Sea World Dr 4" replacement near Vineland	UFA	W	C	USGS
20	282502081422301	Lykes Bros. replacement (S. Burger) 4" near Keene Lake	UFA	Q, W	S	USGS
21	282511081271701	Orangewood #4	UFA	W	S	USGS
22	282528081340901	Bay Lake 8" near Windermere	UFA	W	C	USGS
23	282532081511801	J. M. Barry 8"	UFA	W	S	USGS
24	282543081385801	J. Mathias 4", Lake Hickory Nut	UFA	W	S	USGS
25	282650081262502	Sand Lake Road MW	LFA	W	S	USGS
26	282706081412601	RCID 12"	UFA	W	M	USGS
27	282717081553101	ROMP 101 (L-0056) near Bay Lake	UFA	Q, W	C	USGS
28	282729081443301	Lake Louisa State Park 4" (L-0053)	UFA	Q, W	M	SJRWMD, USGS
29	282738081341401	Lake Sawyer 4" near Windermere	UFA	Q, W	C	USGS
30	282740082012101	Green Swamp L12BD 2" near Bay Lake	UFA	W	M	SWFWMD, USGS
31	282741081585701	Withlacoochee State Forest 3" (Center/South Grades) near Bay Lake	UFA	Q, W	M	USGS
32	282745081283501	Southwest #3 (P-2)	LFA	W	S	USGS
33	282758081392801	Conserv II 1W-2	LFA	W	S	USGS
34	282823081500401	D. Patton 6" near Eva Firetower	UFA	Q, W	S	USGS
35	282835081305201	Palm Lake Dr. 4" near Windermere	UFA	W	C	USGS
36	282838081391401	RIBS II 5-F1A WNW of Avalon Lookout Tower	UFA	Q, W	W	PBG&S
37	282851082035301	Boyette 3"	UFA	W	S	USGS
38	282923081282801	Ivey's Nursery 4", Turkey Lake Road	UFA	W	S	USGS
39	282931081285901	Hidden Springs #4	LFA	W	S	USGS
40	282936081340201	Ross, Lake Butler	UFA	W	S	USGS
41	283001082064702	Richloam Fire Tower 4"	UFA	W	S	USGS

Appendix C. Index to Floridan aquifer system well and spring data-collection sites--Continued

[Site numbers refer to figure 7. Abbreviation for hydrologic unit: LFA, Lower Floridan aquifer; UFA, Upper Floridan aquifer; SP, Upper Floridan aquifer spring. Abbreviation for data type: D, ground-water discharge; Q, water quality; W, ground-water level; --, no data. Abbreviation for frequency of flow and water-level data: C, daily; I, intermittently; IA, currently inactive; M, monthly or bimonthly; Q, quarterly; S, semiannual; W, weekly. Abbreviation for source of data: FLDEP, State of Florida Department of Environmental Protection; LC, Lake County; LO, Land Owner, PBG&S, Parsons Brinckerhoff; SJRWMD, St. Johns River Water Management District; SWFWMD, Southwest Florida Water Management District; USGS, U.S. Geological Survey]

Site number	USGS site identification number	Station name	Hydrologic unit	Data type	Frequency of flow and water-level data	Source of data
42	283006081274101	Kirkman #3	LFA	W	S	USGS
43	283007081575902	GWSI #5 Tower Camp	UFA	Q	I	FLDEP
44	283017081391301	(17830) Davenport Road 4” near Oakland	UFA	Q, W	S	USGS
45	283019081455701	LCFD District 9 Station 1 4” near Crescent Lake, Clermont	UFA	Q, W	S	USGS
46	283028081454701	Country Garden Nursery (S. Tyner) 4”, Clermont	UFA	Q, W	M	USGS
47	283036082105502	Ridge Manor 10”	UFA	W	S	USGS
48	283111081502201	B. DuFrene 10” near Groveland	UFA	W	S	USGS
49	283114081503401	B. DuFrene 2” near Groveland	UFA	Q	M	USGS
50	283116081442301	Rings Pond near Clermont	UFA	W	S	USGS
51	283128081404701	Johns Lake 4” (L-0052)	UFA	Q, W	M	SJRWMD, USGS
52	283204081544901	Mascotte 6” (L-0062) near Mascotte	UFA	Q, W	C	USGS
53	283216081320901	Ocoee South #1 (OR0559) Lower	LFA	W	S	USGS
54	283232081394101	83213902 22S26E25 Edgewater Bch 4” near East Johns Lake	UFA	Q, W	S	USGS
55	283236081290901	Oak Meadows #4 Lower	LFA	W	S	USGS
56	283253081283401	OR0047 6”, Orlo Vista	UFA	Q, W	C	USGS
57	283307081435301	Jacks Lake 2”	UFA	W	S	USGS
58	283314081455501	Clermont (L-0001)	UFA	W	C	USGS
59	283322081415401	Clermont Greater Hills North	LFA	W	S	USGS
60	283325081374001	Oakland 12” #1	UFA	Q, W	S	USGS
61	283355081411701	Site 38 Turnpike, Waits Junction 4” (L-0199)	UFA	Q, W	C	SJRWMD, USGS
62	283357081272201	Pine Hills #1 Lower	LFA	W	S	USGS
63	283400081405100	Apopka (Gourd Neck) Spring near Oakland	SP	D, Q	Q	SJRWMD, USGS
64	283432081530601	Mascotte 8”	UFA	Q	M	USGS
65	283445081573201	H. Fender 6”, SR 50 near Lake/Sumter County Line	UFA	W	M	USGS
66	283510082133701	Croom RR Siding 4” near Croom	UFA	W	S	USGS
67	283530081514501	Dr. Phillips & Sons (Minute Maid Co.) 4” near Lake Lucy	UFA	Q, W	S	USGS
68	283535081545201	G. Barton 4”, 16845 Tuscanooga Road	UFA	Q, W	M	USGS
69	283537082151501	ROMP 103 8” near Brooksville	UFA	W	M	USGS
70	283540081402401	Montverde School 3” intermittent flow	UFA	Q	M	USGS
71	283549081401701	Montverde School 6” freeflow	UFA	Q, W	M	USGS
72	283555081300801	Ocoee Forest Oaks #3	LFA	W	S	USGS
73	283638082025702	Webster 8” #2	UFA	Q, W	M	USGS
74	283638082081501	JC48B SCL RxR	UFA	W	S	USGS
75	283655081412701	Freeflow 4”, Ferndale	UFA	Q, W	M	USGS
76	283718081580201	T. Iley 8”, CR 469 near Center Hill	UFA	W	S	USGS
77	283720081421801	Ferndale Baptist Church 4”	UFA	Q	M	USGS
78	283737081445501	Coca Cola Foods 3”, CR 561 N of Turnpike	UFA	W	M	USGS
79	283804081470601	Clerbrook RV 4” (MW-4)	UFA	W	Q	FLDEP
80	283809081324801	Magnolia Park 6” near Ocoee	UFA	Q	M	USGS
81	283813081325701	UF Agriculture Research Center (St. Foliage) 4”	UFA	W	S	USGS
82	283818081291201	West Regional MW LF-1	LFA	W	S	USGS
83	283828081535701	Sunset Lakes Ski Center 4”, N of Mascotte	UFA	Q	M	USGS
84	283829082123701	JC47 Jumper Creek 4” near Doke	UFA	W	S	USGS

Appendix C. Index to Floridan aquifer system well and spring data-collection sites--Continued

[Site numbers refer to figure 7. Abbreviation for hydrologic unit: LFA, Lower Floridan aquifer; UFA, Upper Floridan aquifer; SP, Upper Floridan aquifer spring. Abbreviation for data type: D, ground-water discharge; Q, water quality; W, ground-water level; --, no data. Abbreviation for frequency of flow and water-level data: C, daily; I, intermittently; IA, currently inactive; M, monthly or bimonthly; Q, quarterly; S, semiannual; W, weekly. Abbreviation for source of data: FLDEP, State of Florida Department of Environmental Protection; LC, Lake County; LO, Land Owner, PBG&S, Parsons Brinckerhoff; SJRWMD, St. Johns River Water Management District; SWFWMD, Southwest Florida Water Management District; USGS, U.S. Geological Survey]

Site number	USGS site identification number	Station name	Hydrologic unit	Data type	Frequency of flow and water-level data	Source of data
85	283830081534901	Sunset Lakes 8", N of Mascotte	UFA	W	M	USGS
86	283840081485001	Novelty Crystal Fire, O'Brien Road 0.1 mi N of US 27	UFA	W	M	USGS
87	283840082154801	Barnhart (CE-25) 6", Nobleton	UFA	W	M	USGS
88	283844081422300	Wolf's Head Spring along RxR Grade near Astatula	SP	D	I	USGS
89	283848081221301	Altamonte Springs #2 Lower #11	LFA	W	S	USGS
90	283849081273401	Ecolog Utilities 6", 2808 Oranole Way near Orange/Seminole County Line	UFA	W	M	USGS
91	283855082003301	Central Packing Processing	UFA	Q	I	FLDEP
92	283903081430100	Bear Spring near Astatula	UFA	--	IA	USGS
93	283905081485401	Novelty Crystal 4", O'Brien Road 0.1 mi S of Florida's Turnpike	UFA	Q	I	USGS
94	283906081290001	Apopka, Sheeler Oaks	LFA	W	S	USGS
95	283917081254501	Altamonte Springs #5 Lower #14	LFA	W	S	USGS
96	283937081422101	Lake Apopka Restoration Area (SJRWMD) 4" freeflow, Clay Island	UFA	Q, W	M	USGS
97	284001081303001	OR0661	UFA	Q	I	FLDEP
98	284003081461401	T. McCormack Nursery 4" near Howey in the Hills	UFA	W	M	USGS
99	284038081443200	Double Run Road Seepage (into Little Lake Harris) near Astatula	SP	D	I	USGS
100	284047081441500	Seepage Run (into Little Lake Harris), CR 561 near Astatula	SP	D	I	USGS
101	284052081212605	Charlotte/North St. (S-1024) Lower	LFA	W	S	USGS
102	284119081234500	Sanlando Springs near Longwood	SP	D, W	S	USGS
103	284120081331701	Minute Maid/Plymouth 12 UFL #1	UFA	Q	M	USGS
104	284122081534401	Groveland Tower 4 (L-0095) near Okahumpka	UFA	Q, W	C	SJRWMD, USGS
105	284127081233400	Palm Springs near Longwood	SP	D, W	S	USGS
106	284128081320901	Apopka Grossenbacher #4 Lower (OR0554)	LFA	W	S	USGS
107	284131082002101	Stuart Ranch 4" near Center Hill	UFA	W	S	USGS
108	284134081564201	Sunshine Peat (prev Hi Acres) 4" near Carson	UFA	Q, W	M	USGS
109	284135081565501	Sunshine Peat (prev Hi Acres) 12" Lower, near Carson	LFA	W	S	USGS
110	284148081232800	Starbuck Spring near Longwood	SP	D, W	S	USGS
111	284230081345301	Plymouth Tower 4" (OR0106)	UFA	Q, W	M	SJRWMD, USGS
112	284233081442801	West Astatula 8"	UFA	W	S	USGS
113	284236081263400	Miami Springs near Longwood	SP	D, W	S	USGS
114	284238081275803	Wekiwa Springs State Park 4" (OR0548)	UFA	Q, W	C	SJRWMD, USGS
115	284241081281800	Barrel Springs, Wekiwa Springs State Park	SP	D	I	SJRWMD
116	284241081402601	Keen Ranch 12" near Lake Jem	UFA	W	S	USGS
117	284243081273600	Wekiwa Springs, Wekiwa Springs State Park	SP	D, Q, W	M	USGS
118	284253081441101	Astatula (J. Swaffer Park) 4"	UFA	Q	I	USGS
119	284258081495701	Grey 4", Punkin Center	UFA	W	M	USGS
120	284317082142601	Wynnhaven Camp 4" near Wahoo	UFA	W	S	USGS
121	284320081410701	Apopka-Beauclair Canal 4" (L-0139) at SJRWMD Field Office	UFA	Q, W	S	USGS
122	284328081515901	Creek Farms 8"	UFA	Q, W	S	USGS
123	284330081360501	World Foliage Resource, Inc., 8" near Zellwood	UFA	Q, W	S	USGS

Appendix C. Index to Floridan aquifer system well and spring data-collection sites--Continued

[Site numbers refer to figure 7. Abbreviation for hydrologic unit: LFA, Lower Floridan aquifer; UFA, Upper Floridan aquifer; SP, Upper Floridan aquifer spring. Abbreviation for data type: D, ground-water discharge; Q, water quality; W, ground-water level; --, no data. Abbreviation for frequency of flow and water-level data: C, daily; I, intermittently; IA, currently inactive; M, monthly or bimonthly; Q, quarterly; S, semiannual; W, weekly. Abbreviation for source of data: FLDEP, State of Florida Department of Environmental Protection; LC, Lake County; LO, Land Owner, PBG&S, Parsons Brinckerhoff; SJRWMD, St. Johns River Water Management District; SWFWMD, Southwest Florida Water Management District; USGS, U.S. Geological Survey]

Site number	USGS site identification number	Station name	Hydrologic unit	Data type	Frequency of flow and water-level data	Source of data
124	284330081464201	Howey in the Hills 14" #3 (L-0591)	UFA	Q, W	I	FLDEP, USGS
125	284340081305101	J. Owens 4", 132 W Ponkan Road near Apopka	UFA	Q	M	USGS
126	284353081292200	Witherington Springs, Wekiwa Springs State Park near Apopka	SP	D	IA	USGS
127	284407081321601	Apopka Northwest #1 Lower	LFA	W	S	USGS
128	284418081532801	Ogden Martin Systems (MW-5) 4", Okahumpka	UFA	W	Q	FLDEP
129	284424081490500	Holiday Springs at Yalaha	SP	D, Q	S	USGS
130	284430081552701	Plantation at Leesburg, SR 470 Spraysite #2, 4" (MW-2B) near Okahumpka	UFA	W	Q	FLDEP
131	284433081483201	LCFD (Dist 8, Stat 1) 4", CR 48, Yalaha	UFA	W	S	USGS
132	284435082011701	Brentwood, CR 526 near Sumterville	UFA	W	S	USGS
133	284437081491700	Sun Eden Spring near Yalaha	SP	D, Q	I	USGS
134	284439082131401	Trail's End Fish Camp 6" near Floral City	UFA	W	S	USGS
135	284445081462101	Lake Yale Groves 8" (L-0043) near Tavares	UFA	W	M	SJRWMD, USGS
136	284452081495400	Mooring Cove Springs near Yalaha	SP	Q	I	USGS
137	284455081494100	Blue Springs, Park Dr near Yalaha	SP	Q	S	USGS
138	284456082053102	ROMP LP-5 Avon Park	UFA	W	M	SWFWMD
139	284504081441501	Astatula 1 Landfill 4" (8B)	UFA	Q, W	Q	LC, USGS
140	284507081540600	Bugg Spring near Okahumpka	SP	D, Q, W	M	LO, USGS
141	284513081310601	Blue Sink, Orange Co. near Rock Springs	UFA	Q	M	USGS
142	284515082050100	Shady Brook Spring #5 (South Panasoffkee Spring Group) near Lake Panasoffkee	SP	D	IA	USGS
143	284516081224001	S. P. Griffin 4", 30 Windsor Isle Road near Lake Mary	UFA	W	M	USGS
144	284516081570701	Asphalt Production Corp. 4", SR 470 near Okahumpka	UFA	W	M	USGS
145	284520081295800	Rock Springs near Apopka	SP	D, Q, W	M	USGS
146	284523082000201	Jones-Hrs 30"	UFA	Q	I	FLDEP
147	284528081530201	Church of God of Prophecy 3" near Okahumpka	UFA	Q, W	S	USGS
148	284529081301001	Rock Springs 4"	UFA	Q, W	S	USGS
149	284541081265201	Rock Springs Run State Reserve Anderson's Pasture 2" freeflow (OR0068)	UFA	Q, W	S	USGS
150	284553081204801	S-0972 Lake Mary #2	UFA	Q	I	FLDEP, USGS
151	284555081414201	C. Givens Farm 4" near Ellsworth	UFA	W	M	USGS
152	284602081391901	Trimble Park Ranger's House	UFA	W	M	USGS
153	284612081303400	Sulphur (Camp) Springs near Mt. Plymouth	SP	D, Q	I	USGS
154	284612082042000	Shady Brook Spring #4 (South Panasoffkee Spring Group) near Lake Panasoffkee	SP	D	IA	USGS
155	284619082035101	ROMP 111 Thompkins Park 8"	UFA	Q, W	M	USGS
156	284634081262004	Rock Springs Run State Reserve (Cluster) 6" (OR0662)	UFA	Q, W	C	USGS
157	284635081280601	FL DER Hidden 2" (OR0463) near Rock Springs	UFA	W	S	USGS
158	284646082023800	Shady Brook Spring #3 (South Panasoffkee Spring Group) near Coleman	SP	D	IA	USGS
159	284708082024600	Shady Brook Spring #2 (South Panasoffkee Spring Group) near Coleman	SP	D	IA	USGS
160	284725081361901	Wolf Sink (LCWA) 6" (L-0600) near Sorrento	UFA	Q, W	M	USGS
161	284728081322201	Florida Central Academy 6", Mt. Plymouth	UFA	W	S	USGS
162	284732081495301	Frog Leg Ln 4" near Cisky Park, Leesburg	UFA	Q, W	M	USGS

Appendix C. Index to Floridan aquifer system well and spring data-collection sites--Continued

[Site numbers refer to figure 7. Abbreviation for hydrologic unit: LFA, Lower Floridan aquifer; UFA, Upper Floridan aquifer; SP, Upper Floridan aquifer spring. Abbreviation for data type: D, ground-water discharge; Q, water quality; W, ground-water level; --, no data. Abbreviation for frequency of flow and water-level data: C, daily; I, intermittently; IA, currently inactive; M, monthly or bimonthly; Q, quarterly; S, semiannual; W, weekly. Abbreviation for source of data: FLDEP, State of Florida Department of Environmental Protection; LC, Lake County; LO, Land Owner, PBG&S, Parsons Brinckerhoff; SJRWMD, St. Johns River Water Management District; SWFWMD, Southwest Florida Water Management District; USGS, U.S. Geological Survey]

Site number	USGS site identification number	Station name	Hydrologic unit	Data type	Frequency of flow and water-level data	Source of data
163	284740081251700	Wekiva Falls Resort flowing borehole	SP	D, Q	I	USGS
164	284742082021900	Fenney Spring (Shady Brook headspring to Lake Panasoffkee) near Coleman	SP	D	IA	USGS
165	284757081320701	L. Knowles 4", Mt. Plymouth	UFA	Q	I	USGS
166	284757081543002	C. R. Williams 4", Caballo Road, Leesburg	UFA	Q, W	S	USGS
167	284759082054102	ROMP LP-6 6", Coleman	UFA	Q, W	M	SWFWMD
168	284802081211101	Hartstock 4", Wilson Ave. near Wilson Corner	UFA	W	M	USGS
169	284802081242101	V. Hermosa 4", Longwood-Markham Rd	UFA	W	M	USGS
170	284808081432801	Tavares 12" #8	UFA	W	S	USGS
171	284810082004001	Hogeye Sink 6" near Wildwood	UFA	W	S	USGS
172	284822081520601	Leesburg #14 Lower	LFA	W	S	USGS
173	284827081403501	D. Bartholow 4" near Tavares	UFA	W	S	USGS
174	284830081522401	Leesburg, #6, Canal St. (L-0592)	UFA	Q	I	FLDEP
175	284842081533001	Leesburg 12", College St. (L-0054)	UFA	W	C	USGS
176	284856081383001	Mt. Dora 20" #3	UFA	Q, W	S	USGS
177	284857081570901	J. Alibrandi 6", SR 44 W of Leesburg near county line	UFA	W	S	USGS
178	284922081250300	Island Spring, Wekiva River	SP	D, Q	I	USGS
179	284923081234801	Yankee Lake Lower (S-1225)	LFA	W	M	SJRWMD, USGS
180	284923081234802	Yankee Lake 4" (S-1230)	UFA	W	M	USGS
181	284929081294901	Abandoned 10" freeflow off SR 46A near Sorrento	UFA	Q, W	S	USGS
182	284934081474801	Lake-Sumter Community College 8" #1 near Leesburg	UFA	W	S	USGS
183	284936081475501	Lake-Sumter Community College QW 2" near Leesburg	UFA	Q	I	USGS
184	284940081303800	Droty Springs near Sorrento	SP	D, Q	I	USGS
185	284954081201101	Anderson 8", Missouri St. at St. Johns River Estates near Lake Monroe	UFA	W	M	USGS
186	285002081215101	S. Cain 3" near Astor Farms	UFA	W	M	USGS
187	285011082034900	Little Jones Creek Spring #3 (North Panasoffkee Spring Group) near Wildwood	SP	D	IA	USGS
188	285028081253301	Seminole State Forest 4" #1 (L-0037)	UFA	Q, W	M	USGS
189	285038081270100	Palm Springs, Seminole State Forest	SP	D, Q	I	USGS
190	285044081312200	Seminole Springs near Sorrento	SP	D, Q, W	IA	USGS
191	285057081321301	Simpson's Horse Training Center 8" (L-0365) near SR 44/46A	UFA	W	S	USGS
192	285102081263900	Blueberry Spring, Seminole State Forest	SP	D, Q	I	USGS
193	285105081263800	Moccasin Springs, Seminole State Forest	SP	D, Q	I	USGS
194	285118081391001	Eustis 16" (L-0593), CR 44A	UFA	Q	I	FLDEP, USGS
195	285121081295600	Messant Spring near Sorrento	SP	D, Q, W	IA	USGS
196	285129081541002	Fruitland Park (abandoned) 6"	UFA	W	S	USGS
197	285134082051800	Little Jones Creek Spring #2 (North Panasoffkee Spring Group) near Wildwood	SP	D	IA	USGS
198	285144081183900	Gemini Springs near DeBary	SP	D, Q, W	M	SJRWMD, USGS
199	285144081475002	Leesburg Fire Tower (L-0290)	UFA	Q, W	M	FLDEP, USGS
200	285150082044001	Wildwood Fire Tower CE3 (JC58) 2", CR 44A	UFA	Q, W	S	USGS
201	285152081542901	Fruitland Park (Cales Memorial Recreation Complex)	UFA	Q	I	FLDEP, USGS
202	285156081372501	B. Stewart Ranch near Eustis	UFA	W	M	USGS

Appendix C. Index to Floridan aquifer system well and spring data-collection sites--Continued

[Site numbers refer to figure 7. Abbreviation for hydrologic unit: LFA, Lower Floridan aquifer; UFA, Upper Floridan aquifer; SP, Upper Floridan aquifer spring. Abbreviation for data type: D, ground-water discharge; Q, water quality; W, ground-water level; --, no data. Abbreviation for frequency of flow and water-level data: C, daily; I, intermittently; IA, currently inactive; M, monthly or bimonthly; Q, quarterly; S, semiannual; W, weekly. Abbreviation for source of data: FLDEP, State of Florida Department of Environmental Protection; LC, Lake County; LO, Land Owner, PBG&S, Parsons Brinckerhoff; SJRWMD, St. Johns River Water Management District; SWFWMD, Southwest Florida Water Management District; USGS, U.S. Geological Survey]

Site number	USGS site identification number	Station name	Hydrologic unit	Data type	Frequency of flow and water-level data	Source of data
203	285207082014501	Wildwood JC57 12", Masters Ave.	UFA	Q, W	M	USGS
204	285208082054100	Little Jones Creek Headspring (North Panasoffkee Spring Group) near Wildwood	SP	D	IA	USGS
205	285224081262400	Shark's Tooth Spring, Seminole State Forest	SP	D, Q	I	USGS
206	285230081242201	Lower Wekiva River State Preserve 2" freeflow #2 (South)	UFA	Q, W	M	USGS
207	285244081471401	Lisbon Baptist Church Grove 8"	UFA	W	M	USGS
208	285257081434201	J. Eichelberger 10" (L-0373), Grand Island	UFA	W	S	USGS
209	285301081285401	Reese 4" near Cassia	UFA	Q, W	S	USGS
210	285310081524101	R. Peters 4", Lake Griffin	UFA	W	M	USGS
211	285318081295200	Blackwater Springs near Cassia	SP	D	IA	USGS
212	285318081340601	Eustis Sand Co. 12" (L-0375)	UFA	Q, W	S	USGS
213	285357081472801	Cabbage Hammock 6" (L-0620)	UFA	W	S	USGS
214	285416081555701	Lady Lake Landfill 4" (LLD06)	UFA	W	M	USGS
215	285419081552801	Lady Lake (L-0594)	UFA	Q	I	SJRWMD, FLDEP
216	285422082001901	Katz 4", Lake Miona boat ramp near Oxford	UFA	W	S	USGS
217	285426081380901	A. B. Marshall (L-0379) near Umatilla	UFA	W	S	USGS
218	285442081181401	Orange City Tower 4" (V-0196)	UFA	Q, W	M	SJRWMD
219	285442081181402	Orange City Tower Lower (V-0780)	LFA	W	S	USGS
220	285452081563201	R. P. Rowley 5" near Lady Lake	UFA	Q, W	S	USGS
221	285454081241201	Lower Wekiwa River State Preserve 2" intermittent flow #1 (North)	UFA	Q, W	M	USGS
222	285504081405901	Austin Groves 8" (L-0380), Umatilla	UFA	W	S	USGS
223	285524081132401	Galaxy Lower (V-0774)	LFA	W	S	USGS
224	285536082044001	G. N. Smith 6", CR 466 near Oxford	UFA	W	S	USGS
225	285539081262901	South Pine Lakes 4", SR 44	UFA	W	S	USGS
226	285543081133803	V-0772	UFA	Q	I	FLDEP
227	285549081530601	Carlton Village Park 10", Clearview Lake	UFA	Q	I	USGS
228	285551081293601	B. Rogers 4", Gourd Lake	UFA	Q, W	M	USGS
229	285600081530001	Carlton Village Park irrigation 6", Clearview Lake	UFA	W	M	USGS
230	285602081344301	K. Kruckenberg 4" intermittent flow, Will Murphy Road near Paisley	UFA	Q, W	M	USGS
231	285606081353601	Coates Tree Farm 4" irrigation	UFA	Q	M	USGS
232	285618081491101	G. Davis 4", Emeralda Island	UFA	Q, W	S	USGS
233	285628081400501	Umatilla Blanding (L-0595)	UFA	Q	I	FLDEP
234	285638081202400	Blue Springs near Orange City	SP	D, Q, W	M	USGS
235	285702081322400	Camp La-No-Che Springs near Paisley	SP	D, Q	I	USGS
236	285707081441101	J. F. Irvine Estate 4" (L-0385) near Lake Yale	UFA	Q, W	S	USGS
237	285743081390201	Altoona Post Office 4", US19	UFA	W	S	USGS
238	285810081234101	Lower Wekiva River St Preserve 4" freeflow	UFA	Q, W	M	USGS
239	285813081142402	V-0777	UFA	Q	I	FLDEP
240	285820081580301	Steeplechase (Stonecrest) Perc Pond Irrigation 4" (MW-1) near Sunset Harbor	UFA	Q	I	FLDEP
241	285827081331401	P. Shokley 6" near Johnson's Corner, Paisley	UFA	W	S	USGS
242	285831081580401	Abandoned 4" near Sunset Harbor	UFA	W	M	USGS

Appendix C. Index to Floridan aquifer system well and spring data-collection sites--Continued

[Site numbers refer to figure 7. Abbreviation for hydrologic unit: LFA, Lower Floridan aquifer; UFA, Upper Floridan aquifer; SP, Upper Floridan aquifer spring. Abbreviation for data type: D, ground-water discharge; Q, water quality; W, ground-water level; --, no data. Abbreviation for frequency of flow and water-level data: C, daily; I, intermittently; IA, currently inactive; M, monthly or bimonthly; Q, quarterly; S, semiannual; W, weekly. Abbreviation for source of data: FLDEP, State of Florida Department of Environmental Protection; LC, Lake County; LO, Land Owner, PBG&S, Parsons Brinckerhoff; SJRWMD, St. Johns River Water Management District; SWFWMD, Southwest Florida Water Management District; USGS, U.S. Geological Survey]

Site number	USGS site identification number	Station name	Hydrologic unit	Data type	Frequency of flow and water-level data	Source of data
243	285859081191001	McGreggor Road 4", SW DeLand	UFA	W	S	USGS
244	285900082072001	CE36 6" (M-0031), Pedro	UFA	Q, W	M	SJRWMD
245	285902081551901	MCFD (District 19, Station 27) 4", Weirsdale	UFA	Q, W	M	USGS
246	285908081470101	Big Bass Lake Recreation Area 4" (M-0046)	UFA	Q, W	M	USGS
247	285920081490501	Nelson's Fish Camp 6" Mar-48 (M-0320) near Ocklawaha River	UFA	W	M	USGS
248	285930081430901	Ocala Forest Campground 6", SR 42 near Altoona	UFA	Q, W	S	USGS
249	285930082022001	W. Sweetz 4", US301 near Summerfield	UFA	W	M	USGS
250	285933081324001	Paisley Fire Tower	UFA	Q	I	USGS
251	285934081262501	LCFD (District 2 Station 2) 4", Lack Mack Road	UFA	Q	I	USGS
252	285935081501201	M-0375	UFA	Q	I	FLDEP
253	285940081522001	K. Scales, Jr., 6" near Weirsdale	UFA	W	M	USGS
254	290026081244701	River Forest, FSR 541 near Forest Hills	UFA	Q	I	USGS
255	290043081232801	River Forest 2" (L-0059) near Crows Bluff	UFA	W	M	SJRWMD
256	290045081295701	Lake Kathryn Recreation Club 4", Pennsylvania St.	UFA	W	M	USGS
257	290047081232501	River Forest 3" (L-0400) near Crows Bluff	UFA	Q, W	S	USGS
258	290047081382801	Pittman Work Center (abandoned) 6" near Altoona	UFA	Q, W	S	USGS
259	290050081381201	Lake Dorr Recreation Area 4"	UFA	Q	I	USGS
260	290052081271201	Central Baptist Youth Camp 4"	UFA	W	M	USGS
261	290130082082001	CE35 4" (M-0042) near Pedro	UFA	W	M	SJRWMD
262	290133082140901	ROMP 119 Marion Oaks 8" near Ocala	UFA	W	C	USGS
263	290138081203201	V-0114 4"	UFA	Q	I	FLDEP
264	290208081250201	St. Francis 2 freeflow near Crows Bluff	UFA	Q, W	M	USGS
265	290220081260400	Mosquito Springs Run, Alexander Springs Wilderness	SP	D, Q	I	USGS
266	290220081485001	Doe Lake Camp 6"	UFA	Q, W	M	USGS
267	290228081382301	LCFD (District 4, Station 6) 4", SR 19 near Altoona	UFA	Q, W	M	USGS
268	290230081123401	USGS 3" on I-4 (V-0118)	UFA	W	S	USGS
269	290237081550501	MCFD (Old Station 12) 4", Ocklawaha	UFA	W	M	USGS
270	290244081302601	Alexander Springs Creek 4", FSR 552B near boat ramp	UFA	W	S	USGS
271	290300081452001	Big Scrub Camp 6"	UFA	Q, W	M	USGS
272	290400082091001	CE33 4" (M-0041) near Ocala	UFA	Q, W	M	SJRWMD
273	290420081311701	Amoco 4" 1A (L-0123), FSR 552B	UFA	W	S	USGS
274	290427081582801	D. Labagh 4", Candler	UFA	W	M	USGS
275	290445081344001	Alexander Springs Recreation Area Supply 4"	UFA	Q	I	USGS
276	290450081343000	Alexander Springs	SP	D, Q, W	M	SJRWMD, USGS
277	290451081344401	Alexander Springs 4" (L-0066)	UFA	W	C	SJRWMD
278	290455081530401	Moss Bluff 8" (M-0013)	UFA	Q, W	M	SJRWMD
279	290512081213601	Glenwood 4" (V-0156)	UFA	Q, W	M	SJRWMD
280	290526081493701	L. Schrimsher 4", near Moss Bluff	UFA	Q, W	M	USGS
281	290541081132903	USGS 05 Lower (V-0012) near DeLand	LFA	W	S	USGS
282	290552082044701	Wolf Sink CE81 4" (M-0058) near Santos	UFA	W	M	SJRWMD
283	290554081390501	Buck Lake Recreation Area handpump 4"	UFA	Q	I	USGS
284	290613081402901	Farles Lake Recreation Area handpump 4"	UFA	Q	I	USGS
285	290614081183301	V-0742	UFA	Q	I	FLDEP

Appendix C. Index to Floridan aquifer system well and spring data-collection sites--Continued

[Site numbers refer to figure 7. Abbreviation for hydrologic unit: LFA, Lower Floridan aquifer; UFA, Upper Floridan aquifer; SP, Upper Floridan aquifer spring. Abbreviation for data type: D, ground-water discharge; Q, water quality; W, ground-water level; --, no data. Abbreviation for frequency of flow and water-level data: C, daily; I, intermittently; IA, currently inactive; M, monthly or bimonthly; Q, quarterly; S, semiannual; W, weekly. Abbreviation for source of data: FLDEP, State of Florida Department of Environmental Protection; LC, Lake County; LO, Land Owner, PBG&S, Parsons Brinckerhoff; SJRWMD, St. Johns River Water Management District; SWFWMD, Southwest Florida Water Management District; USGS, U.S. Geological Survey]

Site number	USGS site identification number	Station name	Hydrologic unit	Data type	Frequency of flow and water-level data	Source of data
286	290628081425301	Ocala NF Lookout Tower Bombing Range (Abandoned Tower #1) 4”	UFA	Q, W	S	USGS
287	290633081375201	Camp Ocala 6” (L-0407), Sellers Lake	UFA	Q, W	S	USGS
288	290647081342101	Alexander Springs 4” (L-0040)	UFA	Q	M	SJRWMD
289	290650081314001	Johnson, Levy Grant near Astor	UFA	Q	S	USGS
290	290708081233101	SJRWMD 4” intermittent flow (V-0280) near Ponce De Leon Springs	UFA	W	S	USGS
291	290748081184201	Thomas 5” near DeLeon Springs	UFA	W	S	USGS
292	290752082121401	J. Downing (Church) 4”, College Road	UFA	W	M	USGS
293	290802081214700	Ponce De Leon Springs near DeLand	SP	D, Q, W	M	SJRWMD, USGS
294	290805081540801	D. Craft 4”, Tomahawk Lake near Lynne	UFA	Q, W	M	USGS
295	290815082025701	CE-40 replacement 3” (M-0269)	UFA	W	M	USGS
296	290820081305001	Alco Fish Camp (Frank Saul) 2” freeflow near Astor	UFA	Q, W	S	USGS
297	290820082032001	USGS CE37 4” (M-0037) near Ocala	UFA	Q, W	M	SJRWMD
298	290828081215101	V-1028	UFA	Q	I	FLDEP
299	290910081360001	Camp McQuarrie (4-H Club Foundation) 6”	UFA	Q, W	S	USGS
300	290950081315501	Astor (A.G. Edwards) 6” (L-0045)	UFA	W	C	USGS
301	290953082031301	CE79 4” (M-0038) near Silver Springs	UFA	W	M	SJRWMD
302	291002081330601	Astor 6” (L-0455)	UFA	Q, W	M	SJRWMD
303	291015081385001	DOT 49 6” (M-0049), SR 19/40	UFA	Q, W	M	SJRWMD
304	291025081263601	V-0506	UFA	Q	I	FLDEP
305	291035081461201	Ocala NF Central Lookout Tower 4” (M-0112) near Lynne	UFA	W	M	USGS
306	291051081495701	Mill Dam Lake Recreation Area Supply 4”	UFA	Q	I	USGS
307	291057081424301	Juniper Springs Recreation Area Supply #2 (M-0115)	UFA	Q	I	USGS
308	291100081422900	Fern Hammock Springs near Ocala	SP	D, Q, W	M	SJRWMD, USGS
309	291100081502001	Mill Dam Lake 6” (SCE-123)	UFA	Q, W	M	USGS
310	291100082010001	USGS CE76 6”, Highway 314 (M-0028)	UFA	Q, W	M	SJRWMD
311	291101081424600	Juniper Springs near Ocala	SP	D, Q, W	M	SJRWMD, USGS
312	291105082005901	FL DEP 4”, Highway 314	UFA	W	M	USGS
313	291110082060001	CE44 6” (M-0032), Ocala	UFA	W	M	SJRWMD
314	291115081592501	Sharpes Ferry Marion DOT5 (Silver Springs 6” Freeflow) near Ocala	UFA	W	C	USGS
315	291115082102901	CE31 replacement 4” (M-0321)	UFA	W	M	SJRWMD
316	291117081540501	Redwater Lake 4” (M-0044)	UFA	Q, W	M	SJRWMD
317	291130082015001	CE47 6” (M-0026) near Silver Springs	UFA	W	M	SJRWMD
318	291136081380001	Juniper Creek South Tributary Seepage near Astor	SP	D	I	USGS
319	291140082052701	CE80 4”, Silver Springs	UF	W	M	SJRWMD
320	291150081282501	Harper’s 8”, Murphy Road	UFA	W	S	USGS
321	291200081390600	Morman Branch Seepage (into Juniper Creek) near Astor	SP	D	I	USGS
322	291216082051501	Ocala (M-0322)	UFA	Q	I	FLDEP
323	291230081594001	Silver Run 3” freeflow (SCE-154) near Silver Springs	UFA	Q, W	M	USGS
324	291257082031100	Silver Springs near Ocala	SP	D, Q, W	C	USGS
325	291258081313701	Ezel’s 4”, SE Lake George	UFA	W	S	USGS
326	291307081393600	Sweetwater Springs along Juniper Creek	SP	D, Q, W	M	SJRWMD, USGS

Appendix C. Index to Floridan aquifer system well and spring data-collection sites--Continued

[Site numbers refer to figure 7. Abbreviation for hydrologic unit: LFA, Lower Floridan aquifer; UFA, Upper Floridan aquifer; SP, Upper Floridan aquifer spring. Abbreviation for data type: D, ground-water discharge; Q, water quality; W, ground-water level; --, no data. Abbreviation for frequency of flow and water-level data: C, daily; I, intermittently; IA, currently inactive; M, monthly or bimonthly; Q, quarterly; S, semiannual; W, weekly. Abbreviation for source of data: FLDEP, State of Florida Department of Environmental Protection; LC, Lake County; LO, Land Owner, PBG&S, Parsons Brinckerhoff; SJRWMD, St. Johns River Water Management District; SWFWMD, Southwest Florida Water Management District; USGS, U.S. Geological Survey]

Site number	USGS site identification number	Station name	Hydrologic unit	Data type	Frequency of flow and water-level data	Source of data
327	291308082024101	Christian Conference Center near Silver Springs	UFA	W	M	USGS
328	291310082045001	CE45 4” (M-0039), Silver Springs	UFA	W	M	SJRWMD
329	291341082003401	Abandoned, CR315 near Lynne	UFA	W	M	USGS
330	291341082142301	Golden Ocala 6”, Ocala	UFA	W	M	USGS
331	291343081254601	R. Jones Fernery 6” (V-0089) near Pierson	UFA	W	C	SJRWMD
332	291351081292502	SJRWMD (V-0577), Shell Harbor Road	UFA	W	M	SJRWMD
333	291443081383700	Silver Glen Springs near Astor	SP	D, Q, W	M	SJRWMD, USGS
334	291445081274001	T. De Witt Taylor School (V-0569)	UFA	Q	I	FLDEP
335	291448081381601	Juniper (Hunt) Club 4” near Silver Glen Springs	UFA	Q, W	S	USGS
336	291458081294201	V-0068 4” near Pierson	UFA	W	C	SJRWMD
337	291508081302801	V-0065	UFA	Q	I	FLDEP
338	291514081515401	Lake Eaton Recreation Area handpump 4”	UFA	Q, W	M	USGS
339	291600081550001	Fore Lake Recreation Area CE55 4” (M-0036)	UFA	Q, W	M	SJRWMD
340	291620081415001	Hopkin’s Prairie Recreation Area handpump 4”	UFA	Q, W	M	USGS
341	291624082090301	Marion Co. Sherriff’s Dept. 4” (M-0419), US301 N of Ocala	UFA	Q	I	FLDEP
342	291640081320901	V-0523	UFA	Q	I	FLDEP
343	291728081390501	Ponderosa Club CE30A 2” freeflow (M-0317) near Lisk Point, Lake George	UFA	Q, W	S	USGS
344	291740081562001	Gores Landing CE54 (M-0025) 6” near Ocala	UFA	Q, W	C	SJRWMD
345	291748081290301	JC Mew Replacement 4” (V-0510)	UFA	W	C	SJRWMD, USGS
346	291750081494001	CE-56 6”, CR 314 near Salt Springs	UFA	W	S	USGS
347	291835081324201	USCE 426 Pine Island 6” freeflow (V-0155), Stoughton House near Seville	UFA	W	S	USGS
348	291849081411401	Lake George 4” (M-0021) near Salt Springs	UFA	Q, W	M	SJRWMD, USGS
349	291941081294201	V-0184 Seville Firetower 4”	UFA	W	M	SJRWMD
350	292019082064201	CE-66 Sparr replacement 4” (M-0063)	UFA	Q, W	M	SJRWMD
351	292056081440901	Salt Springs Civic Association 4”	UFA	W	M	USGS
352	292100081435800	Salt Springs	SP	D, Q, W	M	SJRWMD, USGS
353	292124081345202	Middle Road Upper (P-0736)	UFA	W	M	SJRWMD
354	292138082061601	Johnston C.C. (Black Sink) (M-0012)	UFA	W	C	SJRWMD
355	292143081374601	Drayton Island 2” freeflow (P-0423)	UFA	W	S	USGS
356	292200081510001	CE84 6” (M-0024) near Salt Springs	UFA	Q, W	M	SJRWMD, USGS
357	292204082022801	Fort McCoy Fire Tower 4” (M-0052)	UFA	Q, W	C	SJRWMD
358	292207082115001	Friendship Baptist Church	UFA	W	M	USGS
359	292218081333101	Union Camp (P-0410)	UFA	Q	I	FLDEP
360	292225082053601	Black Sink 10” (M-0284)	UFA	W	M	SJRWMD
361	292240081483101	Grassy Pond Recreation Area handpump 4” (M-0153)	UFA	Q, W	M	USGS
362	292257081353001	P-0469	UFA	Q	I	FLDEP
363	292418081330902	Unknown (P-0705)	UFA	W	M	SJRWMD
364	292440081342601	P-0144	UFA	Q	I	FLDEP
365	292443082003701	MCFD (Stat 2) 4”, Citra	UFA	W	M	USGS
366	292447081370601	Marvin-Jones Road 6” (P-0776)	UFA	W	C	SJRWMD
367	292447081441401	SR 19 near Frontier 4” (P-0427)	UFA	Q, W	M	SJRWMD
368	292521081551200	Wells Landings Springs, Ocklawaha River	SP	D, Q	I	USGS

Appendix C. Index to Floridan aquifer system well and spring data-collection sites--Continued

[Site numbers refer to figure 7. Abbreviation for hydrologic unit: LFA, Lower Floridan aquifer; UFA, Upper Floridan aquifer; SP, Upper Floridan aquifer spring. Abbreviation for data type: D, ground-water discharge; Q, water quality; W, ground-water level; --, no data. Abbreviation for frequency of flow and water-level data: C, daily; I, intermittently; IA, currently inactive; M, monthly or bimonthly; Q, quarterly; S, semiannual; W, weekly. Abbreviation for source of data: FLDEP, State of Florida Department of Environmental Protection; LC, Lake County; LO, Land Owner, PBG&S, Parsons Brinckerhoff; SJRWMD, St. Johns River Water Management District; SWFWMD, Southwest Florida Water Management District; USGS, U.S. Geological Survey]

Site number	USGS site identification number	Station name	Hydrologic unit	Data type	Frequency of flow and water-level data	Source of data
369	292528081383501	P-0270	UFA	Q, W	I	FLDEP
370	292540081552400	Tobacco Patch Landing Spring Group 1a (Group 1 run inflow), Ocklawaha River	SP	D, Q	I	USGS
371	292542081552600	Tobacco Patch Landing Spring Group 1, Ocklawaha River	SP	D, Q	I	USGS
372	292546081513301	CE67 6” (M-0159), FSR 97/75 near Eureka	UFA	W	M	SJRWMD, USGS
373	292548081471201	Lake Delancy Recreation Area handpump 4”	UFA	Q, W	M	USGS
374	292618081412100	Croaker Hole Spring near Welaka	SP	D, Q	I	USGS
375	292622082131801	Huff (M-0367), McIntosh	UFA	W	M	SJRWMD
376	292628081385501	Welaka Fish Hatchery 6” freeflow, Fruitland (P-0396)	UFA	W	S	USGS
377	292654081384900	Beecher Springs near Fruitland	SP	D	S	SJRWMD, USGS
378	292656082125001	Sportsman Cove 2” (M-0351)	UFA	W	M	SJRWMD
379	292725081393500	Forest Springs near Welaka	SP	D	S	SJRWMD
380	292735081394500	Mud Spring near Welaka	SP	D	S	SJRWMD
381	292817081483602	USGS 6” (M-0410), FSR 88/31	UFA	Q, W	M	USGS
382	292824081341501	Thunderbird Airpark (Col. Sauls) 4” (P-0246) near Lake Como	UFA	W	S	USGS
383	292824081443301	Johnson’s Field 4” (P-0472) near Welaka	UFA	Q, W	S	USGS
384	292859081375701	Highway 308B 4” (P-0408), Fruitland	UFA	Q, W	M	USGS
385	292909082095101	(Previously the) Yearling Rest. 4”, Cross Creek	UFA	W	S	USGS
386	292929081572201	MCFD, Orange Springs	UFA	Q	I	USGS
387	292935081402500	Welaka Spring	SP	D	IA	USGS
388	292948081503001	USGS (P-0450), Road 77/77-G	UFA	Q, W	M	SJRWMD
389	293004081443601	Caravell Ranch 4” (P-0585)	UFA	W	S	USGS
390	293021081570600	Camp Seminole Spring, GSC, Orange Springs	SP	D	I	USGS
391	293038081563800	Orange Spring near Orange Springs	SP	D, Q	I	USGS
392	293048081403600	Nashua Spring near Welaka	SP	D	IA	USGS
393	293051081512500	Blue Springs near Orange Springs	SP	D, Q	I	USGS
394	293159081403600	Satsuma Spring near Satsuma	SP	D	S	SJRWMD
395	293113081370301	Pomona Park 6” (P-0382)	UFA	W	S	USGS
396	293234081424101	Rodeheaver Boys Ranch 4” intermittent flow (P-0280)	UFA	W	S	USGS
397	293253082055701	Driscoll 4”, Lake Jeffords	UFA	W	S	USGS
398	293300081523901	CE60 8” freeflow (P-0306)	UFA	Q, W	M	SJRWMD, USGS
399	293420081415601	A. M. Thomas 4” freeflow (P-0462), Stokes Landing	UFA	W	S	USGS
400	293439081524201	3” Freeflow (P-0017) Creek Hwy 315	UFA	W	S	USGS
401	293556082043401	Hawthorne Tower 4” (A-0071)	UFA	W	M	SJRWMD
402	293720081595301	Chesser 6” (P-0008), Putnam Hill	UFA	W	C	USGS
403	293733081474801	Hollister Workctr 4” (P-0510)	UFA	Q, W	M	SJRWMD
404	293744081541601	P-0461, Grassey Lake	UFA	W	S	USGS
405	293806081544901	P-0016 Keller No. 11 Putnam Hill	UFA	W	M	SJRWMD
406	294012081525701	Lake Grandin 6” (P-0772)	UFA	Q, W	S	USGS
407	294308082002201	Swan Lake 10” (P-0001) near Melrose	UFA	Q, W	M	SJRWMD